



UNIVERSITY OF LEEDS

**Modelling Temporal Diffusion of PV Microgeneration
Systems in a Rural Developing Community**

Submitted in Accordance with the Requirements for the Degree of Doctor of
Philosophy

By

Nicholas Nixon Opiyo

Centre for Integrated Energy Research
School of Chemical and Process Engineering
Faculty of Engineering

October, 2016

The candidate confirms that the work submitted is his own, except where work which has formed part of jointly-authored publications has been included. The contribution of the candidate and the other authors to this work has been explicitly indicated below. The candidate confirms that appropriate credit has been given within the thesis where reference has been made to the work of others.

This copy has been supplied on the understanding that it is copyright material and that no quotation from the thesis may be published without proper acknowledgement.

The right of Nicholas Nixon Opiyo to be identified as Author of this work has been asserted by him in accordance with the Copyright, Designs and Patents Act 1988.

List of Publications:

The following publications have been accomplished during the course of this research:

1. **Opiyo, N.**, *Energy Storage for PV-Based Communal Grids*, Journal of Energy Storage **7**: 1-12, 2016. [doi:10.1016/j.est.2016.05.001](https://doi.org/10.1016/j.est.2016.05.001)
2. **Opiyo, N.**, *A Survey Informed PV-Based Cost-Effective Electrification Options for Rural Sub-Saharan Africa*, Energy Policy **91**: 1-11, 2016. [doi:10.1016/j.enpol.2015.12.044](https://doi.org/10.1016/j.enpol.2015.12.044)
3. **Opiyo, N.**, *Power Electronics for PV-Based Communal Grids*, Smart Grid and Renewable Energy **7**: 67-82, 2016. [doi:10.4236/sgre.2016.72004](https://doi.org/10.4236/sgre.2016.72004)
4. **Opiyo, N.**, *Modelling PV-Based Communal Grids Potential for Rural Western Kenya*, Sustainable Energy, Grids and Networks **4**: 54-61, 2015. [doi:10.1016/j.segan.2015.10.004](https://doi.org/10.1016/j.segan.2015.10.004)
5. **Opiyo, N.**, *Modelling Impacts of Scio-Economic Factors on Temporal Diffusion of PV-Based Communal Grids*, Smart Grid and Renewable Energy **6**: 317-332, 2015. [doi:10.4236/sgre.2015.612026](https://doi.org/10.4236/sgre.2015.612026)

Acknowledgements

Firstly, I would like to thank Dr. Caitlin Biedron who gave her all, materially and professionally, to see me through this journey, I will forever be grateful. Secondly, I would like to thank the University of Leeds for giving the opportunity, and enabling me through Leeds International Research Scholarship (LIRS), to read for my PhD here. In particular I would like to thank my supervisors, Dr. Rolf Crook and Prof. Peter Taylor, for carefully guiding me through the whole process. I would also like to thank my former supervisor Dr. Marco Califano for having enabled my admission to the University of Leeds, without which this research would not have been achieved. I am thankful to the accommodation office, and in particular to Rubina Patel, for appointing me as a sub-warden and thus relieving me of a huge financial burden that would have otherwise affected my research. I would like to thank everyone who directly or indirectly contributed to my wellbeing at Leeds and thus to the successful completion of my thesis.

Dedication

In memory of my mother

Marceline Omollo Bwana

You will forever be missed and remembered

Abstract

Development of electricity delivery infrastructures are path-dependent, meaning, each development decision and step affects subsequent steps, and the final outcome. Human actors are therefore the most important variables in any energy development plan as their decisions affect the way a system evolves. Proper policy-planning tools are therefore required to guide decision-makers on least-cost rural electrification topologies. Many factors influence choices of technologies used in rural electrification, the main ones being availability of resources, availability of necessary technical infrastructures, demand, investment costs, and local socio-political and cultural environments. Different modelling tools and techniques have been applied in planning rural electrification paths in many developing countries. However, these often view this problem as a question of expansion of grid coverage through extensions of existing transmission and distribution lines from central power generation stations and seldom address the unique and regionally-specific challenges presented by each developing nation. To the best of our knowledge, no work has captured, in one study, the unique socio-economic, cultural and political environments, and market and technical infrastructural challenges presented by different rural communities in developing nations.

In this work decentralized power systems based on locally available renewable energy resources, in this case solar, are explored as cost-effective electrification alternatives to national utility grid extensions to rural developing communities. An agent-based model (ABM) is developed in Netlogo to provide decision-makers with a user-friendly tool for PV-based rural electrification policy development, planning, and implementation. The model takes into account the complexities and limitations of solar electricity microgeneration technologies, decisions by human actors, geographical factors, and interactions between the three factors in order to capture the overall macro-effects of different micro-decisions in a virtual world; ABMs seek to model individual entities within a complex system and the rules that govern the interactions of the entities within the system, to capture the overall effect of such interactions. The novelty of the model developed in this work is that it simultaneously simulates how technical, socio-economic, and political factors affect temporal diffusion of PV microgeneration systems in a typical rural developing community. The model further simulates how households with PV, driven by demand for more power and other factors, come together to form communal grids. Survey data from Kendu Bay area of Kenya are used to inform the model. Empirical data provided by the Kenyan government are used to validate the model. The model developed in this work could be used by developing nations in their rural electrification planning and implementations, and a test-implementation funded by the Kenyan government is currently underway.

Results show that given various electrification options, households in rural developing communities would overwhelmingly choose small PV microgeneration systems as stepping stones to future grid electrification. This is mainly due to initial basic electricity needs, rapidly falling PV costs, and affordability of such small PV systems; these small PV microgeneration systems allow households to enjoy the benefits of electricity with modest investments while also allowing future modifications with increasing household incomes, increasing power demands, and changing technologies. Another key finding of this research is that as their power demands increase beyond what could be fulfilled by small stand-alone PV systems, most rural households opt for PV-based communal grids as opposed to connecting to the national grids due to low cost, control over a community's own power source, increased reliability and availability, and security of power source. Results also show that increased PV installations, and correspondingly more connections to communal grids, could be realized with introduction of favourable government policies such as subsidies, introduction of favourable microcredit facilities, increased social pressure through advertisements and neighbourhood influence. Furthermore, results indicate that, based on control methods and architectures, start-up and maintenance and operations costs of communal grids could be minimized and thus become more attractive to would be consumers, compared to the national grids.

Table of Contents:

Chapter 1: Introduction and Background.....	1
1.1: Introduction.....	1
1.1.1: Electricity and Development.....	2
1.1.2: Development and Climate Change.....	4
1.2: Microgeneration of Electricity.....	6
1.3: Solar Electricity Microgeneration.....	10
1.4: Communal Grids.....	14
1.5: Concluding Remarks.....	16
1.6: Research Aims and Objectives.....	17
1.7: Thesis Layout.....	18
Chapter 2: Modelling Solar Electricity Microgeneration Systems.....	20
2.1: Introduction.....	20
2.2: PV Power Generators.....	20
2.2.1: PV Modules and Arrays.....	23
2.2.2: Partial Shading.....	26
2.2.3: Maximum Power Point Tracking (MPPT).....	27
2.3: Power Electronics for Microgeneration PV Systems.....	30
2.4: Energy Storage for PV Microgeneration Systems.....	36
2.4.1: Batteries.....	37
2.4.1.1: Lead-Acid (Pb-acid) Batteries.....	38
2.4.1.2: Lithium-Ion (Li-Ion) Batteries.....	38
2.4.1.3: Nickel-Metal Hydride (Ni-MH) Batteries.....	39
2.4.1.4: Nickel-Cadmium (Ni-Cd) Batteries.....	40
2.4.2: Modelling and Simulations.....	41

2.4.2.1: Charging State ($V_p \leq V_{oc}$; $i^* < 0$).....	43
2.4.2.2: Discharging State ($V_p \geq V_{oc}$; $i^* > 0$).....	44
2.4.3: Results and Discussion.....	46
2.4.3.1: Pb-Acid Battery.....	46
2.4.3.2: Li-Ion Battery.....	48
2.4.3.3: Ni-MH Battery.....	49
2.4.3.4: Ni-Cd Battery.....	51
2.5: Concluding Remarks.....	53
Chapter 3: Modelling PV Microgeneration Potential for Kendu Bay Area of Kenya.....	54
3.1: Introduction.....	54
3.2: Solar Radiation.....	54
3.3: Irradiance Data Modelling.....	58
3.4: Methodology.....	62
3.4.1: Clear-Sky Model.....	62
3.4.2: Active-Occupancy Model.....	65
3.5: Results and Discussion.....	67
3.5.1: Single Household Power Demand – Weekend.....	70
3.5.2: Single Household Power Demand – Weekday.....	72
3.5.3: Microgrid and Minigrid.....	73
3.6: Concluding Remarks.....	74
Chapter 4: A Survey of PV Microgeneration Systems in Kendu Bay Area of Kenya.....	76
4.1: Introduction.....	76
4.2: Methodology.....	79
4.2.1: Survey Construction.....	80
4.2.2: Survey Data Collection.....	81

4.3: Results and Discussion.....	83
4.3.1: Individual Households.....	84
4.3.1.1: Grid-Connected Households.....	85
4.3.1.2: Households with Solar Home Systems.....	86
4.3.1.3: Unelectrified Households.....	89
4.3.2: Commercial and Institutional Establishments.....	91
4.3.3: Opinions and Motivations.....	93
4.4: Concluding Remarks.....	93

Chapter 5: Modelling Temporal Diffusion of PV Microgeneration Systems in Kendu Bay Area of Kenya95

5.1: Introduction.....	95
5.2: Methodology.....	96
5.2.1: Cost.....	100
5.2.2: Subsidies.....	102
5.2.3: Neighbourhood Influence.....	104
5.3: Results and Discussion.....	106
5.3.1: Impacts of Subsidies on PV Diffusion.....	110
5.3.1.1: Subsidies/kWh of PV Power Generated.....	110
5.3.1.2: Subsidies/m ² of PV Installed.....	112
5.3.2: Impacts of Neighbourhood Influence on PV Diffusion.....	115
5.3.2.1: Sensing Radius.....	115
5.3.2.2: Neighbourhood Threshold.....	117
5.3.3: Impacts of Costs on PV Diffusion.....	119
5.3.3.1: Impacts of Falling PV Costs.....	119
5.3.3.2: Impacts of Increasing Utility Grid Costs.....	120
5.3.3.3: Impacts of Lending Rates.....	122
5.4: Model Validation.....	124

5.5: Concluding Remarks.....	126
------------------------------	-----

Chapter 6: Impacts of Control Architectures on Temporal Diffusion of PV-Based Communal Grids in Kendu Bay Area of Kenya.....128

6.1: Introduction.....	128
6.1.1: Droop Control.....	128
6.1.2: Inverter Controls.....	130
6.1.2.1: PQ Inverter with Droop Control.....	130
6.1.2.2: VSI Inverter with Droop Control.....	131
6.1.3: Control Architectures.....	132
6.1.3.1: Master Slave (Single Master) Operation.....	132
6.1.3.2: Multi-Master Operation.....	134
6.2: Methodology.....	135
6.2.1: Islanded Communal Grids with Decentralized Storage.....	136
6.2.1.1: DC-Coupled Communal Grids.....	138
6.2.1.2: AC-Coupled Communal Grids.....	140
6.2.2: Islanded Communal Grids with Centralized Storage.....	141
6.2.2.1: DC-Coupled Communal Grids.....	142
6.2.2.2: AC-Coupled Communal Grids.....	143
6.2.3: Grid-Connected Communal Grids.....	144
6.2.3.1: DC-Coupled Communal Grids with Decentralized Storage	147
6.2.3.2: AC-Coupled Communal Grids with Decentralized Storage	148
6.2.3.3: DC-Coupled Communal Grids with Centralized Storage	150
6.2.3.4: AC-Coupled Communal Grids with Centralized Storage	151
6.2.4: Integrated Communal Grids.....	152
6.3: Results and Discussion.....	153
6.3.1: Islanded Communal Grids.....	157
6.3.1.1: DC-Coupled Communal Grids.....	157

6.3.1.2: AC-Coupled Communal Grids.....	158
6.3.2: Grid-Connected Communal Grids.....	159
6.3.2.1: DC-Coupled Communal Grids.....	162
6.3.2.2: AC-Coupled Communal Grids.....	163
6.4: Concluding Remarks.....	165
Chapter 7: Conclusion and Future Work.....	168
7.1: Conclusion.....	168
7.2: Chapter Summaries.....	170
7.3: Future Work.....	173
References.....	175
Appendix A:	188
Appendix B:.....	200
Appendix C:.....	207

List of Figures:

Figure 1.1: World Energy Consumption, 2010-2040 (Quadrillion BTU)	1
Figure 1.2: World Energy Consumption by Fuel Type in Quadrillion BTU	2
Figure 1.3: World Net Electricity Generation by Energy Source, 2010-2040 (Trillion kWh)	2
Figure 1.4: Temporal Rise in Global Carbon Dioxide Emissions from Fossil Fuels	5
Figure 1.5: Temporal Rise in Average Global Temperature	5
Figure 1.6: Temporal Rise in Average Global Temperature	6
Figure 1.7: Global Cumulative Installed PV Capacity, 2000-2013	11
Figure 1.8: Global PV-Generated Electricity 2000-2013	11
Figure 1.9: Cumulative Installed PV Capacity in Leading Countries 2000-2013	12
Figure 1.10: Cumulative PV-Generated Electricity in Leading Countries 2000-2013	12
Figure 1.11: Global Cumulative PV Production 1985-2012	13
Figure 1.12: Global Annual PV Production 2007-2013, with Projection to 2017	13
Figure 1.13: Annual PV Production in Leading Countries 2000-2013	14
Figure 2.1: Schematic Diagram of a Isolated PV power generation System	20
Figure 2.2: Equivalent Circuit Diagram of a PV Cell	21
Figure 2.3: Current-Voltage and Power Voltage Characteristics of a PV Cell	22
Figure 2.4: PV Generator Hierarchy	23
Figure 2.5: BP Solar SX3190 PV-Module Simulink Model	24
Figure 2.6: Effects of Varying Insolation on PV Module Characteristics	25
Figure 2.7: Effects of Varying Temperature on PV Module Characteristics	25
Figure 2.8: Simulink Model for Partial Shading of a BP SX3190 PV Module	26
Figure 2.9: Current-Voltage and Power-Voltage Characteristics of a Partially-Shaded PV Module	27
Figure 2.10: Perturb and Observe Algorithm	28
Figure 2.11: Simulink Model for a PV Array with DC-DC Boost Converter with MPPT	29
Figure 2.12: Comparisons of PV Array Power, Converter Output Power, and Ideal Power at MPP	30

Figure 2.13: Characteristics of the PV Array Showing Maximum Power Point	30
Figure 2.14: Power Electronics in a Grid-Connected PV System	32
Figure 2.15: Simulink Model of a Grid-Connected PV System with DC-DC and DC-AC Converters	32
Figure 2.16: Simulation Results for Different I_{RMSref} Values	33
Figure 2.17: Comparison of V_{DC} and V_{AC} Simulation Results	33
Figure 2.18: Comparison of I_{PV} and I_{AC} Simulation Results	34
Figure 2.19 Comparison of P_{PV} and P_{AC} Simulation Results	34
Figure 2.20: A Grid-Connected PV System with an Automatic Feedback Loop	35
Figure 2.21: Analysis of the Energy Storage Capacitor C	36
Figure 2.22: Circuit Model of a Battery	42
Figure 2.23: Circuit Model of a Battery with Capacitor	42
Figure 2.24: Circuit Model of a Battery with Feedback Loop	43
Figure 2.25: Advanced Circuit Model of a Battery	44
Figure 2.26: Simulink Model of a Battery	45
Figure 2.27: Discharging/Charging Cycles of a Pb-Acid Battery	46
Figure 2.28: Discharging Rate of a Pb-Acid Battery	47
Figure 2.29: Effects of Discharging Current on Rate of Discharge of a Pb-Acid Battery	47
Figure 2.30: Discharging/Charging Cycles of a Li-Ion Battery	48
Figure 2.31: Discharging Rate of a Li-Ion Battery	49
Figure 2.32: Effects of Discharging Current on Rate of Discharge of a Li-Ion Battery	49
Figure 2.33: Discharging/Charging Cycles of a Ni-MH Battery	50
Figure 2.34: Discharging Rate of a Ni-MH Battery	50
Figure 2.35: Effects of Discharging Current on Rate of Discharge of a Ni-MH Battery	51
Figure 2.36: Discharging/Charging Cycles of a Ni-Cd Battery	51
Figure 2.37: Discharging Rate of a Ni-Cd Battery	52
Figure 2.38: Effects of Discharging Current on Rate of Discharge of a Ni-Cd Battery	52
Figure 3.1: Illustration of Zenith and Elevation Angles	55

Figure 3.2: Calculating Solar Radiation on a Tilted PV Module	56
Figure 3.3: Spectral Distributions of AM0, AM1.5G, and AM1.5D	57
Figure 3.4: Schematic Diagram of an AC Coupled Communal Grid	65
Figure 3.5: Sequence of Operation of the Clear-Sky Model	65
Figure 3.6: Sequence of Operation of the Active Occupancy Model	66
Figure 3.7: Comparison of Simulated Clear Sky and Measured Global Irradiance Profiles	67
Figure 3.8: Comparison of Measured Global and Simulated Net Irradiance Profiles	68
Figure 3.9: Comparison of Simulated Clear Sky and Net Irradiance Profiles	68
Figure 3.10: Comparison of Power Generated by One, 25, and 100 SHS	70
Figure 3.11: Active Occupancy and Power Demand on a Weekend	71
Figure 3.12: Generated and Demanded Power on a Weekend	71
Figure 3.13: Exported and Imported Power on a Weekend	72
Figure 3.14: Active Occupancy and Power Demand on a Weekday	72
Figure 3.15: Generated and Demanded Power on a Weekday	73
Figure 3.16: Exported and Imported Power on a Weekday	73
Figure 4.1: Kendu Bay Electrification Topology	85
Figure 4.2: Photos of PV Systems in Kendu Bay	88
Figure 4.3: Correlation between Education and Income Levels	91
Figure 5.1: Sequences of Operation of the Netlogo Model	99
Figure 5.2: A View of the World before Simulations	108
Figure 5.3: A View of the World after Simulations	108
Figure 5.4: Kendu Bay Electrification Topologies	109
Figure 5.5: Kendu Bay Electrification Topologies by Percentages	110
Figure 5.6: Percentage of Electrified Households	110
Figure 5.7: Impacts of Subsidies/kWh on Electrification Topologies after 25 Years	111
Figure 5.8: Impacts of Subsidies/kWh on Electrification Topologies in Percentages after 25 Years	111

Figure 5.9: Percentage of Electrified Households after 25 Years	112
Figure 5.10: Impacts of Subsidies/m ² on Electrification Topologies after 25 Years	113
Figure 5.11: Impacts of Subsidies/m ² on Electrification Topologies in Percentages after 25 Years	113
Figure 5.12: Percentage of Electrified Households after 25 Years	114
Figure 5.13: Impacts of Sensing Radius on Electrification Topologies after 25 Years	115
Figure 5.14: Impacts of Sensing Radius on Electrification Topologies in Percentages after 25 Years	116
Figure 5.15: Percentage of Electrified Households after 25 Years	116
Figure 5.16: Impacts of Neighbourhood Threshold on Electrification Topologies after 25 Years	117
Figure 5.17: Impacts of Neighbourhood Threshold on Electrification Topologies in Percentages after 25 Years	118
Figure 5.18: Percentage of Electrified Households after 25 Years	118
Figure 5.19: Impacts of Falling PV Costs on Electrification Topologies after 25 Years	119
Figure 5.20: Impacts of Falling PV Costs on Electrification Topologies in Percentages after 25 Years	120
Figure 5.21: Percentage of Electrified Households after 25 Years	120
Figure 5.22: Impacts of Increasing Utility Grid Costs on Electrification Topologies after 25 Years	121
Figure 5.23: Impacts of Increasing Utility Grid Costs on Electrification Topologies in Percentages after 25 Years	121
Figure 5.24: Percentage of Electrified Households after 25 Years	122
Figure 5.25: Impacts of Lending Rates on Electrification Topologies after 25 Years	123
Figure 5.26: Impacts of Lending Rates on Electrification Topologies in Percentages after 25 Years	123
Figure 5.27: Percentage of Electrified Households after 25 Years	124
Figure 5.28: Empirical and Simulated Homabay PV Installations Plots	125
Figure 5.29: Empirical and Simulated Ahero PV Installations Plots	125
Figure 5.30: Comparison of Simulated PV Installations Plots	126
Figure 5.31: Comparison of Empirical and Simulated PV Installations Plots	126
Figure 6.1: Generator Connected to Grid	129

Figure 6.2: P-f and Q-V Droops	130
Figure 6.3: A Centrally Controlled Single Master Communal Grid	133
Figure 6.4: A Centrally Controlled Combined VSI-PQ Multi Master Communal Grid	134
Figure 6.5: Islanded DC-Coupled Communal Grid with Decentralized Storage	139
Figure 6.6: Simulink Model of Islanded DC-Coupled Communal Grid with Decentralized Storage	139
Figure 6.7: Islanded AC-Coupled Communal Grid with Decentralized Storage	140
Figure 6.8: Simulink Model of Islanded AC-Coupled Communal Grid with Decentralized Storage	141
Figure 6.9: Islanded DC-Coupled Communal Grid with Centralized Storage	142
Figure 6.10: Simulink Model of Islanded DC-Coupled Communal Grid with Centralized Storage	142
Figure 6.11: Islanded AC-Coupled Communal Grid with Centralized Storage	143
Figure 6.12: Simulink Model of Islanded AC-Coupled Communal Grid with Centralized Storage	144
Figure 6.13: Thevenin Equivalent Circuit of a Feeder (Grid) Connected to an Inverter (PV Source)	146
Figure 6.14: Grid-Connected DC-Coupled Communal Grid with Decentralized Storage	147
Figure 6.15: Simulink Model of Grid-Connected DC-Coupled Communal Grid with Decentralized Storage	148
Figure 6.16: Grid-Connected AC-Coupled Communal Grid with Decentralized Storage	149
Figure 6.17: Simulink Model of Grid-Connected AC-Coupled Communal Grid with Decentralized Storage	149
Figure 6.18: Grid-Connected DC-Coupled Communal Grid with Centralized Storage	150
Figure 6.19: Simulink Model of Grid-Connected DC-Coupled Communal Grid with Centralized Storage	150
Figure 6.20: Grid-Connected AC-Coupled Communal Grid with Centralized Storage	151
Figure 6.21: Simulink Model of Grid-Connected AC-Coupled Communal Grid with Centralized Storage	152
Figure 6.22: Integrated Regional Grid	153
Figure 6.23: Mean Irradiances Hitting the PV Arrays	154
Figure 6.24: Mean Voltages Produced by the PV Arrays	154
Figure 6.25: Mean Currents Generated by the PV Arrays	155

Figure 6.26: Mean Power Outputs from the PV Arrays	155
Figure 6.27: Active and Reactive Power	156
Figure 6.28: Houses Connected to Islanded DC-Coupled Networks	157
Figure 6.29: Percentage of Houses Connected to Islanded DC-Coupled Networks	157
Figure 6.30: Houses Connected to Islanded AC-Coupled Networks	158
Figure 6.31: Percentage of Houses Connected to Islanded AC-Coupled Networks	159
Figure 6.32: Feeder PCC Voltage Performance Using P-f Droop Control Method	160
Figure 6.33: Feeder PCC Voltage Performance Using Q-V Droop Control Method	161
Figure 6.34: Feeder PCC Voltage Performance Using P-Q-V Droop Control Method	162
Figure 6.35: Houses Connected to Grid-Connected DC-Coupled Networks	163
Figure 6.36: Percentage of Houses Connected to Grid-Connected DC-Coupled Networks	163
Figure 6.37: Houses Connected to Grid-Connected AC-Coupled Networks	164
Figure 6.38: Percentage of Houses Connected to Grid-Connected AC-Coupled Networks	164

List of Tables:

Table 1.1: Electricity Access in 2010 - Regional Aggregates	3
Table 1.2: A Comparison of Stand-Alone PV Systems and PV-Based Communal Grids	10
Table 2.1: Properties of BP Solar SX3190	24
Table 2.2: Energy Storage Technologies Comparison	37
Table 2.3: A Comparison of Different Types of Batteries	41
Table 3.1: Section of the Clearness Index Transition Probability Matrix	64
Table 3.2: Comparison of Measured and Simulated Irradiance Data (W/m ²)	69
Table 3.3: Comparison of Power Generated by Single, 25, and 100 SHS (kW)	69
Table 3.4: Comparison of Power Structures for Different SHS Arrangements	74
Table 4.1: Installed PV Capacity by Market Segment	78
Table 4.2: Kenya Communal Grid Potential	79
Table 4.3: Total Populations Households, Survey Samples, and Inclusion Probabilities	83
Table 4.4: Response Rates by Region	84
Table 4.5: Correlation between Education Levels of Heads of Households and Electricity Access	90
Table 4.6: Comparison of Different Electrification Choices for Kendu Bay	94
Table 5.1: Annualized Life Cycle Cost and Levelized Unit Cost of Electricity for a 40 Wp System	107
Table 5.2: Annualized Life Cycle Cost and Levelized Unit Cost of Electricity for a 100 Wp System	107
Table 5.3 Impacts of Subsidies on Electrification Topologies after 25 Years	114
Table 6.1: Typical Line Parameters	132
Table 6.2: Comparison of Additional Power Electronics Required by Networks	156
Table 6.3: Comparison of Houses Connected to Communal Grids under Different Islanded Architectures	159
Table 6.4: Comparison of Houses Connected to Communal Grids under Different Grid-Connected Architectures	165
Table 6.5: Comparison of Houses Connected to Different Communal Grids	165

Chapter 1: Introduction and Background

1.1 Introduction:

International Energy Outlook (IEO) estimates that the current world's energy consumption is about 176 PWh and this is projected to rise by 56% to about 246 PWh by 2040 due to increase in energy demands from developing nations, driven mainly by economic and population growths [1]. During this period, renewable energy and nuclear power will continue to be the world's fastest-growing energy sources at about 2.5% each; fossil fuels, which will still provide about 78% of world's energy needs, will grow at about 1.7%. Figure 1.1 shows the projected global energy consumption trend from 2010 to 2040.

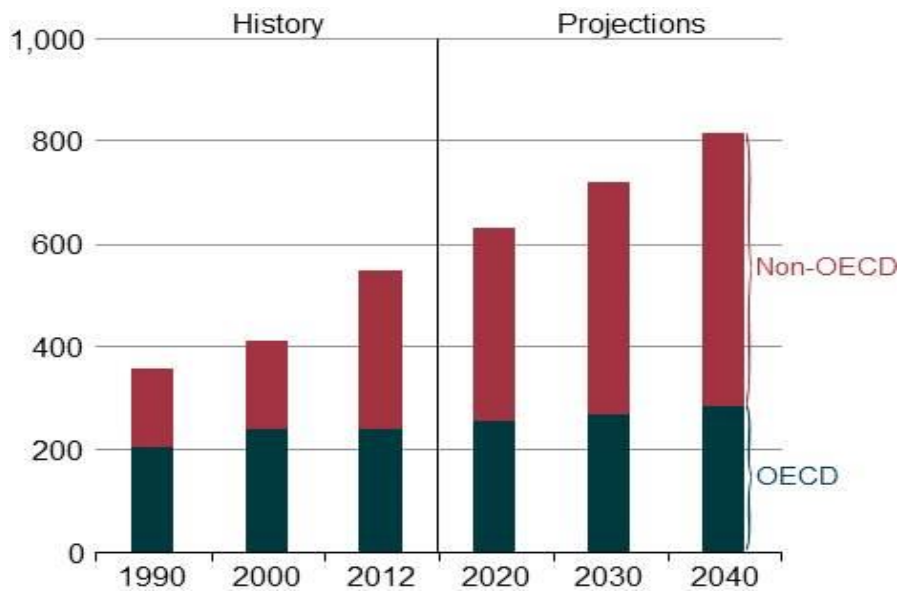


Fig. 1.1: World Energy Consumption, 2010-2040 (Quadrillion Btu) [1]

Concerns for security of energy supplies and environmental degradation by fossil fuel spillages and greenhouse gas emissions have necessitated policies that encourage growth in renewable energy exploration and consumption. As a result, it is projected that the percentage of liquid petroleum consumed, as a share of total global energy demand, will fall from 34% in 2010 to about 28% in 2040 as shown in figure 1.2 below [1]. On the contrary, the use of renewable energy as a share of global total energy consumption will increase from 10% in 2010 to about 15% in 2040, and that of nuclear energy from 5% to 7% [1]. During the same period, electricity generation will grow by 93% from about 20 PWh in 2010 to about 39 PWh in 2040, with generation from renewable energy sources

growing the fastest at an annual rate of 2.8%, followed by those from nuclear and natural gas at rates of 2.5% each, as shown in figure 1.3 [1].

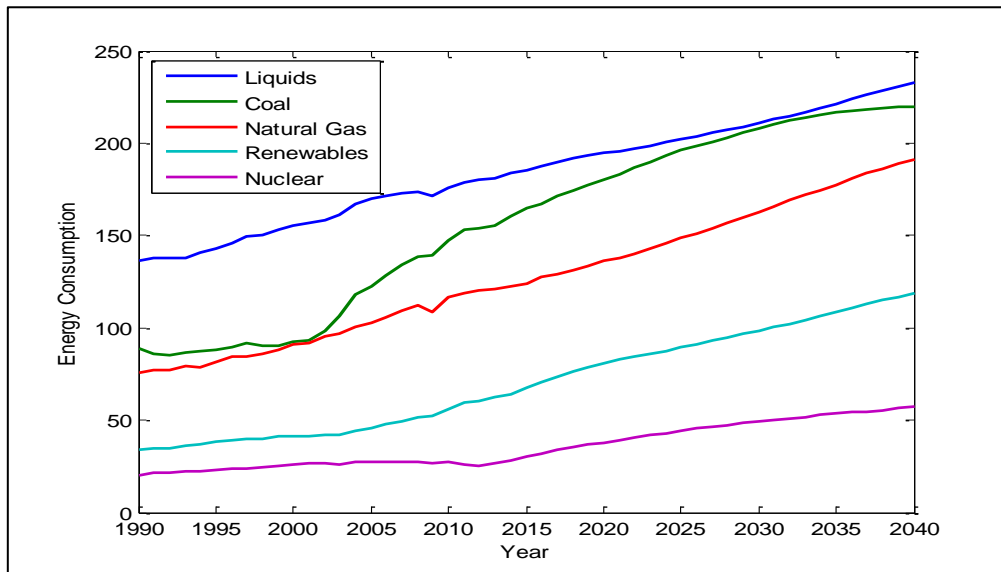


Fig. 1.2: World Energy Consumption by Fuel Type in Quadrillion Btu [1]

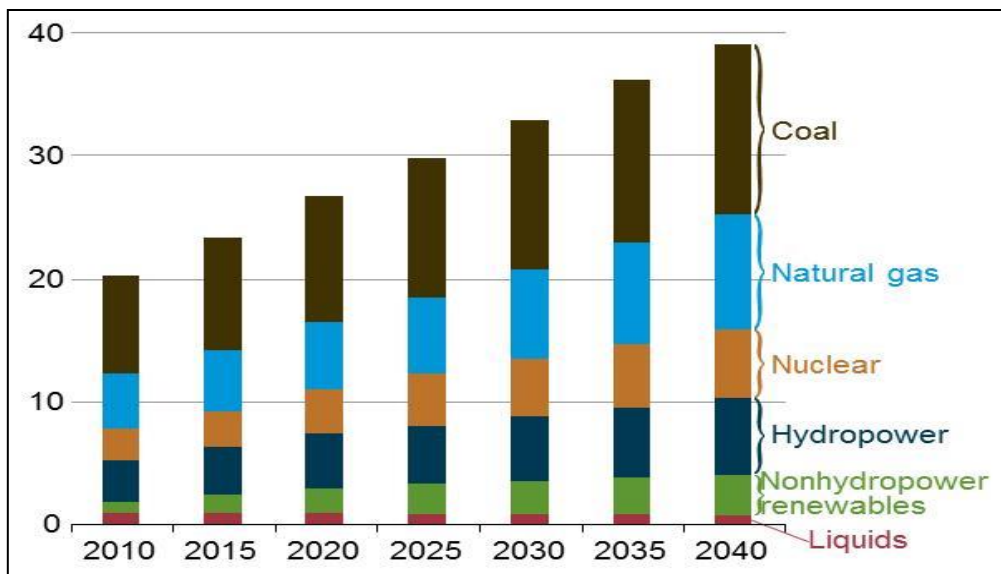


Fig. 1.3: World Net Electricity Generation by Energy Source, 2010-2040 (Trillion kWh) [1]

1.1.1 Electricity and Development

Modern energy services are fundamental to all three pillars of sustainable development, i.e. social, economic, and environmental. Most energy developments must be implemented in line with all aspects of the development process, e.g. energy and communication, energy and health, energy and schools, energy and roads, etc. Energy is therefore a complementary factor to socio-economic

development. Electricity, the main form of modern energy, is crucial to industrialization and easy access to it is an indicator of a nation's standard of living. It is estimated that there are about 1.3 billion people in the world without access to electricity today and that 95% of these people reside in developing nations of Asia and sub-Saharan Africa, 84% of whom are residing in rural areas, and that this trend is expected to continue into 2030 unless investments of over US\$49 billion are made annually into electricity generation, transmission, and distribution [2]. On a more local note, estimates show that the number of people in sub-Saharan Africa without access to electricity will increase from the current 590 million to about 645 million by 2030 mainly due to population growth, and that the majority of these people will still be found in rural areas [2]. Sustained estimated annual investments of about US\$19.1 billion in electricity generation and distribution will have to be made in sub-Saharan Africa for this trend to be arrested [2]. Table 1.1 below summarizes the above information.

Region	Population Without Electricity (millions)	Electrification Rate (%)		
		Total	Urban	Rural
Developing countries	1,265	76.1	92.1	63.7
Africa	590	43	72	24
<i>North Africa</i>	<i>1</i>	<i>99</i>	<i>100</i>	<i>99</i>
<i>Sub-Saharan Africa</i>	<i>589</i>	<i>32</i>	<i>64</i>	<i>13</i>
Developing Asia	628	83	96	74
<i>China & East Asia</i>	<i>157</i>	<i>92</i>	<i>98</i>	<i>88</i>
<i>South Asia</i>	<i>471</i>	<i>70</i>	<i>92</i>	<i>61</i>
Latin America	29	94	98	76
Middle East	18	91	99	75
Transition economies & OECD	2	99.8	100.0	99.5
World	1,267	81.5	94.7	68.0

Table 1.1: Electricity Access in 2010 - Regional Aggregates [2]

Access to electricity-beyond-lighting stimulates rural industrial development by enabling productive use of electricity by small manufacturing enterprises such as welding and carpentry shops and by micro-home enterprises such as mobile phone chargers, or by allowing consumers to switch to cheaper, cleaner, and more convenient sources of electricity for their businesses [3]. Microeconomic activities enabled by access to grid electricity lead to increased employment opportunities which in turn lead to increased incomes and thus improved livelihoods. Electricity also brings with it extended

health benefits as increased incomes enable more rural residents to transition from traditional and harmful cooking fuels such as biomass to modern fuels such as liquid petroleum gas (LPG) which are less harmful; biomasses are major indoor air pollutants for rural households in developing nations, causing about 1.3 million deaths annually as per the latest Global Burden of Disease (GBD) report [4]. In fact, it is estimated that unless urgent measures are taken, noxious smoke from biomass will cause higher annual mortality rates by 2030 than even HIV/AIDS [4]. In addition to clean cooking fuels, electricity also enables access to modern medical equipment such as X-Ray and MRI machines and to cold storage facilities for vaccines and medicines. Even on a smaller scale, the benefits of electricity abound; basic electric lighting alone, usually a replacement for harmful kerosene lanterns, brings with it extended benefits to health and education as improved lighting enables extended hours of studying for school children and extended hours of operation for small businesses, while also providing greater sense of security [3]. Also, basic electricity improves access to information and communication technologies; TVs and radios are major sources of news, business and health information, and distance education [3].

There are two possible routes to rural electrification i.e., through national grid extensions from large central power generation systems or through decentralized systems namely communal grids and stand-alone microgeneration systems. National grid extensions are recommended where the load demands are high enough to make the costs of such investments reasonable. Communal grids are recommended for condensed villages or markets far from national grid lines but with potential economic values to warrant such installations. Stand-alone systems are recommended for isolated homesteads or installations far from existing grid lines, other homesteads, or other installations. The International Energy Agency (IEA) estimates that only 30% of the people currently without access to electricity in sub-Saharan Africa can be cost-effectively served through national grid extensions due to the sparseness of the rural populations, rough terrains, low economic activities, and low load densities. The remaining 70% would be most cost-effectively served through decentralized systems, i.e. communal grids (52.5%) or stand-alone systems (17.5%) [5-9].

1.1.2 Development and Climate Change:

Development and climate change are intrinsically linked given that as countries increasingly industrialize, their greenhouse gas emissions increase and thus their increasing contributions to global warming. Earth's temperature is dependent on a delicate balance between incoming radiation from the sun and outgoing radiation to space, with the latter being strongly affected by the

composition of the earth's atmosphere. Industrialization increases the presence of anthropogenic gases such as carbon dioxide, ozone, and methane, which absorb in the 7-13 μm range, in the atmosphere. This is the range within which 70% of outgoing radiation from the earth's surface should escape into space. Absorption of this radiation by greenhouse gases in the atmosphere therefore leads to increased global temperatures. Figure 1.4 shows a plot of increasing global carbon dioxide emissions from fossil fuels while figure 1.5 shows rise in average global temperatures over the same period [10]. There is a clear correlation between carbon dioxide emissions from burning fossil fuels and increasing global warming, with the atmospheric CO_2 levels estimated to double by 2030, leading to global warming of approximately 1-4°C by 2030, with devastating environmental consequences [11]. Developing nations are predicted to be most affected by the changing environmental conditions since they are the least resilient; industrialization, though a major contributor to environmental pollution, improves a country's ability to cope with the adverse climatic consequences of such pollution [12]. As such, developing regions such as Africa are likely to be the most devastated by global warming.

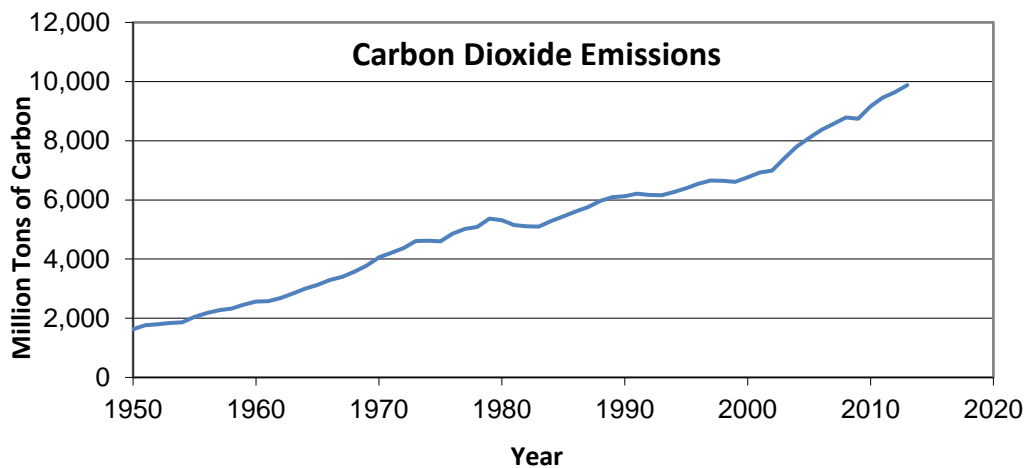


Fig. 1.4: Temporal Rise in Global Carbon Dioxide Emissions from Fossil Fuels [13]

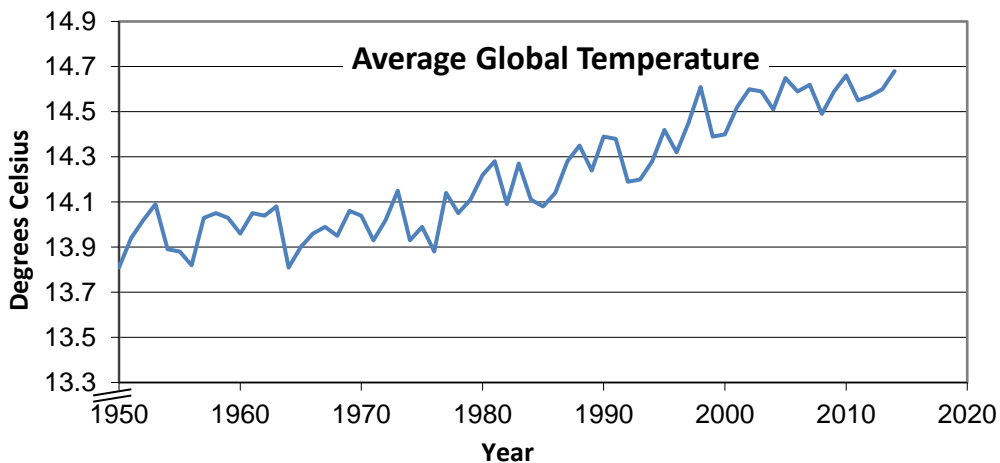


Fig. 1.5: Temporal Rise in Average Global Temperature [13]

As shown in figure 1.6, even though emissions from OECD countries have largely peaked at high numbers of above 3,500 million tons of carbon per annum, emissions from the rest of the world continue to climb rapidly as they industrialize, with the biggest polluters being China and other Asian tigers, India, and Brazil. The least developed regions of sub-Saharan Africa are the least polluters, accounting for less than 3% of total global pollution, a blessing in disguise as they have unique opportunities to pursue green economic paths while industrializing at the same time [14,15].

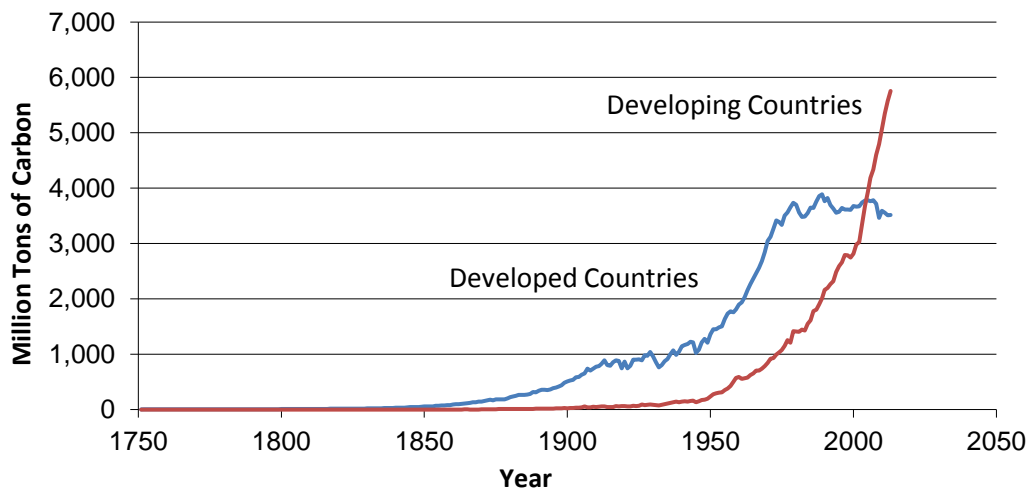


Fig. 1.6: Temporal Rise in Average Global Temperature [13]

1.2 Microgeneration of Electricity:

Lysen noted in his study on photovoltaic systems for rural Bangladesh that the main obstacles to rural electrification in developing nations are the high transmission and distribution losses and costs of grid extensions, disperse rural homesteads coupled with low load demands and governments imposed low tariffs, and nontechnical losses such as illegal connections and theft of power cables and transformers [16]; a typical rural household in a developing nation consumes less than 1 kWh of power per day or about 20-40 kWh per month, much less than that consumed by households in developed nations, leading to high electricity costs, which are usually cross-subsidized by urban consumers. Adner et al noted that the potential for microgeneration systems to disrupt current energy systems, by blurring the traditional boundaries between energy supply and demand, has attracted the attention of both governments and utility companies alike, leading to development of policies geared towards restructuring energy network infrastructures and regulations to meet these new challenges and trends [17-19]. An example is the decision by the Swiss-Swedish energy giant ABB to focus on decentralized generation systems, as opposed to its niche of large-scale centralized generation systems in anticipation of future energy trends [20,21].

Watson researched the roles of domestic electricity generation in bringing the consumer to the core of energy systems operation and development [22]. Chappells et al. reported that the concept of energy co-provision enabled both consumers and energy companies to be actively involved in energy systems [23]. Udwardia and Kumar identified the need for active consumer involvement in co-construction of new products to account for consumer needs and create a sense of shared ownership of the final product [24]. Fliess and Klienaltenkamp noted that extending this approach to service development and delivery puts the consumer at the centre of the focus, encouraging consumer involvement in active co-production or passive consumption [25]. As reported by Van Vliet and Chappells, these concepts are synonymous with energy co-provision, where the household consumer becomes a co-producer and an owner of a microgeneration system [26].

The concept of co-provision allows consumers to choose their levels of involvement in energy production and operation systems, ranging from complete ownership, control and operation, and thus total independence of energy suppliers, to leaving total ownership, operation, and control to a utility company, and instead leasing the system, with an option of co-ownership or full ownership at a later date. Complete ownership is preferred by consumers who are conscious of their energy consumption patterns and the environmental consequences of such, or by consumers in remote rural communities with no grid connections. Shared ownership allows shared operation and control of a microgeneration system between a utility company and a consumer, with the latter benefitting from lower energy bills [27]. Such arrangements are preferred by consumers who know of the socio-economic and environmental benefits of microgeneration systems but who would prefer not to make such investments on their own. The last option is surrendering complete ownership, control, and operation of the microgeneration system to a utility company. In such an arrangement, the consumer leases a microgeneration system from a utility company, allowing him/her to enjoy the socio-economic benefits of such a system without making huge financial investments associated with it [28].

Economic, technical, and social acceptances are the main factors affecting the dissemination of microgeneration technologies around the world. In developed nations for example, the economics of microgeneration is the prevailing factor behind the choices of shared ownership and leasing of microgeneration systems; discrepancies in the tax rules for consumers and energy companies coupled with resistances by utility companies to pay the right prices for electricity imported from domestic producers reduce the appeals of such systems and thus hinder their dissemination. In addition to the economic barriers are technical and regulatory barriers; concerns about technical

standards prompted the development of a new standard, G83, to protect the electricity network and microgeneration systems in the UK in the event of faults [22]. Co-ownership or leasing of the microgeneration systems partially shields consumers from these barriers. In developing nations on the other hand, low load demands coupled with availability of affordable small microgeneration systems tailored to suit those demands make complete ownerships of such systems the most economically sound choices. Moreover, lack of well-developed energy infrastructures and the necessary modern IT and control systems make co-ownership or leasing arrangements very difficult.

As reported by Sauter and others, social acceptance is crucial to successful dissemination of a new technology, and this even more so with microgeneration technologies which impact on individuals' spaces both passively and actively [29-31]. An individual's willingness to participate in the microgeneration process through financial investment, provision of an installation site, or through behavioural change is important for successful uptake of such technologies [32]. Studies have shown that individual households are major contributors to greenhouse gas emissions, especially in developed nations where domestic energy demands are high [33]; microgeneration technologies are being marketed as means to reducing household carbon emissions through zero emissions or through more efficient technologies.

Attitudes towards microgeneration technologies govern their social acceptances; in developed nations consumers are motivated by autonomy, interest in the new technology, environmental concerns, and economic reasons [34]. In developing nations on the other hand, consumers are motivated by availability; people are in need of electricity irrespective of its source, microgeneration technologies just happen to be the most readily available and affordable means of achieving that. In many cases, the environment is an unintended beneficiary. Various studies about opinions and attitudes towards microgeneration systems show overwhelming support for such systems, mainly due to awareness of their socio-economic and environmental benefits [35-37]. However, the majority of those surveyed still did not feel the compulsion to actively participate in their dissemination, leaving that task to the governments, utility companies, and local councils [38,39]. Studies by Dobbyn and Thomas showed that consumers who actively participated in microgeneration technologies by investing in such systems were more conscious of their energy consumption trends, than passive consumers of such technologies, and changed their lifestyles accordingly to meet those standards [40]; the active users were more informed about the operations of their systems and were more attuned to the socio-economic and environmental benefits of such installations than the passive users.

Many rural households in developing nations require electricity basically for lighting and to power small electrical appliances such as mobile phone chargers. These households therefore rarely consume more than 30 kWh per month [41]. In the absence of grid electricity, they use kerosene lanterns or biofuels for lighting. These fuels are health hazards, producing dangerous emissions which affect lungs and eyes, and are also major causes of rural household fires [42]. Some households use batteries to power small electronic appliances, but these require frequent charging at often distant locations where grid electricity is available, making them very costly to operate and maintain. There is therefore a major electricity market vacuum in many rural developing communities, awaiting exploitation. Research shows that for these communities, there is a willingness to pay for electricity microgeneration systems based on locally available renewable energy resources due to the overall socio-economic benefits that such systems offer [43]; additional benefits of microgeneration systems include increased self-sufficiency, perception of enhanced status in the community, increased awareness of the environmental degradation caused by fossil fuels, and higher quality lighting which leads to increased nocturnal social-economic activities [44]. Moreover, microgeneration market infrastructures provide new sources of skilled employment for many rural technicians [45].

The modular nature of microgeneration technologies allows for phased project implementations, enabling households to initiate modest power generation programs, and to modify their systems according to their changing energy needs. The systems are therefore usually used as pre-grid electrification stimulators, sensitizing and readying households for future grid connections, and are thus often abandoned once the latter arrives. This is more so with stand-alone systems which have limited power capacities. However, depending on local resources, capacities, designs and technologies used, communal grids could provide the final solutions to rural electrification in many developing nations and entrench green economies in the process. In fact it is estimated that there will be almost 400TWh of installed communal grid capacity by 2030, about 40% of new installed capacities towards universal electrification in developing nations [2]; communal grids offer many advantages over other options in that when compared to national grids, they are cheaper to put up, with shorter lead times, sized to match local demands, and are modifiable with increasing demands or changing technologies, while when compared to stand-alone systems, they offer access to higher power capacities and more efficient power consumption and management.

A study by Saha on the advantages of communal grids over stand-alone PV systems in a small village in India showed that communal grids offer many benefits over stand-alone systems including better load management, better maintenance and security due to centralized sense of responsibility, and

financial superiority on account of economic viability [46]. Other studies also show that communal grids offer enhanced electrical performance through increased rate of battery charging, high overall efficiency, and low cost of systems due to bulk purchase [47,48]. However, a contrary study by Schmidt-Kuntzer and Schafer in Senegal showed that where the majority of village dwellers only have basic power demands, small and affordable stand-alone systems could be more economical compared to communal grids due to high costs of rural distribution networks associated with the latter [49]. A study by Vallve and Serrasolses showed that there are many cases where stand-alone systems are preferred over communal grids due to the independence they provide to consumers [50]. It is clear from literature that the main factors that influence the choice between stand-alone systems and communal grids are cost of delivered electricity on a life cycle basis, reliability, after sale services, government policies or fiscal incentives, availability of credit facilities, and perceived independence in operations and management. The table below compares the merits and demerits of stand-alone systems versus communal grids.

Stand-Alone	Communal Grid
Offers autonomy and independence over one's own power source and consumption management	Communally owned or by a third party, thus taking away operations management from single individuals
Owner singly responsible for all life cycle maintenance and operations costs	Operations and maintenance costs communally shared through an upfront fee and monthly charges
Sized to supply limited power capacity for single users with 2 to 3 days autonomy in case of low solar radiation	Sized to serve a community and thus offer high power capacity and also with 2/3 days autonomy
Owner singly responsible for PV module security and thus susceptible to theft	PV system communally owned and guarded thus improved sense of security
High costs for operations and maintenance services due to dispersed and remote locations	Centralized systems leads to reduced operations and maintenance services costs
Individual consumer power management often lead to deep discharge of batteries	Centralized power management ensures better monitoring of energy consumption

Table 1.2: A Comparison of Stand-Alone PV Systems and PV-Based Communal Grids [46-50]

1.3 Solar Electricity Microgeneration:

Solar is the cleanest and most abundant source of renewable energy, with an irradiance equivalent to about 223,613 PWh reaching the earth's surface each year, enough to generate electricity for all humans, many times over. In the past, PV power systems were mainly applied as stand-alone power sources for remote crucial installations such as communication towers. However, with

advancements in research and development, coupled with market growth, PV systems have seen massive improvements in both efficiencies and power outputs, leading to falling costs of delivered electricity. This has led to rapid rises in installed PV power systems as alternatives to conventional fossil-fuel-based systems. Figures 1.7 and 1.8 show plots of world's total installed PV capacity and their corresponding PV-generated electricity respectively; installed PV capacity surpassed 140 GW in 2013 and is expected to surpass 302 GW by 2017 due to increase in global demand and growing public awareness of the socio-economic and environmental benefits of solar technologies [51]. In 2012 for example, 31.1 GW of PV was installed around the world, with installations in Europe alone accounting for 55% of that capacity [51]. This was a sharp decline from the year before when Europe accounted for 74% of the global PV market, a clear indication of the globalization trend of the PV market.

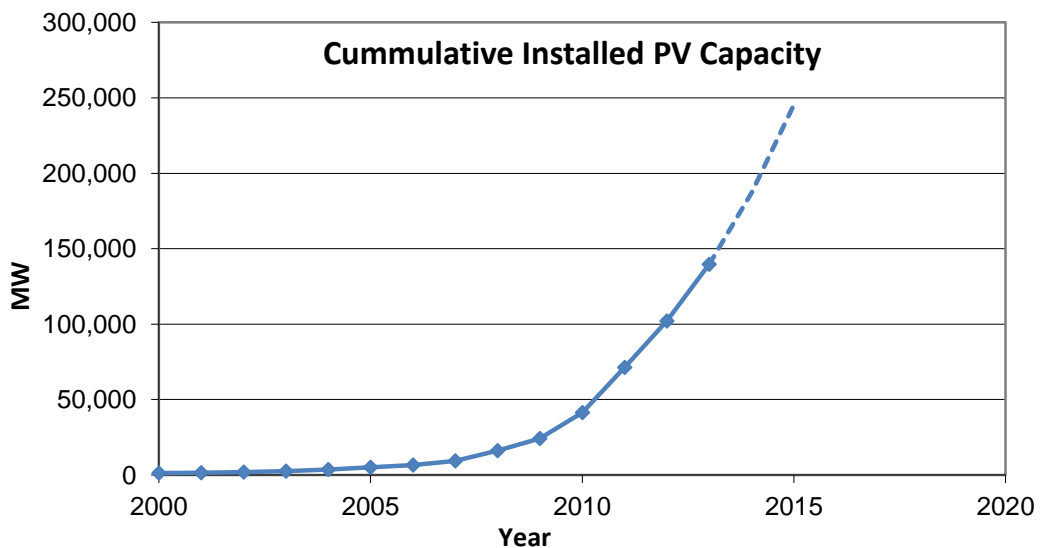


Fig. 1.7: Global Cumulative Installed PV Capacity, 2000-2013 [13]

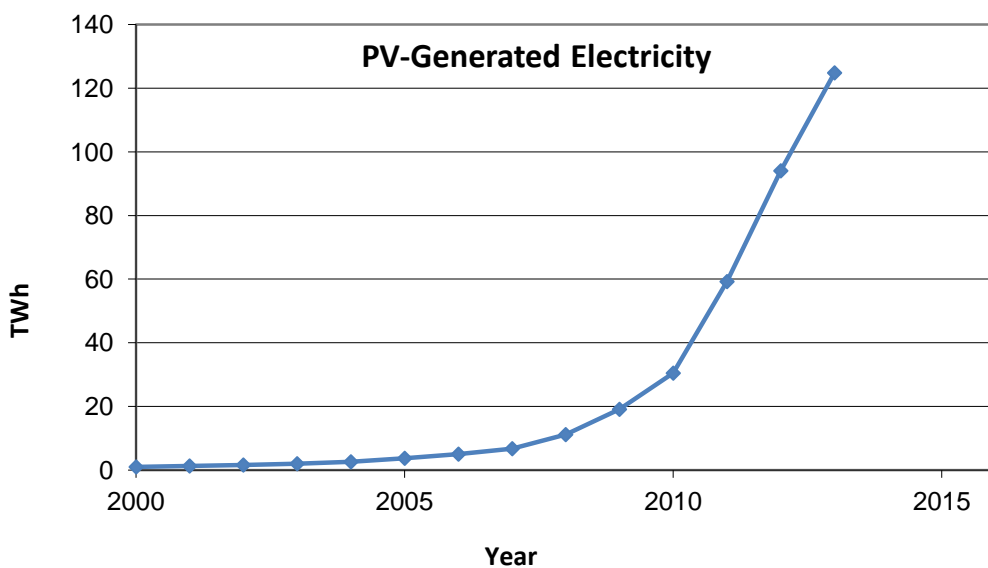


Fig. 1.8: Global PV-Generated Electricity 2000-2013 [13]

Figure 1.9 shows cumulative installed PV capacity in leading countries. Germany still remains the world leader with over 35 TW of installed PV capacity in 2013. This is followed by China which has seen a sharp rise in PV installations, surpassing Italy, Japan, and USA which have been in the market longer. In terms of PV-generated electricity as shown in figure 1.10, Germany still remains the world leader, with about 30 GWh of electricity generated in 2013, followed by Italy, Spain, China, Japan, USA, and India, in order of reducing output [13].

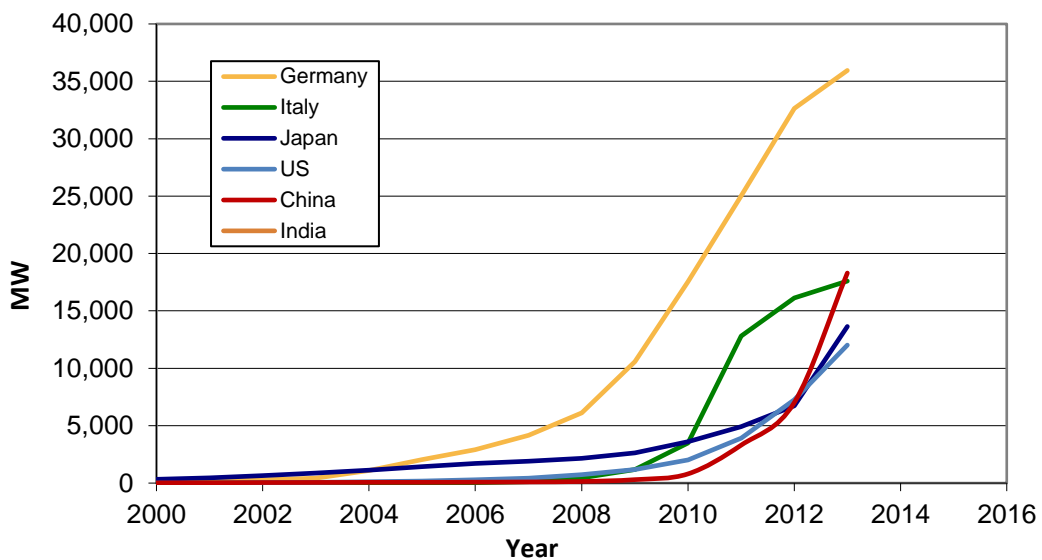


Fig. 1.9: Cumulative Installed PV Capacity in Leading Countries 2000-2013 [13]

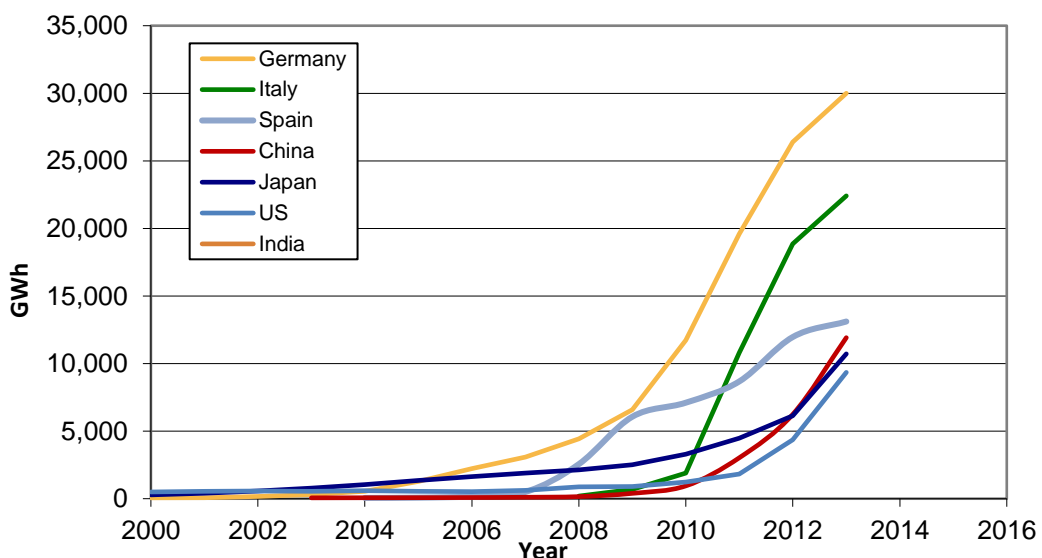


Fig. 1.10: Cumulative PV-Generated Electricity in Leading Countries 2000-2013 [13]

Decades of research and development have also enabled efficient, rapid, and mass production of high quality PV systems (figures 1.11 and 1.12), which have in turn also translated into continuously

falling prices of PV systems [13]. This downward trend is predicted to continue even under major obstacles like unstable governments' policies, global market rebalancing, industry consolidation, and continuing economic crises, leading to sustained growth of installed PV systems; it is estimated that global PV market will reach 2 TWh in 2030 and up to 6,700 TWh, or 20% of global energy consumption, in 2050, based on current global economic and population growth rates [52].

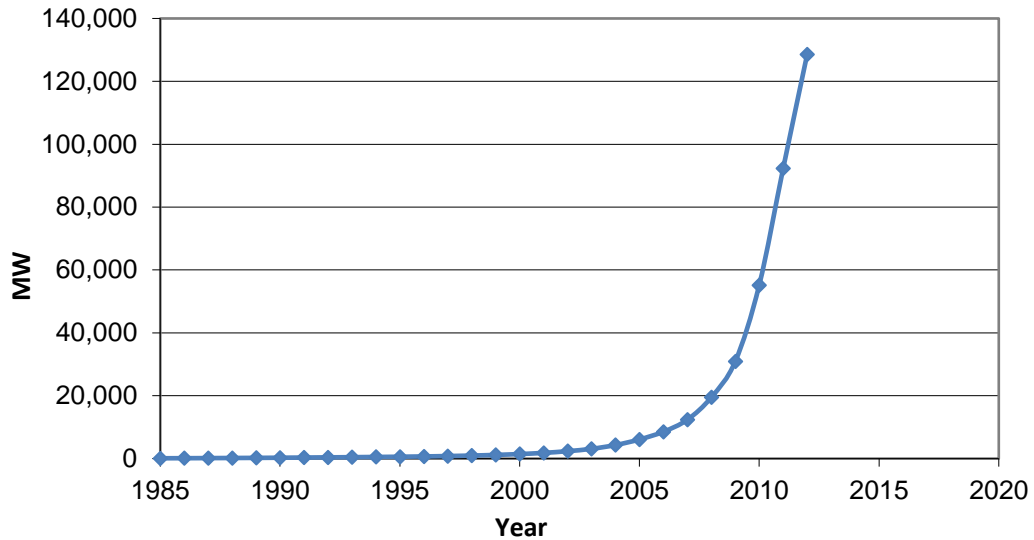


Fig. 1.11: Global Cumulative PV Production 1985-2012 [13]

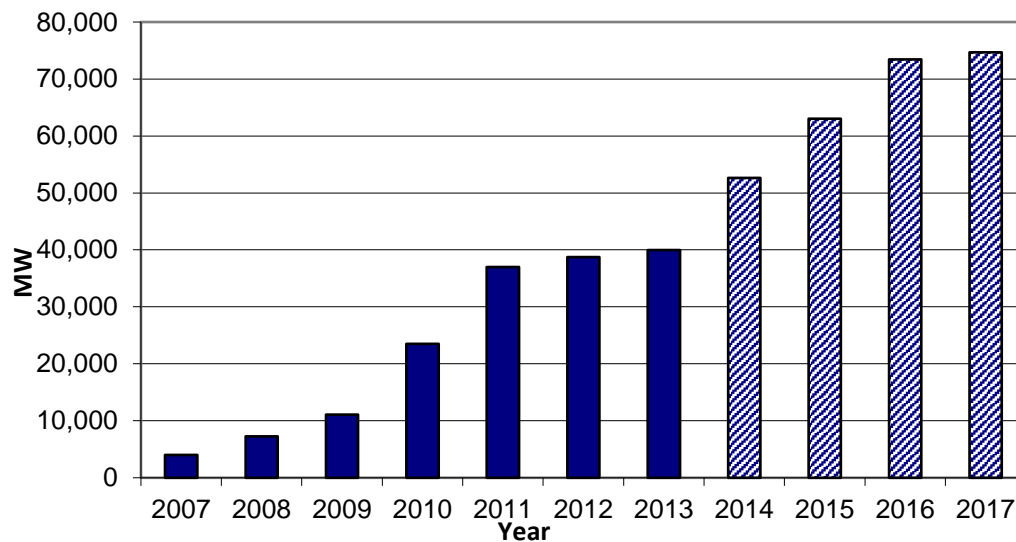


Fig. 1.12: Global Annual PV Production 2007-2013, with Projection to 2017 [13]

Figure 1.13 shows growth in annual PV cells production in leading countries between 2007 and 2013 [13]. There has been a huge growth in PV cells production from about 4 GW in 2007 to nearly 40 GW in 2013. Asian countries have become the largest producers of PV cells with China leading the way followed by Taiwan, Japan, and Malaysia, in that order. Germany is the largest producer of PV cells in Europe.

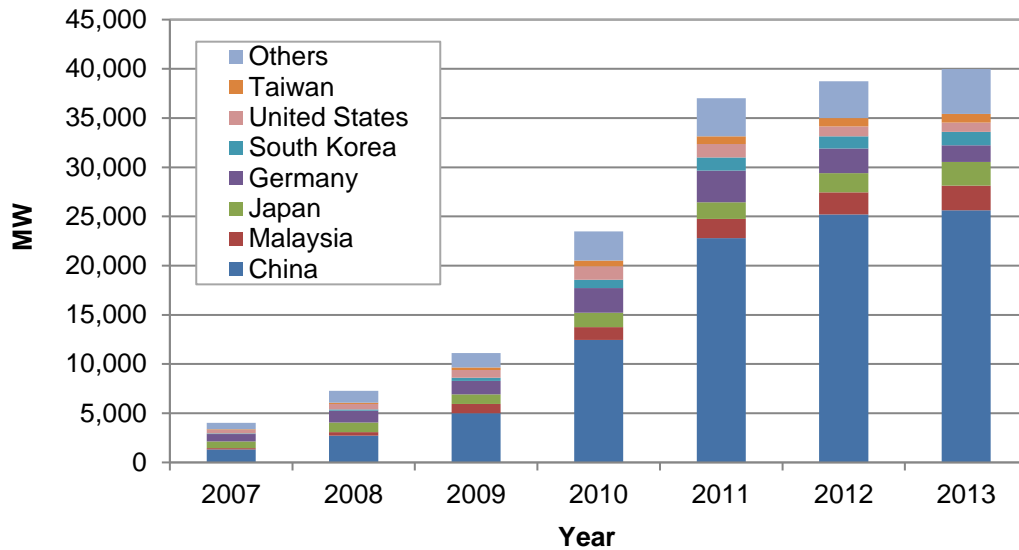


Fig. 1.13: Annual PV Production in Leading Countries 2007-2013 [13]

Even though developing nations remain the least producers of PV systems, their locations along the equatorial belt make them potentially vibrant markets for PV systems; while nations with well-developed electricity infrastructures struggle to sell PV systems to their populations, developing nations with low electrification rates have unique opportunities to build their infrastructures based on green microgeneration systems based on locally available renewable energy resources, and in this case, solar.

1.4 Communal Grids:

A communal grid is defined as a locally confined and independently controlled electric power grid in which a distribution architecture integrates loads and distributed energy resources—i.e. local distributed generators (microgenerators) and energy storage devices—which allows the communal grid to operate in both utility grid-connected and islanded modes. Communal grids can be utility-grid connected to improve system economics, to improve operations, and to improve stability. On the other hand, the utility grid gets to enjoy improved availability, improved stability, and reduced conductor sizes. For a successful interfacing of communal grids to utility grids, power electronics should allow net metering (bi-directional flow of power), peak shaving, advanced communications and control, and fast demand response.

Communal grids can be divided into two groups: minigrids with capacities between 10 kW and 10 MW and microgrids with capacities below 10 kW. Each communal grid comprises of the following two operational systems: small power production and small power distribution. The small power

production comprises of generation and storage subsystems while small power distribution comprises of distribution and consumption subsystems. The generation subsystem includes the power generator, power conditioners, and power management technologies while the distribution subsystems include grid networks for transporting power to individual consumers. Based on design, capacity, and technology, these systems could be AC, DC, earth return, single-phased, or three-phased. The consumption subsystems comprise all the equipment at the end consumer side, i.e. metering, wiring, grounding, and electrical appliances.

The two main operational systems of a communal grid could each be fulfilled by a different operator, or they both could be fulfilled by one operator [53]. There are four communal grid operator models, based on operational systems ownerships, namely utility model, private sector model, community model, and hybrid model [53]. Geographical factors, socio-economic and cultural factors, and regulatory environment are the main factors which determine the best operational model for a given location. In the utility model, the communal grid is owned by a utility company, which in turn, in many developing countries, is usually owned by the central government. Funding for such grids therefore comes from the national treasury. In these arrangements, the utility company runs the communal grid in much the same way as it runs the national grid, and with similar tariffs. Since communal grids are usually non-profitable to utility companies as they are forced to heavily cross-subsidize tariffs, they often reluctantly invest in such ventures, only doing so under direction from central governments.

In private sector models, the communal grid is fully owned by a private entity, from planning stages to operational and management stages. Private equity and commercial loans, together with government grants and subsidies are often used to fund such ventures, with few being fully privately funded. Since private equities and commercial banks are often reluctant to loan for such venture, especially due to lack of working business models and greater risks of defaults involved, a positive policy environment together with public sector loan guarantees are required to encourage private investments into communal grids. A regulatory framework that protects investors and guarantees fair compensation once the communal grid is connected to an expanding national grid, and smooth and safe integration of the two, should be in place before technical and financial designs of a communal grid are made [53].

The private sector model can be implemented using any of the following four approaches: a) franchise approach, b) ABC (Anchor-Business-Community) approach, c) clustering approach, or d) local entrepreneur approach [53]. In the franchise approach, many franchisees are collectively

managed at the franchiser level, minimising the burden to each franchisee. The large number of franchisees bundled together ensures that management cost of the franchising structure does not outweigh income. In the ABC approach, communal grids are established around anchor (A) customers such as factories or large institutions, with extensions to local businesses (B) and domestic customers (C) done to boost revenue. In the clustering approach, a cluster of independent communal grids powering nearby village settlements are operated and managed under one structure to save cost. In the local entrepreneur approach, a permanently based local entrepreneur co-owns, operates, and manages the communal grid and typically acts as an independent power producer selling excess electricity to nearby customers.

In community-based models, the communal grid is owned, operated, and managed by the local community for the benefit of its members. Funding is usually procured through community contributions, commercial loans, and/or grants from NGOs and national governments. Management of the grid could be delegated to a third experienced party, or the locals could be trained to operate and manage the grid themselves. An appropriate tariff must be charged to cover operation and maintenance costs, reinvestment/depreciation, and to pay off any loan in a timely and reliable manner. A cooperative approach may be used to set up a social and decision-making structure to avoid conflicts.

Hybrid models combine different aspect of the three models above. For example, production and distribution systems could be carried out independently by utilities, private operators, or communities or the tasks could be split, and predefined before commissioning, according to who builds, owns, operates, and maintains the system. The two main contractual arrangements that are applied to hybrid models are public-private partnership (PPP) and power purchase agreement (PPA) [53]. In the PPP arrangement, a public partner can finance, own, and manage a communal grid while contracting a private partner to operate and maintain it. In the PPA arrangement, a contract is signed to deliver a pre-agreed quantity of power to a given consumer base. In this case, no single entity owns the production or distribution systems.

1.5 Concluding Remarks:

Centralized electricity generation systems are costly to construct, with long lead times, and are frequently based on fossil fuels and are thus vulnerable to volatile energy prices brought about by global insecurities. Most importantly, fossil fuel spillages and emissions are largely responsible for global warming and related environmental degradation. On the other hand, decentralized electricity

generation systems have short lead times, are reasonably cheap to construct, and are usually based on locally available renewable energy resources making them environmentally friendly. Also, modular nature of renewable energy resources allows for phased projects implementations, allowing even the poorest of nations to initiate modest electricity generation programmes while at the same time allocating resources to pressing development projects. Moreover, they are shielded from energy insecurities of fossil fuels and have thus seen stable downward trends in their costs of installation and generation. For fully electrified developed nations with reliable and stable grid systems, it is difficult to switch to other systems. In developing nations with low electrification rates on the other hand, decentralized systems may be the only cost-effective way to supply electricity to isolated rural communities. Decentralized systems therefore present these nations with unique opportunities to chart green economic futures by developing smarter and greener electricity communal grid systems for their unelectrified rural magnitudes, while stimulating local microeconomic activities at the same time. Today, microgeneration systems based on wind, hydro, solar, geothermal, biomass, or hybridized combinations of the above, implemented either as stand-alone systems or in communal-grid configurations, are widely deployed around the world to provide electricity to remote villages, institutions, and other installations.

1.6 Research Aims and Objectives:

The aim of this research is to investigate potential application of communal grids based on locally available renewable energy resources, in this case solar, in cost-effectively providing electricity-beyond-lighting to rural developing communities. Due to their sparse populations, low power demands, and generally industrial activities, extensions of the national grids to these regions remain unattainable; the research investigates how microgeneration systems could be used as stepping stones to total electrification by stimulating electricity demand and local microeconomic activities. In summary, the research aims to answer the following questions:

- 1) Given various options, how would a typical rural household in a developing community make its electrification choices, and what are the main factors that would influence such a decision?
- 2) Can electricity microgeneration systems based on locally available renewable energy resources be used to cost-effectively provide electricity-beyond-lighting to rural developing communities?
- 3) With a focus of solar electricity microgeneration, how do socio-economic and technical factors such as neighbourhood influence, costs, control, and storage impact on temporal diffusion of such microgeneration systems in a typical rural developing community?

- 4) How do government policies impact on temporal diffusion of electricity microgeneration systems in a typical rural developing community?
- 5) How can all the above factors be simultaneously modelled and simulated, to provide stakeholders and policy makers with a tool for rural electrification planning and development?

The objective of this research, therefore, is to develop a model that could be used by stakeholders in formulating rural electrification policies in developing communities given factors such as local socio-economic demographics, annual climatic conditions, and available resources; the model could be used in prioritizing, planning, and implementing rural electrification projects. To achieve this objective, the following tasks are set and met:

- 1) Model and simulate structures of solar electricity microgeneration systems using Matlab/Simulink with an objective of underscoring important technical aspects of such systems
- 2) Model PV microgeneration potential for Kendu Bay area of Kenya, using a stochastic clear-sky model and active-occupancy model
- 3) Develop and carry out a survey on PV microgeneration systems in Kendu Bay area of Kenya to gather data for the next stage of research
- 4) Model and simulate how different socio-economic factors and decisions by human actors, affect temporal diffusion of PV microgeneration systems in Kendu Bay area, using a survey-informed agent-based-model developed in Netlogo.
- 5) Model and simulate how network architectures affect temporal diffusion of PV-based communal grids in Kendu Bay area
- 6) Make a conclusion of my research

1.7 Thesis Layout:

Chapter 1 deals with literature review; in this chapter, the importance of rural electrification in socio-economic development is discussed. Importance of electricity microgeneration are also highlighted. Solar electricity microgeneration is introduced and reviewed. Communal grids and their structures are also discussed.

In **chapter 2** technical aspects of solar electricity microgeneration systems are modelled and simulated. Specifically this chapter looks at PV power generators, power electronics used with PV power generators, and energy storage systems.

In **chapter 3** a clear-sky model is used to generate high resolution synthetic irradiance data for Kendu Bay area of Kenya, based on empirical data. The data is used to model PV microgeneration potential for the area. This is necessary before a survey is carried out in the area.

In **chapter 4**, having ascertained PV microgeneration potential for Kendu Bay, a survey on PV microgeneration systems in the area is developed and carried out to gather the necessary data for the next stages of the research

In **chapter 5** an agent-based model is developed to model impacts of socio-economic factors on temporal diffusion of solar electricity microgeneration systems in a Kendu Bay area of Kenya

In **chapter 6** impacts of control methods and architectures on temporal diffusion of PV-based communal grids in Kendu Bay area are modelled and simulated.

In **chapter 7** a summary of the research is stated with a discussion of potential future work.

Chapter 2: Modelling Solar Electricity Microgeneration Systems

2.1 Introduction:

In this chapter, having introduced and reviewed the importance of solar electricity microgeneration in chapter 1, a comprehensive review of different components of solar electricity microgeneration systems is carried out in an effort to convey the importance of each component. This is necessary before modelling PV microgeneration potential for Kendu Bay area, which is undertaken in chapter 3. The models developed in this section are applied in chapters 5 and 6 for PV and energy storage modelling and sizing.

A PV microgeneration system consists of PV power generators supplying DC or AC power to a system of loads through a system of power electronics as schematically shown in figure 2.1. The system could either be in an islanded configuration or in a grid-connected configuration. In most cases, since the PV power source (solar radiation) fluctuates with time and environmental conditions, back-up storage systems are used with the PV systems to ensure uninterrupted supply of power at all times. The power electronics comprise of DC-DC converters needed for power conditioning and maximum power point tracking (MPPT), DC-AC inverters in cases of AC loads or utility-grid interfacing, filters to remove harmonic distortions from the inverters, and charge controllers for the energy storage systems. The latter are usually implemented using bi-directional DC-DC buck-boost converters.

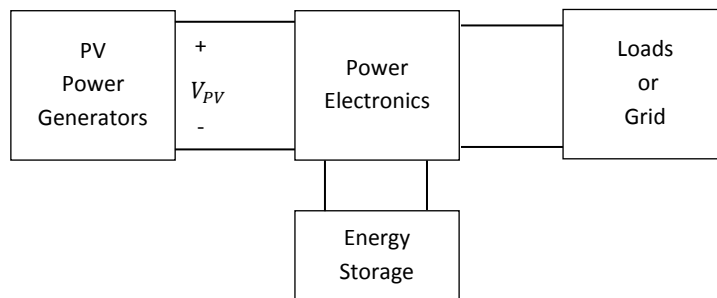


Fig. 2.1: Schematic Diagram of a PV power generation System

2.2 PV Power Generators:

The basic unit of a PV power generation system is a PV cell which is a direct current generator in parallel with a diode, with the current produced being directly proportional to illumination hitting the cell; under darkness a PV cell functions as a p-n junction diode. The most widely accepted and used equivalent circuit of a PV cell is the single diode model shown in shown in figure 2.2 below. The model contains a current source with photo current I_{ph} , diode D , shunt resistance R_p , and series

resistance R_s . R_p models surface leakage along edges of the cell or crystal defects along the junction depletion region while R_s models the resistance of the diffused layer that is in series with the junction as the resistance of the ohmic contacts [54].

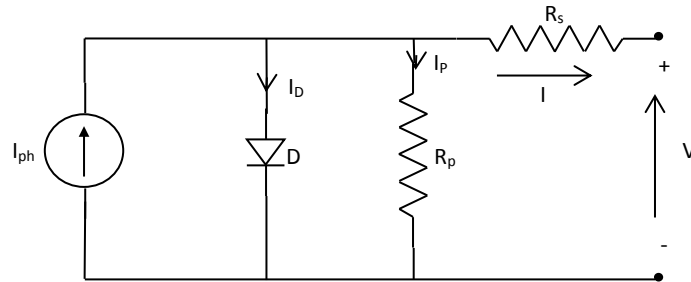


Fig. 2.2: Equivalent Circuit Diagram of a PV Cell [54]

The current through the diode, I_D and the current through the shunt resistance I_p are given by [55]

$$I_D = I_s \left[\exp\left(\frac{q(V + IR_s)}{nkT}\right) - 1 \right] \quad (2.1)$$

$$I_p = \frac{V + IR_s}{R_p} \quad (2.2)$$

where I_s is the cell saturation reverse current, q is the electronic charge, n is the p-n junction ideality factor, k is Boltzmann's constant, and T is the cell junction temperature in kelvin.

The current supplied to the load I , is given by

$$I = I_{ph} - I_s \left[\exp\left(\frac{q(V + IR_s)}{nkT}\right) - 1 \right] - \frac{V + IR_s}{R_p} \quad (2.3)$$

Usually R_p is very large and R_s is very small and therefore the above equation can be simplified to [56]

$$I = I_{ph} - I_s \left[\exp\left(\frac{qV}{nkT}\right) - 1 \right] \quad (2.4)$$

The output power P is expressed as

$$P = VI = \left[I_{ph} - I_D - \frac{V_D}{R_p} \right] V \quad (2.5)$$

Figure 2.3 below shows typical current-voltage and power-voltage characteristics of a PV cell generated using Matlab/Simulink; the four parameters that define the curves are:

- a) Short-circuit current (I_{SC}) which is defined as the current when the voltage across the terminals is zero ($V = 0$) and is given by

$$I_{sc} = I = \frac{I_{ph}}{\left[1 + \frac{R_s}{R_p}\right]} = I_{ph} \quad (2.6)$$

- b) Open-circuit voltage (V_{OC}) which is defined as the voltage across the terminals when the current is zero ($I = 0$) and is given by

$$V_{oc} = \left[\frac{nkT}{q}\right] \ln \left[\frac{I_{ph}}{I_s} + 1\right] \approx \left[\frac{nkT}{q}\right] \ln \left[\frac{I_{ph}}{I_s}\right] \quad (2.7)$$

- c) Maximum power point (MPP or P_{max}) which is defined as the point where the PV cell generates maximum power when supplying a load and is given by

$$P_{max} = I_{max}V_{max} \quad (2.8)$$

Where I_{max} is the maximum generated current and V_{max} is the maximum generated voltage.

- d) Fill factor (FF) which defines the rectangularity of the I-V curve and is given by

$$FF = \frac{I_{max}V_{max}}{I_{sc}V_{oc}} = \frac{P_{max}}{I_{sc}V_{oc}} \quad (2.9)$$

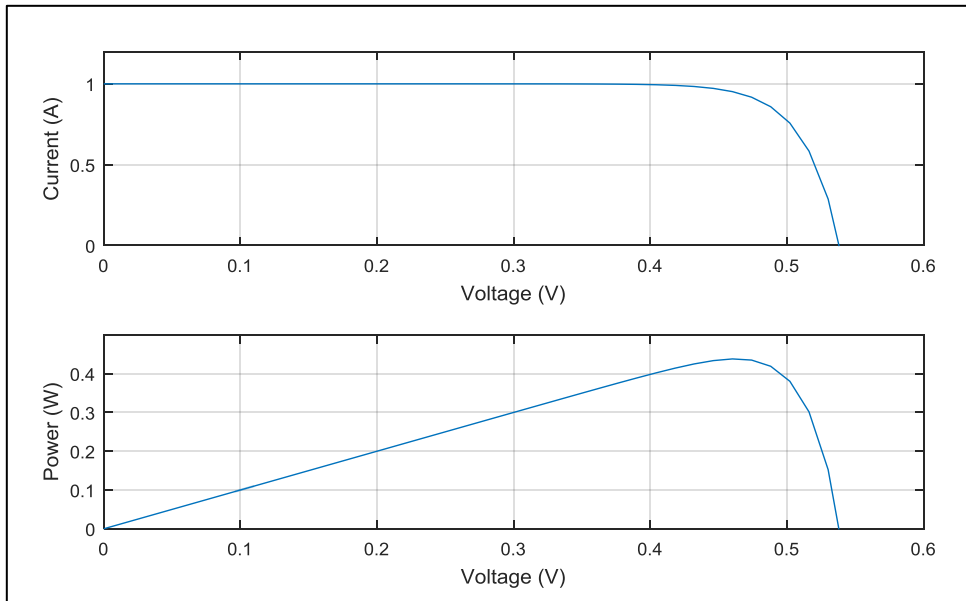


Fig. 2.3: Current-Voltage and Power Voltage Characteristics of a PV Cell

Effects of parameters such as temperature, irradiance, and cell series and shunt resistance on the performances of PV cells have been widely studied and are summarised below [57-61]:

- a) Temperature:
 - Strongly affects saturation current I_S but only slightly affects photocurrent I_{ph} ;
 - V_{OC} has a negative temperature coefficient of about $-2.3mV/^\circ C$ for silicon-based cells.
- b) Solar irradiance: I_{ph} is directly proportional to incoming radiation hitting the cell.
- c) Series resistance: Larger R_s reduces I_{SC} and FF without affecting V_{OC}
- d) Shunt resistance: Smaller R_p reduces V_{OC} and FF without affecting I_{SC}

2.2.1 PV Modules and Arrays:

Output voltage from a single PV cell is too small for any meaningful application. Many cells are therefore connected in series and mounted on a support frame to form a module. Many modules can be connected in series and/or parallel to form an array as shown in figure 2.4. Bypass and/or blocking diodes are used in arrays to reduce loss of power due partial shading or cell/module mismatches.

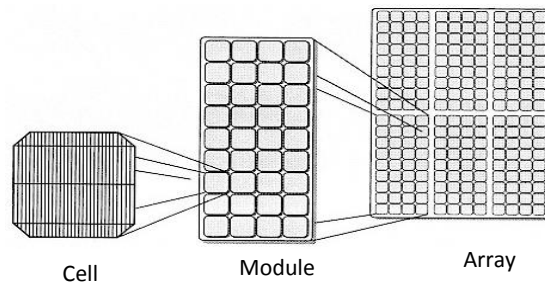


Fig. 2.4: PV Generator Hierarchy

If N_s identical PV cells are connected in series and N_p are connected in parallel to form an array, the current output of the array can be expressed as [57,60]

$$I = N_p \left\{ I_{ph} - I_S \left[\exp \left(\frac{q \left(\frac{V}{N_s} + \frac{I}{N_p} R_s \right)}{nkT} \right) - 1 \right] - \frac{V}{N_s} + \frac{I}{N_p} R_s \right\} \quad (2.10)$$

Since R_p is very large and R_s is very small, the above equation can be simplified further to

$$I = N_p \left\{ I_{ph} - I_S \left[\exp \left(\frac{qV}{N_s nkT} \right) - 1 \right] \right\} \quad (2.11)$$

From the above equation of a single diode, and provided all cells have the same parameters, terminal voltage of a PV array can be expressed as,

$$V = \frac{N_s n k T}{q} \ln \left(\frac{I_{ph} - \frac{I}{N_p}}{I_s} + 1 \right) \quad (2.12)$$

Using data supplied by BP for BP Solar SX3190 190W PV module shown in table 2.1 [62], the model shown below (figure 2.5) was constructed in MATLAB/Simulink. The following parameters are used in the simulations: $n = 1$, $q = 1.602 \times 10^{-19}$, $k = 1.38 \times 10^{-23}$, $T = [0 \ 25 \ 50 \ 75]$, $I_{ph} = [8.38, 8.52, 8.67, 8.09, 8.94]$, $I_s = [1.15 \times 10^{-9}, 4.38 \times 10^{-8}, 9.52 \times 10^{-7}, 1.34 \times 10^{-5}, 0.]$, $R_p = [479.17, 189.67, 120.7, 107.82, 276.73]$, $R_s = [0.249, 0.248, 0.257, 0.278, 0.316]$. The model inputs are ambient solar radiation (S), ambient temperature (T_a), and module operating voltage (V_m). The outputs are current (I_m) and maximum power (P_{max}).

PV Module : BP Solar SX3190	
Number of cells in series	50
Number of cells in parallel	1
Open-circuit voltage V_{oc} (V)	30.6
Short-circuit current I_{sc} (A)	8.5
Voltage at maximum power point V_{max} (V)	24.3
Current at maximum power point I_{max} (A)	7.83
Typical maximum power P_{max} (W)	190.26W

Table 2.1: Properties of BP Solar SX3190 [62]

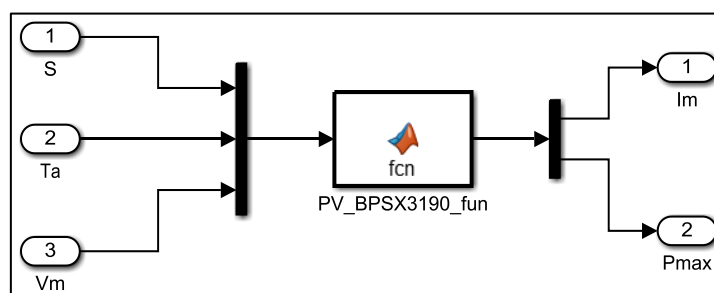


Fig. 2.5: BP Solar SX3190 PV-Module Simulink Model

The current-voltage (I-V) and power-voltage (P-V) characteristics of the PV module at a constant temperature of 25°C and varying solar irradiance are shown in figure 2.6, while the effects of varying temperature on the PV module output at a constant insolation of 1000 W/m² are shown in figure

2.7. If five PV modules with the above characteristics are connected in series to form a string, the voltage at maximum power point (V_{max} (V)) would be $5 \times 24.3 = 121.5$ V while the current at maximum power point (I_{max} (A)) would be 7.83 A. The typical maximum power (P_{max} (W)) output would therefore be 951.28 W. If five such strings are connected in parallel to form a communal grid, V_{max} (V) would 121.5 V, I_{max} (A) would be $5 \times 7.8294 = 39.15$ A, and P_{max} (W) would be 4.76 kW. If ten strings are connected in parallel, V_{max} (V) would 121.5 V, I_{max} (A) would be 78.29 A, and P_{max} (W) would be 9.51 kW. The output of a communal grid is therefore determined by the number of modules in a string and the number of strings connected in series and/or parallel.

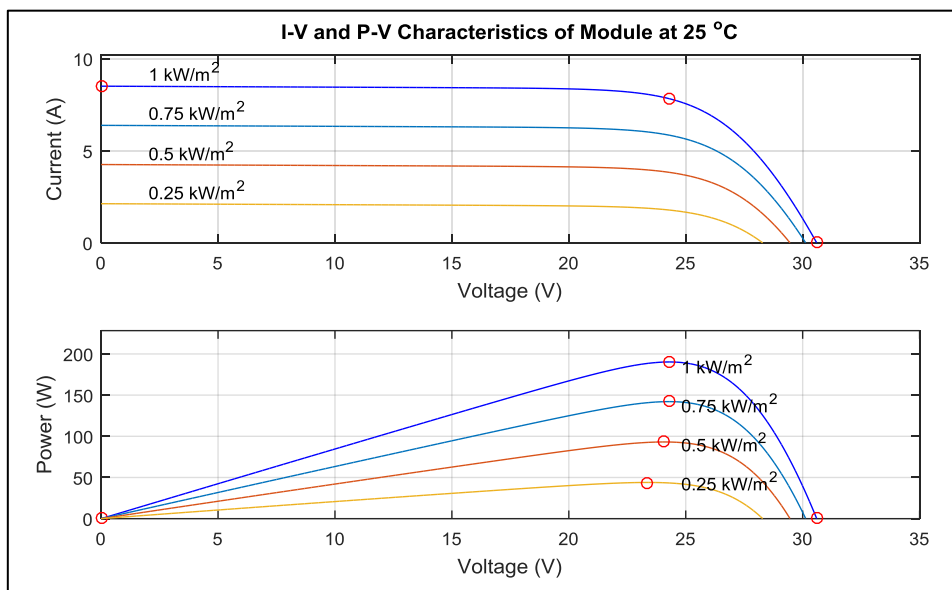


Fig. 2.6: Effects of Varying Insolation on PV Module Characteristics

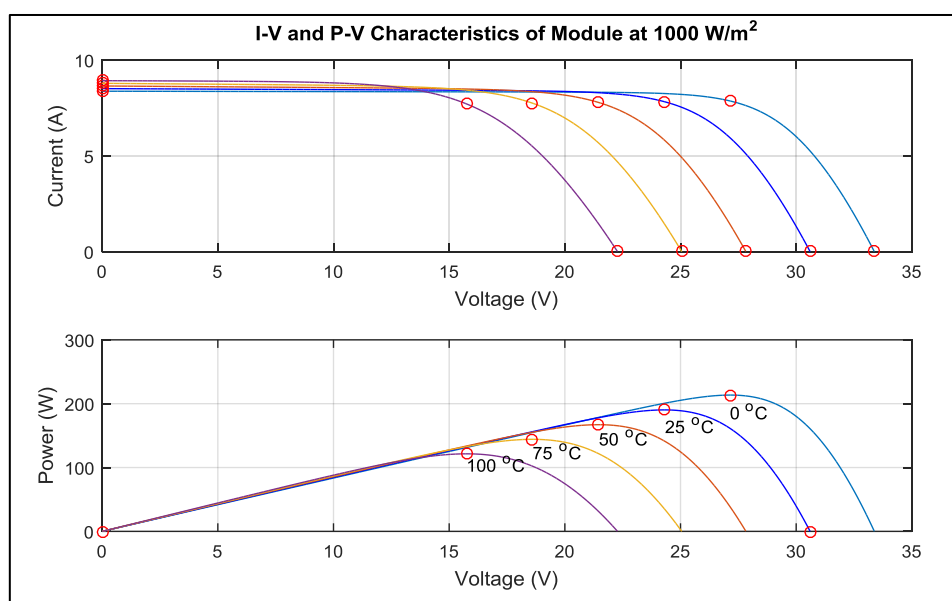


Fig. 2.7: Effects of Varying Temperature on PV Module Characteristics

2.2.2 Partial Shading:

Partial shading due to cell or module mismatches and environmental conditions such as passing clouds or shades from trees or nearby buildings not only leads to hot spots which could damage modules or entire arrays, but are also some of the main causes of reduced performances by PV systems. If one PV cell/module amongst others connected in series has a lower I_{ph} due to shading, damage, etc., it operates as a load for the other cells and is thus reverse biased. This cell will therefore spend energy instead of producing it, leading to a rise in cell temperature. Unchecked increases in temperature could lead to damage of the cell/module, or even the entire array. Bypass diodes connected in parallel with PV modules are used to correct this problem [63]. If modules with different V_{OC} are connected in parallel, the module with the lower V_{OC} will operate as a load, again leading to increases in temperature which could damage the module or the entire array. This problem is solved by connecting blocking diodes in series with modules [63].

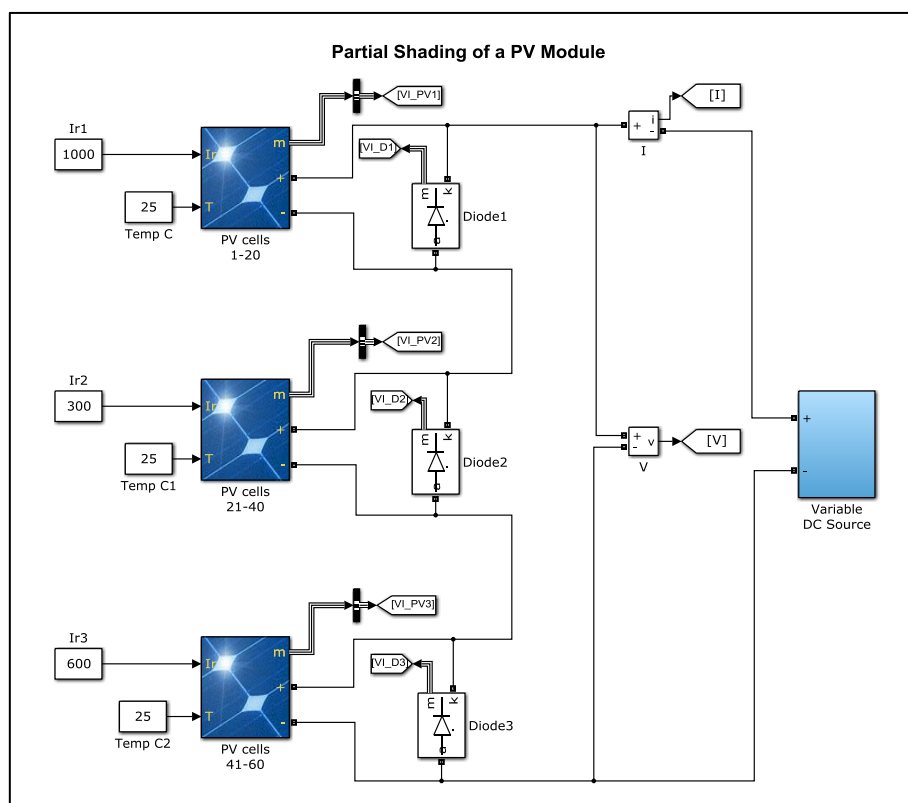


Fig. 2.8: Simulink Model for Partial Shading of a BP SX3190 PV Module

Figure 2.8 above shows a Matlab/Simulink model used to simulate partial shading of a 60 cell BP Solar SX3190 module. The module comprises of three strings of PV modules connected in parallel with bypass diodes that allow current flow in case of partial shading. Each string contains 20 cells connected in series. String 1 (cells 1-20) is under full illumination of 1000 W/m², string 2 (cells 21-40)

is under 300 W/m^2 illumination, while string 3 (cells 41-60) is under 600 W/m^2 illumination. The temperature for the entire module is kept constant at $25 \text{ }^\circ\text{C}$. The module is connected to a variable voltage source for measuring its I-V and P-V characteristics.

Figure 2.9 shows plots of global I-V and P-V characteristics of the module. The plots exhibit three maxima corresponding to different illumination points (shading). The global maximum power point, indicated by the red circle, is 34% lower than the maximum power.

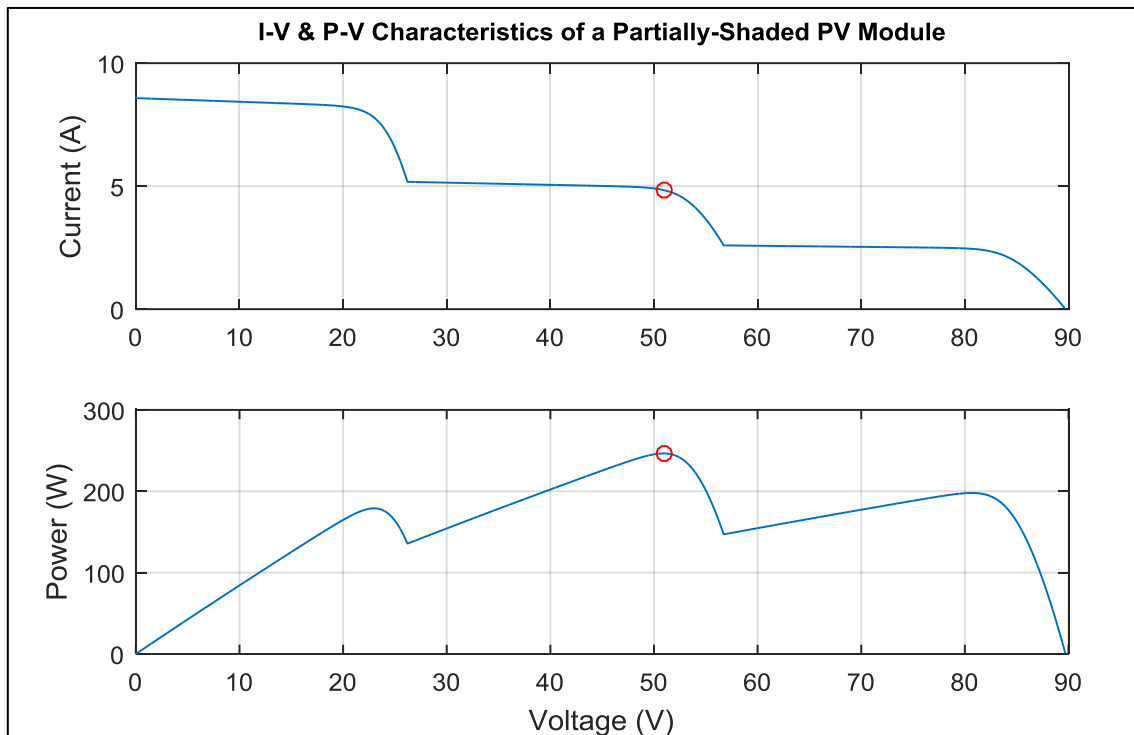


Fig. 2.9: Current-Voltage and Power-Voltage Characteristics of a Partially-Shaded PV Module

2.2.3 Maximum Power Point Tracking (MPPT):

PV generators exhibit maximum power points (MPP) which vary with changing weather and environmental conditions. To extract maximum power from a PV system therefore, it is necessary to track the MPP. This is done using a DC-DC converter with MPPT controller. Tracking speed, stability, and cost are some of the aspects taken into consideration when designing a good MPP tracker. Tracking efficiency is given by [64]

$$\eta_{MPPT} = \frac{\int_0^t P_{actual}(t)dt}{\int_0^t P_{max}(t)dt} \quad (2.13)$$

where P_{actual} is the actual power produced by a PV system while P_{max} is the theoretical maximum power that the PV system is rated to produce.

The most common methods used for MPPT include perturb and observe (P&O), incremental conductance (IncCond), open-circuit and constant voltage, intrinsic ripple (InRip), and short-circuit current. Of these, P&O is the most widely applied method in PV systems. The method employs the hill climbing algorithm shown below in figure 2.10 [65,66]. It works by creating a perturbation in terminal DC voltage of the PV array and observing its effects on output power of the array. If power increases with perturbation then it continues to make perturbations in the same direction, otherwise the direction is reversed. P&Os have slow tracking speeds and oscillations around MPPs [65]. Use of variable step-sizes has been applied to try to minimise this problem [66].

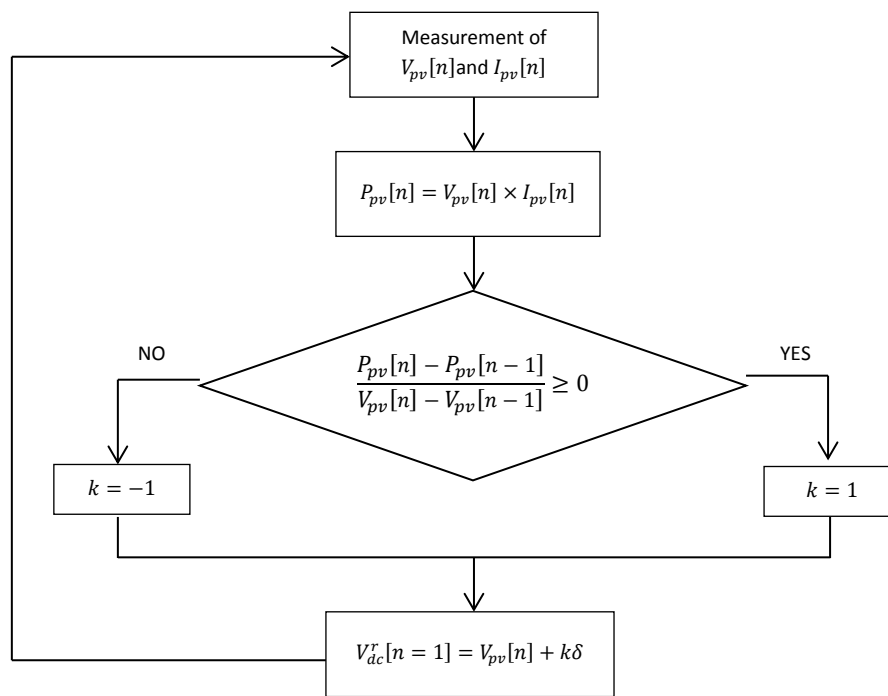


Fig. 2.10: Perturb and Observe Algorithm

From the figure, δ is a voltage increase step and a design parameter dependent on tracking speed accuracy of the algorithm. It is given by [65,66]

$$\delta = \frac{V_{MPP}}{(freq)(step)} \quad (2.14)$$

where V_{MPP} is the voltage at maximum power point, $freq$ is the frequency of the MPPT algorithm in Hz, and $step$ is a design parameter.

The Simulink model shown in figure 2.11 below is used to implement the P&O method. The MPPT algorithm adjusts DC-DC control variable so that the PV array operates at the maximum power point. The array consists of 6 x 85 W PV modules connected in series, ideally producing 510 W. It is assumed, in the example below, that the Boost output voltage $V_{out} = V_{DC}$ is constant. I_{ref} is used as the control variable for the Boost converter. PV array current ideally tracks the Boost input current reference: $I_{PV} = I_{ref}$. The converter boosts DC voltage from 103.4 V to 200 V. The converter uses the MPPT system to automatically vary the duty cycle in order to generate the required voltage to extract maximum power. The MPPT function is implemented by means of a MATLAB function block that generates embeddable C code.

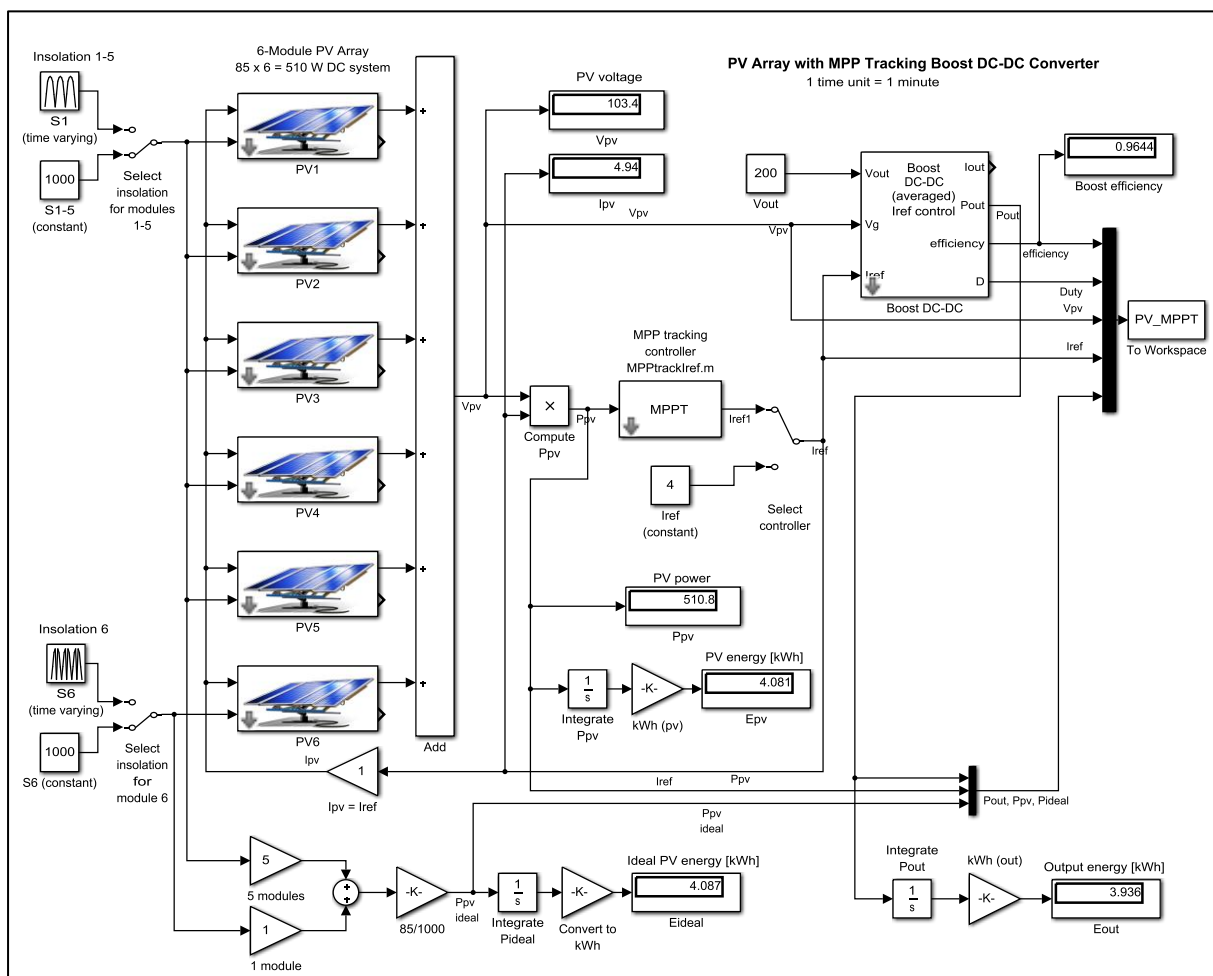


Fig. 2.11: Simulink Model for a PV Array with DC-DC Boost Converter with MPPT

Figure 2.12 shows a comparison of PV array output power and ideal power at maximum power point while figure 2.13 shows the I-V and P-V characteristics of the PV array at 1000W/m² and 25°C. The point of maximum power (MPP) is shown on the figure. The boost conversion efficiency is determined to be 96.44%

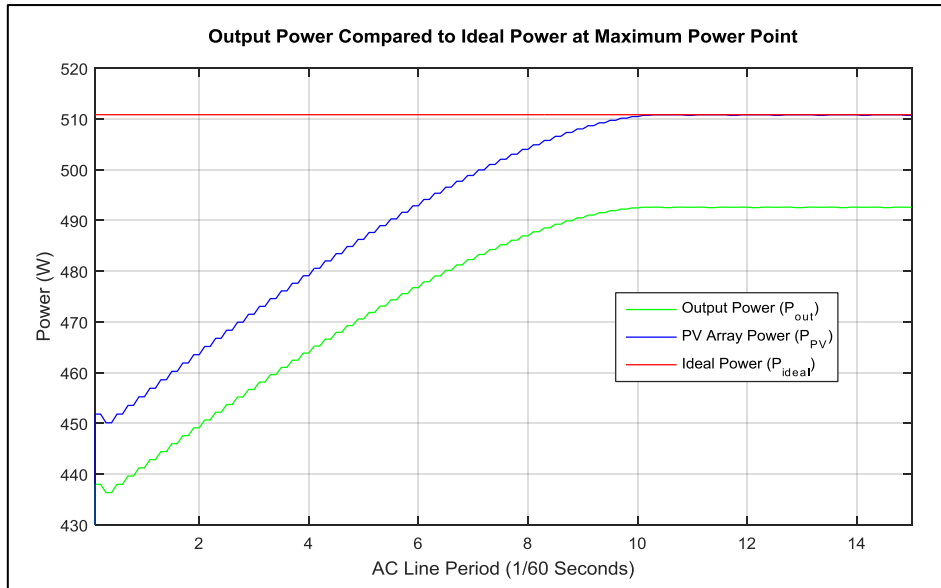


Fig. 2.12: Comparisons of PV Array Power, Converter Output Power, and Ideal Power at MPP

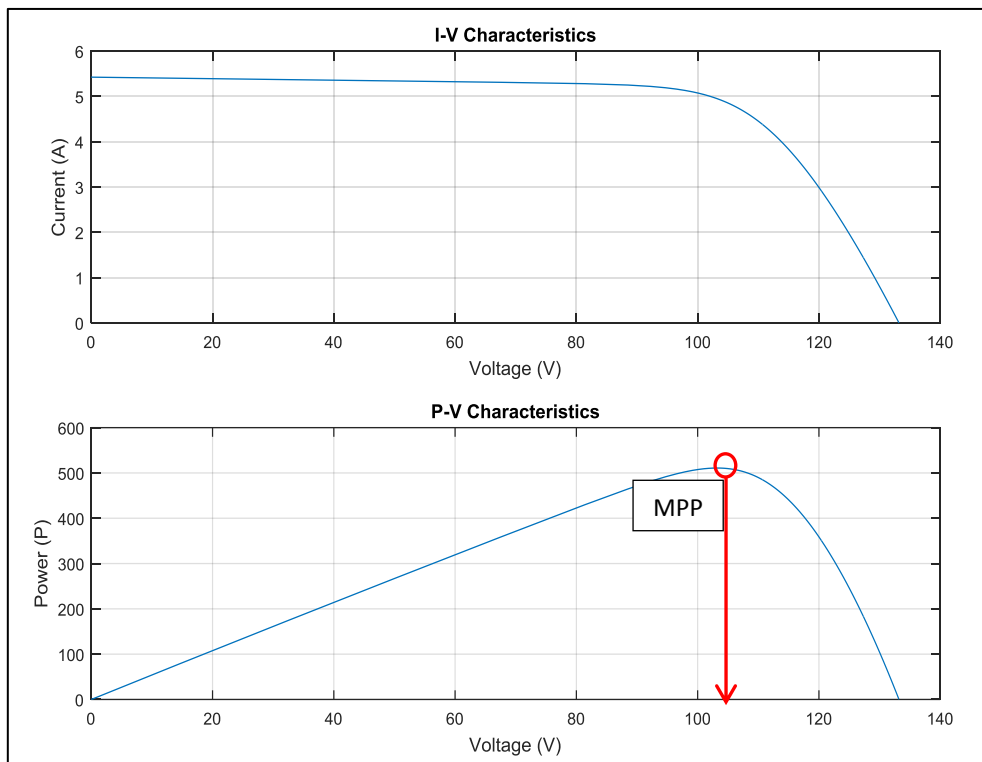


Fig. 2.13: Characteristics of the PV Array Showing Maximum Power Point

2.3 Power Electronics for PV Microgeneration Systems:

Power electronics used in PV power microgeneration systems are essential for power conditioning, maximum power point tracking, efficient voltage step-up or step-down, power inversion, battery

charge/discharge controlling, charge storage, and grid interfacing. They are therefore crucial parts of PV power microgeneration systems. The main power electronic devices used in PV systems are DC-DC converters and DC-AC inverters.

The main functions of DC-DC converters are to operate the PV power generator at maximum power point under all conditions and to efficiently step up/down the voltage from the PV source to a stable DC voltage of desired magnitude. They are also used for controlling battery charging and discharging. The four basic DC-DC converters used with PV systems are Buck, Boost, Buck-Boost, and Cuk converters.

DC-AC Inverters are used in PV systems to convert DC generated voltage into AC voltage for AC loads or for utility grid interfacing and to control the active and reactive power [67-70]. A maximum power point tracker (MPPT), implemented using a DC-DC converter, is usually used with DC-AC inverters to ensure extraction of maximum power from the PV system. Filters with active damping are used to reduce harmonics from the inverters. Typically voltage source inverters (VSI) are used when interfacing PV systems with a utility grid. These usually have buck characteristics, i.e., output voltage is usually lower than input voltage. However, step-up transformers can be used to boost the voltage. Capacitors are used to form DC links between DC-AC inverters and DC-DC converters to decouple power fluctuations in the AC and DC sides. Inverters with transformers are also used to provide galvanic isolation between PV generators and the utility grid.

Figure 2.14 shows a schematic diagram of power electronics in a grid connected PV system without a back-up battery. The function of the DC-DC boost converter is to operate the array at maximum power point under all conditions and to efficiently step up V_{PV} to a higher DC voltage V_{DC} . The DC-AC inverter generates an AC output current i_{ac} in phase with the AC utility grid voltage v_{ac} and also balances the average power delivery from the PV array to the grid,

$$P_{ac} = P_{PV} \times \eta_{DC-DC} \times \eta_{DC-AC} \quad (2.15)$$

The aim is to achieve a power-conversion-efficiency close to 100%, i.e.

$$\eta_{converter} = \frac{P_{ac}}{P_{PV}} = \frac{V_{RMS} I_{RMS}}{V_{PV} I_{PV}} \quad (2.16)$$

The purpose of the capacitor is to provide energy storage to balance the difference between P_{PV} and instantaneous power $p_{ac}(t)$. The system is disconnected from the grid if the utility loses power.

The control variable for the DC-AC inverter is the RMS current reference I_{RMSref} . The DC/AC inverter current $i_{ac}(t)$ is controlled so that it is in phase with the grid voltage $v_{ac}(t)$ and so that its RMS value equals the reference; $I_{RMS} = I_{RMSref}$

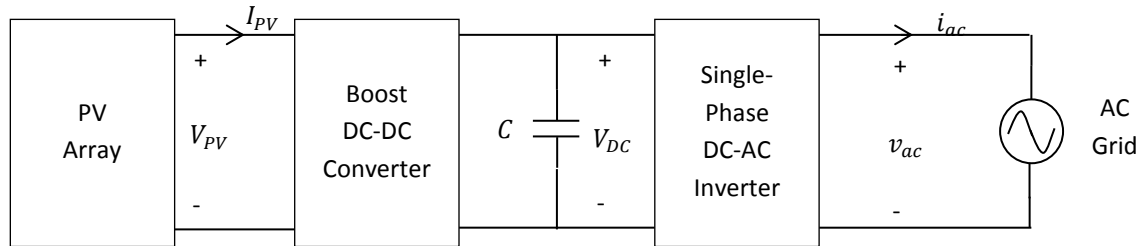


Fig. 2.14: Power Electronics in a Grid-Connected PV System

Figure 2.15 below shows a Simulink model of a grid-connected 6 module PV array with a DC-DC boost converter and a DC-AC inverter used to implement the above diagram. Each module is rated 85Wp and therefore if the PV array operates at ideal conditions, total power generated (P_{PV}) should be 510 Wp.

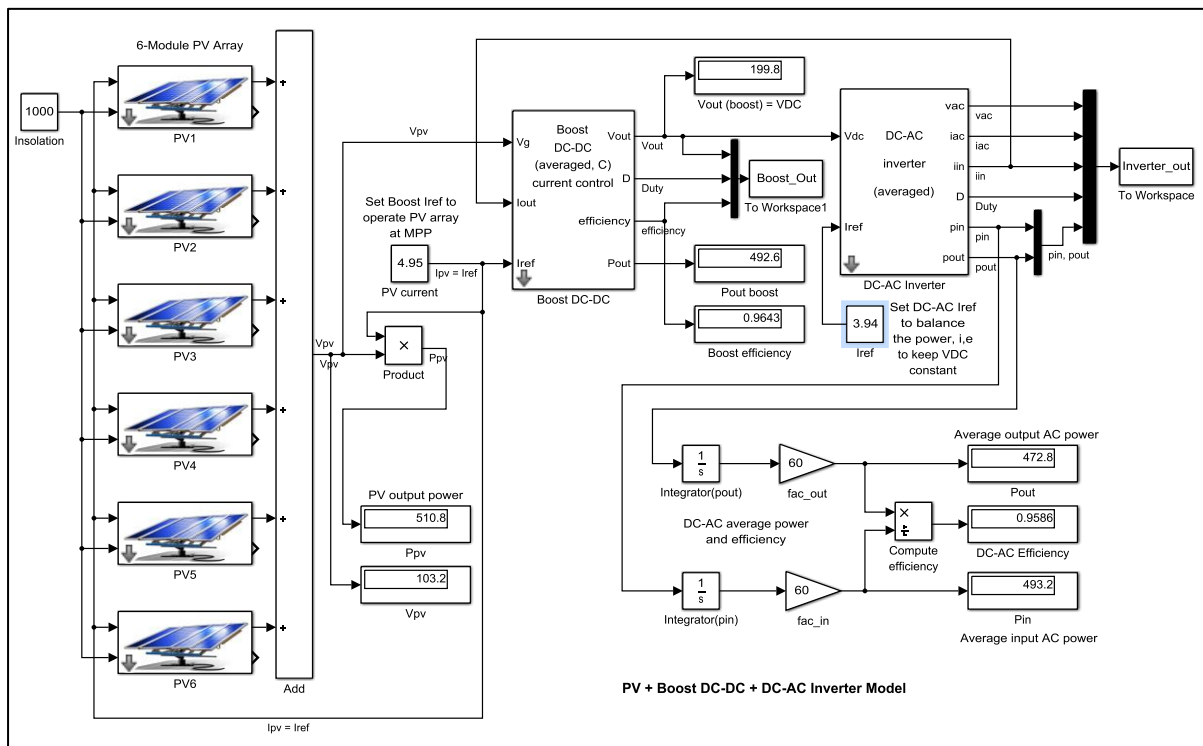


Fig. 2.15: Simulink Model of a Grid-Connected PV System with DC-DC and DC-AC Converters

The AC grid RMS is set at 120 V while AC line frequency is set at 60 Hz. In this simulation, the PV array voltage output $V_{PV} = 103.2$ V, current output $I_{PV} = 4.95$ A, and power output $P_{PV} = 510.8$

W. These three values are fed into the DC-DC boost converter which then outputs a V_{DC} of 199.8 V, representing a 96.6% boost in V_{PV} . The boost power out $P_{PV} = 492.6$ W, meaning the DC-DC converter has 96.43% efficiency. If we run the simulation using different values of I_{RMSref} and observe the output voltage $V_{out}(t) = V_{DC}(t)$, we can determine the right I_{RMSref} when $P_{ac} \approx P_{PV}$ and thus achieving nearly 100% conversion efficiency; in this case the ideal I_{RMSref} was determined to be 3.94 A, as shown in figure 2.16.

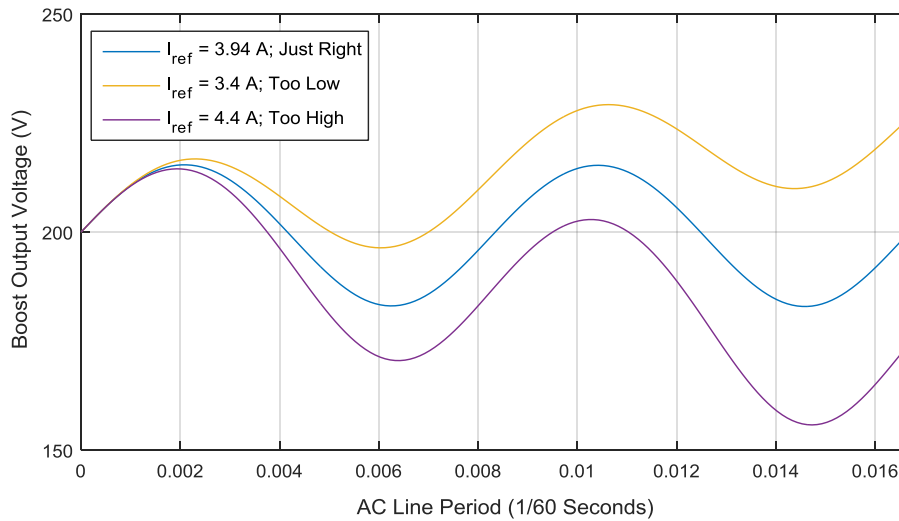


Fig. 2.16: Simulation Results for Different I_{RMSref} Values

The V_{DC} from the boost converter is input into the DC-AC inverter where it is inverted into V_{AC} for grid interfacing. Figure 2.17 below shows a comparison of V_{DC} and V_{AC} . While V_{DC} ripples around 200 V with a mean of 199.5 V, V_{AC} is a sine wave with amplitude of 169.7 V and a mean of 0 V, and a frequency and period that matches that of the grid it is interfaced with.

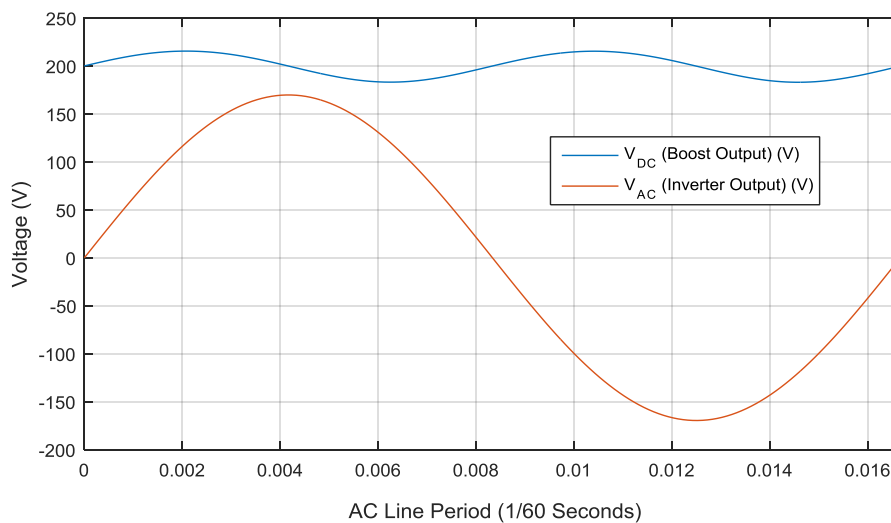


Fig. 2.17: Comparison of V_{DC} and V_{AC} Simulation Results

Similarly, figure 2.18 shows a comparison of I_{PV} and I_{AC} from the DC-AC inverter. I_{PV} ripples between 0 A and 4.95 A, while I_{AC} is a sine wave with an amplitude of 5.57 A and a mean of 0 A, and a frequency and period that matches that of the grid it is interfaced with.

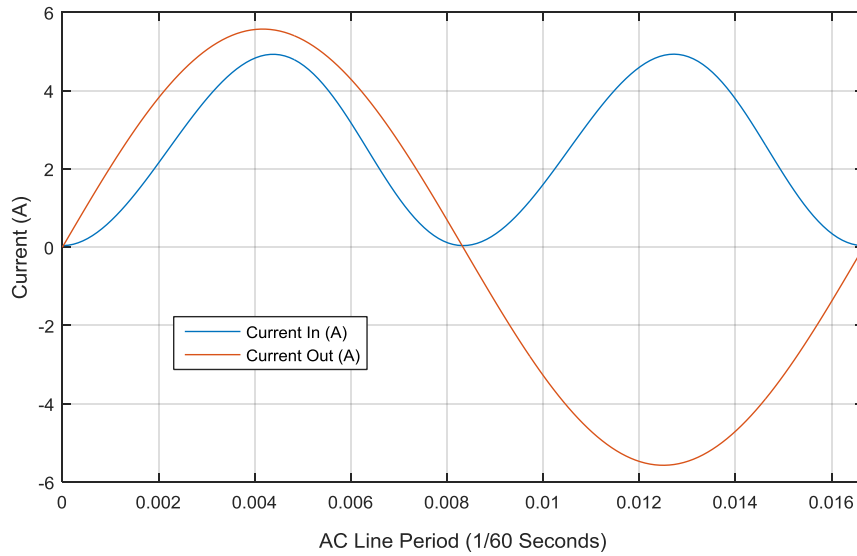


Fig. 2.18: Comparison of I_{PV} and I_{AC} Simulation Results

As shown in figure 2.19, the averaged input AC power is 493.2 W while the averaged output AC power is 472.8 W, therefore the DC-AC inverter efficiency is 95.86%. From equation 2.16, the overall conversion efficiency is given by

$$\eta_{converter} = \frac{P_{ac}}{P_{PV}} = \frac{472.8}{510.8} \times 100 = 92.56\% \quad (2.17)$$

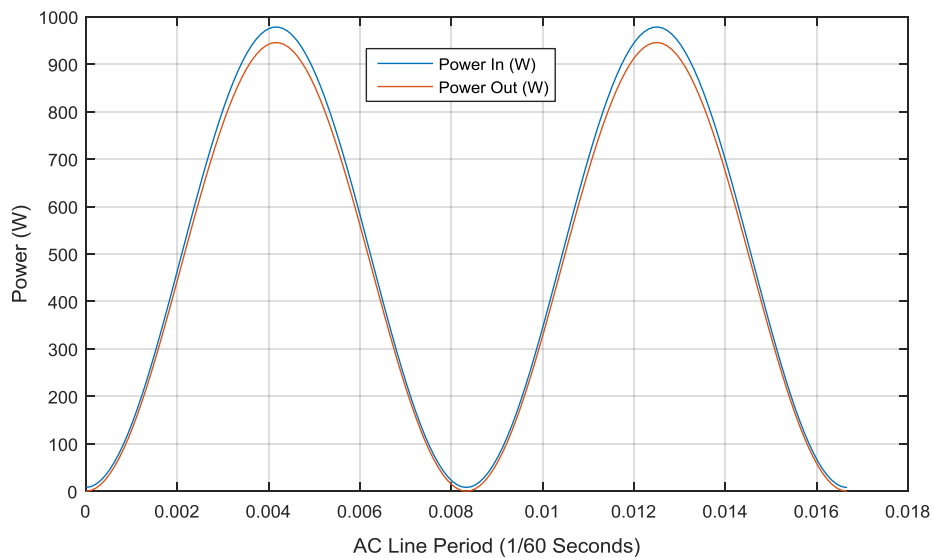


Fig. 2.19: Comparison of P_{PV} and P_{AC} Simulation Results

Average power balance can be implemented through an automatic feedback control as shown in figure 2.20 below. The voltage V_{DC} is sensed and compared to a reference value V_{DCref} and the difference is the error signal of the feedback controller. If the error is positive ($V_{DC} > V_{DCref}$), the compensator increases I_{RMSref} . If the error is negative ($V_{DC} < V_{DCref}$), the compensator decreases I_{RMSref} . In steady state ($V_{DC} = V_{DCref}$), the error signal is zero as I_{RMSref} is automatically adjusted by the automatic feedback controller so that it is just right and the average power delivered to the AC grid, P_{ac} matches the power generated by the PV array, P_{PV} .

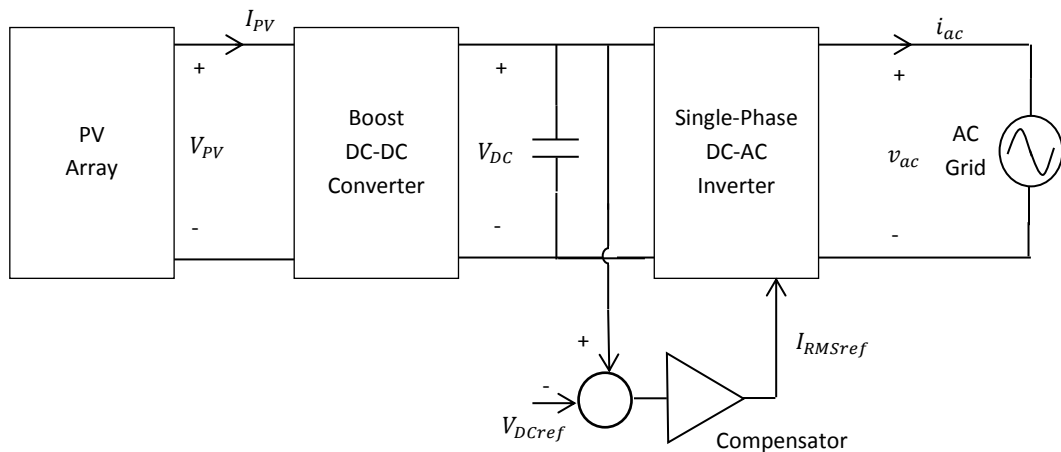


Fig. 2.20: A Grid-Connected PV System with an Automatic Feedback Loop

Figure 2.21 shows an analysis of storage capacitor C . As mentioned earlier, capacitor C provides energy storage necessary to balance instantaneous power delivered to the grid.

$$P_{ac} - p_{ac}(t) = P_{ac} - p_{ac}(1 - \cos 2\omega t) = P_{ac} \cos 2\omega t \quad (2.18)$$

The magnitude of the resulting ripple voltage ΔV_{DC} at twice the AC line frequency ($2 \times 60\text{Hz} = 120\text{Hz}$) depends on the average power P_{ac} and capacitance C . The energy supplied to the capacitor during charging from V_{DCmin} to V_{DCmax} , i.e. when $P_{ac} > p_{ac}(t)$, is given by

$$\Delta E_C = \int_{-T_{ac}/8}^{T_{ac}/8} P_{ac} \cos 2\omega t \, dt = \frac{P_{ac}}{2\omega} \int_{-\pi/2}^{\pi/2} \cos \theta \, d\theta = \frac{P_{ac}}{\omega} \quad (2.19)$$

This energy must match the change in energy stored on the capacitor;

$$\Delta E_C = \frac{1}{2} C V_{DCmax}^2 - \frac{1}{2} C V_{DCmin}^2 = C (V_{DCmax} - V_{DCmin}) \frac{V_{DCmax} + V_{DCmin}}{2} \approx C V_{DC} \Delta V_{DC} \quad (2.20)$$

Solving for the ripple voltage we get

$$CV_{DC}\Delta V_{DC} = \frac{P_{ac}}{\omega} \quad (2.21)$$

And therefore

$$\Delta V_{DC} = \frac{P_{ac}}{CV_{DC}\omega} \quad (2.22)$$

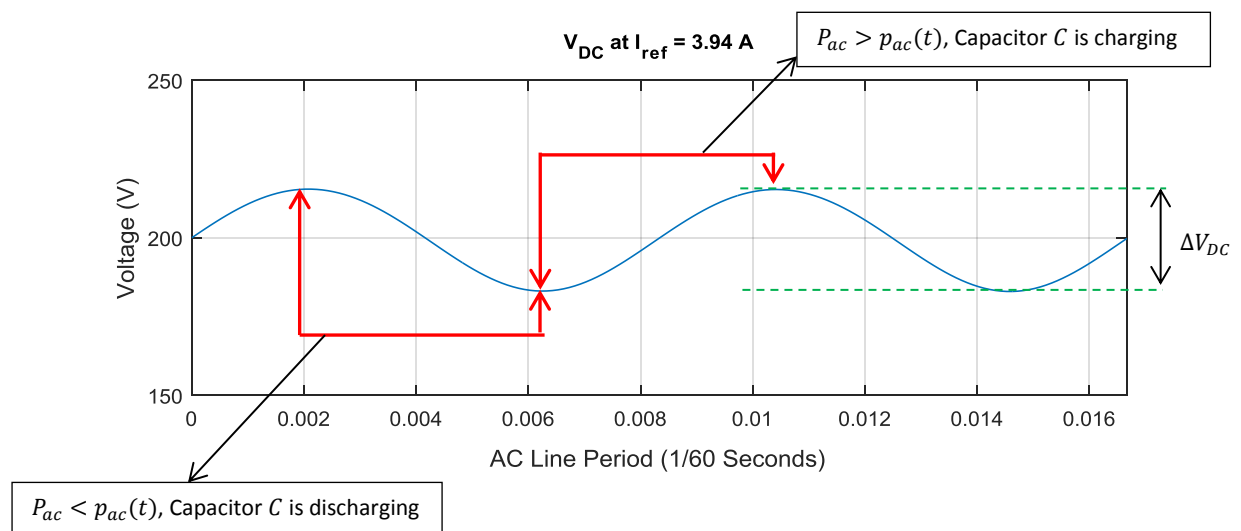


Fig. 2.21: Analysis of the Energy Storage Capacitor C

2.4 Energy Storage for PV Microgeneration Systems:

Energy storage systems are used in decentralized power systems for energy management, load levelling or peak shaving, for power bridging, and for power quality improvements [71-74]. Energy management functions require the energy storage system to serve for long durations of time compared to the other functions [71-74]. Power bridging functions require energy storage systems to serve for a few seconds to a few minutes [71-74]. For power quality improvements, the energy storage systems are required for only fractions of a second [71-74]. The main energy technologies include pumped hydro, compressed air energy storage (CAES), flywheels, superconducting magnetic energy storage (SMES), and electrochemical storage [75-79].

Table 2.2 below compares the properties of different energy storage technologies. It is noteworthy that batteries have a wider range of in all aspects of comparison. This is because there are very many

types of batteries that are commercially available, with each type optimizable for different purposes and applications.

	Supercapacitor	Battery	Flywheel	SMES	Fuel Cell	Pumped Hydro	CAES
Charge Time	1-30 s	0.3-5h	0.5-2h	0.1-5h	0.3-5h	10-50h	1-50h
Reverse Time (S)	0.01	0.01	0.1	0.01	360	10	360
Energy Density (Wh/kg)	1-10	30-130	5-50	10-50	20-30	0.2-0.7	20-50
Power Density (W/kg)	10^3 - 10^5	10 - 10^2	10^2 - 10^4	10^3 - 10^4	10^2 - 10^3	Not relevant	Not relevant
Rated Power (MW)	0.01-5	0.01-90	0.1-10	1-50	0.01-90	500-5000	100-1000
Life Cycle	$>10^6$	10^3	10^4 - 10^6	$>10^6$	10^3	10^4 - 10^6	10^4 - 10^5
Efficiency	$>95\%$	60-99%	85-90%	$>95\%$	40-60%	70-85%	75-80%
Capital Cost (\$/kW)	300-500	300-3000	3000-5000	700-3000	700-3000	700-2000	700-1500
Siting Requirement	Close to load	Close to load	Close to load	Substations/generators	Close to load	Geological consideration	Geographical consideration

Table 2.2: Energy Storage Technologies Comparison [75-79]

In pumped hydro systems, excess energy during low demand periods is used to pump water from a lower reservoir into an uphill reservoir from where it can be used to generate electricity during high power demands by natural flow of water through turbines back to the lower reservoir. In CAES systems compressed air is used to feed a gas turbine to generate electricity when necessary. In flywheels energy is stored in the form of mechanical kinetic energy and is converted back into electricity by the use of 4-quadrant power converters. SMESs store energy in magnetic fields using superconducting coils with high magnetic fields. The stored energy can be discharged as electric current by connecting it to a load. Electrochemical storage systems store energy as chemical energy which can then be converted into electricity through chemical reactions. They include fuel cells, supercapacitors, and batteries.

2.4.1 Batteries:

Batteries are the main storage devices used in PV power systems; they are used to operate PV systems near their maximum power points (MPP), to power electrical loads at stable voltages, and to supply surge currents to electrical loads and inverters. The two main classes of batteries are primary

batteries and secondary batteries. Primary batteries cannot be recharged and are thus not applicable in PV systems. Examples include carbon-zinc and lithium batteries used in consumer electronics. Secondary batteries can be recharged and are thus used in PV systems. The most common battery types used with PV systems are lead-acid, lithium-ion, nickel-metal hydride, and nickel-cadmium.

2.4.1.1 Lead-Acid (Pb-Acid) Batteries:

The positive electrode in a Pb-acid battery is composed of lead dioxide (PbO_2) while the negative electrode is composed of porous lead (Pb). The electrolyte is composed of 6 molar sulphuric acid (H_2SO_4).

During discharge the following reactions occur at the electrodes:

- a) Positive electrode: $PbO_2 + SO_4^{-2} + 4H^+ + 2e^- \rightarrow PbSO_4 + 2H_2O$
- b) Negative electrode: $Pb + SO_4^{-2} \rightarrow PbSO_4 + 2e^-$
- c) Overall: $Pb + PbO_2 + 2SO_4^{-2} + 4H^+ \rightarrow 2PbSO_4 + 2H_2O$

Reactions at the positive and negative electrodes lead to formation of lead sulphate coats around the electrodes which lead to reduction of the acid electrolyte. Since lead sulphate is a poor conductor of electricity, further reactions are limited; charging of the battery forces electrons to flow from the positive electrode to the negative electrode, reversing the 'sulphation' process [80].

The main advantages of lead acid batteries include the following: a) they are low cost as they benefit from maturity of technology, b) they are widely available and therefore it is easier to find parts, and c) they handle abuse (overcharge or over-discharge) better than other batteries [80]. The main disadvantages are that they have shorter shelf-lives compared to emerging technologies and that they are more sensitive to temperatures compared to other technologies [80]. They also suffer leakages which can lead to damage of the batteries [80]. Also, lead is harmful to humans and to the environment and could lead to waste lands, reduced IQ in children, abdominal pains, damage to liver and kidney, or even cancer, to name a few.

2.4.1.2 Lithium-Ion (Li-Ion) Batteries:

The positive electrode in a Li-ion battery is composed of a lithiated form of a transition metal oxide, usually lithium cobalt oxide ($LiCoO_2$) or lithium manganese oxide ($LiMn_2O_4$) while the negative electrode is composed of carbon (C), usually graphite (C_6). The electrolyte is composed of solid

lithium salt electrolytes (LiPF_6 , LiBF_4 , or LiClO_4) and organic solvents (ether). During discharge, the following reactions occur at the electrodes, where $0 < x < 1$:

- a) Positive electrode: $\text{LiCoO}_2 \rightarrow \text{Li}_{1-x}\text{CoO}_2 + x\text{Li}^+ + xe^-$
- b) Negative electrode: $x\text{Li}^+ + xe^- + 6\text{C} \rightarrow \text{Li}_x\text{C}_6$
- c) Overall: $\text{LiCoO}_2 + \text{C}_6 \rightarrow \text{Li}_{1-x}\text{CoO}_2 + \text{Li}_x\text{C}_6$

During discharge, the cobalt Co is oxidized from Co^{3+} to Co^{4+} while the reverse (reduction) occurs during charging.

Li-ion batteries do not accept a high initial charging current well. Also, cells in a battery pack need to be equalized to avoid falling below the minimum cell voltage of about 2.85V/cell. Therefore, Li-ion batteries need to be initially charged with a constant current profile, and thus require a charger. Typical float voltage is above 4V (usually 4.2V). Carbonaceous materials used in all Li-ion batteries lead to formation of a solid electrolyte interface (SEI) around the carbon electrodes as a result of non-reversible chemical reactions between the carbon electrodes and lithium ions [81]. As the SEI gets thicker, it leads to capacity decline and to eventual stoppage of the battery performance [81]. The lifetime and cyclability of a Li-ion cell therefore depends on its SEI layer [81].

Advantages of Li-ion batteries include the following: a) they are lighter and smaller than lead acid batteries of similar capacities, b) they have longer shelf-lives (replacement every 5-7 years as opposed to 1.5-2 years with sealed lead acid), c) they can withstand up to 60°C without degradation and thus have no need for air conditioning, d) they have faster recharge times and 20-25% higher turnaround charge efficiency compared to Pb-acid batteries, e) they have greater discharge cycles (5-10x), f) they have a full depth of discharge capability, g) they can be easily and remotely monitored, h) they require no servicing or watering, i) they have no need for hydrogen gas extraction provisions, j) the time between recharges is 26 weeks as opposed to 2 weeks for sealed lead acid, k) fewer cells in series are needed to achieve a given voltage, and l) there are not deposits with every charge/discharge cycle and thus 99% efficiency is achievable [82]. The main disadvantage of Li-ion batteries is that they are very expensive compared to other technologies.

2.4.1.3 Nickel-Metal Hydride (Ni-MH) Batteries:

The positive electrode of an Ni-MH battery is composed of nickel oxyhydroxide ($\text{NiO}(\text{OH})$) while the negative electrode is composed of a metal hydride such as AB_2 (where A is titanium and/or vanadium, and B is zirconium or nickel, modified with chromium, cobalt, iron, and/or manganese) or AB_5 (where A is a rare earth mixture of lanthanum, cerium, neodymium, and/or praseodymium, and

B is nickel, cobalt, manganese, and/or aluminium).The electrolyte is composed of potassium hydroxide (KOH).

During discharge, the following reactions occur at the electrodes:

- a) Positive electrode: $NiO(OH) + H_2O + e^- \rightarrow Ni(OH)_2 + OH^-$
- b) Negative electrode: $MH + OH^- \rightarrow M + H_2O + e^-$
- c) Overall: $NiO(OH) + MH \rightarrow Ni(OH)_2 + M$

The electrolyte is not affected because it does not participate in the reaction.

Ni-MH batteries do not accept a high initial charging current well and are thus not suitable for charging with a constant-voltage method. Float voltage is about 1.4V while minimum voltage is about 1V. Advantages of Ni-MH batteries include the fact that they are less sensitive to high temperatures than Li-ion and Lead-acid batteries and that they can handle abuse (overcharge or over-discharge) better than Li-ion batteries. The main disadvantages are that more cells in series are needed to achieve a given voltage, compared to similarly sized Li-ion or Pb-acid batteries, and that they are very expensive.

2.4.1.4 Nickel-Cadmium (Ni-Cd) Batteries:

The positive electrode of a Ni-Cd battery is composed of nickel oxyhydroxide (NiO(OH)), same as with Ni-MH batteries, while the negative electrode is composed of cadmium. The electrolyte is composed of potassium hydroxide (KOH), as in Ni-MH batteries.

During discharge, the following chemical reactions occur at the electrodes:

- a) Positive electrode: $2NiO(OH) + 2H_2O + 2e^- \rightarrow 2Ni(OH)_2 + 2OH^-$
- b) Negative electrode: $Cd + 2OH^- \rightarrow Cd(OH)_2 + 2e^-$
- c) Overall: $2NiO(OH) + Cd + 2H_2O \rightarrow 2Ni(OH)_2 + Cd(OH)_2$

The electrolyte is not affected because it does not participate in the reaction.

As with Ni-MH batteries, Ni-Cd batteries do not accept a high initial charging current well and are thus not suitable for charging with a constant-voltage method. Float voltage is about 1.4V while minimum voltage is about 1V. The main advantage of Ni-Cd batteries is that they are less sensitive to high temperatures than all other batteries. Also, they handle abuse (overcharge or over-discharge)

better than Li-ion. The main disadvantages are that more cells in series are needed to achieve a given voltage and that they are very expensive.

Table 2.3 below shows a comparison of different parameters of the four batteries discussed above.

	Lead-Acid	Ni-Cd	Ni-MH	Li-ion
Cell Voltage (V)	2	1.2	1.2	3.6
Specific Energy (Wh/kg)	1-60	20-55	1-80	3-100
Specific Power (W/kg)	<300	150-300	<200	3-100
Energy density (kWh/m ³)	25-60	25	70-100	80-200
Power density (MW/m ³)	<0.6	0.125	1.5-4	0.4-2
Maximum cycles	200-700	500-1000	600-1000	3000
Discharge time range	> 1min	1 min -8 hr	> 1min	10 s – 1 hr
Cost (\$/kWh)	125	600	540	600
Cost (\$/kW)	200	600	1000	1100
Efficiency (%)	75-90	75	81	99

Table 2.3: A Comparison of Different Types of Batteries [83,84]

2.4.2 Modelling and Simulations:

The main parameters used in modelling a battery are [85]:

- a) Internal resistance: this is caused by charge and discharge conditions of a battery and increases as battery efficiency decreases
- b) Self-discharge resistance: this is caused by electrolysis of water at high voltage levels and by leakage current at terminals when voltage levels are low
- c) Charge and discharge resistances: these are due to electrolyte, plate, and fluid resistances
- d) Polarization capacitance: this is caused by chemical diffusion that occurs within the electrolyte terminals
- e) Terminal voltage: this is the voltage across the battery terminals and a load
- f) Open circuit voltage: this is the voltage across battery terminals with no load

Equation of state of charge (*SoC*) of a battery is given by [86]

$$SoC = \alpha SoC_c + (1-\alpha)SoC_v \quad (2.23)$$

where α ($\in [0,1]$) is the weight factor, SoC_c is the current-based state of charge, and SoC_v is the voltage-based state of charge.

SoC is a function of time and can thus alternatively be expressed as

$$SoC_c(t) = SoC_c(0) - \frac{1}{Q} \int_0^t I(t) dt \quad (2.24)$$

where Q is the battery capacity in (Ah), and relates the battery current I to SoC .

Many battery models have been developed for different applications. Electrochemical models describe a battery using a set of six coupled differential equations. These models are used in battery designs. Electric circuit models are mainly used in electrical engineering to study the electrical properties of batteries. Figure 2.22 shows a circuit model of a battery.

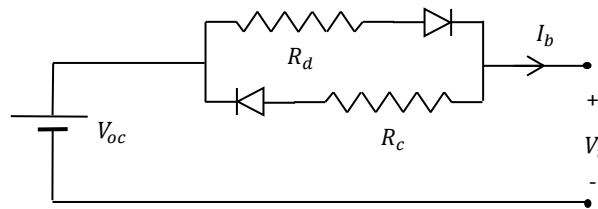


Fig. 2.22: Circuit Model of a Battery

R_d and R_c represent internal resistances which are on or off during discharging and charging, respectively; during charging and discharging, one diode conducts while the other is reverse biased. Parameters of the two internal resistances account for the loss in energy, electrical or non-electrical. It is noteworthy that the two diodes are just for modelling purposes and are thus not physically implanted in battery structures.

To simulate chemical diffusion of electrolytes and the resultant effect of causing transient currents within the battery, a capacitor is added to the model as shown in figure 2.23 [87]

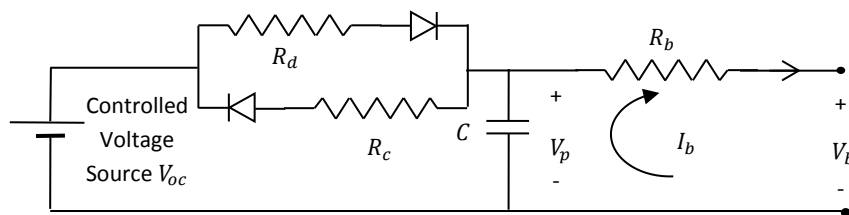


Fig. 2.23: Circuit Model of a Battery with Capacitor

A proportional feedback loop controller can be added to the above model, as shown in figure 2.24 below, to provide the model with a voltage source that is controlled and in series with a resistance. This enables the model to simulate a charge and a discharge process with the controlled voltage based on the SOC of the battery [87].

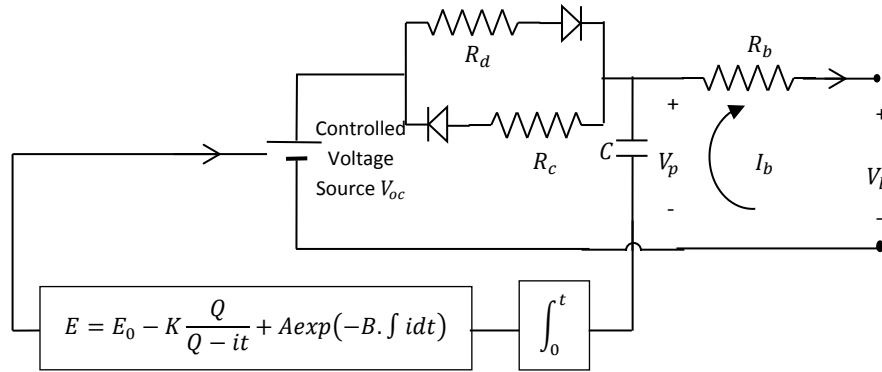


Fig. 2.24: Circuit Model of a Battery with Feedback Loop

The controlled voltage source is described by the following equation [87]

$$E = E_0 - K \frac{Q}{Q - it} + A \exp(-B \cdot \int idt) \quad (2.25)$$

where E is the no-load voltage (V), E_0 is the battery constant voltage (V), K is the polarization (V) voltage, Q is the maximum battery capacity (Ah), $\int idt$ is the actual battery charge (Ah), A is the exponential zone amplitude (V), and B is the exponential zone time constant inverse (Ah)⁻¹.

2.4.2.1 Charging State ($V_p \leq V_{oc}$; $i^* < 0$):

During charging, the feedback loop controller compares the difference in SOC and some predefined values of SOC to determine whether the battery has reached the lowest specified value of SOC. If the lowest set value is reached, the DC machine begins to charge the battery at a pre-set charge current. The DC machine acts as a battery charger. This process is described by equations 2.26, 2.27, and 2.28 for Pb-acid, Li-ion, and Ni-MH and Ni-Cd batteries, respectively [86-88]:

$$f_1(it, i^*, i, Exp) = E_0 - K \cdot \frac{Q}{it + 0.1 \cdot Q} \cdot i^* - K \cdot \frac{Q}{Q - it} \cdot it + Laplace^{-1} \left(\frac{Exp(s)}{Sel(s)} \cdot \frac{1}{s} \right) \quad (2.26)$$

$$f_1(it, i^*, i) = E_0 - K \cdot \frac{Q}{it + 0.1 \cdot Q} \cdot i^* - K \cdot \frac{Q}{Q - it} \cdot it + A \cdot \exp(-B \cdot it) \quad (2.27)$$

$$f_1(it, i^*, i, Exp) = E_0 - K \cdot \frac{Q}{|it| + 0.1 \cdot Q} \cdot i^* - K \cdot \frac{Q}{Q - it} \cdot it + Laplace^{-1} \left(\frac{Exp(s)}{Sel(s)} \cdot \frac{1}{s} \right) \quad (2.28)$$

where it is extracted capacity (Ah), i is battery current (A), i^* is the low frequency current dynamics (A), $Exp(s)$ is the exponential zone dynamics (V), $Sel(s)$ represents the battery mode and equals 1 during charging and 0 during discharge,

2.4.2.2 Discharging State ($V_p \geq V_{oc}$; $i^* > 0$):

During discharge, a feedback loop controller measures the difference in SOC and some predefined SOC values to determine whether a pre-set maximum value of SOC has been reached. This process is described by the following set of equations for Pb-acid, Li-ion, and Ni-MH and Ni-Cd, respectively [86-88]:

$$f_2(it, i^*, i, Exp) = E_0 - K \cdot \frac{Q}{Q - it} \cdot i^* - K \cdot \frac{Q}{Q - it} \cdot it + Laplace^{-1} \left(\frac{Exp(s)}{Sel(s)} \cdot 0 \right) \quad (2.29)$$

$$f_2(it, i^*, i) = E_0 - K \cdot \frac{Q}{Q - it} \cdot i^* - K \cdot \frac{Q}{Q - it} \cdot it + A \cdot \exp(-B \cdot it) \quad (2.30)$$

$$f_2(it, i^*, i, Exp) = E_0 - K \cdot \frac{Q}{Q - it} \cdot i^* - K \cdot \frac{Q}{Q - it} \cdot it + Laplace^{-1} \left(\frac{Exp(s)}{Sel(s)} \cdot 0 \right) \quad (2.31)$$

The above equations for charging and discharging states can be incorporated into the battery circuit model to give the model shown in figure 2.25 below. The model is later used in chapter 6 for energy storage modelling.

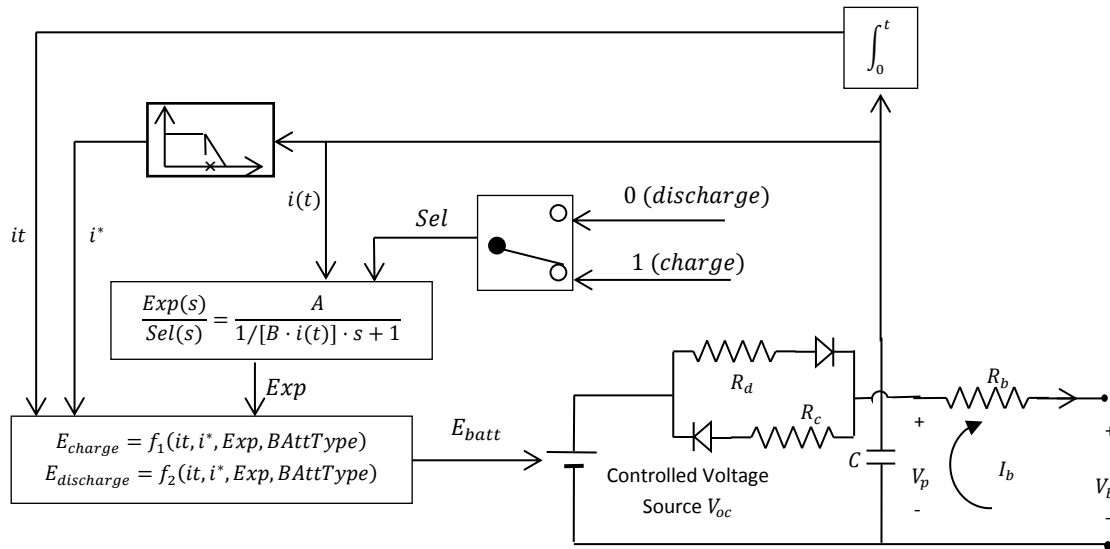


Fig. 2.25: Advanced Circuit Model of a Battery

The following assumptions are made in the model:

- Internal resistance is assumed to be constant during charging and discharging
- Parameters for the model are based upon values found from discharging and charging cycles
- There is no change in capacity of the battery or in the amplitude of the current
- Self-discharging state is not represented
- The battery is deemed to have no effect on the stored memory

The generic Simulink model shown in figure 2.26 below is used to implement the above circuit model. The mask labelled 'Battery' implements a generic battery that models Pb-acid, Li-ion, Ni-MH, and Ni-Cd batteries. The type of the battery to be modelled is selected under parameters of the mask. A particular battery type's parameters are automatically loaded when it is selected in the mask. These parameters cannot be modified and are based on manufacturers' data sheets. In the mask parameter tab, nominal voltage (V) represents the end of the linear zone of the discharge characteristics while rated capacity (Ah) is the minimum effective capacity of the battery. The initial state of charge is set at 100%. The mask labelled the DC Machine charges the battery at a constant charge current. It is turned on if a pre-set minimum value of SOC is reached. The feedback loop controller takes measurements of SOC at different intervals and compares them to pre-defined values of SOC upper and lower limits. If the upper limit is reached, charging stops while if the lower limit is reached, charging begins. The feedback loop controller therefore determines when to charge the battery via the DC machine. The data output is fed into a scope and the simulation output feeds to workspace where obtained voltage, SOC, DC motor speed, and armature current are recorded.

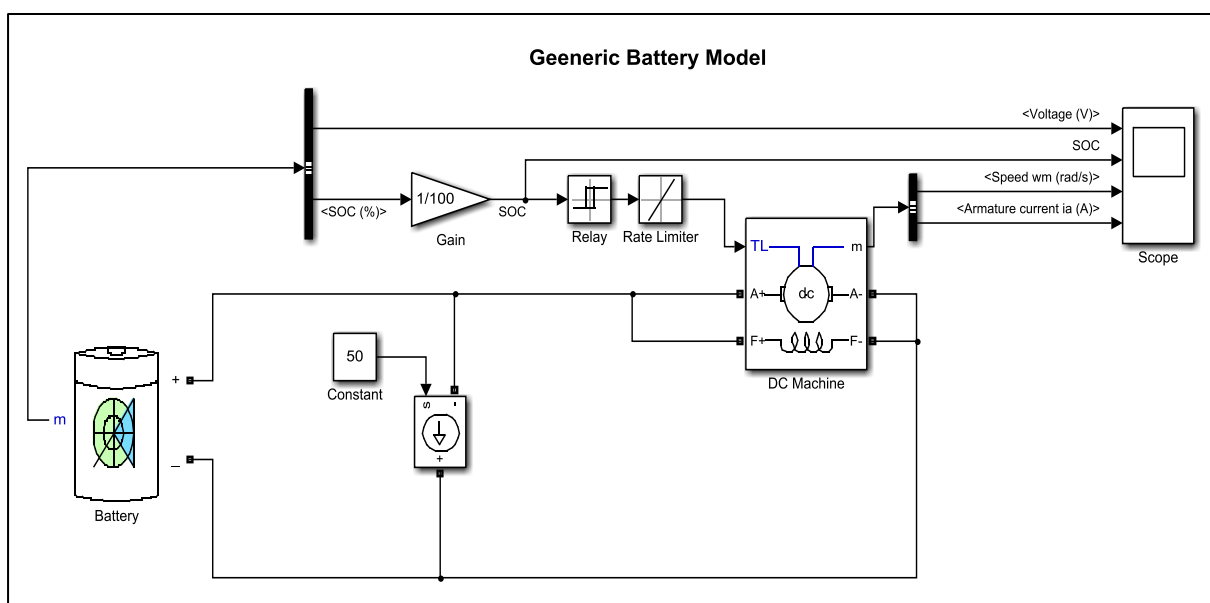


Fig. 2.26: Simulink Model of a Battery

2.4.3 Results and Discussion:

2.4.3.1 Pb-Acid Battery:

The following parameters were used for the Pb-acid battery: Nominal voltage (V) = 24; internal resistance (Ohms) = 0.0016; nominal discharge current (A) = 30; rated capacity (Ah) = 150; capacity at nominal voltage (Ah) = 46.54; and initial state-of-charge = 100%. Figure 2.27 shows plots of battery voltage and state of charge with time. Initially the state of charge is 1 (100%) and the battery voltage is at 24 V. The battery then begins to discharge with time. When the SOC reaches 0.4, the feedback loop controller instructs the DC machine to start charging the battery. This continues until the SOC reaches 0.8 when charging stops and the discharging process begins again. This cycle is repeated for the duration of the simulation. Pb-acid batteries have optimum voltage window and lifetime in the 0.4 to 0.8 SOC range. These simulation results therefore validate the model.

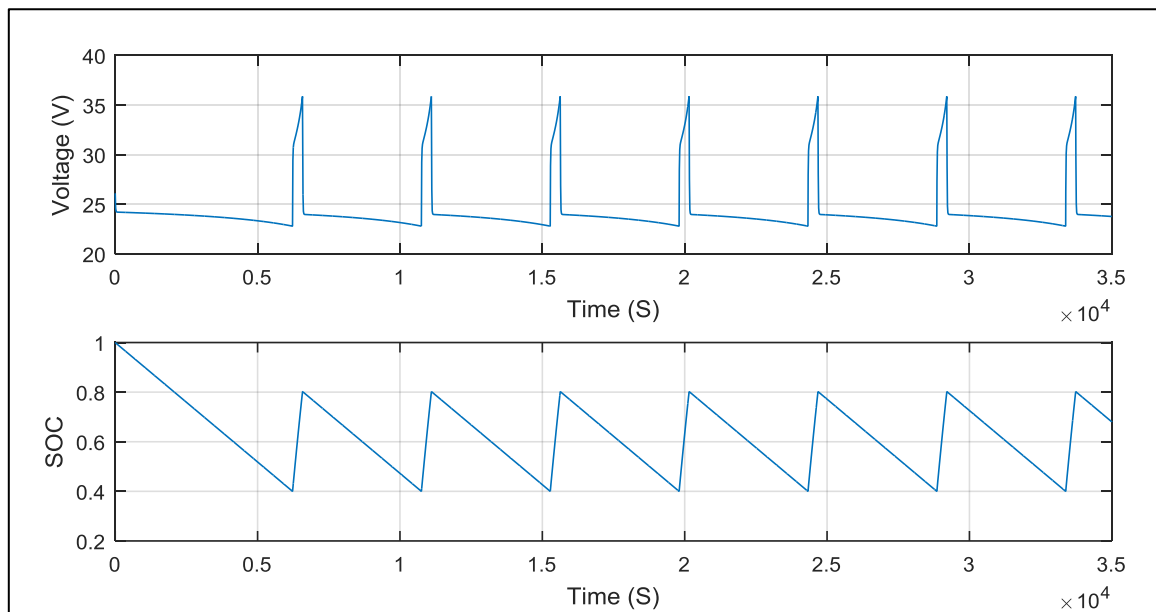


Fig. 2.27: Discharging/Charging Cycles of a Pb-Acid Battery

Depth of discharge (DOD) of a battery refers to the lowest permissible SOC. Deep cycle and large batteries can withstand up to 80% DOD (20% SOC). A battery's life is directly dependent on its DOD and charging/discharging cycles it experiences over its lifetime. Figure 2.28 shows a plot of voltage discharge rate and of SOC. It takes about 6,250 seconds for the battery to discharge to minimum SOC and for the charging process to begin. The rate at which a battery is discharged affects its capacity and lifetime [89]; if discharging occurs too quickly, a battery's capacity is significantly diminished while if discharging occurs more slowly, the capacity is enhanced.

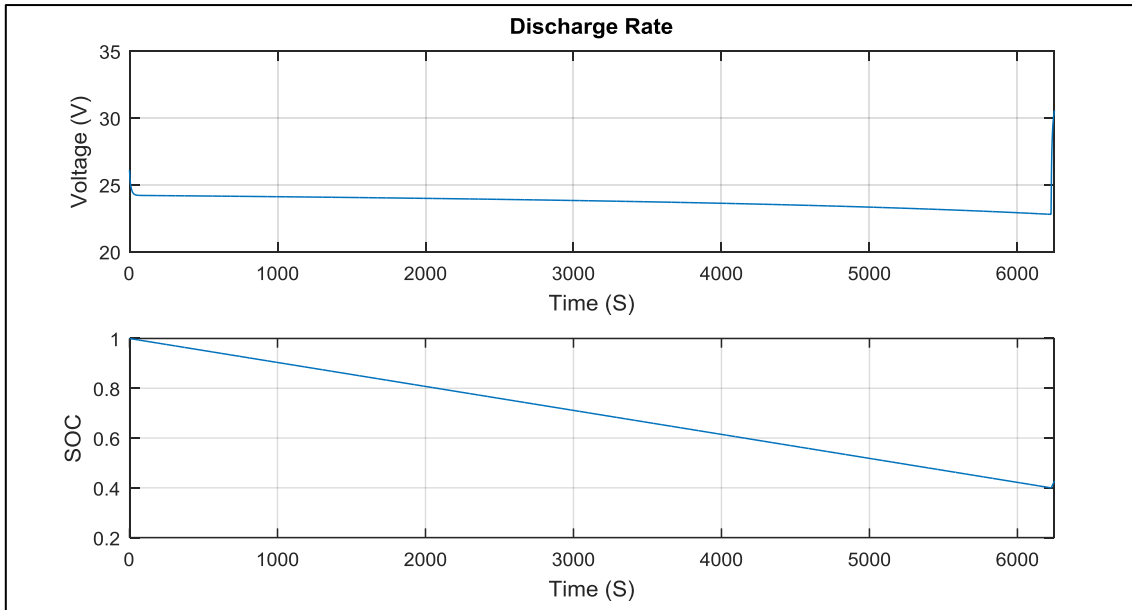


Fig. 2.28: Discharging Rate of a Pb-Acid Battery

Battery capacity is a function of time and rate of its discharge; a battery's capacity decreases as its discharge rate increases, a phenomenon called Peukert's effect [89]. According to this law, the capacity of a battery can be found by plotting the discharge rate. Peukert's effect is given by [89]

$$C = I^K t \quad (2.32)$$

Where C is the battery capacity at 1A discharge rate, I is the discharge current, K is Peukert coefficient (typically between 1.1 and 1.3), and t is time.

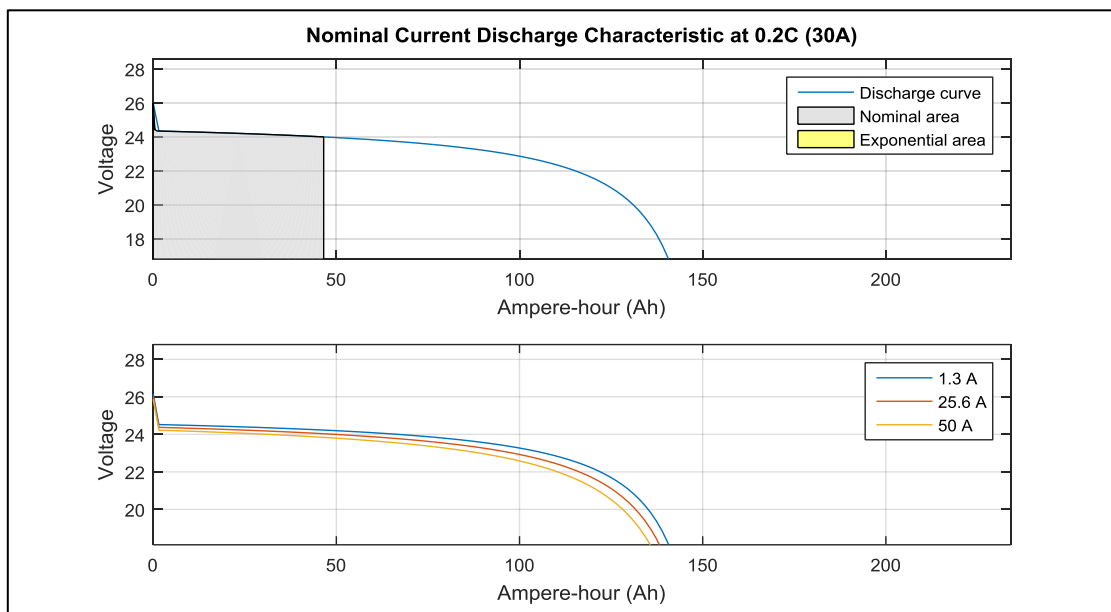


Fig. 2.29: Effects of Discharging Current on Rate of Discharge of a Pb-Acid Battery

Figure 2.29 above shows the effects of discharging current on nominal voltage; the voltage is significantly affected by the rate of discharge with lower discharge currents leading to slower discharge rates while higher discharge currents lead to faster discharge rates. It has the smallest nominal area of all battery technologies considered in this section and thus the shortest discharge cycle.

2.4.3.2 Li-Ion Battery:

The following parameters were used for the Li-ion battery: Nominal voltage (V) = 24; internal resistance (Ohms) = 0.0016; nominal discharge current (A) = 65.22; rated capacity (Ah) = 150; capacity at nominal voltage (Ah) = 135.65; and initial state-of-charge = 100%. Figure 2.30 shows plots of battery voltage and state of charge with time. Initially the state of charge is 1 (100%) and the battery voltage is at 24 V. The battery then begins to discharge with time. When the SOC reaches 0.4, the feedback loop controller instructs the DC machine to start charging the battery. This continues until SOC reaches 0.9 when charging stops and the discharging process begins again. This cycle is repeated for the duration of the simulation; Li-ion batteries have a larger SOC range than that of Pb-acid batteries.

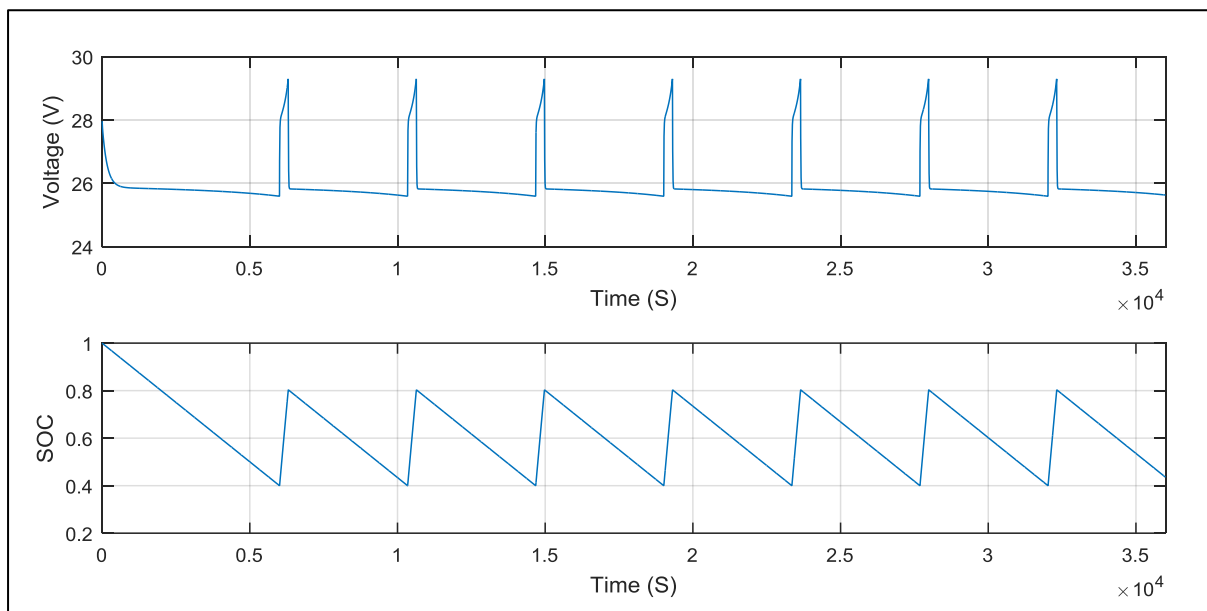


Fig. 2.30: Discharging/Charging Cycles of a Li-Ion Battery

Figure 2.31 shows a plot of voltage discharge rate and of SOC. It takes about 6,000 seconds (for the battery to discharge to minimum SOC and for the charging process to begin. This is a faster charging/dischARGE rate compared to a Pb-Acid battery of similar capacity as discussed above.

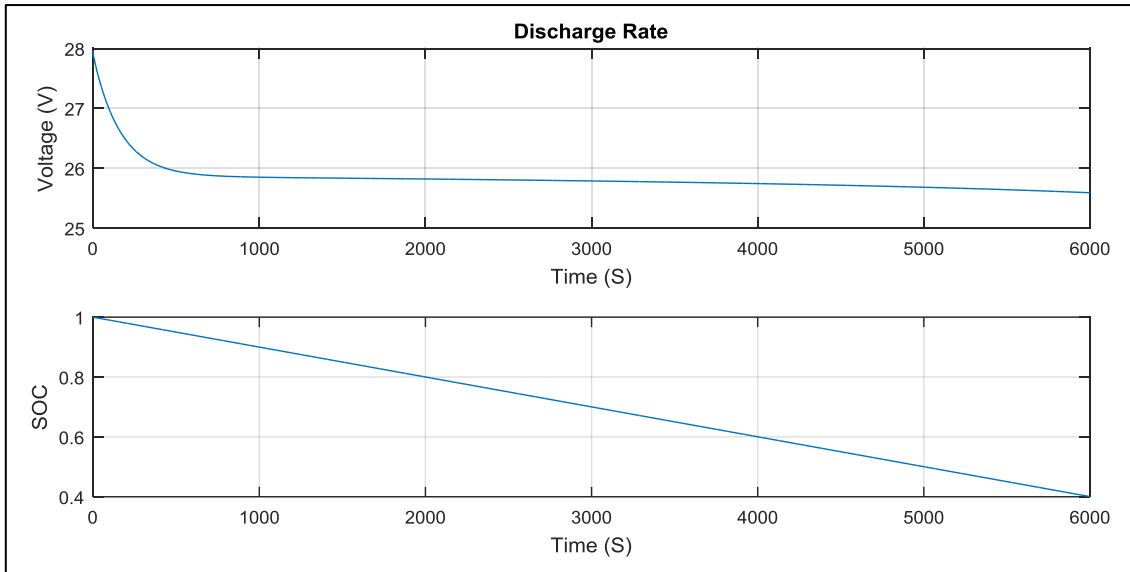


Fig. 2.31: Discharging Rate of a Li-Ion Battery

Figure 2.32 shows effects of discharging current on nominal voltage; as with a Pb-acid battery, the voltage is significantly affected by the rate of discharge with lower discharge currents leading to slower discharge rates while higher discharge currents lead to faster discharge rates. The nominal area is much larger than that of Pb-Acid battery, indicating a longer discharge cycle.

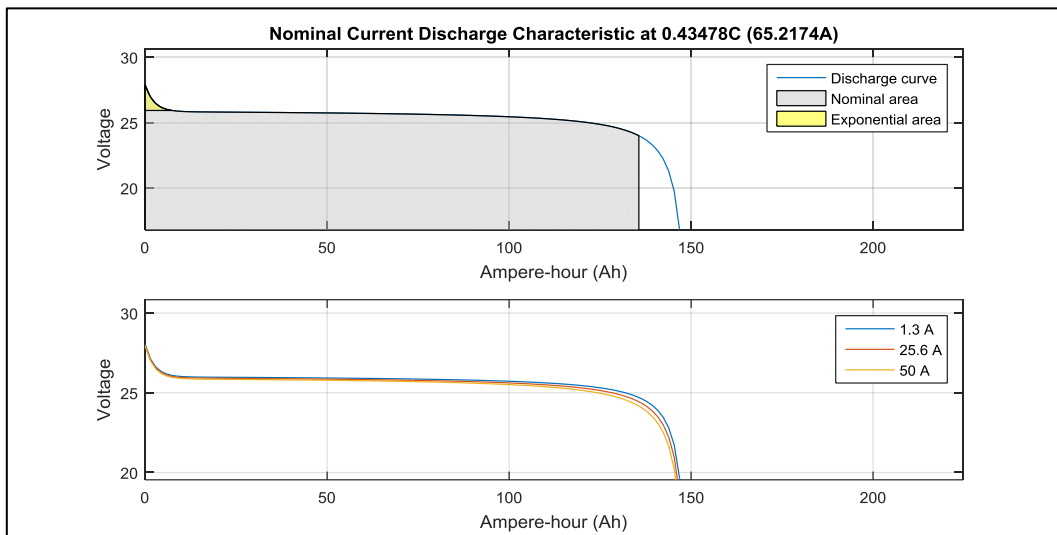


Fig. 2.32: Effects of Discharging Current on Rate of Discharge of a Li-Ion Battery

2.4.3.3 Ni-MH Battery:

The following parameters were used for the Ni-MH battery: Nominal voltage (V) = 24; internal resistance (Ohms) = 0.0016; nominal discharge current (A) = 30; rated capacity (Ah) = 150; capacity at nominal voltage (Ah) = 144.23; and initial state-of-charge = 100%. Figure 2.33 shows plots of

battery voltage and state of charge with time. Initially the state of charge is 1 (100%) and the battery voltage is at 24 V. The battery then begins to discharge with time. When the SOC reaches 0.4, the feedback loop controller instructs the DC machine to start charging the battery. This continues until SOC reaches 0.8 when charging stops and the discharging process begins again. This cycle is repeated for the duration of the simulation; Ni-MH batteries have a SOC range similar to that of Pb-acid batteries.

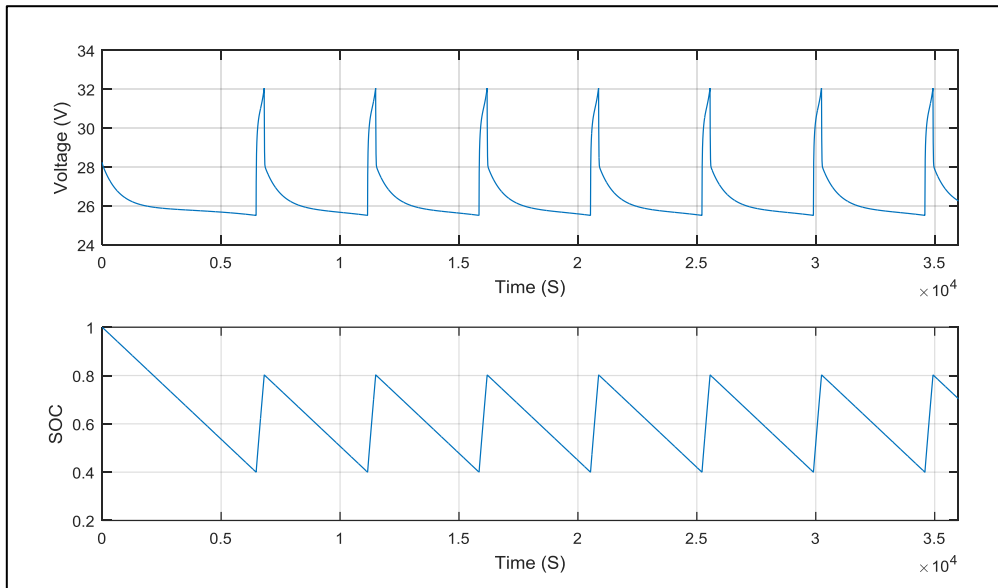


Fig. 2.33: Discharging/Charging Cycles of a Ni-MH Battery

Figure 2.34 shows a plot of voltage discharge rate and of SOC. It takes about 6,500 seconds for the battery to discharge to minimum SOC and for the charging process to begin.

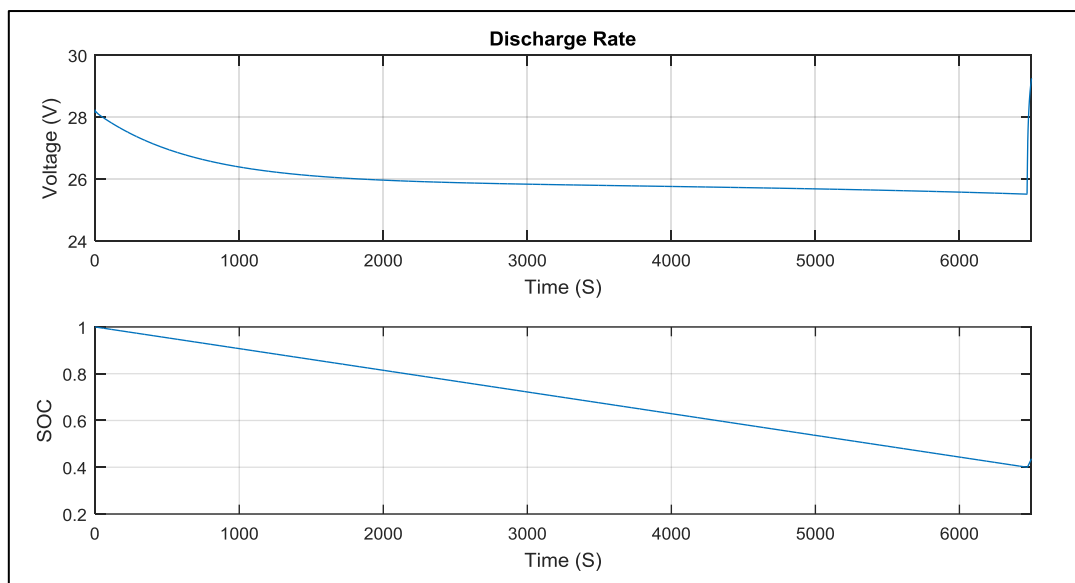


Fig. 2.34: Discharging Rate of a Ni-MH Battery

Figure 2.35 shows the effects of discharging current on nominal voltage; as with Pb-acid and Li-ion batteries, the voltage is significantly affected by the rate of discharge with lower discharge currents leading to slower discharge rates while higher discharge currents lead to faster discharge rates. The nominal area is larger than Li-Ion or Pb-Acid batteries.

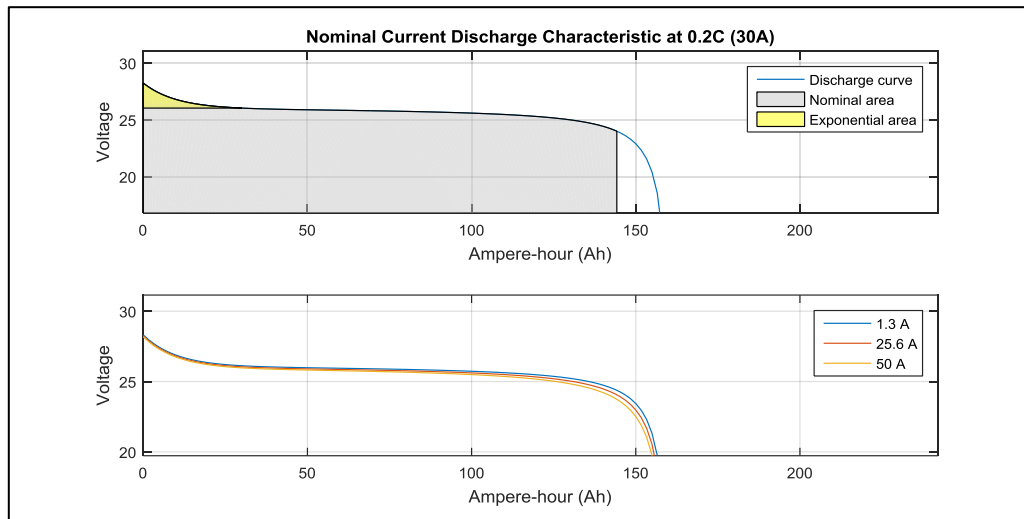


Fig. 2.35: Effects of Discharging Current on Rate of Discharge of a Ni-MH Battery

2.4.3.4 Ni-Cd Battery:

The following parameters were used for the Ni-Cd battery: Nominal voltage (V) = 24; internal resistance (Ohms) = 0.0016; nominal discharge current (A) = 30; rated capacity (Ah) = 150; capacity at nominal voltage (Ah) = 144.2; and initial state-of-charge = 100%. Figure 2.36 below shows plots of battery voltage and state of charge with time. Initially the state of charge is 1 (100%) and the battery voltage is at 24 V.

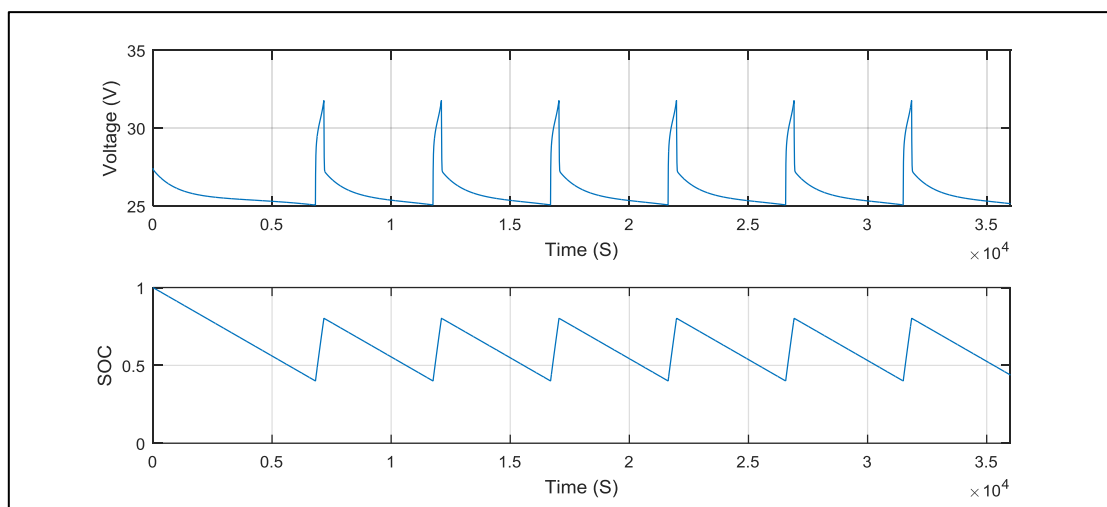


Fig. 2.36: Discharging/Charging Cycles of a Ni-Cd Battery

The battery then begins to discharge with time. When the SOC reaches 0.4, the feedback loop controller instructs the DC machine to start charging the battery. This continues until SOC reaches 0.8 when charging stops and the discharging process begins again. This cycle is repeated for the duration of the simulation; Ni-Cd batteries are quite similar to Ni-MH batteries and also have a SOC range similar to that of Pb-acid batteries.

Figure 2.37 shows a plot of voltage discharge rate and of SOC. As with the Ni-MH battery, it takes about 6,500 seconds for the battery to discharge to minimum SOC and for the charging process to begin. This is slower than Pb-acid and Li-ion batteries.

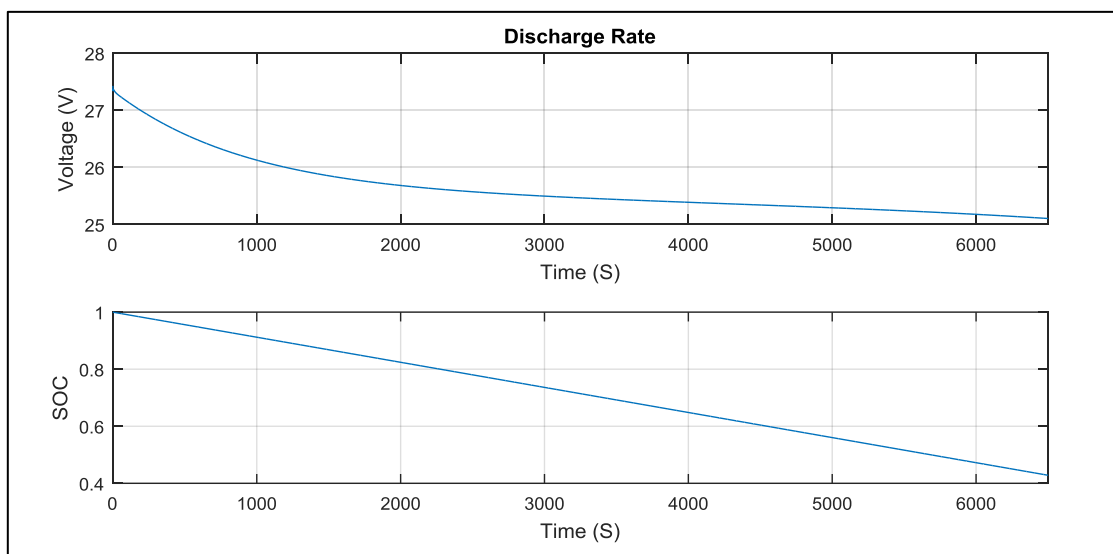


Fig. 2.37: Discharging Rate of a Ni-Cd Battery

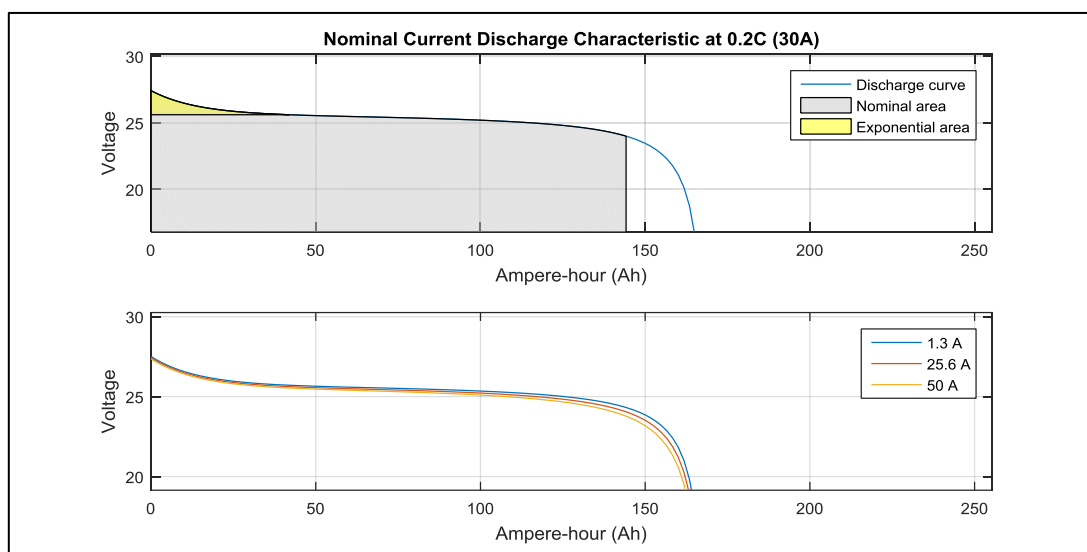


Fig. 2.38: Effects of Discharging Current on Rate of Discharge of a Ni-Cd Battery

Figure 2.38 above shows the effects of discharging current on nominal voltage. As with Pb-acid, Li-ion, and Ni-MH batteries, the voltage is significantly affected by the rate of discharge with lower discharge currents leading to slower discharge rates while higher discharge currents lead to faster discharge rates. The nominal area is the same as with Ni-Cd batteries and larger than in Li-Ion or Pb-Acid batteries.

2.5 Concluding Remarks:

In this chapter, PV power microgeneration systems have been reviewed and modelled. In the first section, PV power generators are reviewed, modelled and simulated. This section simulates I-V and P-V characteristics of solar cells, modules, and arrays in different configurations. Factors affecting PV power output such as partial shading and maximum power point are also modelled and simulated. In the second section, PV power electronics are reviewed, modelled and simulated. PV systems need converters for maximum power point tracking, power conditioning, grid interfacing, and voltage buck or boost. Different types of converters/inverters are explored. In the third section, energy storage technologies are reviewed. Batteries are essential for islanded PV systems and for stability in grid-connected PV systems. The merits and demerits of different battery technologies are explored. Four of the most common battery technologies used with PV systems, i.e., Pb-acid, Li-ion, Ni-MH, and Ni-Cd have been modelled and simulated in Matlab/Simulink. Results show that Li-ion batteries have faster charging/discharging rates and higher efficiencies compared to the other types of batteries. Ni-MH and Ni-Cd batteries have the longest discharge cycles and thus the largest nominal areas, making them the longest lasting for the rates sizes. Cadmium, however is very toxic and therefore the technology is not widely used in batteries for PV systems.

Chapter 3: Modelling PV Microgeneration Potential for Kendu Bay Area of Kenya

3.1 Introduction:

In this chapter, having reviewed and modelled solar electricity microgeneration systems in chapters 1 and 2, PV microgeneration potential for Kendu Bay area of Kenya is modelled and simulated. This is to ascertain the area's PV microgeneration capacity, necessary prior to conducting a survey of PV systems in the area. The models developed in this chapter, and their simulation results, are also used in chapters 5 and 6 to generate household power demand profiles. Kendu Bay area of Kenya was chosen as the ideal case study for this research because of many factors including its proximity to the equator, its socio-economic demographics which resembles those of many rural communities in Kenya, and other East African nations, and the present author's familiarity with the area, having been born and lived the area for most of his life.

3.2 Solar Radiation:

The sun emits radiation in all directions, with only a portion of this reaching the earth's surface. The solar constant, average incident power per unit area on a plane orthogonal to the sun's rays outside the earth's atmosphere, is expressed as $S = 1,367 \text{ W/m}^2$ [90]. Atmospheric absorption, coupled with scattering by molecules and particles, affect the distance travelled, and thus the intensity and spectrum of the sun's rays that pass through the atmosphere to the earth's surface. The optical path travelled by the photons that reach the earth's surface can be modelled in terms of air mass number (AMn), defined as [90]

$$AMn = \frac{1}{\cos \theta} \quad (3.1)$$

where $n = \sec \theta$ where θ is the zenith angle, the angular height of the sun measured from the vertical, and is given by

$$\theta = 90^\circ - \alpha \quad (3.2)$$

where α is the elevation (altitude) angle, angular height of the sun measured from the horizontal.

During equinoxes, the zenith angle at solar noon equals the latitude of the sites. Figure 3.1 below shows an illustration of zenith and elevation angles.

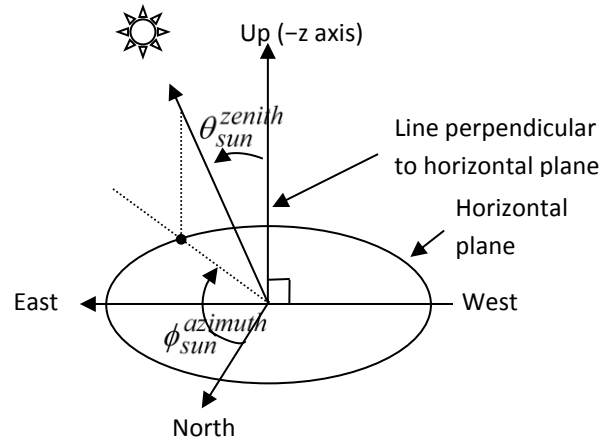


Fig. 3.1: Illustration of Zenith and Elevation Angles [90]

The elevation angle is given by

$$\alpha = \sin^{-1}[\sin \delta \sin \varphi + \cos \delta \cos \varphi \cos(HRA)] \quad (3.3)$$

where φ is the latitude of the PV module location and δ is the declination angle given by

$$\delta = \sin^{-1}\{\sin(23.45^\circ) \sin B\} \quad (3.4)$$

where 23.45° is the earth's tilt and

$$B = \frac{360}{365}(DOY - 81) \quad (3.5)$$

where DOY is the day of the year, with January 1st given as $d = 1$.

From equation 3.3, HRA is the hour angle and it is given by

$$HRA = 15^\circ(LST - 12) \quad (3.6)$$

where LST is the local solar time and is given by

$$LST = LT + \frac{TC}{60} \quad (3.7)$$

where LT is the local time while TC is the time correction factor, given by

$$TC = 4(Longitude - LSTM) + EoT \quad (3.8)$$

where $LSTM$ is the Local Standard Time Meridian and is given by

$$LSTM = 15^\circ \cdot \Delta T_{GMT} \quad (3.9)$$

where ΔT_{GMT} is the difference of the local time (LT) from Greenwich Mean Time (GMT) in hours.

From equation 3.8, EoT is the equation of time in minutes and it corrects the earth's axial tilt and eccentricity. It is given by

$$EoT = 9.87 \sin 2B - 7.53 \cos B - 1.5 \sin B \quad (3.10)$$

The current produced by a PV cell is directly dependent on the photon flux and the angle between the PV module and the sun. Azimuth angle is the compass direction from which the sunlight is coming. It varies with latitude, day of the year, and time of the day, and is given by

$$Azimuth = \cos^{-1} \left[\frac{\sin \delta \cos \varphi - \cos \delta \sin \varphi \cos(HRA)}{\cos \alpha} \right] \quad (3.11)$$

During equinoxes, the azimuth angle equals 90° at sunrise and 270° at sunset irrespective of the latitude. Elevation and azimuth angles are crucial for proper orientation of a PV module. The power density on a PV module is highest when it is orthogonal to sun rays. Figure 3.2 shows parameters used to calculate solar radiation on a tilted PV module.

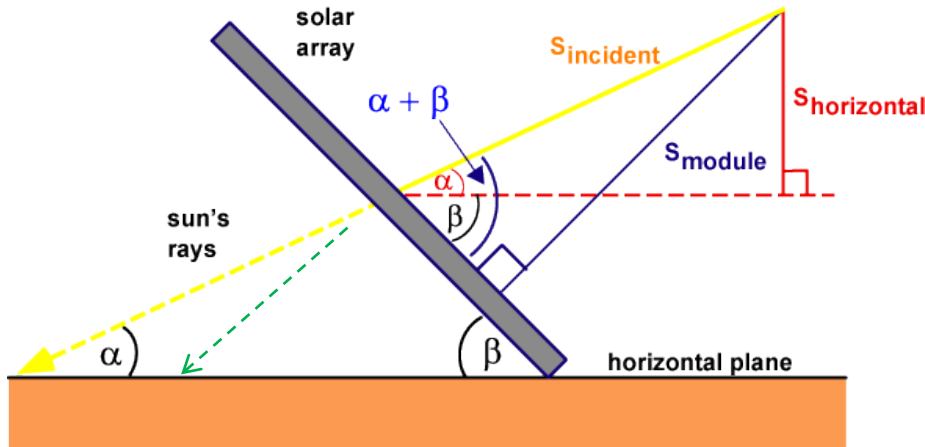


Fig. 3.2: Calculating Solar Radiation on a Tilted PV Module [91]

Solar radiation incident on a tilted module (S_{module}) is given by [91]

$$S_{module} = S_{incident} \sin(\alpha + \beta) \quad (3.12)$$

where $S_{incident}$ is the solar radiation measured orthogonal to the sun rays, α is the elevation angle, and β is the tilt angle of the module measured from horizontal. Solar radiation measured from horizontal ($S_{horizontal}$) is given by [91]

$$S_{horizontal} = S_{incident} \sin \alpha \quad (3.13)$$

Since the radiation absorption rate is proportional to the photon energy, both the intensity and distribution of the radiation over different photon energies affect the efficiency of a solar cell [91]. Air mass number (AMn) is used to define the optical path travelled by the photons that reach the earth's surface [92]. AM0 corresponds to solar spectrum outside the earth's atmosphere and is used for extra-terrestrial PV applications. AM1 corresponds to the minimum possible optical path travelled by the sun's rays through the atmosphere to the earth's surface, i.e. direct overhead cast. AM1.5-direct (AM1.5D) and AM1.5-global (AM1.5G) are the standard solar spectra for terrestrial applications; AM1.5D spectrum represents solar radiation as received directly from the sun after atmospheric losses while AM1.5G adds indirect radiation coming from a 2π field-of-view, due to Rayleigh scattering by molecules in the atmosphere and ground reflection, to the AM1.5D spectrum [93]. Figure 3.3 shows plots of AM0, AM1.5G, and AM1.5D spectra.

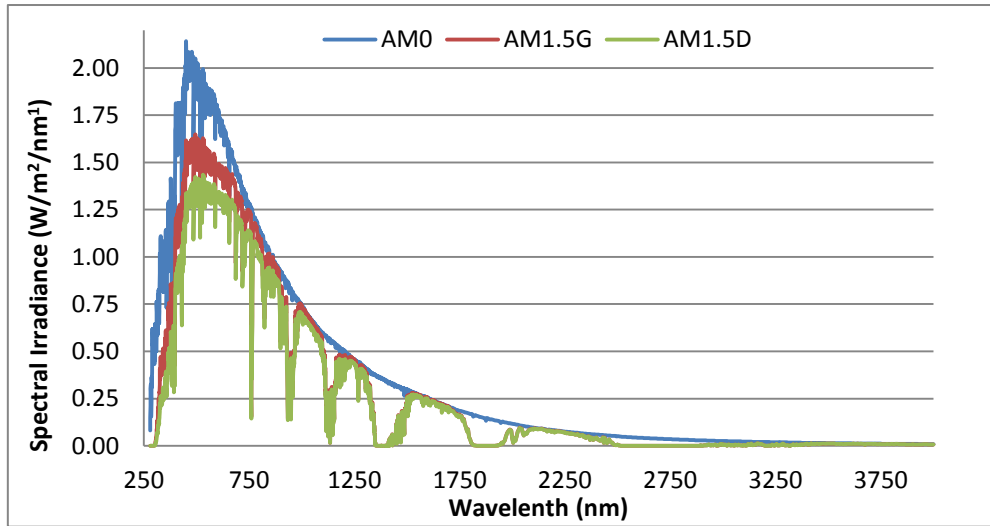


Fig. 3.3: Spectral Distributions for AM0, AM1.5G, and AM1.5D

The intensity of direct solar irradiance on a solar module orthogonal to the sun's rays on a given day is given by

$$I_D = 1.353 \times 0.7(AM^{0.678}) \quad (3.14)$$

and it increases with altitude. On a clear day, the global irradiance on a module orthogonal to the sun's rays is given by

$$I_G = 1.1 \times I_D \quad (3.15)$$

and the power density on the module is equal to the incident power density, and reduces as the angle between the sun rays and the module changes ($\cos \theta$), eventually reaching zero when the rays are parallel to the plane (angle to module normal = 90°). A location's latitude, longitude, day of the year, and time of the day are all necessary for complete irradiance modelling. External irradiance directly affects the amount of power generated by a solar home system and thus the net power exported or imported by a household. It also directly affects a household's power demand, especially as pertains to lighting and heating. Heavy cloud cover could mean increased lighting and heating demands while at the same time meaning a reduction in PV output.

3.3 Irradiance Data Modelling:

Photovoltaic systems directly convert sunlight into electricity and therefore irradiance data is necessary for modelling a PV system's performance for a given location and time since variations in solar radiation directly translate into variations in the power output of a PV system. High resolution empirical irradiance data for specific locations and times are not always available necessitating the use of models to estimate such data. Clear sky models are often used to estimate solar irradiance as a function of the solar elevation angle, site altitude, aerosol concentration, water vapour, and other atmospheric conditions, under cloudless and cloudy conditions [94,95]. Even on the clearest of days about 25% of radiation from the sun is scattered and absorbed as it passes through the atmosphere. Part of the scattered irradiance is directed towards earth and is called diffuse irradiance. This also includes radiation reflected from the earth's surface. Total radiation on a horizontal surface, global horizontal irradiance (*GHI*), is a sum of direct normal irradiance (*DNI*) and diffuse radiation on a horizontal surface, i.e.

$$GHI = Diffuse + DNI \times \cos \theta \quad (3.16)$$

where θ is the zenith angle.

Clear sky models can be divided into three groups namely: very simple models, simple models, and complex models. Very simple clear sky models are calculated using only empirical data and the

zenith angle and are thus less accurate for sites other those whose empirical data were used to calibrate the models [94-96]. Examples of very simple clear sky models include:

Daneshyar-Paltridge-Proctor (DPP) model developed in 1978 and expressed as [97,98]

$$DNI = 950.2[1 - \exp(-0.075(90^\circ - \theta))] \quad (3.17)$$

$$Diffuse = 14.29 + 21.04(\frac{\pi}{2} - \theta \frac{\pi}{180}) \quad (3.18)$$

$$GHI = Diffuse + DNI \times \cos \theta \quad (3.19)$$

Kasten-Czeplak (KC) model developed in 1980 and expressed as [99]

$$GHI = 910 \times \cos \theta - 30 \quad (3.20)$$

Haurwitz model developed in 1979 and expressed as [100,101]

$$GHI = 1098 \times \cos \theta \times \exp\left(\frac{-0.057}{\cos \theta}\right) \quad (3.21)$$

Berger-Duffie (BD) model developed in 1979 and expressed as [94]

$$GHI = I_0 \times 0.70 \times \cos \theta \quad (3.22)$$

where I_0 is the extraterrestrial normal incident irradiance

Adnot-Bourges-Campana-Gicquel (ABCG) model developed in 1979 and expressed as [94]

$$GHI = 951.39 \times (\cos \theta)^{1.15} \quad (3.23)$$

Robledo-Soler (RS) model developed in 2000 and expressed as [102]

$$GHI = 1159.24 \times (\cos \theta)^{1.179} \times \exp[-0.0019 \times (90^\circ - \theta)] \quad (3.24)$$

Meinel model developed in 1976 and expressed as [103,104]

$$DNI = I_0 \times 0.7^{AM_n^{0.678}} \quad (3.25)$$

And the Laue model developed in 1970 and expressed as [103,104]

$$DNI = I_0 \times [(1 - 0.14 \times \alpha) \times 0.7^{AM^{0.678}} + 0.14 \times \alpha] \quad (3.26)$$

where α is the elevation angle.

Simple clear sky models add basic atmospheric parameters such as air pressure, temperature, relative humidity, aerosol, and Rayleigh scattering to the parameters used in very simple clear sky models. Examples include the Kasten model expressed as [105]

$$GHI = 0.84 \times I_0 \times \cos \theta \times \exp[-0.027 \times AM \times (f_{\alpha 1} + f_{\alpha 2}(TL - 1))] \quad (3.27)$$

where TL is the Linke Turbidity factor [106] and

$$f_{\alpha 1} = \exp(-\alpha/8000) \quad (3.28)$$

$$f_{\alpha 2} = \exp(-\alpha/1250) \quad (3.29)$$

Complex models are more accurate than simple models but also require many more inputs such as ozone, aerosols, and perceptible water. An example is the MAC model which takes into account effects of Rayleigh scattering by molecules, the ozone layer, aerosols, and water vapour [107,108]. It is represented by the following set of equations:

$$GHI = DNI \times \cos \theta + D_R + D_A \quad (3.30)$$

$$DNI = I_0(T_0 T_r - a_w) T_a \quad (3.31)$$

$$D_R = I_0 \cos \theta T_0 (1 - T_r)/2 \quad (3.32)$$

$$D_A = I_0 \cos \theta (T_0 T_r - a_w)(1 - T_a) \omega_0 f \quad (3.33)$$

where D_R is the Rayleigh scatter, D_A represents scattering by aerosol, ω_0 is the spectrally-averaged single scattering albedo for aerosol, f is the ratio of forward total scattering by aerosols, a_w is the absorptivity of water vapour, T_r is the transmissivity due to Rayleigh scattering, T_a is the transmissivity due to absorption by aerosols and is between 0.84 and 0.91 [109], and T_0 is the transmissivity of the ozone layer given by

$$T_0 = 1 - a_0 \quad (3.34)$$

where a_0 is the absorption coefficient by ozone and is given by

$$a_0 = \frac{0.1082 \times x_0}{1 + 13.86 \times x_0^{0.805}} + \frac{0.00658 \times x_0}{1 + (10.36 \times x_0)^3} + \frac{0.00218}{1 + 0.0042 \times x_0 + 3.23 \times 10^{-6} \times x_0^2} \quad (3.35)$$

where x_0 is the equivalent length of the radiation path through the depth of the ozone layer in the atmosphere (μ_0) and is given by

$$x_0 = AM_n \times \mu_0 \quad (3.36)$$

Transmissivity due to Rayleigh scattering, T_r , is given by

$$T_r = 0.9768 - 0.0874 \times AM_n + 0.010607552 \times AM_n^2 - 8.46205 \times 10^{-4} \times AM_n^3 + 3.57246 \times 10^{-5} \times AM_n^4 - 6.0176 \times 10^{-7} \times AM_n^5 \quad (3.37)$$

The absorptivity of water vapour in the atmosphere, a_w , is given by

$$a_w = \frac{0.29 \times x_w}{(1 + 14.15 \times x_w)^{0.635} + 0.5925 \times x_w} \quad (3.38)$$

where x_w is the length of the radiation path through thickness of the water vapour layer in the atmosphere and is given by

$$x_w = AM_n \times \frac{4.93u}{T} \times \exp\left(26.23 - \frac{5416}{T}\right) \quad (3.39)$$

where u is the humidity while T is the temperature.

There are many other complicated clear sky models developed and published in various academic sources including the Bird model which was developed after Bird and Hulstrom analysed and compared six different clear-sky models to spectral baseline dependence on aerosol transmittance, transmittance after Rayleigh scattering, water vapour transmittance, and ozone transmittance [110-112], and the REST2 model which was developed by Gueymard after analysing 11 clear-sky models to test their validity and performances [113,114].

In this chapter, solar microgeneration potential for rural Kenya is modelled and simulated to ascertain its viability as an alternative route to rural electrification-beyond-lighting. Minutely global irradiance data for a location of interest, Kendu Bay in this case, is synthetically generated using a simple clear sky model. The data is then used to simulate and generate PV microgeneration data for

the given area. A stochastic active-occupancy model is used to generate minutely household power demand data based on a household's occupancy, time of the day, and day of the week using a list of common household appliances found in a modern Kenyan household. The power demand data are then compared to the PV generation data to determine whether enough power is produced over a given period to satisfy a household's demands. Communal grids comprising of 25 and 100 similar households are also simulated in AC-coupled configurations to explore their potential applications in providing high capacity power (electricity-beyond-lighting) to rural households.

3.4 Methodology:

3.4.1 Clear-Sky Model:

The clear sky model requires the following inputs: empirical global irradiance data of the location of interest, latitude, longitude, solar position, time of the day, and day of the year [115-118]. The model generates minutely data over 24 hours per simulation run. Empirical global irradiance data for Kenya provided by the Kenya Meteorological Department (KMD), with the desired resolution, are only available for the following locations and only for the 15th of March 2007: Nairobi (central Kenya), Mombasa (southern/costal Kenya), Kisumu (western Kenya), and Garrisa (north eastern Kenya). The model can be used to generate synthetic irradiance data for any day, using the one set of available irradiance data. Moreover, the empirical data from the above locations could be applied to areas within their vicinities due to negligible variations in climatic patterns. In this case, the data for Kisumu are used to generate data for Kendu Bay. The equation of time is used to provide a relationship between solar noon and local time at a given longitude. The model then calculates the clear sky radiation (*CSR*) using the following equation

$$CSR = (K_B + K_D)R_E \quad (3.40)$$

where K_B is the clearness index of the direct beam component of the solar radiation, K_D is the transmissibility index of the diffuse component of the solar radiation, and R_E is the extraterrestrial radiation and is given by

$$R_E = \frac{S \cos \theta}{d^2} \quad (3.41)$$

where S is the solar constant and equals 1367 W/m^2 , θ is the zenith angle, d^2 is a function of the day of the year (*DOY*) and is given by

$$d^2 = \frac{1}{1 + 0.033 \cos\left(\frac{2\pi \times DOY}{365}\right)} \quad (3.42)$$

The clearness index of the direct beam component of the solar radiation, K_B is given by

$$K_B = 0.98 \exp\left[\frac{0.00146P}{K_t \sin \beta} - 0.075 \left(\frac{W}{\sin \beta}\right)^{0.4}\right] \quad (3.43)$$

where K_t is the turbidity coefficient and its value is between 0 and 1, with 1 representing a clear day. β is the sun angle, P is the atmospheric pressure, and W is the perceptible water given by

$$W = 0.14e^a P + 2.1 \quad (3.44)$$

where e^a is the actual vapour pressure and is given by

$$e^a = e^0 \frac{Rh}{100} \quad (3.45)$$

where Rh is the relative humidity while e^0 is a saturated vapour pressure coefficient given by

$$e^0 = 0.618 \exp\left(\frac{17.27T}{T + 237.5}\right) \quad (3.46)$$

where T is the temperature.

Transmissibility index for the diffuse component of the solar radiation, K_D , is expressed as

$$K_D = 0.35 + 0.36K_B \text{ for } K_B > 0.15 \quad (3.47)$$

or

$$K_D = 0.35 - 0.36K_B \text{ for } K_B > 0.15 \quad (3.48)$$

Once the model has calculated and generated the minutely clear sky irradiance data, it then generates a stochastic clearness index (K_C) using the following formula [119]

$$K_C = \frac{I_{MG}}{CSR} \quad (3.49)$$

where I_{MG} is the measured minutely global irradiance data.

Transition Probability Matrix (TPM) of the clearness index is constructed using measured minutely global irradiance data. The TPM estimates the probability of transition from one possible clearness

state to any other possible state. The measured minutely global irradiance data for a specific location over one-year period was separated into 12 separated data series for each month of the year, with each data series consisting of between 40,320 to 44,640, depending on the month. Climatic variations due to seasonal changes are negligible as Kenya sits astride the equator with no noticeable seasonal variations. This makes use of a year's worth of data adequate. The probability of transition is determined by counting the number of times a value is followed by another value and dividing by the number of times the value appears in the time series of data. Each TPM is constructed with a range of 0.01 to 1 along the horizontal and vertical axes of the matrix. The probability of transition between the values on the vertical axis and the values on the horizontal axis are then determined thus generating a TPM where the probability of transition between each possible clearness index is quantified. Table 3.1 below shows a portion of the TPM. Transitions occur from left to right, with the numbers in bold showing current state.

	To State										
		0.1	0.2	0.3	0.4	0.5	0.6	0.7	0.8	0.9	1.0
From State	0.1	0.00	0.00	0.00	0.00	0.00	0.00	0.00	0.01	0.00	0.01
	0.2	0.00	0.00	0.00	0.00	0.00	0.01	0.01	0.01	0.00	0.01
	0.3	0.00	0.01	0.00	0.01	0.00	0.01	0.02	0.02	0.02	0.01
	0.4	0.00	0.00	0.00	0.00	0.00	0.01	0.00	0.01	0.02	0.00
	0.5	0.00	0.01	0.01	0.00	0.01	0.00	0.01	0.01	0.02	0.01
	0.6	0.00	0.00	0.00	0.00	0.00	0.02	0.02	0.00	0.00	0.01
	0.7	0.00	0.00	0.00	0.00	0.00	0.00	0.01	0.00	0.01	0.01
	0.8	0.00	0.00	0.00	0.00	0.00	0.01	0.00	0.00	0.01	0.01
	0.9	0.00	0.00	0.00	0.00	0.01	0.01	0.00	0.00	0.01	0.01
	1.0	0.00	0.00	0.00	0.00	0.00	0.00	0.01	0.00	0.01	0.00

Table 3.1: Section of the Clearness Index Transition Probability Matrix

Given the clearness index, net global irradiance, I_{NG} , can be calculated by multiplying simulated minutely clearness index by the corresponding clear sky irradiance data as expressed below

$$I_{NG} = K_C \times CS \quad (3.50)$$

For simulation of PV power generation, the model requires inputs of the module surface area, orientation, and efficiency, and then uses the generated net global radiation data (I_{NG}) to calculate the generated power by a single household and by 25 and 100 such similar households connected in AC-coupled communal grids as schematically shown in figure 3.4 below. AC coupling allows for generated power to be distributed around a grid easily for high voltage systems, in addition to

providing higher efficiency for loads operating during the day. In this configuration, generated power is immediately converted into AC and then interconnected with the AC loads. Power is converted back into DC to recharge the batteries pack.

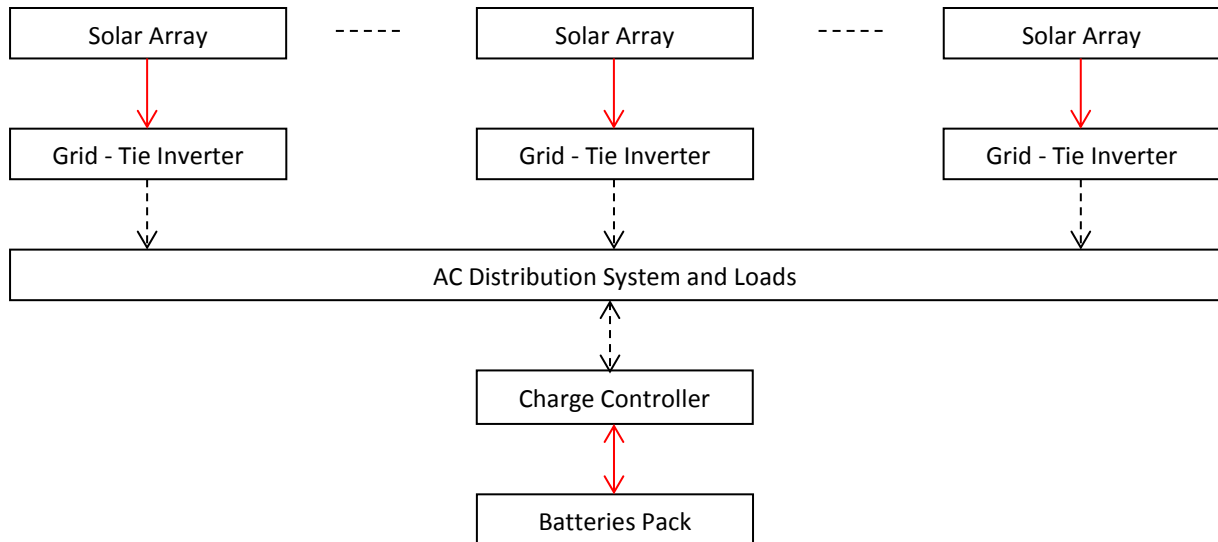


Fig. 3.4: Schematic Diagram of an AC Coupled Communal Grid

Figure 3.5 below summarizes the sequences of operation of the clear-sky model.

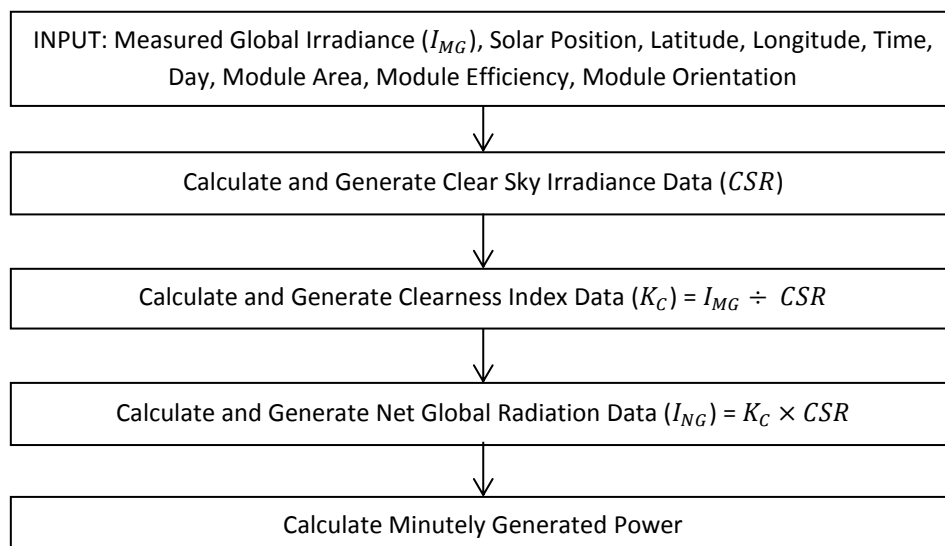


Fig. 3.5: Sequence of Operation of the Clear-Sky Model

3.4.2 Active-Occupancy Model:

A domestic electricity demand model developed and validated by Richardson et al is adopted for use in this research [120]. Minutely household power demand data is generated using stochastically

allocated load profiles based on the time of the day, on the day of the week (weekday or weekend), and on the level of active occupancy from the following list of appliances based on data from the Kenya's Central Bureau of Statistics (KCBS): Fridge/Freezer, Radio/CD Player, Clock, Telephone (Charger), Iron, Personal Computer, Printer, Fan, Water Dispenser, TV, VCR/DVD, DSTV Box, Hob, Oven, Microwave, Kettle, Toaster, Washer, Dryer, Water Heater (Shower), and Lighting [121]. Each appliance is assigned an annual energy demand in kWh/y using data from KCBS. All appliances are assumed to be off at the beginning of each simulation run. Appliances on standby are also assumed to be off. Due to limited demand profiles data, appliances are assumed to have constant power demands when switched on.

Given a total number of residents in a house, the active occupancy model stochastically assigns the number of active people in the house at a given time, and uses this data to allocate appliances accordingly, based on the time of the day, and on the day of the week [120-123]. An activity profile, the probability of a specific appliance being on at certain times or during specific activities, for example the TV being on at night or the hob and the oven being on during cooking, is assigned to every appliance to enable varying allocation of appliances during the simulation. The active occupancy profiling enables sharing of appliances or correlated use of appliances to be taken into account when simulating demand. Active occupancy and domestic electricity demand simulation runs are used with generation data to calculate power exported by a household. Power is exported if power demanded is less than power generated. Since the active occupancy model is stochastic, different results are obtained for every simulation run. Figure 3.6 summarizes the sequences of operation of the active occupancy model:

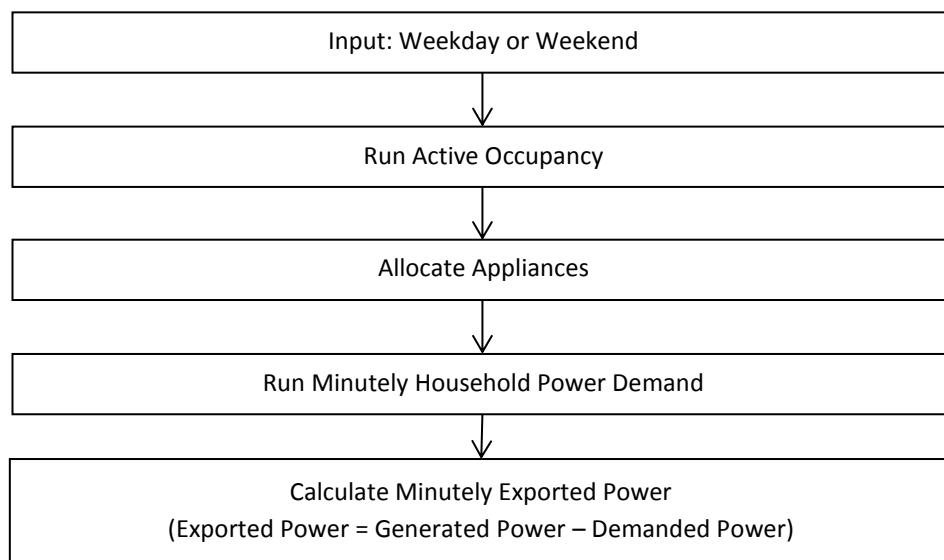


Fig. 3.6: Sequence of Operation of the Active Occupancy Model

3.5 Results and Discussion:

Empirical minutely global irradiance data provided by the Kenya Meteorological Department is compared to simulated clear sky and net irradiance data to ascertain the validity of the clear-sky model. The active-occupancy model is based on a validated model by Richardson et al [120] and no further validation was done.

Figure 3.7 shows a comparison of measured global irradiance data for Kisumu on the 15th of March 2007 and simulated clear-sky irradiance data for Kendu Bay for the same day. As mentioned before, due to their proximity, about 20 km apart, empirical data from Kisumu can be used to model synthetic data for Kendu Bay. The two plots fit well; in both cases, there is evenly distributed daylight of about 12 hours with 8 hours of strong irradiance, peaking at about noon. For the empirical data plot, there are many occasions of attenuations caused by changing weather patterns (passing clouds), but the overall shape of the curve is easily visible. Due to semi-aridity of the region, as with most of rural Kenya, the cloud cover is limited and hardly lasts.

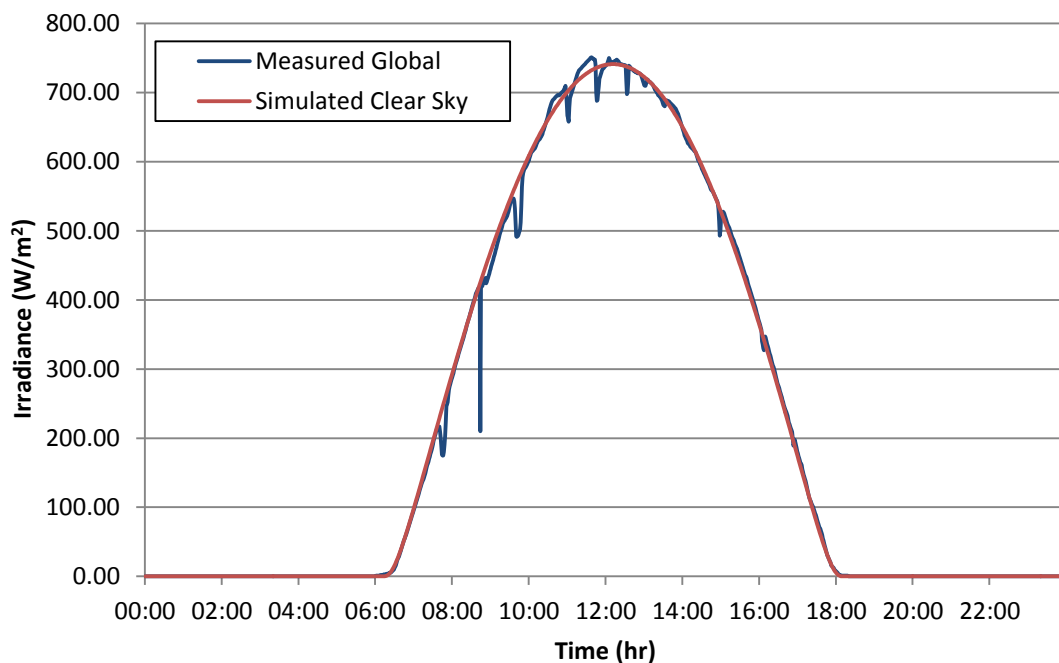


Fig. 3.7: Comparison of Simulated Clear Sky and Measured Global Irradiance Profiles

Figure 3.8 shows a comparison of measured global and simulated net radiation data while figure 3.9 shows plots of simulated clear-sky and net radiation profiles. Net radiation is the product of clear-sky radiation and clearness index. The plots show a relatively clear day with short cloudy moments;

every simulation run produces different clearness index result due to the stochastic nature of the model, and thus different net radiation profile. The simulated net radiation data fits well with measured data and with simulated clear sky data, further giving validity to the clear-sky model. Table 3.2 shows a partial representation of the above information.

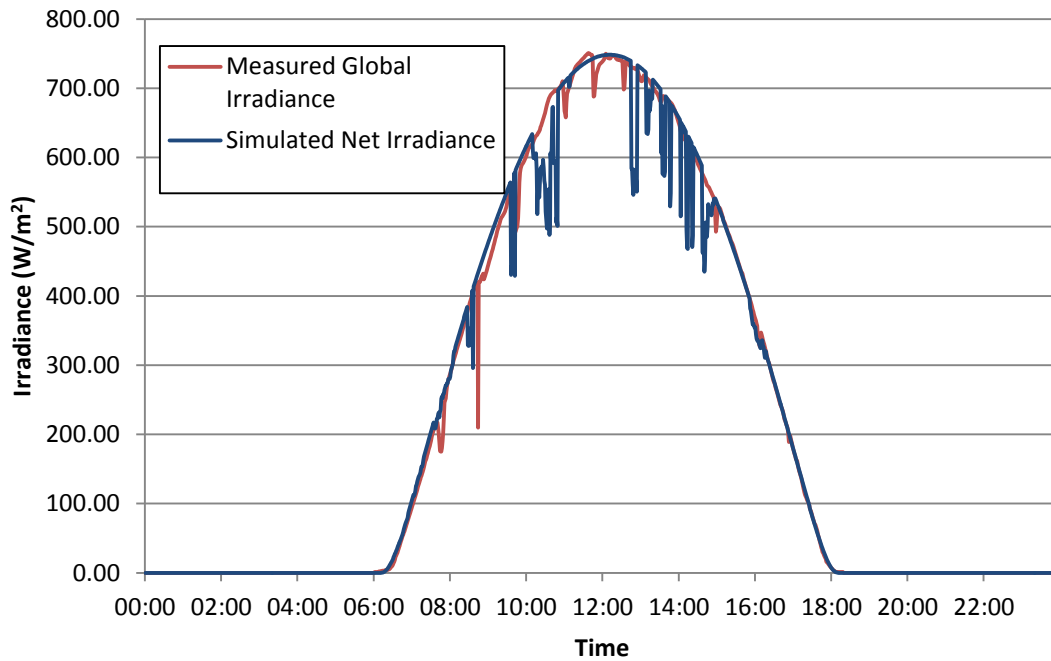


Fig. 3.8: Comparison of Measured Global and Simulated Global Irradiance Profiles

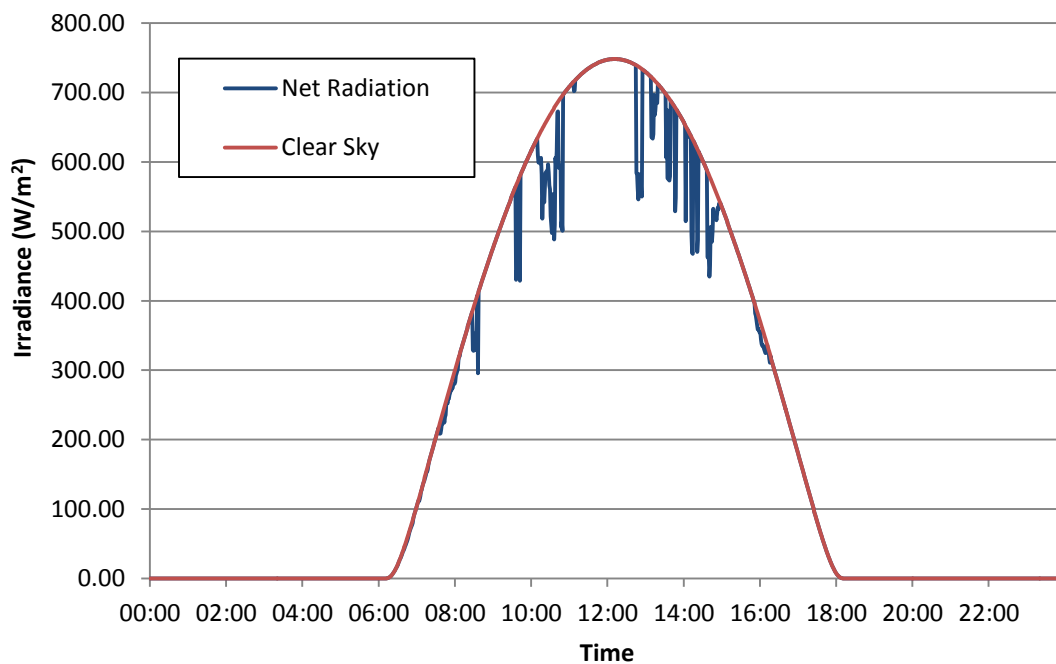


Fig. 3.9: Comparison of Simulated Clear Sky and Global Irradiance Profiles

Time	Measured Global Irradiance	Simulated Clear Sky	Simulated Clearness Index	Simulated Global Radiation
06:00	0.00	0.00	1.00	0.00
07:00	96.00	106.07	1.00	106.07
08:00	288.00	301.31	0.94	283.23
09:00	445.00	477.43	1.00	477.43
10:00	603.00	616.75	1.00	616.75
11:00	667.00	708.91	1.00	708.91
12:00	739.00	747.41	1.00	747.41
13:00	711.00	729.57	1.00	729.57
14:00	648.00	656.63	1.00	656.63
15:00	517.00	533.70	1.00	533.70
16:00	367.00	369.66	0.96	354.87
17:00	178.00	178.27	1.00	178.27
18:00	7.00	6.89	1.00	6.89
19:00	0.00	0.00	1.00	0.00

Table 3.2: Comparison of Measured and Simulated Irradiance Data (W/m²)

Table 3.3 shows a partial representation of the comparisons of power generated by a single solar home system, a microgrid of 25 such systems, and a minigrid of 100 such systems, while figure 3.10 shows plots of comprehensive data on the same.

Time	Singe SHS	25 SHS (Microgrid)	100 SHS (Minigrid)
06:00	0.00	0.00	0.00
07:00	0.16	3.98	15.91
08:00	0.42	10.62	42.48
09:00	0.72	17.90	71.61
10:00	0.93	23.13	92.51
11:00	1.06	26.58	106.34
12:00	1.12	28.03	112.11
13:00	1.09	27.36	109.43
14:00	0.98	24.62	98.49
15:00	0.80	20.01	80.05
16:00	0.53	13.31	53.23
17:00	0.28	6.69	26.74
18:00	0.01	0.26	1.03
19:00	0.00	0.00	0.00

Table 3.3: Comparison of Power Generated by Single, 25, and 100 SHS (kW)

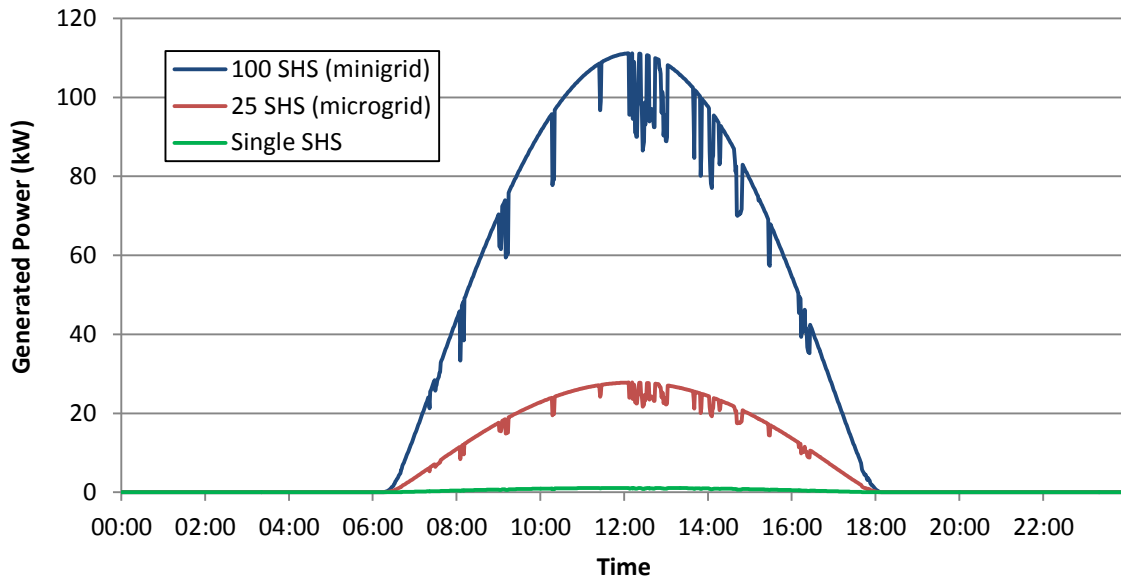


Fig. 3.10: Comparison of Power Generated by One, 25, and 100 SHS

The plots correlate because they are based on the same simulated irradiance data. For this simulation run, a total of 7.87 kWh is generated by a single solar home system with an area of 15 m², rated efficiency of 10%, and orientation of 0°. Ignoring ohmic losses, the microgrid generated a total of 196.65 kWh while the minigrid generated 786.60 kWh. Gridding provides an effective storage method for generated power as it is difficult to match demand to supply at any given moment due to continuously changing weather patterns and household activities. Gridding, therefore, enables efficient power management.

3.5.1 Single Household Power Demand – Weekend:

Figure 3.11 shows plots of active occupancy and power demand for a weekend simulation run. Each simulation run produces different result from the previous one due to stochastic nature of the model, with many occasion of reactive power being shown on the plot. The demand profile is determined by social factors such as usual family gathering times such as meal times, school and work times, etc. Many runs would be needed to see a true emerging pattern. In this simulation run, there is limited activity in the morning but this changes in the afternoon from when we see increased activity into late night. As expected, activity and power demand correlate. A total of 6.78 kWh is demanded for this simulation run. The power demand data are used to calculate power exported to the grid. For this particular simulation run, a total of 7.87 kWh was generated by the PV system of which 6.21 kWh was exported to the grid, meaning a self-consumption of about 1.66 kWh. The PV system generates enough power for this household' demands, however, demand and supply times do not always match and therefore a total of 5.12 kWh was imported from the grid. Without

the grid, a properly sized battery pack would need to be provided to cater for this mismatch, otherwise generated power would go to waste.

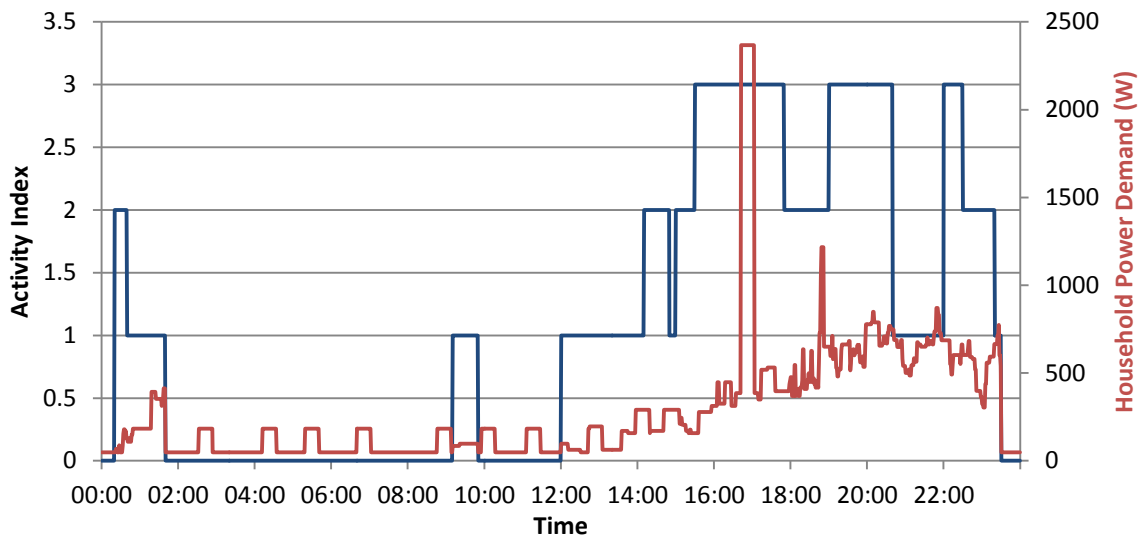


Fig. 3.11: Active Occupancy and Power Demand on a Weekend

Figure 3.12 shows plots of generated and demanded power for a weekend simulation run. No power is generated during the night, meaning all power demanded during this period is imported from the grid, in case of lack of appropriate power pack. On the other hand, most of PV power is generated during the day, when, according to activity index, there is little demand. Most of this power is exported to the grid.

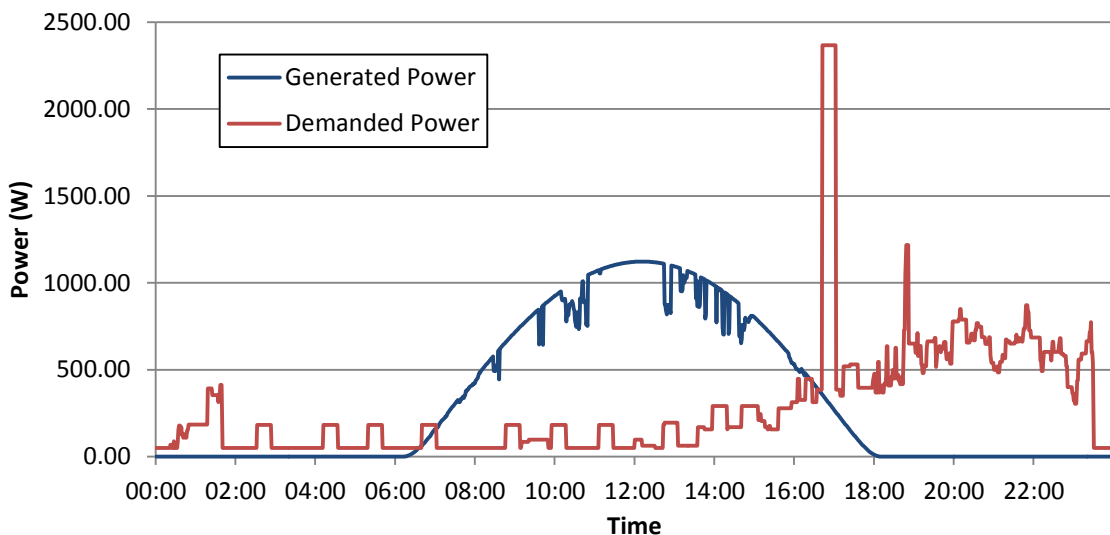


Fig. 3.12: Generated and Demanded Power on a Weekend

Figure 3.13 shows plots of imported and exported power. Power is imported when there is no solar insolation and thus zero generation by the PV system. On the other hand, power is exported during

the day when the PV system is generating electricity. Overall, the system exports more power than it imports; a net of 1.09 kWh is sold by this household to the grid.

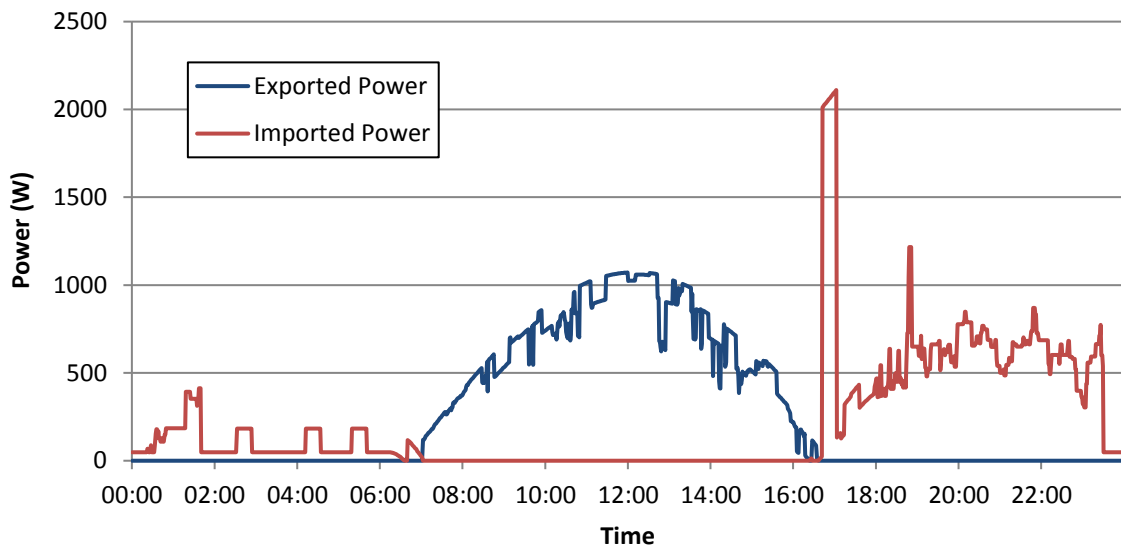


Fig. 3.13: Exported and Imported Power on a Weekend

3.5.2 Single Household Power Demand – Weekday:

Figure 3.14 shows plots of active occupancy and domestic power demand for a weekday simulation run. The occupants are mainly active between 6 and 8 am and again in the evening after 4.00 pm. These are the times when people prepare to go to work or to school and when people return from work or from school; household activities are highest during these periods and thus the correlated power demands.

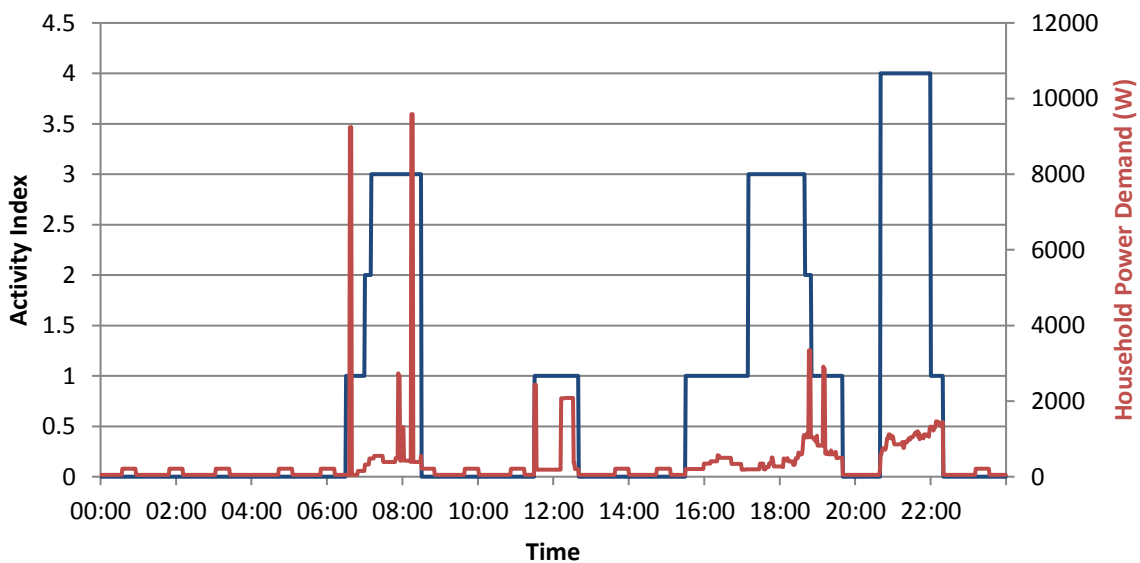


Fig. 3.14: Active Occupancy and Power Demand on a Weekday

Figure 3.15 shows plots of generated and demanded power while figure 3.16 shows plots of exported and imported power. A total of 7.96 kWh is demanded, of which 5.66 kWh is imported from the grid; the household exports a total of 5.57 kWh from the PV system after a self-consumption of 2.3 kWh. Overall, more power is imported than exported; the household buys a net of 0.09 kWh from the grid. The two moments of power spikes in the morning could indicate use of an appliance which demands large amount of power. The appliance is used for only a short moment at a time.

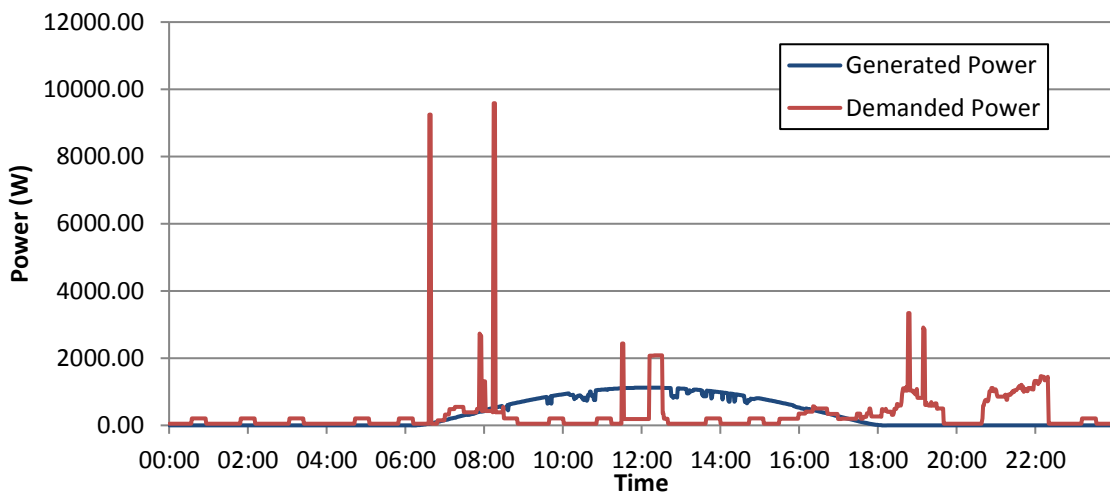


Fig. 3.15: Generated and Demanded Power on a Weekday

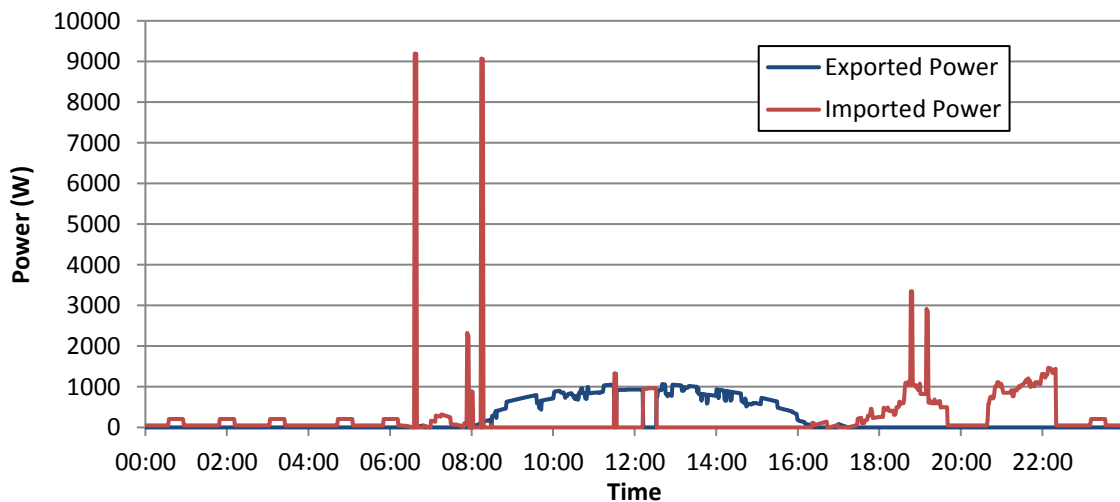


Fig. 3.16: Exported and Imported Power on a Weekday

3.5.3 Microgrid and Minigrid:

Table 3.4 below summarizes the different power structures for a single household, a microgrid of 25 such households, and a minigrid of 100 such households. All the systems are based on a 100 Wp PV system and different results would be obtained with differently sized systems.

Power (kWh)	Weekend			Weekday		
	Single SHS	25 SHS (Microgrid)	100 SHS (Minigrid)	Single SHS	25 SHS (Microgrid)	100 SHS (Minigrid)
Generated	7.87	196.65	786.60	7.87	196.50	786.60
Demanded	6.78	159.60	651.75	7.96	179.25	721.80
Imported	5.12	121.35	498.30	5.66	123.50	476.40
Self-Consumption	1.66	38.25	153.45	2.30	55.75	245.40
Exported	6.21	158.40	633.15	5.57	140.90	541.20
Net Export/Import	1.09 (sold)	37.05 (sold)	134.85 (sold)	-0.09 (bought)	17.40 (sold)	64.80 (sold)

Table 3.4: Comparison of Power Structures for Different Arrangements of 100 Wp PV Systems.

For a weekend simulation run, 25 similar households connected in a microgrid configuration would demand a total of about 159.60 kWh against a generation of 196.65 kWh. 121.35 kWh would be imported from the national grid against an export of 158.40 kWh, leaving a self-consumption of about 38.25 kWh. Overall, the system would export more power than it consumes, selling about 37.05 kWh to the grid. A minigrid of 100 households would demand about 651.75 kWh against a generation of 786.60 kWh. About 498.3 kWh would be imported from the grid while 633.15 kWh would be exported to the grid. The overall self-consumption would be about 153.45 kWh. A net of 134.85 kWh would be sold to the grid. For a weekday simulation run, about 179.25 kWh is demanded by the microgrid, of which 123.50 kWh is imported from the grid. A total of 140.90 kWh is exported by the system, leaving a self-consumption of about 55.75 kWh. Overall the system exports more power than it imports, with the difference being 17.4 kWh, which is sold to the grid. The minigrid demands about 721.80 kWh of electricity, of which 476.4 kWh is imported. A total of 541.20 kWh is exported, leaving a self-consumption of about 245.4 kWh. Again, more power is exported by the minigrid than is imported, with the difference being 64.8 kWh, which is sold to the grid.

3.6 Concluding Remarks:

High resolution irradiance data based on a location of interest, Kendu Bay, Kenya, is simulated using a stochastic clear-sky model and based on available empirical data from a nearby location with similar climatic condition, i.e., Kisumu, Kenya. The irradiance data is used to model and simulate PV microgeneration potential for a single household, 25 households, and 100 households, taking into account module surface areas, efficiencies, and orientations. Minutely household power demands

are modelled and simulated using a stochastic active occupancy model. The results are used to calculate power imported and exported by the household(s) on a minutely basis, and overall. Results show that there is great potential for solar microgeneration in Kendu Bay, with strong solar insolation throughout the year; there are little seasonal variations and little cloud cover, boosting PV microgeneration potential. For efficient generation and consumption, results show that connecting many solar home systems into communal grids reduces power losses due to improper storage or due to demand versus generation mismatches; a single household imported more power than it exported during a weekday simulation run while 25 or 100 such households connected in a communal grid exported more power than they imported. The stochastic nature of the household power demand model produces different demand profiles for every simulation run, however, it is clear from the data obtained that gridding enables more efficient power consumption than stand-alone systems. In addition, gridding provides effective storage for generated power while also reducing the overall expenses incurred by an individual household vis-à-vis battery costs. Based on these results, a survey of solar home systems was carried out in Kendu Bay area to collect data on their installations and on factors affecting choices of electrification in the area, with survey findings then applied to further research on rural electrification options for rural Kenya.

Chapter 4: A Survey of PV Microgeneration Systems in Kendu Bay Area of Kenya

4.1 Introduction:

In this chapter, having modelled and simulated the potential for PV power generation in Kendu Bay area of Kenya in chapter 3 and obtained satisfactory results, a household survey was developed and carried out to identify patterns and sources of electrification in the area. Broadly, the survey sought to identify the reasons behind different household electrification choices and how those choices affected other energy use patterns such as cooking fuels, appliances etc., within the same household. Specifically, the survey sought to gather as much information as possible on PV installations in the area to identify key drivers of such installations. As mentioned in chapter 3, Kendu Bay area of Kenya was chosen as the most suitable location for this survey because of its proximity to the equator and thus good solar generation potential, its population distribution which mirrors those of other rural towns all over Kenya, and its socio-economic activities, which also mirror those of other small towns all over Kenya.

Kenya's national electrification rate stands at 23%, with the situation being even worse in rural areas where over 76% of the population resides; latest figures show that rural grid electrification rate stands at less than 5% [124]. The country still heavily relies on unsustainable low-grade forms of fuel, especially biomass (firewood and charcoal), for its primary energy needs. In 2014 for example, biomass accounted for 69% of all energy consumed in Kenya [124]. During the same period, electricity accounted for only 9% of the total energy consumed, with petroleum and petroleum products accounting for the remaining 22%, and for 25% of the national import bill in 2014 [124]. Overreliance on imported petroleum and petroleum products makes Kenya vulnerable to global energy insecurities and has thus made it suffer considerably due to fluctuations in petroleum prices; the first oil-shock of 1973-1974 interrupted Kenya's robust post-colonial economic growth, nearly sending it into recession [121]. The second oil shock of 1979 sent Kenya's economy into a nosedive that persisted through the global recession of the early 1980s. Recently, political unrest in Northern Africa and the Middle East has again adversely affected the country's rebounding economy, leading to increased inflation rates with no commensurate increases in wages.

Kenya's energy policy and a core pillar of its millennium development goals is to provide clean, sustainable, affordable, and secure energy for all of its citizens. Towards this end, it has embarked

on an ambitious plan to achieve a 100% national electrification rate by 2030 by putting up large central power plants based on coal and natural gas, both not currently mined in Kenya, and which will thus add to its import expenditure [124]. In the meantime, the government has started to expand its national grid network, from the current 3,767 km to about 16,000, in anticipation of increased power capacity [124]. As with many developing nations, Kenya's national grid is strained and plagued by frequent power blackouts, high system losses, and poor maintenance, and is therefore unreliable; extensions of the national grid have only resulted in further strain on the system and therefore in further reduction in quality of services to those already grid-connected [125]. Kenya can still cost-effectively, and in a timely manner, achieve universal electrification if it formulates more suitable and achievable policies to exploit its vast renewable energy resources. Such policies could include provision of subsidies towards renewable energy systems, removal of tax duties on imported renewable energy technologies and systems, and provisions of microcredit facilities to enable rural households purchase small PV systems.

Renewable energy has the potential to enhance energy security and reliability in Kenya while generating income and employment, and to enable the country to make substantial foreign exchange savings by reducing dependence on imported petroleum and petroleum products. With an average solar insolation of over 6.5 kWh/m²/day all year round, and about 8 hours of strong sunlight daily, Kenya's geographical location astride the equator makes it a potentially vibrant solar energy market. The country's solar energy potential is about 1.86 PWh/year, enough to satisfy its energy demands many times over [126]. However, effectively harnessing this free source of energy still remains a challenge mainly due to lacklustre government support and underappreciation of its potential; even though the Kenyan PV market is amongst the most vibrant in Africa, it has mainly evolved with little government support or regulatory policies, apart from at its inception. In the early 1990s, the total installed PV capacity in Kenya was 1.5 MWp, with government or donor sanctioned installations accounting for about two-thirds of the total capacity [126]. By 2000, the market had more than doubled to 3.9 MWp, with household installations accounting for about 75% of the total installations [124]. Annual growth rates have been between 10 and 15% since the 1990s, with the current annual installations estimated at between 1-2MWp, driven mainly by the demands for small solar home systems (SHS) of between 20 and 100 Wp [124-127].

Table 4.1 shows the PV market structure in Kenya today [124]. Solar home systems account for about 75% of the total installed PV capacity, or for 6-8 MWp. Government and donor funded large PV projects, which once dominated the PV market in Kenya, now account for between 20% and 25%

or about 2 MWp of the installed capacity. PV systems for remote communication installations, which pioneered the entry of solar technology into the Kenyan market, now account for a negligible segment of the market. However, even with such vibrancy, the installed PV capacity is still significantly lower than the nation’s potential. PV powered communal grids have hardly grown in Kenya due to lack of knowledge on the socio-economic benefits of such arrangements, lack of government support and regulation, and most importantly, lack of organizational structures necessary to establish and run such ventures.

Market Segment	Estimated Installed Capacity
SHS and Small-Scale Enterprises	6-8MWp
Off-grid Community Systems	1.5MWp
Off-grid Schools	0.5MWp
Remote Communication Installations	100-150kWp
Off-grid Tourism Establishments	50kWp
Overall Market Size	8-10MWp

Table 4.1: Installed PV Capacity by Market Segment, 2015 [124]

Kenya has 22 recorded communal grid systems, 19 of which are government owned and were set up in rural towns of strategic administrative and commercial importance. All of these systems were originally based on large diesel-generators, however, due to energy insecurities and improving renewable energy technologies, 7 of these systems have now been hybridized with PV and wind systems, and similar plans are afoot for the remaining 12 minigrids [124]. There are also plans by Kenya’s Rural Electrification Authority to construct 27 new green minigrids (based entirely on wind and PV), to combat low levels of rural electrification. However, these are plans which have been in place for years now but have not yet been implemented. The 3 privately owned minigrids in Kenya are based on renewable energy resources; there is a communally-owned pico-hydro system set up in central Kenya to serve a local village of about 60 residents and 2 PV minigrids recently set up in costal Kenya to service a local NGO and neighbouring communities, and in Naivasha to serve a flower farm.

Minimum potentials for a communal grid are a minimum of 5km from existing national grid lines and minimum population density of 250 people/km² [5-7,128-130]. Maximum potential for a communal grid are a minimum of 20km from existing national grid lines and a minimum population density of 300 people/km² [5-7, 128-130]. As per latest estimates, Kenya has a population of about 44 million

people, only about 33% of whom (about 14.5 million) can be cost-effectively electrified through national grid extensions [103,106]. 66% of the population (about 28.8 million) live in areas with densities above 250 people/km². Of these, the communal grid population, those living over 5km from existing national grid lines, is about 10 million, or 23% of the national population [121,124]. The remaining 44% of the population (about 18.9 million) can currently be cost-effectively electrified through stand-alone systems. However, with increasing demands and population growth, this number is also expected to shrink as more and more portions of this group fall into the communal grid category.

Table 4.2 shows communal grid potential for Kenya. From the table, it is clear that rural and off-grid villages in Kenya can leapfrog into sustainable electricity access through solar microgeneration systems, especially PV-based communal grids, as long term solutions rather than as temporary solutions as national grid lines are awaited to arrive; the communal grids could provide ‘electricity-beyond-lighting’ to stimulate local microeconomic activities and enhance livelihood.

Kenya	Wind	Hydro	Biomass	Solar	Total
Population targeted by communal grids (>250hab/km ² & >5km of MV), in millions	2.24	1.02	1.02	5.9	1.02
Share of population for a given technology	22%	10%	10%	63%	
Average energy consumption over 20 Yr. (GWh/Yr.)	568	258	258	1,497	2,582
Penetration rate (%)	33%	87%	80% (RH) 50% (SC)	40%	
Total Energy need @ Yr5 (GWh)	329	150	150	868	1,497
Total Power need @ Yr5 (MW)	62	28	28	163	281
Renewable Device capacity (MW)	153			238	391
Carbon emission Diesel-MG (kTCO ₂ eq/Yr.)	244	292	756	779	2,070
Carbon emission National grid (kTCO ₂ eq/Yr.)	153	184	476	490	1 303

Table 4.2: Kenya Communal Grid Potential [124]

4.2 Methodology:

Kendu Bay is a small rural community situated in western Kenya at 0° 21' S, 34° 38' E and occupies an area of about 200km². It is situated in a basin along Lake Victoria and experiences semi-arid climatic conditions. Administratively, Kendu Bay is a town council within Homabay County and is also the district headquarter of Rachuonyo East District. It has a population of about 29 thousand people residing within three main locations namely, Pala, Gendia, and Kanam. The main economic activities

are fishing and subsistence farming which, due to poor rainfall, occurs mainly near the shores of Lake Victoria and along a local permanent river called Awach. The main source of employment is civil service with many people working as administrators, clerks, teachers, police officers, or health officers. Other sources of employment are small scale businesses and consumer services, small scale manufacturing enterprises, and mining. Due to its proximity to the equator, Kendu Bay is blessed with plenty of sunlight all year round making it a potentially vibrant market for solar technology. Even though national electricity distribution lines along the two main roads across it places all of its residents within 10km of the grid, less than 4% of residents and businesses in Kendu Bay are actually connected to the grid, begging the question, what are the reasons behind such low electrification rates? The majority of residents still depend on biomass fuels for cooking, ironing, warming, and in some cases, lighting. Many more also depend on kerosene for lighting and cooking, situations mirrored in many other rural Kenyan communities.

4.2.1 Survey Construction:

A comprehensive survey questionnaire was prepared before embarking on the survey as shown in the appendix. The main questions asked in the survey were:

1. Do you have a PV installed? If yes
 - a. What is the capacity?
 - b. What was the total cost of the installed system?
 - c. What are the powered appliances in order of priority?
 - d. What was the motivation for installing PV?
 - e. What problems have you encountered with your system?
 - f. What is the level of education of head of household (the one who makes energy decisions)?
 - g. What is the level of household monthly income and source?
 - h. How has household income changed in the past 5 years and how has this change affected your energy choices?
 - i. What are the choices of cooking and heating fuels?

2. If you don't have PV, is the household electrified? If yes
 - a. What is the source of electricity?
 - b. Reasons behind electrification choice?
 - c. What are the powered appliances in order of priority?
 - d. What are the energy choices for cooking and heating?

- e. Household monthly income and source?
 - f. How has household income changed in the past 5 years and how has this change affected your energy choices?
 - g. Head of household level of education?
3. If the household is unelectrified, what are the reasons behind that?
- a. What are the energy choices for lighting, cooking, and heating?
 - b. What is the household monthly income and source?
 - c. How has household income changed in the past 5 years and how has this change affected your energy choices?
 - d. Head of household level of education?
4. Opinion and Motivation?
- a. What are the reasons behind your energy choices?
 - b. Did your environmental concerns influence your energy choices?
 - c. What is your opinion on the national grid?
 - d. What is your opinion on the large central coal and gas power plants being constructed by the government?
 - e. What is your opinion on electricity microgeneration based on local renewable energy resources?
 - f. Would you support policy change to encourage exploitation and adoption of renewable energy resources?
 - g. Do you about communal grids (explain if they don't)?
 - h. Would you join a communal grid based on PV systems?

The questions were carefully incorporated into the survey questionnaire, taking into account the sensitivity of some of the questions, and local cultural inhibitions; an ethics review was completed through the University of Leeds and approved before embarking on the survey and every surveyed household signed a consent form, please see the appendix.

4.2.2 Survey Data Collection:

The survey was divided into three major sections, i.e. demographic information, technical information, and opinions and other comments. The demographic section sought to identify the education and income levels of the heads of the household and to relate this to the type (traditional, transitional, or modern) and sizes of the houses and households. In this survey traditional houses

are defined as houses with grass-thatched roofs and with walls and floors constructed with clay soil mixed with cow-dung. Transitional houses are traditional houses with corrugated iron sheets for roofs. Modern houses are described as houses constructed with either bricks (red bricks are locally baked) or stones (also locally mined). The roofs are usually made of corrugated iron sheets.

The technical information section sought to identify energy sources and choices, and reasons behind such choices. Specifically, this section sought to identify the sources of household electricity, if any, and technical specifications of the same. Choices of cooking fuels were also sought as these were later compared to education and income levels to identify any emerging patterns. The opinions and comments section sought to obtain the respondents' opinions on national grid electricity compared to other available options, i.e., solar home systems. Comments on centralized power generation based on fossil fuels versus communal gridding based on locally available renewable resources were also sought as environmental pollution was a major motivation for this study.

The main factor considered when grouping the households was whether a household was electrified or not, i.e., households with grid electricity were grouped together, households with PV were grouped together, and unelectrified households were also grouped together. The unelectrified households were then further divided into three groups according to levels of household incomes. This grouping made it easier to interpret responses to survey questions as households with similar energy patterns were grouped together.

Without recorded physical addresses, random sampling of potential respondents was done using google maps; the survey area was divided into three regions based on administrative boundaries, namely Gendia, Kanam, and Pala to ensure equal distribution of samples and to make it easier to manage the travel logistics. The surveyed households were those nearest to the main roads. Every 5 households were surveyed, unless a household with PV appeared before the next sample count, in which case, the sampling would begin afresh from the house with PV. The three regions have the following populations: 11,312, 9,219, and 8,987 and corresponding households of 2,833, 2,312, and 2,248, respectively [160]. The surveyed samples were divided into two sections namely, commercial and institutional establishments which covered 3 schools and 15 shops, and individual households which covered 537 households, representing about 7.3% of the population of Kendu Bay. Table 4.3 below shows the population of each region and the corresponding survey household sample sizes, and inclusion probabilities. Inclusion probability in a region is given by dividing the region's households sample by its total households. The inclusion probability of Gendia is the lowest because it has the highest population and most sparse population. Still, it produced the highest number of

samples for this survey. Kanam and Pala had almost equal inclusion probabilities. The overall inclusion probability of 0.073 is an average of the three regional probabilities.

Region	Population	Households	Sample (households)	Inclusion Probability
Gendia	11,312	2,833	183	0.065
Kanam	9,219	2,312	179	0.077
Pala	8,987	2,248	175	0.078
Kendu Bay (Total)	29,518	7,393	537	0.073

Table 4.3: Total Populations Households, Survey Samples, and Inclusion Probabilities

Data collection was done through face-to-face and door-to-door interviews, with the responses filled into paper questionnaires before compilation into a laptop computer. This was deemed viable and the best option after a risk and cost analysis. The head of the household, the person responsible for making energy decisions, answered on behalf of the whole household. During data compilation, the households were divided into three groups as follows: those with grid electricity, those without grid electricity but with installed solar home systems, and those without grid electricity or solar home systems, i.e., no source of electricity. This division also inadvertently grouped the households according to income and education levels. Those without any source of electricity were further divided into three groups depending on income and education levels.

4.3 Results and Discussion:

The main sources of electricity for Kendu Bay residents are the national grid and small solar home systems (SHS). National grid lines pass along the main two roads in the area, Kendu-Oyugis and Ahero-Kendu-Homa Bay, while SHS are widely retailed by local vendors, and especially Africa Retail Traders (ART) which has a large shop in Kendu Bay town. The SHS come in two standard packages: a 45 W system with a 12V 100Ah lead acid battery and a non-grid-tie DC/AC inverter installed at a cost of \$250, and a 100W system with a 24V 100Ah lead acid battery pack and a non-grid-tie DC/AC inverter installed at a cost of \$400. Both of these systems are cheaper than the grid electricity connection fee of \$750. ART sells the SHS to civil servants on an interest-free hire-purchase arrangement payable over 6 months, with deductions taken directly from purchasers' salaries every month. Other buyers have to pay the full amounts before installations. Those without access to electricity use kerosene lanterns or firewood for lighting. Small diesel generators and car batteries are sometimes used for emergency power generation or lighting, especially during social gatherings, but are never operated on a long term basis due to high operation and maintenance costs. The main

sources of cooking fuels are firewood, charcoal, kerosene, and liquid petroleum gas (LPG). Firewood is freely collected from local bushes and shrubs while locally burned charcoal are easily accessible and cheap. The few people who use kerosene and/or LPG for cooking are considered well off individuals by local standards. Kerosene is sold by local vendors while LPG is sold at petrol stations in Kendu Bay town.

4.3.1 Individual Households:

The survey samples were divided into three groups namely: positive respondents, non-respondents, and ineligible respondents. The total response rate is found by taking into consideration the sizes of these groups. Of the 537 households approached, 513 households were classified as positive respondents, representing a 95.5% response rate. 18 households, or 3.4%, were recorded as non-respondents because home owners were either not present at the time of the survey or chose not open their doors. Six households, or 1.1%, were recorded as ineligible respondents because heads of household (those who make energy decisions) were not present at the time of the survey. The primary quality indicator of the surveyed households mirrors the response rate and is given by

$$\frac{\text{positive repondents}}{\text{total sample} - \text{inelegible samples}} \times 100\% \quad (4.1)$$

In this case, the quality indicator was 96.6%. For commercial and institutional establishments (schools and shops), the quality factor was 100%. Table 4.4 below shows response rate by region. Pala had the highest response rate followed by Kanam and then Gendia. There was no particular pattern or reason to this. Of the 513 households classified as positive respondents, 16 had grid electrification, representing 3.1% of the sample, and in line with the local electrification data [160]. Twenty-four households had installed solar home systems for electrification, representing 4.7% of the sample, while 473 household (92.2%) had no access to electricity of any source.

Region	Sample	Positive Respondents	Non-Respondents	Ineligible Respondents	Quality Indicator
Gendia	183	173	7	3	96.1%
Kanam	179	171	6	2	96.6%
Pala	175	169	5	1	97.1%
Kendu Bay(Total)	537	513	18	6	96.6%

Table 4.4: Response Rates by Region

Figure 4.1 captures the above information.

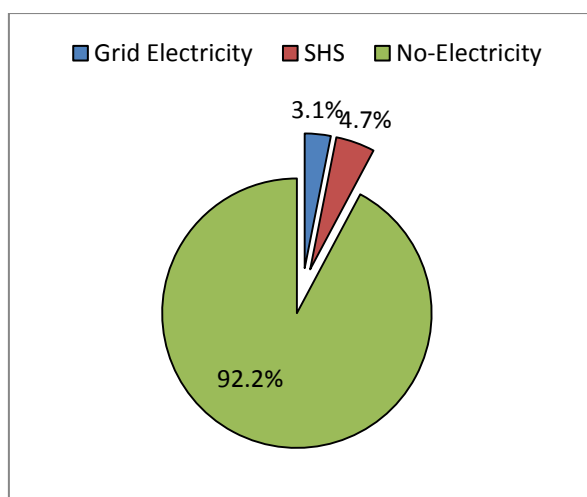


Fig. 4.1: Kendu Bay Electrification Topology

4.3.1.1 Grid-Connected Households:

All households with grid electricity were situated along existing national grid lines, i.e. the two main roads in the area. Their monthly incomes were above \$400 and were thus considered well off by local standards and their household appliances mirrored those of modern households. For these households the cooking fuels of choice were LPG and charcoal. All of the heads of household in this group had college degrees and were either employed as high level civil servants or self-employed as successful entrepreneurs. All of the houses in this category were classified as modern. One household in this category had purchased a SHS for backup power during blackouts while one, which originally had a grid-connected SHS, sold the SHS to remain only with grid connection. Due to lack of governing policies and grid-tie inverters, neither SHS was connected to the grid.

According to 94.6% of grid connected respondents, the main reason for grid connection decisions was need for electricity-beyond-lighting while final decisions on whether or not to connect to the grid depended on the proximity of a household to existing national grid lines and on its ability to afford grid connection fees and related expenses. Grid electricity comes with many benefits, key amongst which are listed below:

- Unlimited power supply enables households to acquire modern household electrical appliances such as fridges, microwaves, and fans which in turn make their lives easier and more enjoyable.

- Grid electricity lighting as an alternative to kerosene lanterns not only means higher quality lighting but also healthier living and studying environment, as soot from lanterns has been shown to be as bad an environmental polluter as soot from burning biomass fuels.
- Access to unlimited power motivates people to acquire TVs and radios, major sources of news and information, which in turn leads to improved knowledge on world affairs, gender related issues and equality, distance learning, and important health news and information.
- Access to grid electricity enables households to start and run home-based microenterprises such as mobile phone charging kiosks, as neighbours with phones but no access to electricity take their phones for charging at a small fee. This augments a household's income.
- Unlimited access to electricity also provides improved sense of security through high quality lighting, encouraging more nightly social activities such as group studies, and thus stimulating communal social development.
- Access to grid electricity is presumed to be an indication of a household's wealth, and thus elevates its social status within the community.

Even though grid connection comes with many benefits, it also comes with many obstacles and problems, with the main ones being:

- High connection fee - all households connected to the grid complained of high connection fees, making grid out of reach of many would-be consumers. This is an unnecessary obstacle to rural electrification.
- System strain and unreliability – all households complained of frequent blackouts brought about by strain on the system. These made grid electricity quite unreliable, which is detrimental for those with small business which could not be operated without electricity.
- Corruption – 98% of households complained of having to pester and bribe technicians before their applications for grid connections could be processed. Moreover, all households with grid complained of uneven monthly bills, even after periods of prolonged blackouts.

4.3.1.2 Households with Solar Home Systems:

The majority (81%) of households with small PV systems were situated far from existing national grid lines, making such connections too costly. Twelve of the systems were rated 45 Wp and were mainly used for basic lighting, to charge mobile phones, and in some cases, to power small radios during the day. Eleven of the systems were rated 100 Wp and these were also used for basic lighting, to charge mobile phones, power small radios, and in one case, to power a small TV for short intervals, mainly during prime time news times (7pm and 9 pm). One system was customized to 400 Wp and used to

power a small colour TV and a small under-the-counter fridge. For this category of households, the main choices of cooking fuels were firewood and charcoal, and in some few cases, LPG. The heads of household in this category also had college level education, but earned between \$250 and \$400 per month. Most were employed as medium level civil servants. The remaining portion owned and operated their own small businesses. All of the houses in this category were classified as modern. For these people, the need for basic electricity was the main driver behind decisions to install PV systems, as seen in the capacities of the systems installed.

The main reasons for lack of grid connection could be summarized as follows:

- High grid connection fee – All of the households in this group reported the high grid connection fee as the main hindrance to grid electricity. This might change now that the Kenyan government has announced scrapping of the grid connection fee (however, this is done every election cycle but has never actually been implemented).
- Need for basic electricity – 83.3% of the households in this category needed electricity for lighting, to charge mobile phones, and in some few cases (16.7%), to power small TVs and radios. Small solar homes systems therefore provided enough electricity to satisfy their needs.
- Grid unreliability (strain) – impacts of social factors (word-of-mouth) from households with grid electricity within a given neighbourhood led to lesser grid connections as many people with grid complained of frequent and long blackouts.
- Corruption – 98% households with grid also complained of uneven monthly bills, demand of kickbacks from technicians, and general corruption in the system. This dissuaded many would-be consumers from investing in grid connections.

In addition to the negative image of the national grid, the following factors motivated households to install solar home systems:

- Cost – affordability of small solar homes systems was the main factor that influenced final decisions to install them (reason cited by 95.8% of respondents); compared to grid connection fee, basic solar homes systems are more affordable.
- Neighbourhood influence – apart from 3 early adopters, the rest of households with SHS in Kendu Bay (87.5%) were motivated by neighbourhood influence. Neighbourhood influence took three forms often working in combination, i.e.:
 - Observation – most households installed solar home systems after observing similar installations in their neighbourhoods, with their friends, or with their families and presuming their socio-economic benefits.

- Word-of-mouth – many households also installed PV systems after hearing about their benefits from neighbours, colleagues, family, or friends, or after enquiring about them after observations.
- Social pressure – this mainly took the form of marketing and it was done through billboards, word-of-mouth, and mass media. ART marketed solar home systems through schools and civil servants and by offering interest-free hire-purchase arrangements.
- Social status – elevated social status within the society brought about by a visibly installed solar home system drove many households (70.8%) which could afford basic systems to adopt them.
- Reliability – reliability of solar home systems and control over one’s own power source also drove people who could afford such systems to adopt them, according to 83.4% of respondents.

Figure 4.2 shows photos of PV systems installed in Kendu Bay.



Fig. 4.2: Photos of PV Systems in Kendu Bay Taken During Survey

Even though solar homes systems are generally advantageous, their limited power capacities drive households with increasing incomes and thus more household electrical appliances to transition to

grid electricity to meet the increasing power demands. Other obstacles to PV diffusion in Kendu Bay area included:

- Ignorance – Many people did not know that PV systems can be customized to meet their changing power demands and were thus stuck with the standard 45Wp and 100Wp systems sold locally. This could be blamed on limited market infrastructures and monopoly which limited consumers' choices and knowledge on PV systems.
- Cost – Since all PV products and components are usually imported, the general cost of PV systems in Kenya is higher than it is in developed nations. This makes even the most basic of PV systems out of reach of over 92% of Kendu Bay residents, thus hindering adoptions.
- Lack of government support – As has been reported elsewhere, PV growth in Kenya has occurred with very little support from the government and this was evident in Kendu Bay; more people could afford PV systems if positive incentives and policies were introduced. Rapid development of PV in Europe, USA, China, and Japan happened as a result of massive government support, this is lacking in sub-Saharan Africa, mainly due to lack of resources but also due to lack of knowledge of potential economic benefits of such incentives and policies.

4.3.1.3 Unelectrified Households:

The last group, composed of 92.2% of Kendu Bay residents, comprised of households without access to electricity of any source. For this group, the main hindrance to electrification was cost; all the households in this group could not afford upfront basic solar home systems or grid electricity connection fees. They therefore mainly used kerosene lanterns for lighting, and in rare cases of extreme poverty, used freely collected firewood for the same purpose. For easier classification, this group was further divided into three smaller groups according to income and educational level as elaborated below:

- Group 1 comprised of households with monthly incomes of between \$200 and \$250 and could thus save to purchase small solar home systems within a year or so. Eighty-nine households falling into this category were interviewed, representing 18.8% of unelectrified households. Nearly all of the heads of household in this category were educated up to tertiary colleges, and were either employed as low-level civil servants or were small business owners. These households used kerosene lanterns for lighting and firewood and charcoal for cooking. All of the houses in this category were classified as transitional. Due to their income levels, households in this group could be motivated to install basic solar home systems through provisions of proper microcredit facilities.

- Group 2 comprised of households with monthly incomes of between \$75 and \$200. Two-hundred and twenty-four households in this category were interviewed representing 47.4% of the unelectrified households. Most of the heads of household in this group were educated up to high school and were employed as skilled casual labourers. The houses in this category were traditional. Kerosene lanterns were used for lighting while firewood was used for cooking. These households earned too little to be able to transition to the SHS income category within 5 years. They were also too risky to lend to and could therefore not be offered credit facilities.
- Group 3 comprised of households with less than \$75 in monthly incomes. One-hundred and sixty households in this category were interviewed representing 33.8% of unelectrified households. Heads of household in this category were educated up to primary school level and were mostly employed as unskilled casual labourers; these households heavily depended on subsistence farming for their food sources. For this group, kerosene lanterns, and in many cases, firewood was used for lighting, while firewood was also used for cooking. Households in this category generally live in serious poverty with unstable incomes and can therefore not be considered for credit facilities.

From the above data, it is clear that nearly 25% more residents of Kendu Bay can be motivated to install PV systems almost immediately through provisions of proper credit facilities, positive government incentives and policies, and subsidies. These are the grid connected 3.1%, group 1 of the unelectrified, and top earners of group 2 of the unelectrified. The data also shows that there is a clear correlation between households' income levels and heads of household education levels, with the highest educated heads of households having highest incomes and thus able to afford grid connection fees or solar home systems and also able to build modern houses for their families. They are followed by those with tertiary college education, with the people in this category able to afford basic solar home systems and modern houses. The unelectrified group had heads of household educated up to high school or primary school level. Due to their lack of specialized skills therefore, these people could not be employed in high paying jobs and thus could not afford grid connection fee or basic solar home systems. Table 4.5 and figure 4.3 below capture the above information.

Highest Education Level	Surveyed Houses	% of Total	No Electricity	Grid	SHS
Primary School	160	31.2	160	0	0
Secondary School	228	44.4	224	0	4
Tertiary College	113	22.1	89	5	19
University	12	2.3	0	11	1

Table 4.5: Correlation between Education Levels of Heads of Households and Electricity Access

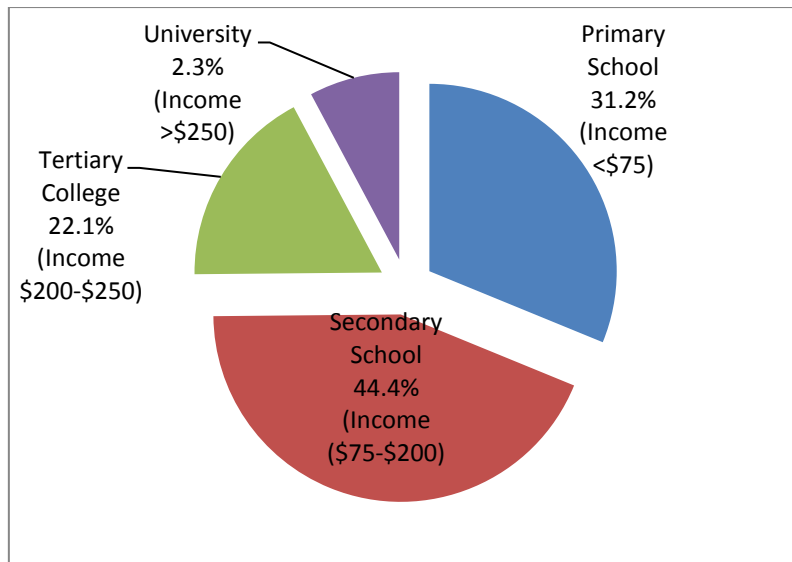


Fig. 4.3: Relation between Education and Income Levels

4.3.2 Commercial and Institutional Establishments:

In this category, three public primary schools and 15 private shops were interviewed, with 100% response rate recorded. Of the three schools, 1 had grid electricity, 1 had solar systems installed on the roofs, and 1 had no source of electrification whatsoever. In all of these school, pupils in standards 6-8 were required to attend compulsory dawn (5-7.30 am) and evening (6-9 pm) tutorial classes, periods during which lighting was required. Pupils in the school without electricity used kerosene pressure lamps for lighting. This means that parents with children in classes 6-8 had to pay a monthly kerosene fee, an additional burden for the majority of poor rural households. In addition, these lamps are very dangerous, frequently exploding and causing fires. The government has promised to electrify this school using solar home systems in the coming budget year.

The school with a solar system and the one with grid connection were electrified for free under a government's rural electrification programme targeted at public institutions. Electrification has brought about many immediate advantages over kerosene pressure lamps with the main ones being:

- Improved quality lighting – Quality lighting enables better studying during tutorial lessons, reducing strain on pupil's eyes.
- Improved personal safety – As reported above, kerosene pressure lamps are quite dangerous and often explode, causing serious health risk to pupils within its vicinity. This risk is eliminated by electrification.

- Improved sense of security – Quality lighting provides an improved sense of security to the young pupils during their tutorial lessons.
- Elimination of kerosene fee – Parents with pupils in classes 6-8 do not have to pay the kerosene fee anymore, a major relief for these poor rural residents.
- Access to national teaching programs – Kenya runs national lessons through radios and TV and these can only be tuned in to if there is electricity. Electrification therefore enables access to more information and lessons necessary for the curriculum.

Of the 15 shops interviewed, 3 had grid electricity connections, 4 had solar home systems installed, while 8 had no source of electrification whatsoever. The three shops with grid electricity were all located in Kendu Bay town centre where two major transmission and distribution lines intersect. The shops with solar home systems were located at Benga and Oriang markets, far from existing grid electricity lines. The shops without electricity were also located at the above two markets, far from existing grid lines.

The shops with electrification, be it grid or solar home systems, reported improved business activities through extended hours of operation, ability to offer quality and efficient services, and better sense of security. In particular, ability to power fridges enabled shop owners to stock cold drinks or perishable goods, enabled chemists to stock a wide variety of medication, and enabled food vendors to have larger stocks. For service providers like barber shops or salons, access to electricity enabled them to offer efficient and quicker services, allowing for more customer flow and correlated income.

As with individual households, shops with grid electricity complained of frequent blackouts which adversely affected stocks, especially perishable goods, and of corruption with often unexplainable uneven monthly bills. One of the shops in this category installed an automatic backup generator to supply power during blackouts as his shop could not function without electricity. For those with solar home systems, the 100% complained about limited power capacity; the installed systems were mainly used for basic lighting as appropriately sized systems proved too expensive to these people and without subsidies or credit facilities, they are on their own. For 100% of shops without electrification, the main obstacle was cost; high grid connection fees or PV prices kept many of these shops unelectrified. Most of these shops were small family or owner operated business such as carpentry shops, food kiosks, or small chemists. They all envied their neighbours with electricity as this translated into better profit margins. They all blamed lack of government support through incentives or microcredit facilities for their predicaments.

4.3.3 Opinions and Motivations:

Most of the households in Kendu Bay area of Kenya are not aware of global warming or have heard very little about it. Respondents' environmental concerns therefore had no influence on energy choices among the households surveyed. Most of the households also did not know that the government was in the process of constructing large central power plants, roughly 600km away. This was mainly due to poor communication from the government and lack of engagement with poor rural communities. All of the households without electricity in Kendu Bay preferred to be electrified one day, and did not mind the future source of their electricity, as long as it was cost-effective and affordable. Although preferences are not being driven directly by environmental concerns, significant environmental benefits result from the current situation as small PV systems are the most affordable initial electrification option in the area at this time.

Furthermore, all surveyed households in Kendu Bay area had low opinions of the national utility grid, describing it as unreliable and too expensive. Most people (98%) complained about corruption in the system, with uneven monthly bills and officials asking for bribes, in addition to high connection fees, in order to process connection applications. For these reasons, all households voiced support for decentralized electricity microgeneration based on PV systems. Even though a PV-based communal grid was a new concept to the majority of the households, they all supported the idea, indicating a willingness to form, or join, such a grid if it meant access to reliable and cost-effective grid-quality power. All households in the area also voiced support for national policy change as it pertains to renewable energy resources. Specifically, 99% of the respondents wanted the government to remove all taxes on renewable energy technologies and products in order to reduce their costs. Respondents also wanted the government to introduce subsidies in order to encourage more independent power generation. Most households (82.7%) asked for some kind of government grants or soft-loans to help with PV purchases or modifications.

4.4 Concluding Remarks:

A survey on electrification topologies in Kendu Bay area of Kenya was carried out with a broad aim of establishing the drivers of different electrification choices. Specifically, the survey aimed to gather comprehensive data on PV systems installed in Kendu Bay area for applications in future modelling and simulations of temporal PV diffusions in a typical rural developing community. Results show that currently 92.2% of Kendu Bay households are unelectrified due to financial barriers, 4.7% have basic

electricity through small PV systems, while 3.1% are connected to the national grid. From the survey, we can report that the four possible routes to electrification in Kendu Bay area are through national grid connections, through installations of stand-alone PV systems, through formations and connections to communal grids, or through grid-connected PV systems. As there are currently no communal grids in Kendu Bay, only the first three options are operational. However, with more homes installing PV systems, the potential for communal grid formations remain high. From the survey, it is clear that there is a serious distrust of the government run national grid system, with many respondents describing it as too unreliable due to frequent and long-lasting blackouts, too expensive due to high connection fee, or too corrupt with technicians demanding kickbacks and customers complaining of uneven monthly bills. For these people, any affordable and reliable alternative would be preferred. On the other hand, typical stand-alone PV systems offer limited power capacity and hardly provide electricity beyond lighting; a properly sized system to meet all of a household’s power demands would be too expensive for most of Kendu bay residents, since as it currently stands, 92.2% cannot afford even the most basic of PV systems. Small stand-alone PV systems therefore cannot stimulate rural micro-economic activities. Communal grids based on PV systems could provide the bridge between stand-alone systems and the national grid by providing sustainable, clean, and affordable electricity-beyond-lighting to rural residents.

Table 4.6 below compares the merits and demerits of different potential electrification topologies for Kendu Bay area.

Electrification Option	Merits	Demerits
National Grid	<ul style="list-style-type: none"> • Unlimited power capacity 	<ul style="list-style-type: none"> • Unreliable • Expensive • Plagued with corruption • Not trusted
Stand-Alone SHS	<ul style="list-style-type: none"> • Affordable • Reliable • Short lead time • Clean • Individual control 	<ul style="list-style-type: none"> • Limited power capacity • Properly sized systems are too expensive
Communal Grid	<ul style="list-style-type: none"> • High power capacity • Communal control • Affordable • Reliable • Short lead times 	<ul style="list-style-type: none"> • Lack of reliable implementation models • Difficult to finance • Difficult to organize/implement

Table 4.6: Comparison of Different Electrification Choices for Kendu Bay

Chapter 5: Modelling Temporal Diffusion of PV Microgeneration Systems in Kendu Bay Area of Kenya

5.1 Introduction:

In this chapter, after having gathered and analysed necessary survey data in chapter 4, an agent-based model (ABM) is developed as a tool for evaluating temporal diffusion of PV microgeneration systems in Kendu Bay area of Kenya, and by extension, similar developing communities. The model takes into account the complexities and limitations of solar electricity microgeneration technologies, decisions by human actors, geographical factors, and the interaction between the three factors. ABMs seek to capture the overall macro-effects of different micro-decisions in a virtual world; they model individual entities within a complex system and the rules that govern the interactions between the entities within the system, to capture the overall effect of such interactions. The model developed in this section is used to simulate how households in Kendu Bay area would make their electrification choices over a given period of time, given various electrification options. Many factors influence choices for different electrification options with the primary ones being cost, household income, social factors such as neighbourhood influence, source availability, and government policies such as subsidies; the model simulates how these factors influence choices of household electrification. Observations made from this study can be applied to many similar locations in sub-Saharan Africa. But most importantly, the model can be used by policy-makers in formulating rural electrification policies and in planning, prioritizing, and implementing rural electrification projects in Kenya.

Development of electricity delivery infrastructures are path-dependent, meaning, each development decision and individual step affects subsequent steps, and the final outcome. Human actors are therefore the most important variables in any energy development plan as their decisions affect the way a system evolves. Proper policy-planning tools are therefore required to guide decision-makers on least cost rural electrification pathways. Many factors influence choices of technologies used in rural electrification, the main ones being availability of resources, demand, investment costs, and local socio-political and cultural environments. Different modelling tools and techniques have been applied in planning rural electrification paths in many countries. However, these often view this problem as a question of expansion of grid coverage through extensions of existing transmission and distribution lines from central power generation stations and seldom address the unique and regionally-specific challenges presented by many developing nations [131-133]. In most of sub-

Saharan Africa for example, grid electricity is often unreliable, plagued with frequent blackouts, poor maintenance, and low quality of service. In these regions, expansions of the national grids often result in further strain on the systems and thus in further reduction in the quality of services provided to those already grid-connected [134]. Bhattacharyya and Timilsina point to models that can capture a developing nation's unique context as a key input for future policy formulation, while Urban et al point to the lack of focus to date on off-grid technologies based on locally available renewable energy resources and on the prevailing socio-economic and cultural factors [135,136]. The model developed in this work uniquely and simultaneously captures the impacts of local socio-economic and technical factors on temporal diffusion of PV microgeneration systems while also taking into consideration, local cultural and political factors. The model simulates how, given various electrification options, households in a typical rural developing community would make their electrification choices, and how the above factors influence and impact on those decisions.

5.2 Methodology:

In this section an agent-based model is developed in Netlogo to simultaneously simulate impacts of socio-economic and technical factors on temporal diffusion of PV microgeneration system in Kendu Bay area of Kenya. Netlogo was chosen for this work because it is widely accepted by scholars as one of the best environments for socio-economic agent-based modelling [137]. Moreover, it is free to download and use. The following agents are created in the model: a) a representation of the environment and the solar potential in it, b) the populations in it that require electricity, c) PV seeds that would use the environment to produce electricity, d) links which are used by households with PV to connect to communal grids, and e) a central observer or stakeholder who determines the strategies and preferences for PV diffusions. Through these agents and the rules created for their interactions, the model is used to simulate the way decisions and preferences by human actors affect PV diffusion.

Based on survey data in chapter 4, 92.2% of Kendu Bay residents do not have access to electricity of any source and thus depend on harmful kerosene lanterns and firewood for lighting and cooking. Another 4.7% have small PV systems for basic lighting and to power small electronic appliances such as mobile phone chargers, and in some cases, small radios and even black and white TVs. The remaining 3.1% have access to grid electricity, and these are mainly well-off households by local standards. Even though the majority of the unelectrified households in Kendu Bay are situated within 10 km of existing MV national grid distribution lines, they are hindered from connecting to

the grid by high connection fees and unreliability of the grid caused by strain on the system and corruption. For Kendu Bay residents, the intermediate step between being unelectrified and being grid connected is owning a small PV system for lighting and mobile phone charging.

A Markov chain can be used to define temporal transitions between different electrification states in Kendu Bay given a vector of initial states. Let $S = \{s_1, s_2, \dots, s_t\}$ be a random process in the discrete time space \mathcal{E} . If transitions between the states, say from s_i to s_j occurs with a probability $\mathbb{P}_{ij}(t)$ that satisfies the Markov property, then the set of state S is called a Markov chain. $\mathbb{P}_{ij}(t)$ is called a transition probability while matrix of transition probabilities is called a transition probability matrix.

Markov property is satisfied if

$$\mathbb{P}(s_{t+1}|s_1, \dots, s_{t-1}, s_t) = \mathbb{P}(s_{t+1}|s_t) \quad (5.1)$$

for every sequence s_1, \dots, s_t, s_{t+1} of elements of \mathcal{E} and for every $t \geq 1$, where the first part of the equation represents conditional probability of an event one step into the future beyond time t while the second part represents conditional probability of an event in the future given just the present. The transitions in this model occurs through continuous time Markov process.

A transition probability matrix (TPM) is expressed as

$$TPM = \begin{bmatrix} p_{00} & p_{01} & \cdots & p_{0S} \\ p_{10} & p_{11} & \cdots & p_{1S} \\ p_{20} & p_{21} & \cdots & p_{2S} \\ \vdots & \vdots & \vdots & \vdots \\ p_{S0} & p_{S1} & \cdots & p_{SS} \end{bmatrix} \quad (5.2)$$

Each row represents all transition probabilities out of a single initial state and must therefore sum to 1. If a Markov chain has r states and an initial conditions vector x_0 , then a transition probability matrix after n steps is given by

$$x_0 \mathbb{P}_{ij}^n = \sum_{k=1}^r x_0 (\mathbb{P}_{ik}^n \mathbb{P}_{kj}) \quad (5.3)$$

At present, there are 5 possible electrification states for Kendu Bay, namely: 1) Not-Electrified (NE), 2) National-Grid (NG), 3) single-household PV systems (PV), 4) grid-connected PV systems (PVNG), and Communal-Grid (CG). Based on data collected from the Kendu Bay survey, the following initial

conditions apply: NE = 92.2%, NG = 3.1%, PV = 4.7%, PVNG = 0%, and CG = 0%. A vector of initial condition can therefore be expressed as

$$x_0 = \begin{pmatrix} \text{NE} & \text{PV} & \text{CG} & \text{NG} & \text{PVNG} \\ 0.922 & 0.047 & 0.000 & 0.031 & 0.000 \end{pmatrix} \quad (5.4)$$

Since there are no theories to predict how transitions can occur between these states, and since we cannot propose transition probabilities a priori, data from the Kendu Bay survey are used to estimate the transition probabilities using the frequency of transitions between given states. Ability to afford a given electrification source is the ultimate factor which decides transitions between different states. Other factors such as neighbourhood influence and government policies are used to model the final decisions on whether to choose a specific means of electrification or not, but not whether one can transition to that electrification state.

The survey data revealed that, all households with grid electricity had monthly incomes of above \$400. We can therefore make this a condition for grid connection; ability to afford the connection fee and related charges. All households with PV had incomes of between \$250 and \$400 while unelectrified households earned below \$250. The unelectrified households were further divided into three groups with 18.8% earning between \$200 and \$250, 47.4% earning between \$75 and \$200, and the remaining 33.8% earning below \$75 per month. From the Kendu Bay survey data, we can estimate that households' incomes increase annually at an average rate of 6.87%. Keeping all financial thresholds constant, we can estimate that after 1 year 5.3% of unelectrified households could transition to the greater than \$250 income bracket and thus be able to afford basic PV systems. Similarly, 20.8% of households in the PV category could transition to income brackets greater than \$400 after 1 year, and thus become grid connected if they so choose.

Based on the Kendu Bay survey data the following assumptions can be made:

- A household that can afford to connect to the national grid can also afford to join a communal grid and that both grid options offer equal power benefits.
- A household that has PV and has decided to become connected to a grid can choose to do so while selling off the PV system or having a grid connected PV system, both with equal probabilities.
- A household with a grid connection can choose to install PV for backup power during blackouts with a 6.3% probability.
- A household with a grid-connected PV system can also choose to sell off the PV system with a 6.3% probability.

Using the above probabilities and assuming that a house once connected to the grid cannot be disconnected (power may be cut off due to lack of payment of bills but the grid will still be extended to the household), the following TPM can be estimated after 1 year of transitions

$$\begin{matrix} & \begin{matrix} \text{NE} & \text{PV} & \text{CG} & \text{NG} & \text{PVNG} \end{matrix} \\ \begin{matrix} \text{NE} \\ \text{PV} \\ \text{CG} \\ \text{NG} \\ \text{PVNG} \end{matrix} & \begin{bmatrix} 0.947 & 0.053 & 0.000 & 0.000 & 0.000 \\ 0.000 & 0.792 & 0.104 & 0.052 & 0.052 \\ 0.000 & 0.000 & 1.000 & 0.000 & 0.000 \\ 0.000 & 0.000 & 0.000 & 0.937 & 0.063 \\ 0.000 & 0.000 & 0.000 & 0.063 & 0.937 \end{bmatrix} \end{matrix} \quad (5.5)$$

After n years, the probability of a household being in one of the 5 possible states (x_n) is given by

$$x_n = x_0 \times TPM^n \quad (5.6)$$

where TPM^n is the transition probability matrix after n years.

The chart below shows the sequences of execution in the program.

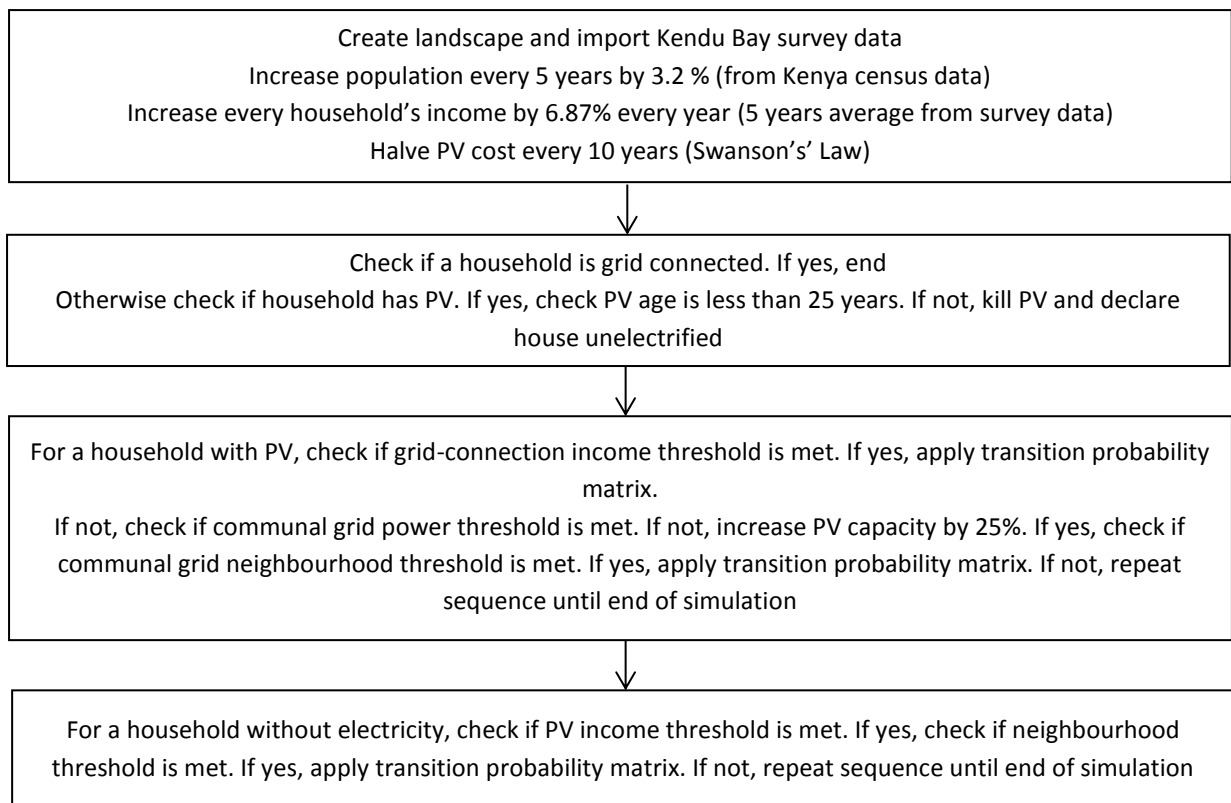


Fig. 5.1: Sequences of Operation of the Netlogo Model

A household without a PV system must first develop the idea to install one given the following main factors: cost, subsidies, and neighbourhood influence as discussed below.

5.2.1 Cost:

Based on Kendu Bay survey data, 92.2% of households do not have PV systems due to cost. Cost is therefore the dominant factor in a PV installation decision. The transition probability matrix is based on the ability of a household to afford a given electrification option after a given number of years. Each year, therefore, the probability that a household is in one of the 5 possible electrification states is given by equation 5.6. PV is only installed if a household can afford it and if:

$$LUCE_{PV} < C_{A/kWh} \quad (5.7)$$

where $C_{A/kWh}$ is avoided cost per kWh, i.e., the prevailing national grid electricity cost per kWh and equals \$0.20/kWh as per current Kenyan rates, while $LUCE_{PV}$ is the levelized unit cost of delivered electricity and is given by

$$LUCE_{PV} = \frac{ALCC_{PV}}{W_p \times EHFS \times 365 \times CUF} \quad (5.8)$$

where W_p is the rated peak Watt capacity of the PV module and is based on a household's activity profile and power demand (chapter 3), $EHFS$ is the equivalent hours of full sunshine per day and equals 8 (chapter 3), CUF is the capacity utilization factor which incorporates non-utilization and outages of systems due to various reasons and equals 0.9 based on Kendu Bay survey data, and $ALCC_{PV}$ is the annualized life cycle cost which is calculated by summing up the cost of all of its individual components, i.e. the module, battery, charge controller, and appliances multiplied by their respective capital recovery factors plus operations and maintenance costs. It is expressed as

$$ALCC_{PV} = (C_{0PV} \times CRF_{PV}) + (C_{0batt} \times CRF_{batt}) + (C_{0cc} \times CRF_{cc}) \\ + (C_{0appl} \times CRF_{appl}) + C_{O\&M} \quad (5.9)$$

where C_{0PV} is the capital cost of the PV module and is set at \$1.40/Wp based on Kenya's PV costs, C_{0batt} is the capital cost of the battery and is set at \$0.95/Ah based on the price of a typical 48V 100 Ah battery in Kenya, C_{0cc} is the capital cost of the charge controller and is set at \$28.50 as per Kenyan rates, and C_{0appl} is the capital cost of appliances and is averaged at \$75 per household

based on typical load profiles of 95% of households with PV systems in Kendu Bay. CRF_{PV} , CRF_{batt} , CRF_{cc} , and CRF_{appl} are the capital recovery factors of the PV module, the battery, the charge controller, and appliances, respectively, while $C_{O\&M}$ is the operations and maintenance cost and is set at \$2.50/year based on Kendu Bay survey data.

Capital recovery factor (CRF) is calculated using the formula

$$CRF = \frac{i(1+i)^n}{(1+i)^n - 1} \quad (5.10)$$

where i is the discount rate and is set at 12% based on average Kenya's central bank rates over the past 12 months, while n is the life of the particular component being considered, i.e. 25 years for PV modules/arrays, 5 years for batteries, 5 years for converters/inverters/charge controller, and 10 years for appliances (cumulative load). Based on these figures, $CRF_{PV} = 0.1339$, $CRF_{batt} = 0.2774$, $CRF_{cc} = 0.2774$, and $CRF_{appl} = 0.1770$.

For a communal grid consisting of N households, levelized unit cost of delivered electricity ($LUCE_{CGrid}$) is given by

$$LUCE_{CGrid} = \frac{ALCC_{CGrid}}{CGrid_{PV} \times EHFS \times 365 \times CUF} \quad (5.11)$$

where $CGrid_{PV}$ is the capacity of the communal grid (PV array) in kWp and is based on the activity profiles of all households connected to the communal grid, $EHFS$ is the equivalent hours of full sunshine per day and equals 8, CUF is the capacity utilization factor which incorporates non-utilization and outages of systems due to various reasons and is maintained at 0.9, and $ALCC_{CGrid}$ is the annualized life cycle cost of the communal grid and is given by

$$\begin{aligned} ALCC_{CGrid} = & [(C_{0CGrid_{PV}} \times CRF_{PV}) + (C_{0CGrid_{batt}} \times CRF_{batt}) \\ & + (C_{0pcu} \times CRF_{pcu})] \times [CGrid_{PV} \times R]^b \\ & + [(C_{0dn} \times L) + (C_{0sc} \times N)] \times CRF_{pdn} + C_{CGrid_{O\&M}} \end{aligned} \quad (5.12)$$

where $C_{0CGrid_{PV}}$ is the capital cost of the PV array and associated mounting structures and is set at \$1,400/kWp, $C_{0CGrid_{batt}}$ is the capital cost of the battery bank and associated structures and equals \$0.95/Ah $\times N$, C_{0pcu} is the capital cost of the power conditioning unit (power electronics) and equals \$28.50 $\times N$, CRF_{pcu} is the capital recovery factor of the power conditioning unit and equals

0.2774, C_{0dn} is the capital cost of the power distribution network per km and equals \$2,500 for Kendu Bay, C_{0sc} is the capital cost of service connections including internal wiring and appliances per household serviced and equals \$125 based on similar networks in Kenya, L is the length of the distribution network in km and is initially set at 1 km for a neighbourhood radius of 500 m, CRF_{pdn} is the capital recovery factor of the distribution network including the service connections and is calculated to be 0.1770, $C_{CGrid_O\&M}$ is the cost of operating and maintaining the communal grid and is estimated to be $\$2.50 \times N$, R is the benchmark unit cost of the communal grid and is set at \$1,400/kWp, and b is a scale factor for incorporating cost reduction in overall cost of the communal grid, without the power distribution network (pdn), due to bulk purchasing of the components used in the grid. Its effect is uniformly distributed over all components of the communal grid, minus the distribution network. It is set at 0.95.

5.2.2 Subsidies:

Studies show that positive government incentives and subsidies are largely responsible for rapid growths in PV installations in developed nations which have proper market and technical infrastructures necessary for implementation of such policies; Beise's research on diffusions of technologies across national boundaries found that positive government policies significantly stimulated diffusion of PV across many countries, underscoring the importance of government intervention in adaptations of new technologies [138]. A comparable study by Guidolin et al also found that positive government policies in the form of incentives and subsidies positively influenced PV diffusions across 11 countries [139]. Wustenhagen found that positive government policies, especially feed-in-tariffs (FiT), were largely responsible for the boom in PV installations in Germany [140]. Zhang et al found that in addition to positive regional governments' policies, costs also played significant roles in PV diffusion across Japan [141]. In developing nations on the other hand, limited resources restrict governments' abilities to subsidize new technologies as priorities are given to crucial projects. Since there are no PV related subsidies in Kenya, the value is initially set to zero. To investigate impacts of subsidies on temporal diffusion of PV systems in Kendu Bay area, we simulate impacts of increasing subsidies per kWh of PV electricity generated and increasing subsidies per m² of PV installed.

Subsidies per kWh (S_{kWh}) is given by [91]

$$S_{kWh} = C_{PV/kWh} - C_{A/kWh} \quad (5.13)$$

where $C_{PV/kWh}$ is the PV generation cost per kWh and is given by

$$C_{PV/kWh} = \frac{C_{PV-Total}}{(E_{PV-Total} \times L_{PV})} \quad (5.14)$$

where $C_{PV-Total}$ is the total PV cost, $E_{PV-Total}$ is the total PV output, and L_{PV} is PV lifetime and is set at 25 years based on Kendu Bay data.

Total PV cost ($C_{PV-Total}$) is given by

$$C_{PV-Total} = (C_{0PV} - S_{m^2}) \times \varepsilon_{PV} \times A \times AF \quad (5.15)$$

where C_{0PV} is the capital cost of the PV module per Wp and is set at \$1.40 based on Kendu Bay data, S_{m^2} is subsidies per m^2 and is initially set to zero, ε_{PV} is PV efficiency and is set at 15% based on Kendu Bay data, A is roof area available under PV Installation and is randomly set between $10m^2$ and $50m^2$, and AF is an accounting factor given by

$$AF = (1 + r)^{L_{PV}} \quad (5.16)$$

where r is the lending rate; if a household purchases PV on credit, lending rate (r) on the loan is used for accounting factor AF calculations. For cash buyers, $r = 0$.

Total PV output $E_{PV-Total}$ (kWh) is given by

$$E_{PV-Total} = I_{PV} \times PR \times \varepsilon_{PV} \times A \quad (5.17)$$

where PR is the performance ratio which takes into account losses from components, environmental factors, etc., and is initially set at 0.75, while I_{PV} in kWh/m^2 is the irradiation on tilted panels and is given by [91]

$$I_{PV} = I_{incident} \sin(\alpha + \beta) \quad (5.18)$$

where $I_{incident}$ is the solar radiation measured orthogonal to the sun rays, α is the elevation angle, and β is the tilt angle of the module measured from horizontal, as expressed by equations 3.3 – 3.13 in chapter 3.

5.2.3 Neighbourhood Influence:

Rogers' theory of Diffusion of Innovations (DOI) states that diffusion of a new technology into a given market depends on its relative advantage, compatibility, ease of use, and social acceptance amongst other factors [142]. According to this theory, different attitudes towards the new technology affect initial adoption rates, with more acceptances experienced with time after observations of the benefits of the new technology have been made [142]. Studies show that social acceptance is crucial to successful dissemination of a new technology, and even more so with solar home systems which impact on individuals' spaces both passively and actively [143-145]. An individual's willingness to participate in the microgeneration process through financial investment, provision of an installation site, or behavioural change is important for successful uptake of such technologies [146]. Attitudes towards microgeneration technologies govern their social acceptances; in developed nations consumers are motivated by autonomy, interest in the new technology, environmental concerns, and economic reasons [146-149]. In developing nations on the other hand, consumers are motivated by availability; people are in need of electricity irrespective of its source, and microgeneration technologies just happen to be the most readily available and cost-effective means of achieving electrification. In many cases, the environment is an unintended beneficiary.

A major factor in social acceptance is neighbourhood influence. Knowledge of a new technology is necessary for a consumer to make an informed decision on its adoption, but this is difficult with nascent technologies such as PV where information is asymmetrical, with producers being in better positions to test the technology than consumers, contributing to their initial slow diffusions in new markets [150-153]. In such cases, neighbourhood influence from early and independent adopters play important roles in increased future adoption rates [154-156]. Bollinger and Gillingham argue that neighbourhood influence begins to play a more important role once early adopters have installed a new technology [156]; they infer that visibility of a new technology (PV installed on roofs) coupled with word-of-mouth about benefits of the new technology leads to increased adoption within a given neighbourhood or sensing radius [157]. Weber and Rode researched on the impacts of observational learning, or visibility of a new technology, on adoption of PV installations, while ignoring the effects of social interactions or word-of-mouth [157]. They found that, even though visibility played an important role in PV diffusion, its effect was more localized to immediate neighbours thus to a small sensing radius [157].

It is difficult to model the impacts of different non-quantitative social aspects on the adoption of a new technology. However, a measurable parameter such as sensing-radius, the radius within which

a household can 'sense' its neighbours, and neighbourhood-threshold, the minimum percentage of neighbours within a given sensing radius that must have adopted a new technology for a household to consider doing the same, can be modelled and varied to explore the impacts of such parameters on the adoption of a new technology. If we assign a coefficient of innovation p to early adopter and a coefficient of imitation q to neighbourhood influence, the probability that a household deciding on PV installation actually adopts at time t is given by [158]

$$(p + qF(t)) \quad (5.19)$$

where $F(t)$ is the proportion of adopters at time t . Without neighbourhood influence, $p > 0, q = 0$, while without early adopters $p = 0, q > 0$.

The probability density function for a house that is deciding on PV installation at a time t is given by

$$f(t) = (p + qF(t))(1 - F(t)) \quad (5.20)$$

And the corresponding cumulative density function is given by

$$F(t) = \frac{1 - \exp(-(p + q)t)}{1 + \frac{q}{p} \exp(-(p + q)t)} \quad (5.21)$$

Given a market potential factor m , cumulative adoption of PV at a time t is given by $F(t) \times m$. Coefficients p and q , and market factor m are considered environmental variables to account for the changing and unstable environment within which diffusion of a new technology occurs. Initial and independent adoption decisions are mainly influenced by perceived or measured costs, social pressures such as advertising campaigns, a level of awareness of the new technology, attitudes towards the new technology such as environmental concerns in case of PV, and social demographics such as education and income levels. These factors are captured in the coefficient of innovation p . Perceived and spoken (word-of-mouth) benefits of the new technology are captured in the coefficient of imitation q . Geographical factors such as location and demographics will determine the market saturation levels which are then captured in the market potential factor m . Preferences for specific product attributes such as cost and environmental benefits can influence adoption timing decisions of new technologies as reported in studies by Kim and Srinivasan [159] and by Islam and Meade [160].

As previously mentioned, a household without PV must first develop the idea to install PV given the cost, subsidies, and neighbourhood influence. The idea to install PV returns true if

$$\frac{H_{PV/SR}}{H_{Total/SR}} \times 100 > T_{SR} \quad (5.22)$$

where $H_{PV/SR}$ is the number of households with PV within a given sensing radius (SR), $H_{Total/SR}$ is the total number of households within the same sensing radius, and T_{SR} is the neighbourhood threshold. For Kendu Bay, the initial sensing radius is set at 500m based on population distribution; a sensing radius below 500m limits impacts of neighbourhood influence on a household to one's own clan, based on homestead and farm distributions. The initial neighbourhood threshold is set at 10%; simulation results showed that values below 10% showed no impact (influence) on PV diffusion.

To be allowed to join a communal grid, a household must have electricity needs beyond lighting and must demonstrate this by having installed PV of a given minimum capacity (power-threshold). They must also be within a given sensing radius of other houses with PV that meet the power-threshold. The idea to join a communal grid returns true if

$$\frac{H_{CGRID/SR}}{H_{Total/SR}} \times 100 > T_{SR} \quad (5.23)$$

where $H_{CGRID/SR}$ is the number of households with PV within the sensing radius that meet the power-threshold and $H_{Total/SR}$ is the total number of households within the same sensing radius.

5.3 Results and Discussion:

Tables 5.1 and 5.2 respectively show the annualized life cycle costs (ALCC) and the levelized unit cost of delivered electricity (LUCE) of a PV system with a 40 Wp module and a system with a 100 Wp module, which comprise 99% of all systems installed in rural Kenya as most households only initially need electricity for basic lighting and maybe to charge mobile phones and other small electronic appliances such as radios. It is clear from the tables that as the capacity of the installed system increases, the levelized unit cost of delivered electricity rapidly falls.

System with 40 Wp Module				
Components	Capital Cost (\$)	Life (Years)	CRF	Annualized Cost (\$)
Module (40 Wp)	60	20	0.1339	8.70
Battery (12 V, 40 Ah)	45	5	0.2774	12.48
Charge Controller	25	5	0.2774	6.94
Appliances	75	10	0.1770	13.28
Balance-of-Systems	120	10	0.1770	21.24
O&M	-	-	-	2.50
Total	325	-	-	59.14
Power Output (kWh)	-	-	-	105.12
LUCE (\$/kWh)	-	-	-	0.56

Table 5.1: Annualized Life Cycle Cost and Levelized Unit Cost of Electricity for a 40 Wp System

System with 100 Wp Module				
Components	Capital Cost (\$)	Life (Years)	CRF	Annualized Cost (\$)
Module (100 Wp)	125	20	0.1339	16.74
Battery (24 V, 100 Ah)	90	5	0.2774	24.97
Charge Controller	35	5	0.2774	9.71
Appliances	100	10	0.1770	17.70
Balance-of-Systems	150	10	0.1770	26.55
O&M	-	-	-	2.50
Total	500	-	-	98.17
Power Output (kWh)	-	-	-	262.8
LUCE (\$/kWh)	-	-	-	0.37

Table 5.2 Annualized Life Cycle Cost and Levelized Unit Cost of Electricity for a 100 Wp System

Figures 5.2 and 5.3 show the view at year 0 and after 25 years, respectively. The landscape is coloured green with the lighter areas being hill tops. Black houses are those that are unelectrified. Houses deciding on installing PV are coloured white while those that have installed PV are coloured yellow. Houses with PV that meet the communal grid-power-threshold and are deciding on joining communal grids are coloured red. Houses that have joined communal grids are coloured blue and are linked to other houses in the communal grid through grey links (grid lines). From the figure, it is clear that nearby communal grids join together to form even larger regional grids.

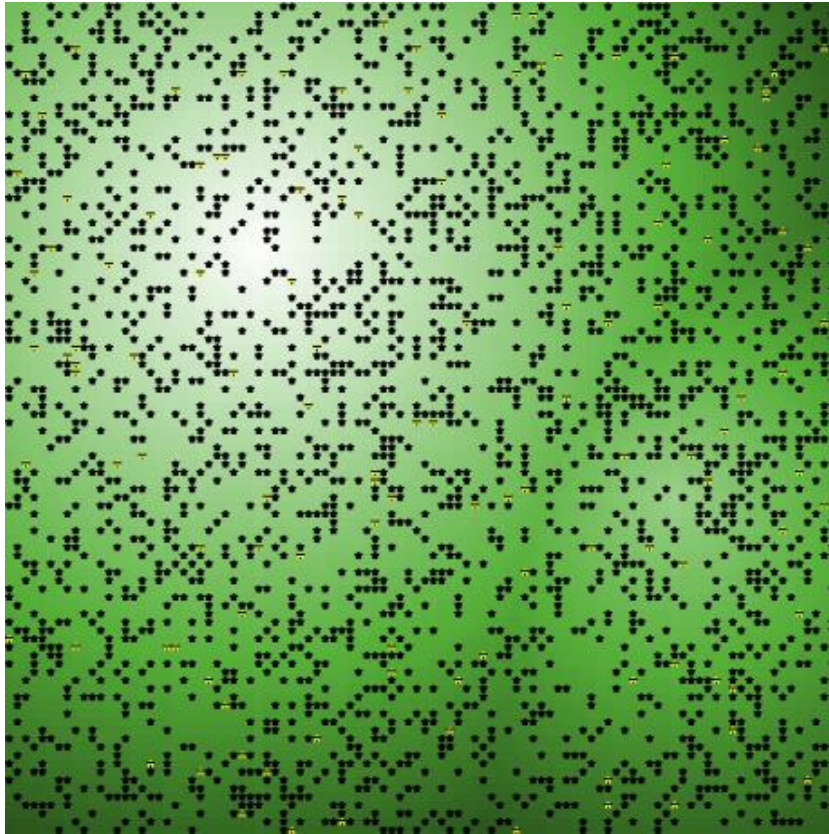


Fig. 5.2: A View of the World before Simulations (Key to colour chamber on preceding paragraph - page 107)

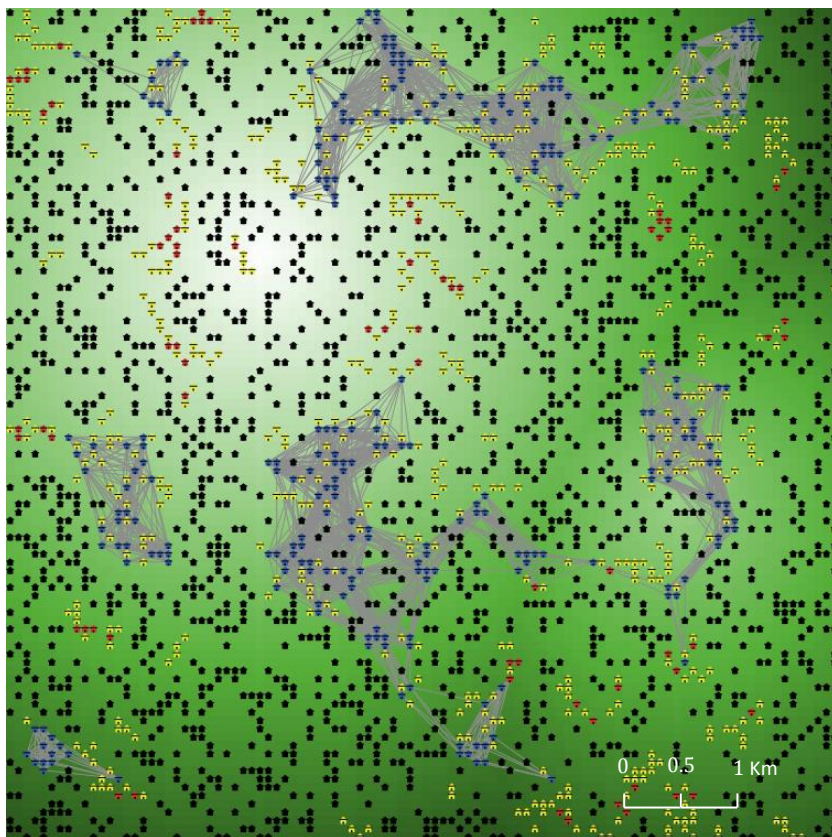


Fig. 5.3: A View of the World after Simulations after 25 Years (Key to colour chamber on preceding paragraph - page 107)

Figure 5.4 shows a graph of households with PV installations, households connected to communal grids, and households connected to the national grid after 25 years while figure 5.5 shows plots of their corresponding percentages. Currently (at year zero) there are 347 households with PV installations in Kendu Bay area, representing 4.7% of all households. Similarly, there are 229 households connected to the national grid, representing 3.1% of all households; there are currently no communal grids in Kendu Bay and thus zero connections. After 25 years, 4,325 households would have installed PV, representing 44.1% of all households. This massive growth is attributable to many factors with the main ones being falling PV costs coupled with increasing households' incomes, increasing neighbourhood influence due to increasing PV installations, increasing awareness of the socio-economic and environmental benefits of PV systems, and generally increasing PV efficiencies and thus increasing outputs for similarly sized systems.

As more households install PV over the years, and as households' electricity demands increase, more and more households will start looking for ways of increasing their access to electricity; therefore, households will start coming together to form communal grids or to join already existing communal grids. Specifically, households connected to communal grids are estimated to grow from zero to about 2,410 after 25 years, representing 24.6% of all households. This massive growth is attributable to the same factors as those that influence PV installations. Moreover, communal grids are sized to match demands and can therefore be set up with small initial investments. Also, they are modifiable with increasing demands or with changing technologies, and could thus be expanded with increasing incomes. Even though households connected to the national grid will also grow from 229 to 1,323 after 25 years, representing 13.5% of all households and 23.4% of all electrified households., electrification through PV systems and PV-based communal grids will grow at a faster pace, representing 76.6% of all electrified households.

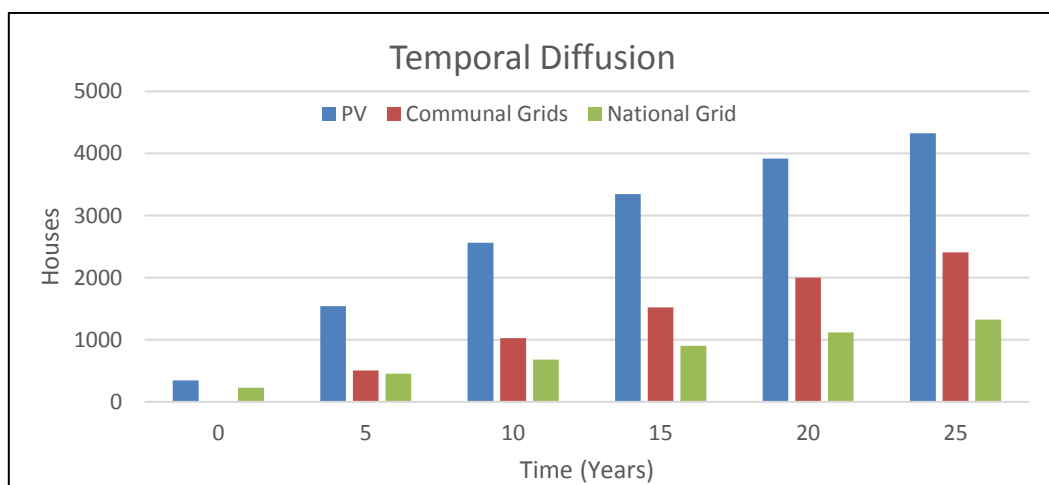


Fig. 5.4: Kendu Bay Electrification Topologies

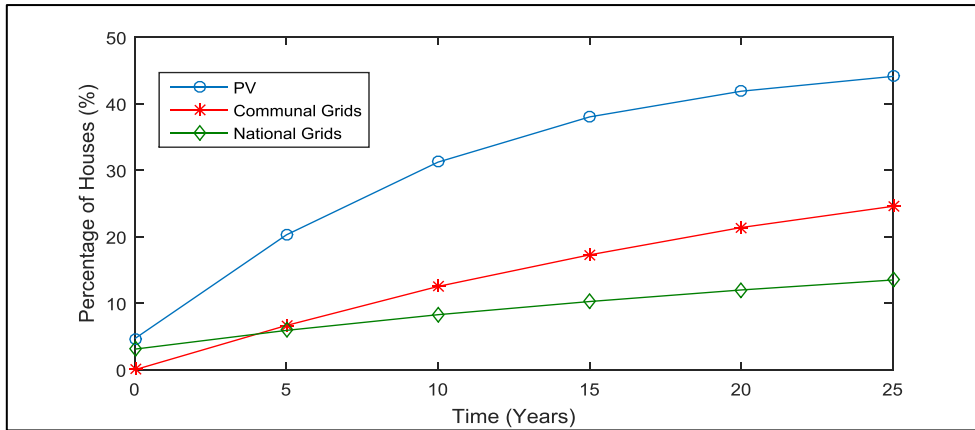


Fig. 5.5: Kendu Bay Electrification Topologies by Percentages

Overall electrification rate increases from 7.8% at year zero to 57.6% after 25 years as shown in figure 5.6 below. Majority of these, 44.1%, will be electrified through PV systems of varying sizes, 24.6% will be electrified through communal grids, and 13.5% through the national grid.

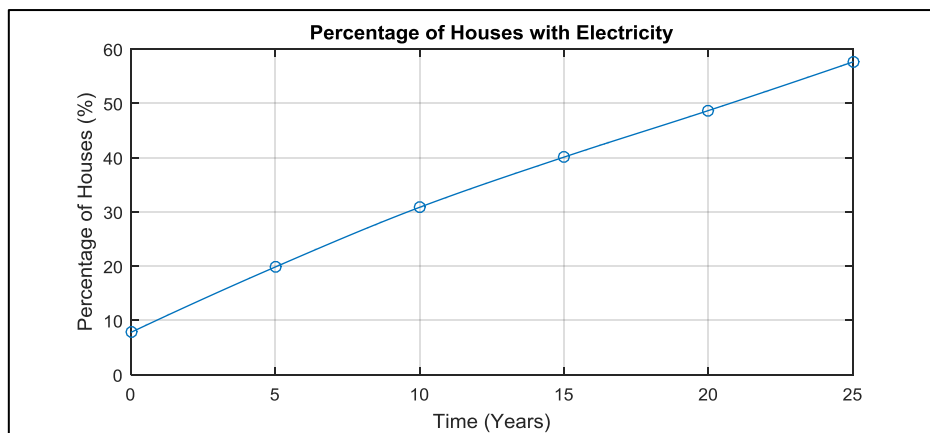


Fig. 5.6: Percentage of Electrified Households

5.3.1 Impacts of Subsidies on PV Diffusion:

In this section we simulate how introduction of subsidies would impact on temporal diffusion of PV systems and PV-based communal grids in Kendu Bay area. Currently there are no functional subsidies in Kenya and therefore both values are initially set to zero.

5.3.1.1 Subsidies/kWh of PV Power Generated:

Figure 5.7 shows a graph of households with PV, households connected to communal grids, and households connected to the national grid as functions of increasing subsidies/kWh of power generated, after 25 years, while figure 5.8 shows plots of their corresponding percentages. Without subsidies 4,325 households would have installed PV after 25 years, representing 44.1% of all

households. If a subsidy of \$0.10/kWh is introduced, the number of households with PV after 25 years jumps to 5,067, representing 51.7% of all households, and an increase of 17.2% in PV installations. A subsidy of \$0.20/kWh would lead to 5,591 PV installations, representing 57% of all households and an increase of 29.3% in PV installations. Similarly, introduction of a subsidy of \$0.30/kWh would lead to 5,827 PV installations, or 59.4% of all households, and an increase of 34.7% in PV installations. As PV installations increase, so do communal grid formations and/or connections. Without subsidies, 2,410 households would have connected to communal grids after 25 years, representing 24.6% of all households. This figure increases to 2,791 with introduction of a subsidy of \$0.10/kWh, representing 28.5% of all households, and an increase of 15.8% in communal grids connections. Similarly, subsidies of \$0.20/kWh and \$0.30/kWh would lead to 3,217 (32.5%) and 3,685 (37.6%) communal grids connections, respectively and representing increases of 33.5% and 52.9%, respectively.

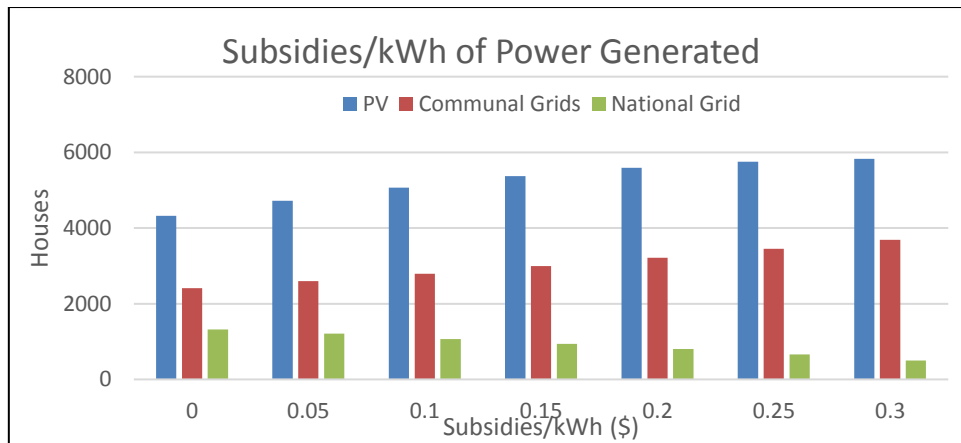


Fig. 5.7: Impacts of Subsidies/kWh on Electrification Topologies after 25 Years

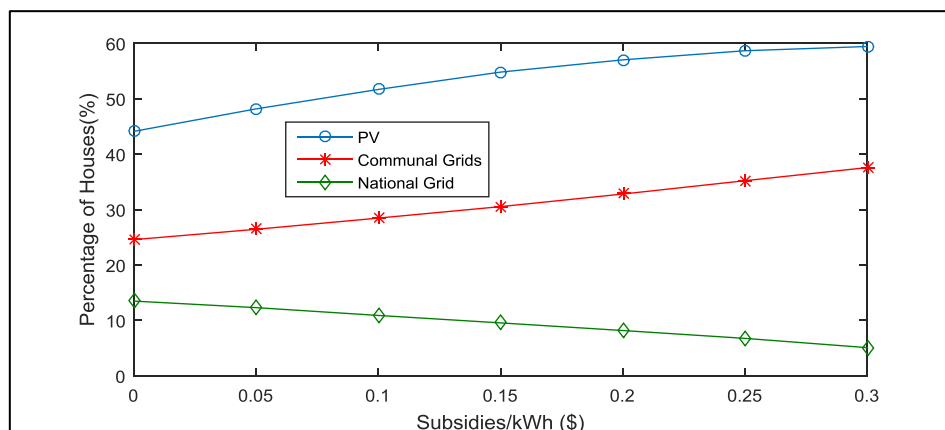


Fig. 5.8: Impacts of Subsidies/kWh on Electrification Topologies in Percentages after 25 Years

As PV installations increase, and as more households opt for PV-based communal grids, connections to the national grid fall. Specifically, without subsidies, 1,323 households would have connected to

the national grid after 25 years. This falls to 1,069 with introduction of a subsidy of \$0.10/kWh, and even further to 802 and 499 with introductions of subsidies of \$0.20/kWh and \$0.30/kWh, respectively. In percentage terms, national grid connections fall from 13.5% with no subsidies to 5.1% with subsidies of \$0.30/kWh. Overall, introduction of subsidies/kWh leads to a logarithmic rise in the number of electrified households as shown in figure 5.9 mainly due to increased PV installations. Specifically, with no subsidies, the percentage of electrified households after 25 years will have risen to 57.6%. With a subsidy of \$0.15/kWh, the percentage of electrified households after 25 years rises to 64.2% while with a subsidy of \$0.30/kWh, the percentage rises to 66.6%. The overall rise in electrification rate is logarithmic, meaning, increments in subsidies become less insignificant with time.

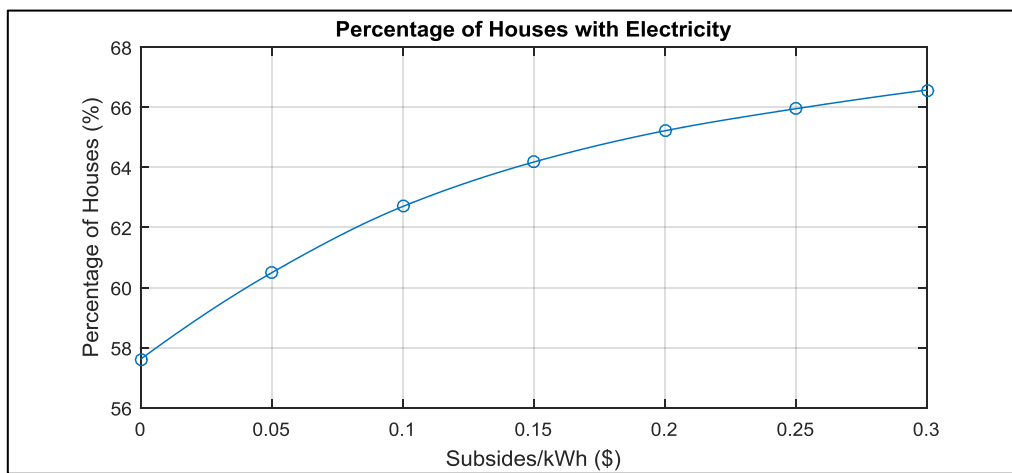


Fig. 5.9: Percentage of Electrified Households after 25 Years

5.3.1.2 Subsidies/m² of PV Installed:

Figure 5.10 shows a graph of households with PV, households connected to communal grids, and households connected to the national grid as functions of increasing subsidies/m² of PV installed, after 25 years, while figure 5.11 shows plots of their corresponding percentages. Without subsidies 4,325 households would have installed PV after 25 years, representing 44.1% of all household. If a subsidy of \$50/m² is introduced, the number of households with PV after 25 years jumps to 5,023, representing 51.2% of all households, and an increase of 16.1% in PV installations. A subsidy of \$100/m² would lead to 5,601 PV installations, representing 57.1% of all households and an increase of 29.5% in PV installations. Similarly, introduction of a subsidy of \$150/m² would lead to 6,012 PV installations, or 61.4% of all households, and an increase of 39% in PV installations. As PV installations increase so do communal grids formations and connections. Without subsidies, 2,410 households would have connected to communal grids after 25 years, representing 24.6% of all

households. This figure increases to 2,829 with introduction of a subsidy of \$50/m², representing 28.9% of all households, and an increase of 17.4% in communal grids connections. Similarly, subsidies of \$100/m² and \$150/m² would lead to 3,254 (33.2%) and 3,689 (37.6%) communal grids connections, respectively, which represents increases of 35% and 53.1% in connections, respectively. As PV installations increase, and as more households opt for PV-based communal grids, connections to the national grid fall with increasing subsidies/m². Specifically, without subsidies, 1,323 households would have connected to the national grid after 25 years. This falls to 1,129 with introduction of a subsidy of \$50/m², and even further to 923 and 701 with introductions of subsidies of \$100/m² and \$150/m², respectively. In percentage terms, national grid connections fall from 13.5% with no subsidies to 7.2% with subsidies of \$150/m².

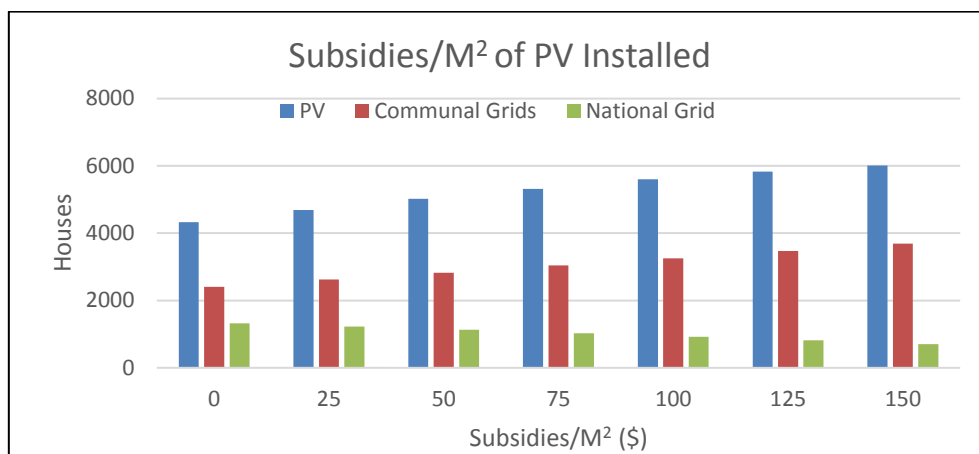


Fig. 5.10: Impacts of Subsidies/m² on Electrification Topologies after 25 Years

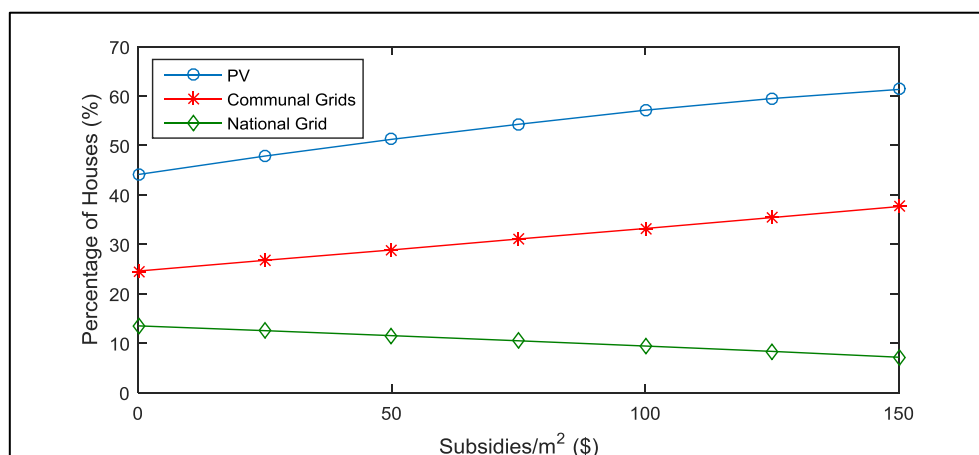


Fig. 5.11: Impacts of Subsidies/m² on Electrification Topologies in Percentages after 25 Years

Overall, introduction of subsidies/m² leads to a logarithmic rise in the number of electrified households as shown in figure 5.12 mainly due to increased PV installations. Specifically with no subsidies, the Percentage of electrified households after 25 years will have risen to 57.6%. With a

subsidy of \$75/m², the percentage of electrified households after 25 years rises to 64.7%. Similarly, with a subsidy of \$150/m², the percentage rises to 68.5%.

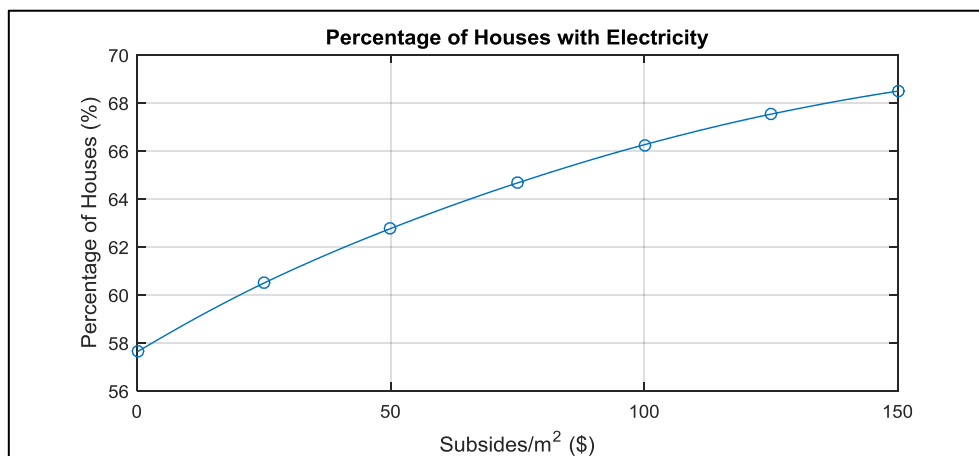


Fig. 5.12: Percentage of Electrified Households after 25 Years

Table 5.3 below summarizes the above information. It is clear from the results that introduction of either capital or energy subsidies would lead to increased PV installations which would in turn lead to increased connections to communal grids. The increases in PV installations due to introduction of either of the subsidies is insignificant, leading us to believe that both would simulate PV installations with equal measure. Also, electrification through PV-based systems of various sizes will rise at a faster pace than through national grid connections. Subsidies should only be given to households that are able and willing to install PV. The minimum household income level is therefore set at \$200. It is important to note that subsidies commit future governments to financial burdens and there may be concern over lack of commitment to promises made by previous governments.

Houses after 25 years	Subsidies/kWh (\$)		
	0	0.15	0.30
Houses with PV	4325	5374	5827
Houses Connected to Communal Grids	2410	2994	3685
Houses Connected to National Grid	1323	937	499
Houses after 25 years	Subsidies/m² (\$)		
	0	75	150
Houses with PV	4325	5321	6012
Houses Connected to Communal Grids	2410	3046	3689
Houses Connected to National Grid	1323	1027	701

Table 5.3 Impacts of Subsidies on Electrification Topologies after 25 Years

5.3.2 Impacts of Neighbourhood Influence on PV Diffusion:

In this section we simulate how increasing neighbourhood influence, modelled as sensing radius and neighbourhood threshold, would impact on temporal diffusion of PV systems and PV-based communal grids in Kendu Bay area.

5.3.2.1 Sensing Radius:

The default sensing radius is set at 0.5 km, based on Kendu Bay's population distribution and socio-economic demographics as discussed in section 5.2.3. Figure 5.13 shows a graph of households with PV, households connected to communal grids and households connected to the national grid as functions of increasing sensing radius, after 25 years, while figure 5.14 shows plots of their corresponding percentages. If the sensing radius is increased from 0.5 km to 1 km, the number of households with PV installations increases from 4,325 to 4,617 after 25 years, representing 47.1% of all households and an increase of 6.8% in PV installations. Similarly, increasing the sensing radius to 1.5 km and to 2 km would result in 4,909 and 5,204 PV installations after 25 years, respectively and representing 50.1% and 53.1% of all households, respectively. Increasing sensing radius means increasing neighbourhood influence, and thus increasing PV installations. As more households install PV, and as their power demands increase, so do connections to communal grids. Specifically, if the sensing radius is increased from 0.5 km to 1 km, the number of households connected to communal grids would increase from 2,410 (24.6%) to 2,635 (26.9%) after 25 years, representing an increase of 9.3% in connections. Similarly, increasing the sensing radius to 1.5 km and to 2 km would result in 2,869 (29.3%) and 3,092 (31.5%) communal grid connections, respectively, representing increases of 19% and 28.3%, respectively. Increasing communal grid connections is indicative of increasing household power demands and greater preference for PV systems.

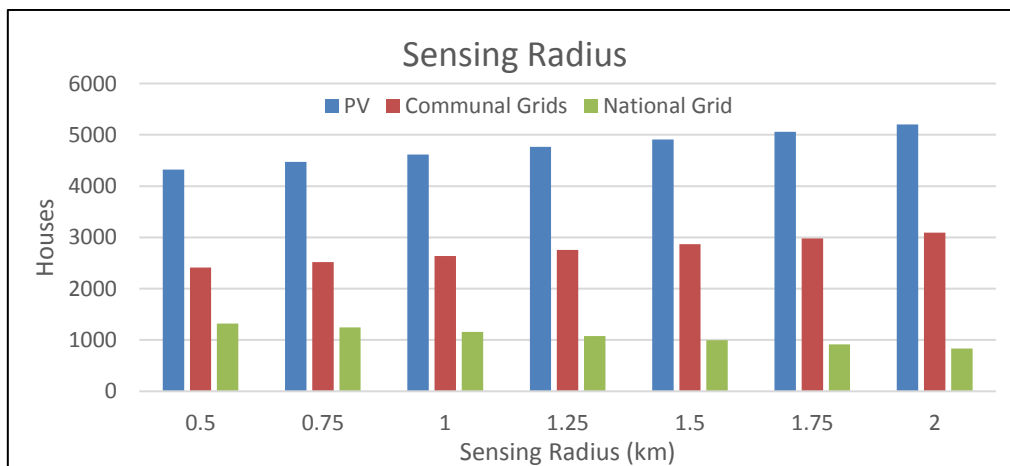


Fig. 5.13: Impacts of Sensing Radius on Electrification Topologies after 25 Years

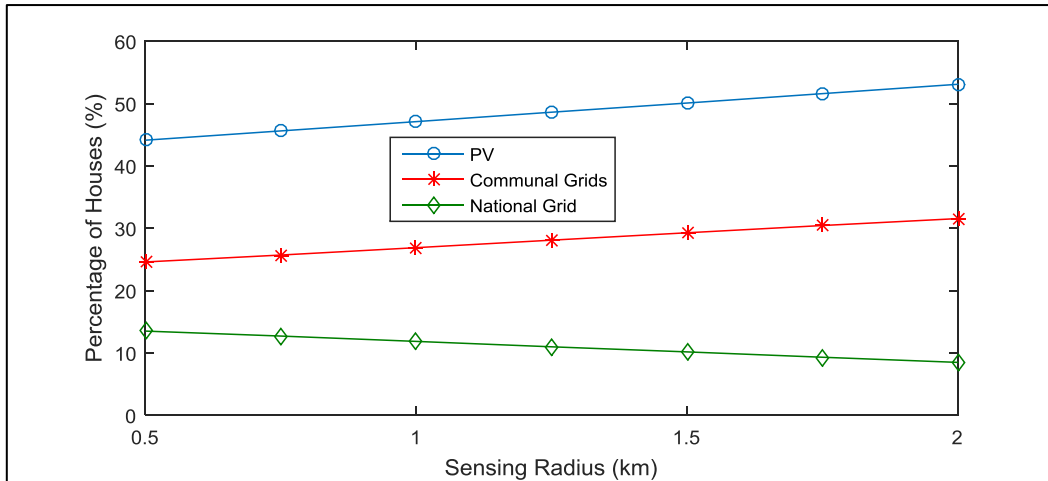


Fig. 5.14: Impacts of Sensing Radius on Electrification Topologies in Percentages after 25 Years

As electrification through PV systems increase with increasing sensing radius, electrification through the national grid connections falls. Specifically, connections to the national grid falls from 1,323 (13.5%) to 1,161 (11.8%) if the sensing radius is increased to 1 km. If the sensing radius is increased to 1.5 km, national grid connections fall to 996 (10.2%). Increasing the sensing radius to 2 km would result in further fall in houses electrifying through the national grid to 831, representing 8.5% of all households. So, even though now only 3.1% of Kendu Bay households are electrified through the national grid, increases in national grid connections over 25 years slow with increasing sensing radius as increasing neighbourhood influence positively impacts on PV installations.

Overall, the electrification rate linearly increases with increasing sensing radius as shown in figure 5.15, from 5,658 households at 0.5 km sensing radius after 25 years, representing 57.6% of all households, to 6,035 households at 2 km sensing radius, representing 61.6% of all households

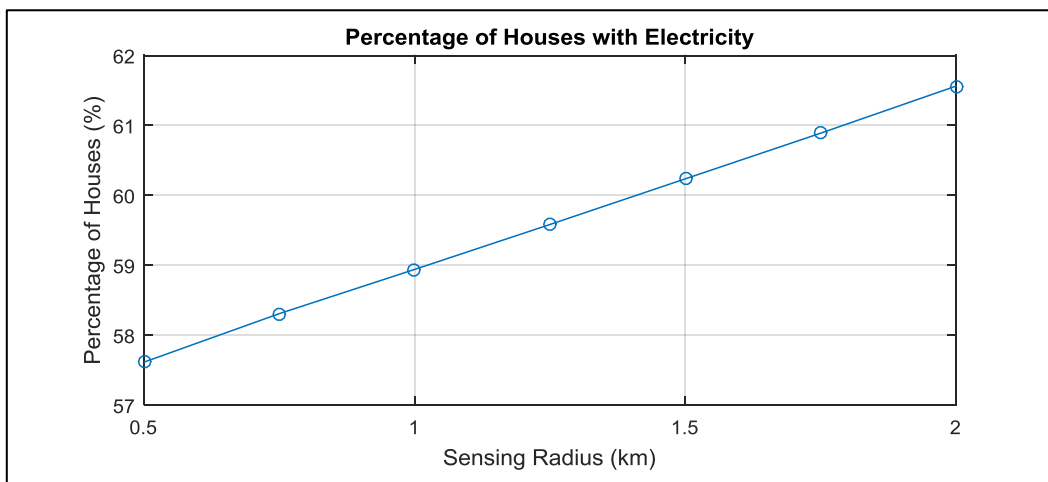


Fig. 5.15: Percentage of Electrified Households after 25 Years

5.3.2.2 Neighbourhood Threshold:

As discussed above, neighbourhood threshold is the minimum percentage of neighbours within a given sensing radius (neighbourhood) that must have installed PV for a given household to consider doing the same. It is an important parameter in measuring neighbourhood influence and in calculating the percentage of early, or independent, adopters. The objective is to determine what optimal percentage of households must have installed PV for nearby neighbours to start noticing. Figure 5.16 shows a graph of households with PV, households connected to communal grids, and households connected to the national grid as functions of increasing neighbourhood threshold, after 25 years, while figure 5.17 shows plots of their corresponding percentages. With no neighbourhood threshold, 4,325 household would have installed PV after 25 years, representing 44.1% of all households. Imposing a neighbourhood threshold of 5% would result in 4,065 PV installations after 25 years, representing 41.5% of all households, and a fall of 6% in PV installations. Similarly, if a neighbourhood threshold of 10% is imposed, total PV installations after 25 years falls even further to 3,617, representing 36.9% of all households and a fall of 16.4% in PV installations after 25 years. A similar trend is observed if a neighbourhood threshold of 15% is imposed, leading to a 31.4% fall in total PV installations after 25 years. As PV installations fall so do connections to communal grids. With no neighbourhood threshold, 2,410 household would have connected to communal grids after 25 years, representing 24.6% of all households. Imposing a neighbourhood threshold of 5% would result in 2,108 communal grids connections after 25 years, representing 21.5% of all households, and a fall of 12.5% in communal grids connections. Similarly, if a neighbourhood threshold of 10% is imposed, total communal grids connections after 25 years falls even further to 1,722, representing 17.6% of all households and a fall of 28.5% in communal grid connections after 25 years. A similar trend is observed if a neighbourhood threshold of 15% is imposed, leading to a 47.8% fall in communal grids connections after 25 years.

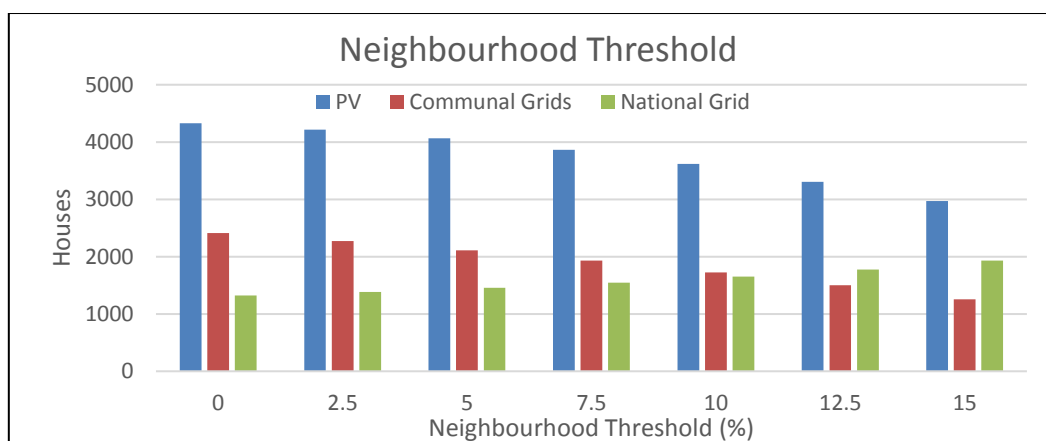


Fig. 5.16: Impacts of Neighbourhood Threshold on Electrification Topologies after 25 Years

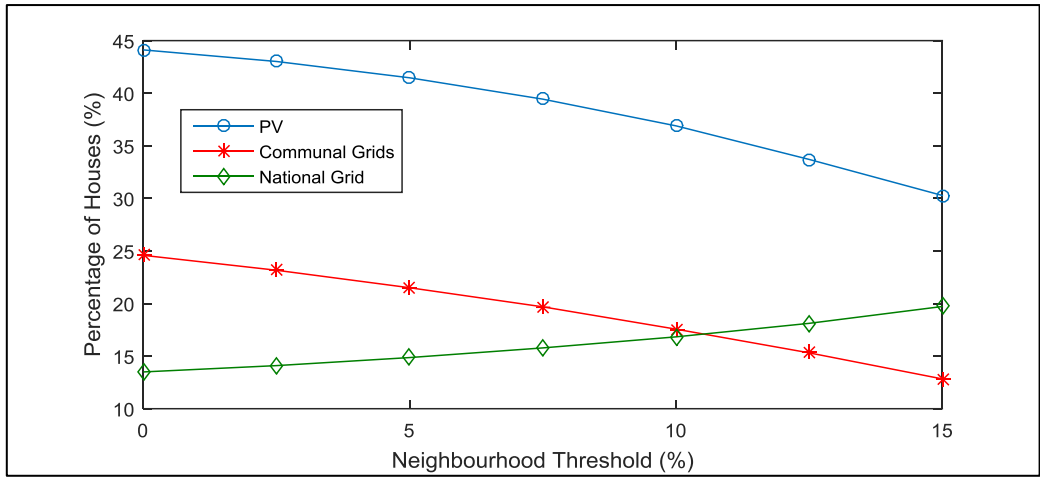


Fig. 5.17: Impacts of Neighbourhood Threshold on Electrification Topologies in Percentages after 25 Years

Falling PV installations and corresponding communal grid connections push people to look for other means of electrifications, in this case, the national grid; connections to the national grid increases from 1,323 with no neighbourhood threshold, representing 13.5% of all households, to 1,933 with introduction of 15% neighbourhood threshold, representing 19.7% of all households and an increase of 46.1% in national grid connections.

Increasing neighbourhood threshold leads to fewer people being electrified after 25 years as fewer people will be able to install PV since majority of Kendu Bay residents cannot afford national grid connection fees, or prefer not to connect to it due to other reasons. Specifically, and as shown in figure 5.18, without neighbourhood threshold, 57.6% of Kendu Bay residents would be electrified after 25 years, mainly through small PV systems. This number falls to 56.3% with introduction of a neighbourhood threshold of 5%, and even further to 53.7% and 50% with introduction of thresholds of 10% and 15%, respectively.

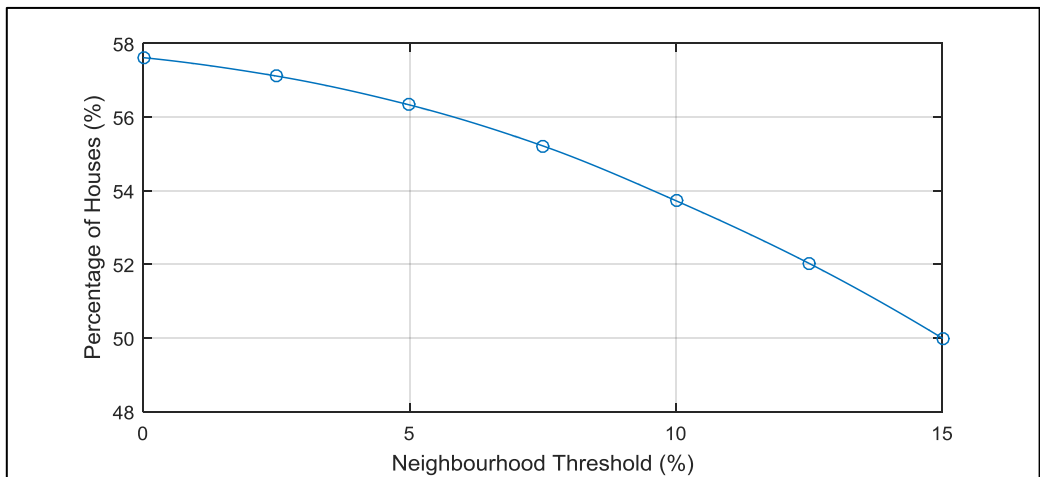


Fig. 5.18: Percentage of Electrified Households after 25 Years

5.3.3 Impacts of Costs on PV Diffusion:

Currently, 92.2% of Kendu Bay households are unelectrified due to inability to afford small PV systems or national grid connection fees. In this section we simulate how generally falling PV costs, generally increasing utility grid costs, and different lending rates for PV purchases would impact on future electrification topologies in Kendu Bay area.

5.3.3.1 Impacts of Falling PV Costs:

Figure 5.19 shows a graph of households with PV, households connected to communal grids, and households connected to the national grid as functions of generally falling PV costs, after 25 years; figure 5.20 shows plots of their corresponding percentages. PV systems are generally more expensive in developing countries and effectively costs about \$1.40/Wp in Kenya. At this price, 4,325 household would have installed PV after 25 years, representing 44.1% of all households. As PV costs continue to fall, installations will correspondingly rise with a PV cost of \$1.00/Wp leading to 4,749 installations after 25 years, and representing 48.4% of all households. If PV costs fall to \$0.40/Wp, PV installations after 25 years would increase to 6,058, representing 61.8% of all households.

As PV installations increase so do communal grid connections or formations; with the current PV costs of \$1.40/Wp, 2,410 households would have connected to communal grids after 25 years, representing 24.6% of all households. If PV costs were to drop to \$1.00/Wp, 2,517 households would have connected to communal grids after 25 years, representing 25.7% of all households. Similarly, if PV costs fall to \$0.40/Wp, 3,427 households would have connected to communal grids after 25 years, representing 35% of all households.

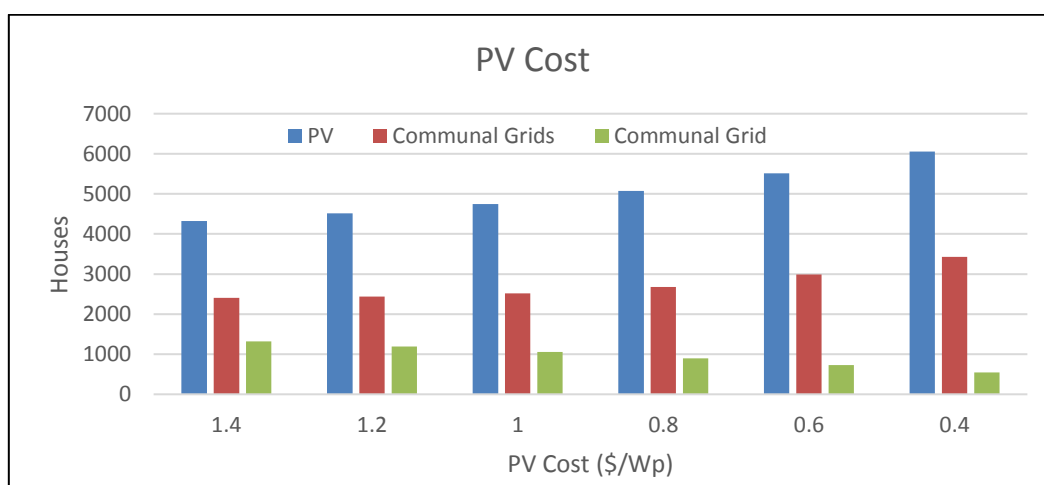


Fig. 5.19: Impacts of Falling PV Costs on Electrification Topologies after 25 Years

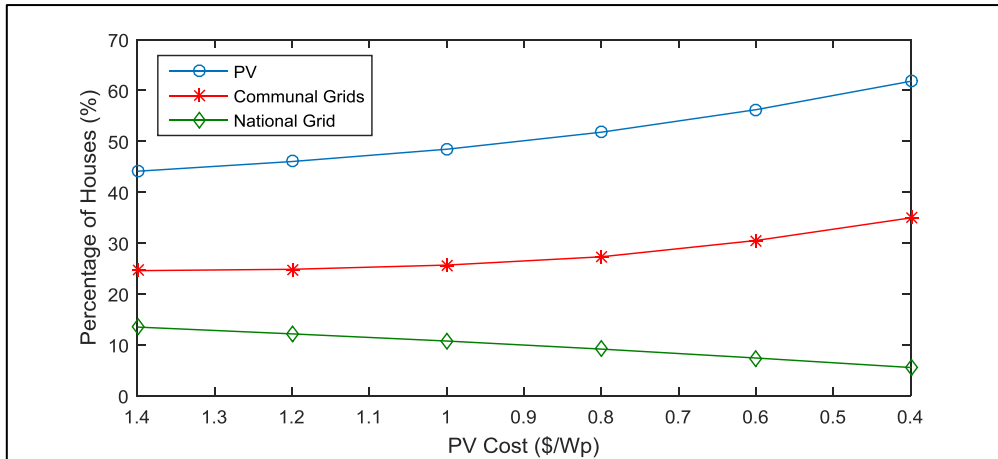


Fig. 5.20: Impacts of Falling PV Costs on Electrification Topologies in Percentages after 25 Years

As electrification through PV systems increases with falling PV costs, electrification through national grid connections falls. Specifically, connections to the national grid falls from 1,323 (13.5%) to 1,054 (10.8%) if PV costs fall from \$1.40/Wp to \$1.00/Wp. Similarly, a further fall in PV costs to \$0.40/Wp would lead to even further declines in electrification though the national grid, with only 554 households being connected to the national grid after 25 years, representing 5.5% of all households. As shown in the cubic fit of figure 5.21, overall electrification rate exponentially grows with falling PV costs as more households install PV and join communal grids.

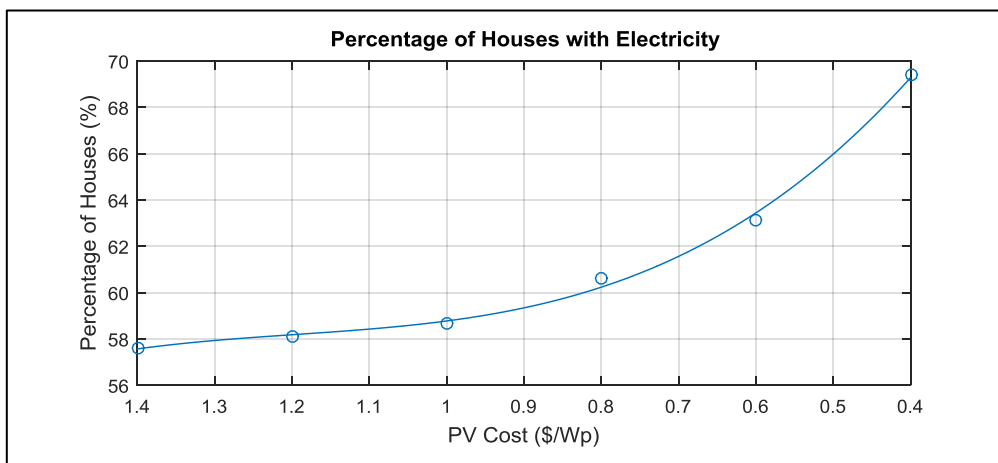


Fig. 5.21: Percentage of Electrified Households after 25 Years

5.3.3.2 Impacts of Increasing Utility Grid Costs:

As PV costs continue to fall, utility grid costs inevitably will continue to rise; figure 5.22 shows a graph of households with PV, households connected to communal grids, and households connected to the national grid as functions of generally increasing utility grid costs, after 25 years; figure 5.23 shows plots of their corresponding percentages. Currently grid electricity costs about \$.20/kWh in

Kendu Bay. At this price, 4,325 households would have installed PV after 25 years, representing 44.1% of all households. As grid costs continue to rise, PV installations will correspondingly rise, with a grid cost of \$0.22/kWh leading to 4,578 installations after 25 years, representing 46.7% of all households. If grid costs rise to \$0.25/kWh, PV installations after 25 years would increase to 5,456, representing 55.7% of all households. As PV installations increase so do communal grid connections or formations; with the current grid costs of \$0.20/kWh, 2,410 households would have connected to communal grids after 25 years, representing 24.6% of all households. If grid costs were to increase to \$0.22/kWh, 2,577 households would have connected to communal grids after 25 years, representing 26.3% of all households. Similarly, if grid costs rise to \$0.25/kWh, 3,321 households would have connected to communal grids after 25 years, representing 33.9% of all households.

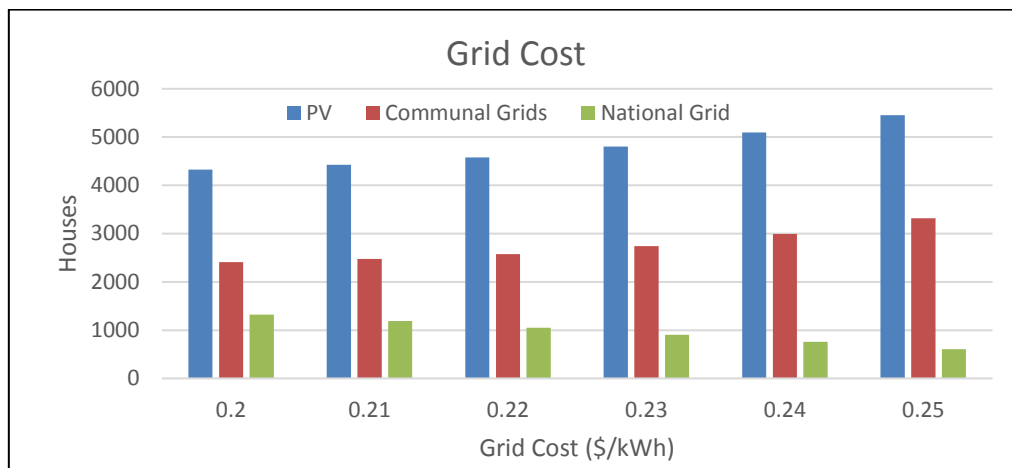


Fig. 5.22: Impacts of Increasing Grid Costs on Electrification Topologies after 25 Years

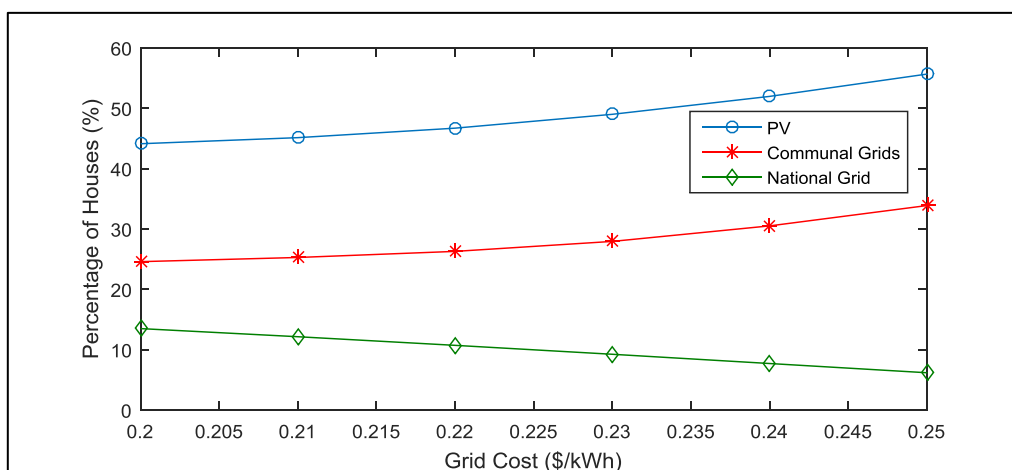


Fig. 5.23: Impacts of Increasing Grid Costs on Electrification Topologies in Percentages after 25 Years

As national grid costs rise, and as electrification through PV systems increase, electrification through national grid connections falls. Specifically, connections to the national grid falls from 1,323 (13.5%)

to 1,051 (10.7%) if grid costs rise from \$0.20/kWh to \$0.22/kWh. Similarly, a further rise in grid costs to \$0.25/kWh would lead to even further decline in electrification through the national grid, with only 606 households being connected to the national grid after 25 years, representing 6.2% of all households. As shown in the cubic fit of figure 5.24, overall electrification rate exponentially grows with increasing grid costs as more households install cheap PV systems and join communal grids.

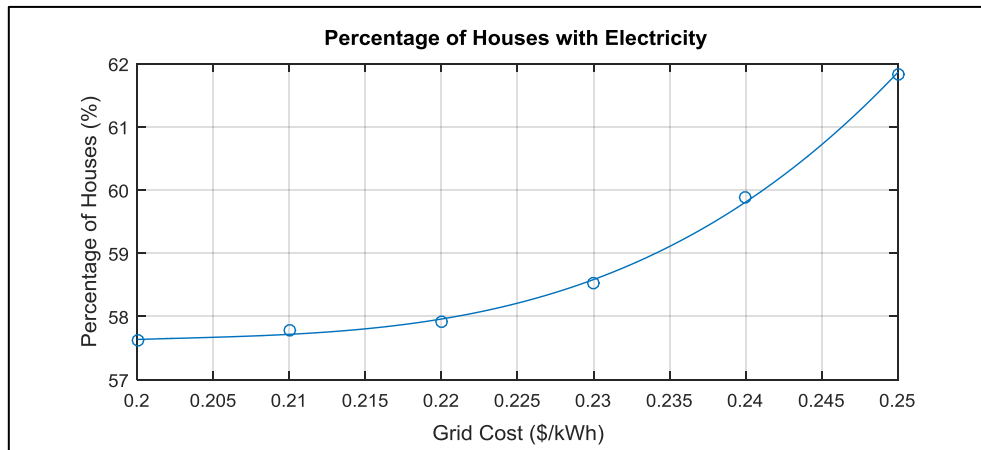


Fig. 5.24: Percentage of Electrified Households after 25 Years

5.3.3.3 Impacts of Lending Rates:

Most PV systems installed by households in Kendu Bay area are small systems with capacities of between 20 Wp and 100 Wp mainly due to basic power demands. Most of these systems are usually bought on cash basis because they are affordable and also due to lack of proper credit facilities to cater to low-income households. To stimulate rural economic growth however, electricity-beyond-lighting is required and this can only be provided through grid electrification. In such cases, larger systems would need to be installed by households to sustain the grid. Such large systems are not easily affordable and thus the need for proper microcredit facilities; in this section the impacts of lending rates on formations of communal grids are explored.

Figure 5.25 shows a graph of households with PV, households connected to communal grids, and households connected to the national grid as functions of increasing lending rates after 25 years; figure 5.26 shows their corresponding percentages. If all PV systems installed in Kendu Bay were purchased on cash basis, 4,325 households would have installed PV after 25 years, representing 44.1% of all households. If a credit facility is introduced with an interest rate of 1% over 5 years, the number of households with PV installations will increase to 4,621, representing 47.14% of all households, representing an increase of 6.8% in PV installations. Total PV installations after 25 years begin to fall as interest rates rise, falling to zero for lending rates above 7%.

Similarly, communal grid formations or connections after 25 years would increase from 2,410 for cash purchases to 2,699 for credit purchases with lending rates of 1% for 5 years. This would then begin to fall with increasing lending rates, falling to zero for lending rates above 6%. On the other hand, connections to the national utility grid will initially fall before beginning to rise again as PV installation fall; low lending rates stimulate PV installations by enabling more households to purchase systems on credit over reasonable payback periods. Increasing PV installations stimulate more power demands and thus formations of communal grids which in turn lead to increased rural microeconomic activities. Increased economic activities lead to increased rural socio-economic development.

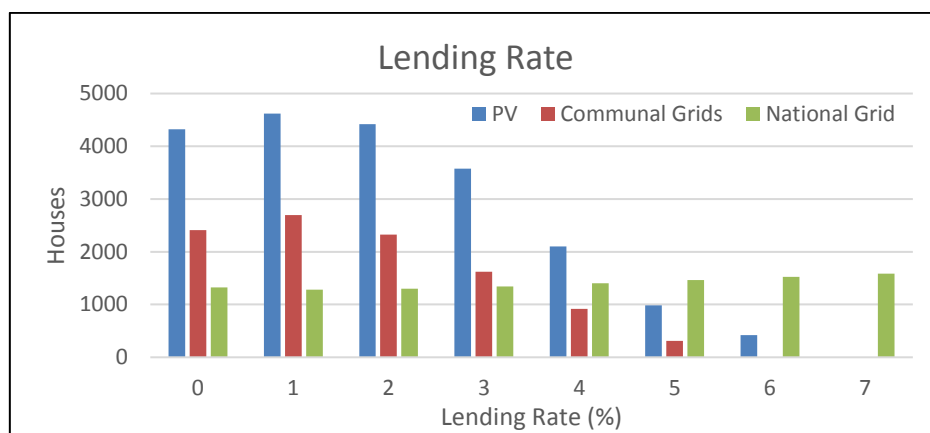


Fig. 5.25: Impacts of Lending Rates on Electrification Topologies after 25 Years

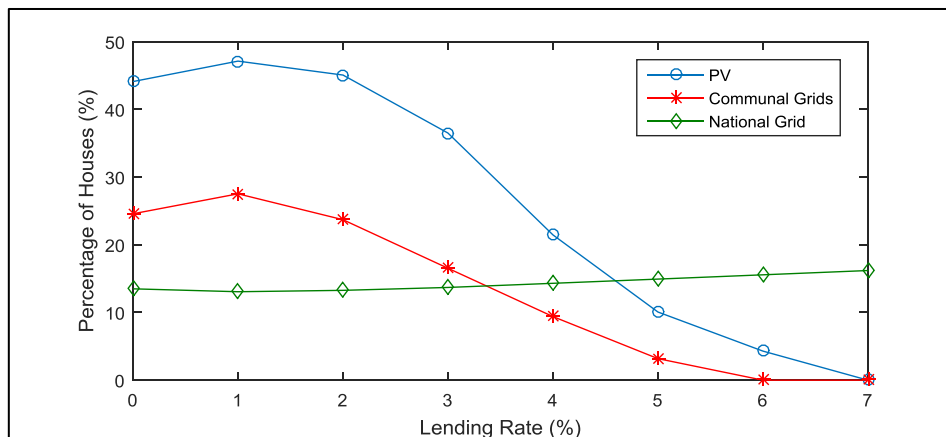


Fig. 5.26: Impacts of Lending Rates on Electrification Topologies in Percentages after 25 Years

Overall, and as shown in figure 5.27, electrification rate exponentially decays with increasing lending rates, as fewer and fewer homes are able to afford PV systems on credit while grid electricity cost will continue to inevitably rise. Many rural households in developing nations are not able to afford small PV systems upfront due to high levels of poverty. Proper and favourable credit facilities must therefore be availed to these people to encourage them to install such systems. High lending rates in

many developing nations brought about by high inflation rates and weak currencies have made the costs of borrowing to be out of reach of many would-be investors. Commercial establishments need to be able to recover costs of lending to consumers within a reasonable timeframe and it would be unbeneficial to lend at no interest. This explains why very few commercial financial institutions are willing to lend for PV installations. A solution lies in guarantees from national governments and even in government funded microcredit facilities to offer low interest rates. Another solution lies in hire-purchase arrangements as seen in Kendu Bay where civil servants can purchase PV systems from the main vendor on interest-free credit with the total cost payable in 6 equal monthly instalments. This arrangement benefits both the buyer and the vendor.

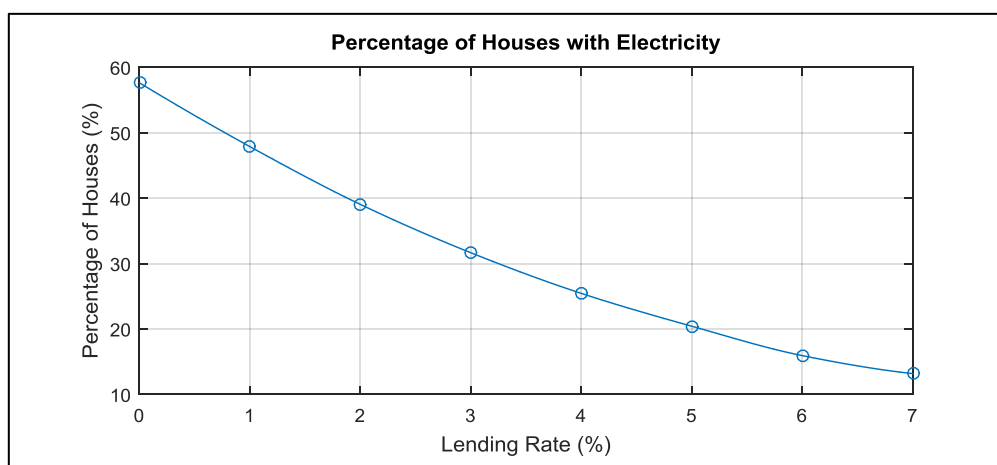


Fig. 5.27: Percentage of Electrified Households after 25 Years

5.4 Model Validation:

Empirical PV installations data from 1985 to 2010 obtained from the Kenya's Ministry of Energy and Petroleum for two separate locations with similar geolocation data to Kendu Bay, i.e. Homabay and Ahero [161], are used to validate the model. The two towns were also chosen because in 1985, their populations of 31,063 (Homabay) and of 26,322 (Ahero) mirrored that of Kendu Bay (29,518) in 2015 [121]. Moreover, both areas are mainly occupied by people of the same ethnic and cultural backgrounds as Kendu Bay and would thus respond similarly to given socio-economic and cultural factors. The PV installations data are obtained by the government from retailers who also perform the tasks of installing and repairing the purchased systems.

PV installation data for Homabay at year zero (1985) was input into the model and then simulated over 25 years. Figure 5.28 shows a comparison of simulated and empirical data for Homabay after 25 years. For empirical data, year 1985 is taken as year zero while year 2010 is taken as year 25. It is assumed that PV costs in 1985 were lower than current costs but that household income levels then

were also lower than income levels today by a similar ratio. The errors range between 0.01 and 0.05, making the model reasonably accurate. In all simulations, increasing population and falling PV costs are taken into account using available census data from the Kenyan Government [121].

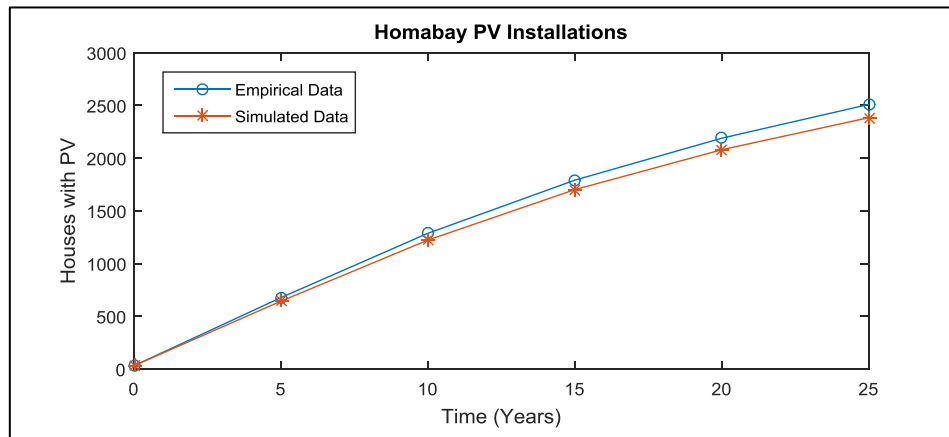


Fig. 5.28: Empirical and Simulated Homabay PV Installations Plots

A similar comparison was done for PV installations in Ahero and the results are as shown in figure 5.29. Here again, it is assumed that PV costs in 1985 were lower than current costs but that household income levels then were also lower than income levels today by a similar ratio. The error is below 0.05, further validating the model.

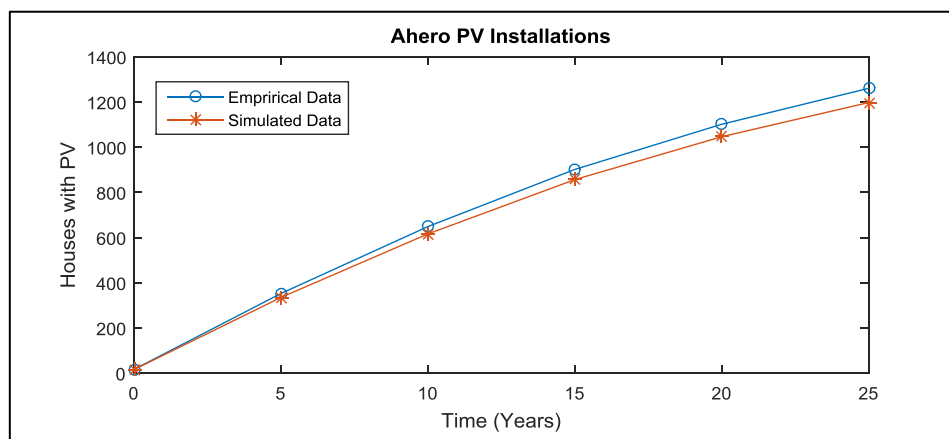


Fig. 5.29: Empirical and Simulated Ahero PV Installations Plots

Figure 5.30 shows comparisons of simulated PV installations for Homabay, Ahero, and Kendu Bay after 25 years while figure 5.31 shows a plot of empirical (Homabay and Ahero) and simulated (Kendu Bay) PV installations data after 25 years. The plots show similar trends in PV installations, with Kendu Bay installations being greater than the other two due to rapidly falling PV costs and increasing awareness of their benefits. The plots further validate the model.

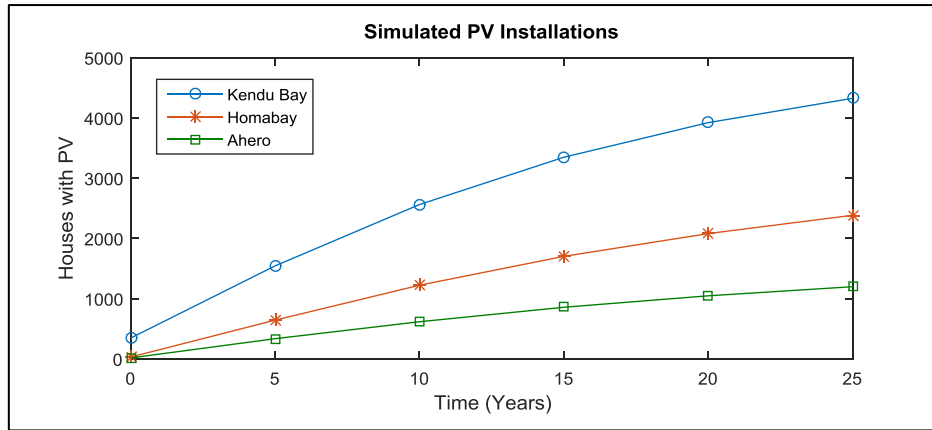


Fig. 5.30: Comparison of Simulated PV Installations Plots

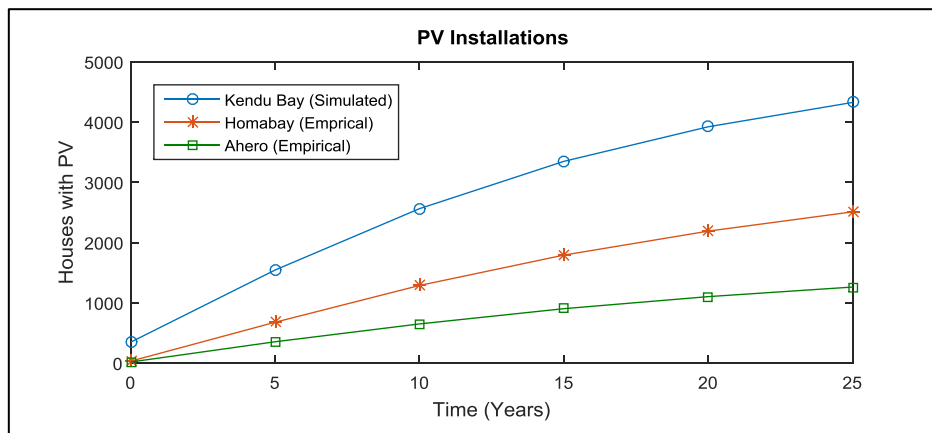


Fig. 5.31: Comparison of Empirical and Simulated PV Installations Plots

Further and more accurate validation of the model will be done after a follow up survey in the future. The current validation assumes that the ratio of PV cost to household income level in 1985 and similar to current ratios, making difference in diffusion of PV installations insignificant. This is not a very accurate assumption.

5.5 Concluding Remarks:

In this chapter, temporal diffusion of PV microgeneration systems in Kendu Bay area is modelled and simulated using an agent-based model developed in Netlogo. Results show that after 25 years, more households will be electrified through PV systems than through the national grid. Specifically, results show that the electrification rate in the area will steadily rise from the current 7.8% to 57.6%. Of the electrified households, 44.1% will be electrified through PV systems, with 24.6% being connected to communal grids. Another 13.5% will be electrified through the national grid. These trends are attributable to rapidly falling PV costs coupled with the availability of small PV systems tailored for rural households with basic electricity needs. These systems enable rural households to make

modest investments into PV systems, tailored to meet their basic power demands. Moreover, with increasing incomes and power demands, households could modestly modify their systems in a step-wise fashion. These systems therefore act as electricity demand stimulators by introducing households to the benefits of electricity. Results also show that, as their power demands increase, more households with PV choose to form or join communal grids as opposed to the national utility grid, due to greater affordability and reliability.

Furthermore, results show that the introduction of subsidies would lead to further increases in PV installations, leading to a substantial rise in the percentage of electrified households. In this chapter, impacts of both capital and energy based subsidies were simulated, with results showing that both led to significant increases in PV installation, with the difference between the two subsidies being negligible. This is a clear indication of the willingness of many rural households to install PV, with affordability being a major hindrance. The model developed in this work was meant to investigate the potential application of PV-microgeneration systems in cost-effectively supplying electricity-beyond-lighting to rural developing communities. The above findings demonstrate that the Government of Kenya can increase its rural electrification rate by introducing favourable subsidies to entice more people to install PV. The merits and demerits of both types of subsidies could be debated, but energy based subsidies enable the government to avoid direct capital investments in a household's own PV system. It could therefore be more affordable for developing countries with less capital. These favourable policies, together with the provision of affordable microcredit facilities, would lead to increased PV installations; implementation of such policies is therefore the recommendation being proposed to the Government of Kenya and to other developing nations.

Impacts of social factors on PV installation in Kendu Bay area of Kenya were also modelled and simulated. Results show that increasing neighbourhood influence, modelled as sensing radius and neighbourhood threshold, would lead to increased PV installations and subsequent communal grid connections. This is because as more households install PV within a given sensing radius (neighbourhood), a threshold is reached where a household begins to take notice. With increasing observations, greater communication via word of mouth, and elevated social status of those with PV, a household is increasingly pressured to consider doing the same. This leads to more PV installations within a given area as a result of greater neighbourhood influence. Potential methods to increase neighbourhood influence within a given community include increased advertisements through posters, billboards, or even the local radio and TV channels, community outreach through chiefs and other local leaders, roof-top mounting of PV systems to increased external visibility, and compensated referrals, as is currently being done by ART in Kendu Bay.

Chapter 6: Impacts of Control Architectures on Temporal Diffusion of PV-Based Communal Grids in Kendu Bay Area of Kenya

6.1 Introduction:

In this chapter, having modelled and simulated impacts of costs, subsidies, and neighbourhood influence on temporal diffusion of PV microgeneration systems in Kendu Bay area of Kenya, we now look at how network architectures and related power electronics would impact on costs, and thus on temporal diffusion of PV-based communal grids in a rural developing community such as Kendu Bay. The main objective of this research is to explore the potential application of PV-based communal grids in cost-effectively supplying electricity-beyond-lighting to such rural developing communities.

A PV-based communal grid can be defined as a collection of distributed PV generation systems, distributed energy storage devices, and distributed loads, operating as a single and controllable system capable of supplying power to an area of service. They should be operable in both grid-connected and islanded modes. Power electronics interfaces and controllers are used in communal grids to ensure quality, reliable, and independent power supply at all times. A control system must be able to disconnect and reconnect the communal grid from the utility grid, maintain voltage and frequency levels in islanded mode of operation, and facilitate a black start after a system failure [162]. The main drivers of communal grids are demand, cost, technical aspects, and environmental concerns [163]. These factors influence the control strategy applied to a communal grid and consideration will need to be given to issues such as load sensitivity, number of distributed generators in the communal grid, power quality requirements, ownership of the communal grid and distributed generators, distances between the distributed generators, the existing communication infrastructure, each distributed generator's energy source, and whether the communal grid is predominantly an exporter or importer of electricity [164-166].

6.1.1 Droop Control:

Droop control method is the most widely used approach in PV power systems to enable automatic load sharing between different distributed PV systems and to extend operating range of active (P) and reactive (Q) power ratings of a given inverter [167,168]. The method requires P and Q to be measured in order to droop the frequency (f) and voltage (V) accordingly such that the inverter mimics the behaviour of a synchronous generator [167,168]. A reactive power voltage (Q-V) droop

control is used to control point of common coupling (PCC) voltage magnitude while an active power frequency (P-f) droop control is used to control the frequency of the system in islanded mode [167]. For a simplified analysis, consider a two-bus synchronous generator connected to a high voltage (HV) transmission network as shown in the figure 6.1 below. The power produced at the generator terminal is expressed as [169]

$$P = \frac{E}{R^2 + X^2} [XV \sin \delta + R(E - V \cos \delta)] \quad (6.1)$$

$$Q = \frac{E}{R^2 + X^2} [-RV \sin \delta + X(E - V \cos \delta)] \quad (6.2)$$

where δ is the voltage angle.

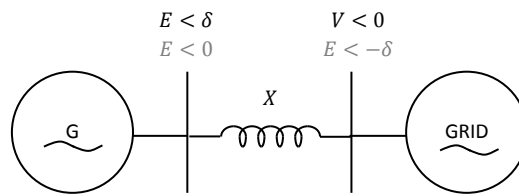


Fig. 6.1: Generator Connected to Grid

Since HV networks have high reactance (X) and low line resistance (R), and thus high X/R ratios, the line resistance can be ignored and equations 6.1 and 6.12 reduced to [169]

$$P = \frac{VE \sin \delta}{X} \quad (6.3)$$

$$Q = \frac{E^2 - VE \cos \delta}{X} \quad (6.4)$$

Usually, δ is very small (zero) and therefore $\cos \delta \cong 1$ and $\sin \delta \cong \delta$. Equations 6.3 and 6.4 can therefore be simplified further to [169]

$$\delta \approx \frac{PX}{VE} \quad (6.5)$$

$$E - V \approx \frac{QX}{E} \quad (6.6)$$

The reactive power Q can therefore be controlled by the difference in voltage between E and V , and the active power P , by the voltage angle δ . The voltage angle δ can be expressed in terms of angular frequency ω (radians/second), and therefore in terms of electrical frequency f (hertz) as [170]

$$\delta = \int \Delta\omega dt = \frac{1}{2\pi} \int \Delta f dt \quad (6.7)$$

The relationship outlined above allows automatic load sharing between many synchronous generators (SGs) when combined with P-f droop control as shown in figure 6.2a [162,163]; a change in load will cause frequency variation at the terminal of each SG. Active power will flow from regions of higher frequency to regions of lower frequency. Frequency variations within the network will eventually drift to an average steady state value [163]. The new steady state frequency will be proportional to the change in power, as shown in Figure 6.2b [162].

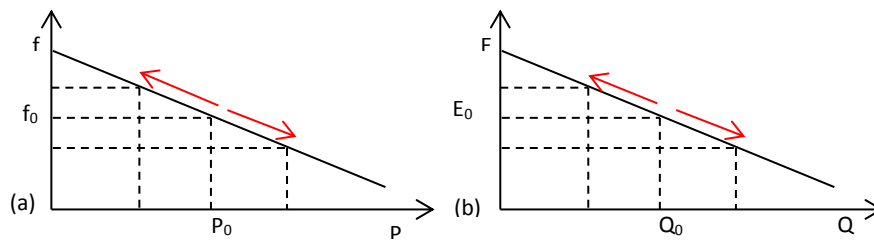


Fig. 6.2: P-f and Q-V Droops

6.1.2 Inverter Controls:

Inverters are used to interface communal grids with utility grids and can be classified according to modes of operation as PQ or V-f (also known as voltage source inverter (VSI)). A PQ inverter controls the real (P) and reactive (Q) power by adjusting the magnitude of the output real and reactive current. It therefore operates as a voltage controlled current source [171]. A voltage source inverter controls the voltage (V) and frequency (f) at the output terminal, and thus operates as a voltage source [170,171]. The mode of an inverter operation is chosen depending on a communal grid's architecture and control strategy, and may change depending on whether the communal grid is islanded or grid-connected. Unlike synchronous generators, inverters do not have rotors and thus no natural connection between frequency and active power. To achieve stable operation with multiple distributed PV systems, the inverters are controlled so that they mimic the characteristics of synchronous generators with P-f and Q-V droop controls [172]. For a PQ inverter, these droops are implemented as (*f*) and (*V*) functions, whereas a VSI uses (*P*) and (*Q*) droops [173].

6.1.2.1 PQ Inverter with Droop Control:

As opposed to a synchronous generator that uses its rotor speed as the frequency input for the P-f droop controller, a PQ inverter does not set the frequency, but rather measures the grid frequency using a phase lock loop (PLL) and then operates at that measured frequency [170-172]. The inverter

will adjust its power accordingly, by comparing the measured frequency to a reference (nominal grid frequency) value accordingly. This relationship is can be modelled as [170-172]:

$$P(f) = P_0 - (f_{set} - f)k_f \quad (6.8)$$

where P_0 is the power delivered by the inverter at setpoint frequency f_{set} and k_f is the gradient of the droop, which determines how much the active power P will change in response to a change in frequency f . When a Q-V droop is used, the PQ inverter measures the terminal voltage and compares this to the reference value. The reactive power is adjusted by altering the reactive component of the inverter current [171]. This reactive power adjustment is expressed as [170-172]:

$$Q(V) = Q_0 - (V_{set} - V)k_v \quad (6.9)$$

where Q_0 is the reactive power delivered/consumed by the inverter at setpoint voltage V_{set} and k_v is the gradient of the droop, which determines how much the reactive power Q will change in response to a change in voltage V .

6.1.2.2 VSI Inverter with Droop Control:

A VSI with droop control uses measured active power output to generate the VSI frequency and measured reactive power output to generate the VSI voltage [169]. It thus operates like a synchronous generator. This process can be modelled by equations 6.10 and 6.11 below [169]:

$$f(P) = (P_0 - P)k_p - f_{set} \quad (6.10)$$

where K_p is the gradient of the droop, which determines how much the frequency will change in response to a change in power P .

$$V(Q) = (Q_0 - Q)k_q - V_{set} \quad (6.11)$$

where K_q is the gradient of the droop, which determines how much the voltage will change in response to a change in reactive power Q .

The conventional droop control relies on the inductive nature of transmission lines and is thus based on the assumption that the line resistance (R) is much less than the reactance (X), i.e., high X/R ratio and therefore active power flow is predominately a function of the voltage angle (δ) [173]. This is the case for high voltage (HV) and medium voltage (MV) lines, but it is not so for low voltage (LV) networks as shown in table 6.1 below.

Type of line	R (Ω/km)	X (Ω/km)	R/X
Low voltage	0.642	0.083	7.7
Medium voltage	0.161	0.190	0.85
High voltage	0.06	0.191	0.31

Table 6.1: Typical Line Parameters [174]

For systems with LV transmission networks and thus high line resistance, the low X/R ratio causes a coupling effect between active and reactive power, rendering Q-V droop control method ineffective in achieving required voltage regulation in such systems [175]. A solution to this problem has been proposed by Alatrash et al., in which a control system that incorporates virtual reactance at the terminals of the VSI is used [176]. The idea behind this method is to emulate the higher reactance of MV and HV distribution lines. Abusara et al. proposed a control strategy that employs both virtual inductance to remove harmonic disturbances and a real time integration filter to eliminate the need for measuring average power [177].

6.1.3 Control Architectures:

The two general control structures used in communal grids are centralized control and decentralized control [178,179]. In centralised control, a central controller (CC) determines the operating points of the communal grid and sends this information via communication systems to some or all the distributed PV systems and potentially to some of the loads throughout the communal grid network. In decentralised control a virtual communication system independently determines the operating points of each decentralized PV system and load within the communal grid network, effectively eliminating the need for communication links and thus increasing system reliability as well as reducing cost [178]. This enables easy and cost-effective expansion of the communal grid by enabling decentralized PV systems and loads to have plug-and-play capabilities [178]. The two configurations can be implemented under two main modes of operation, i.e., master slave or multi master [180].

6.1.3.1 Master Slave (Single Master) Operation:

In this mode of operation, all the inverters in the network operate in PQ mode when the communal grid is connected to the utility grid, since the latter controls the voltage and frequency. In islanded

mode, a single master inverter switches to VSI mode to provide the voltage and frequency references while the remaining distributed PV systems continue to operate in PQ mode [171]. The system can operate in either a centralised configuration or in a decentralised configuration. In centralized configuration a single VSI acts as the voltage and frequency reference while all of the other inverters operate in PQ current source mode. The load is equally shared across each inverter such that the current produced from the master is used as a reference for the PQ inverters. The operating current is communicated to them in real time. This configuration is therefore only possible with high speed communication links and is thus difficult to expand [163]; it is therefore not recommended for communal grids which require modularity in design. Figure 6.3 shows a centrally controlled master slave operation [170,181].

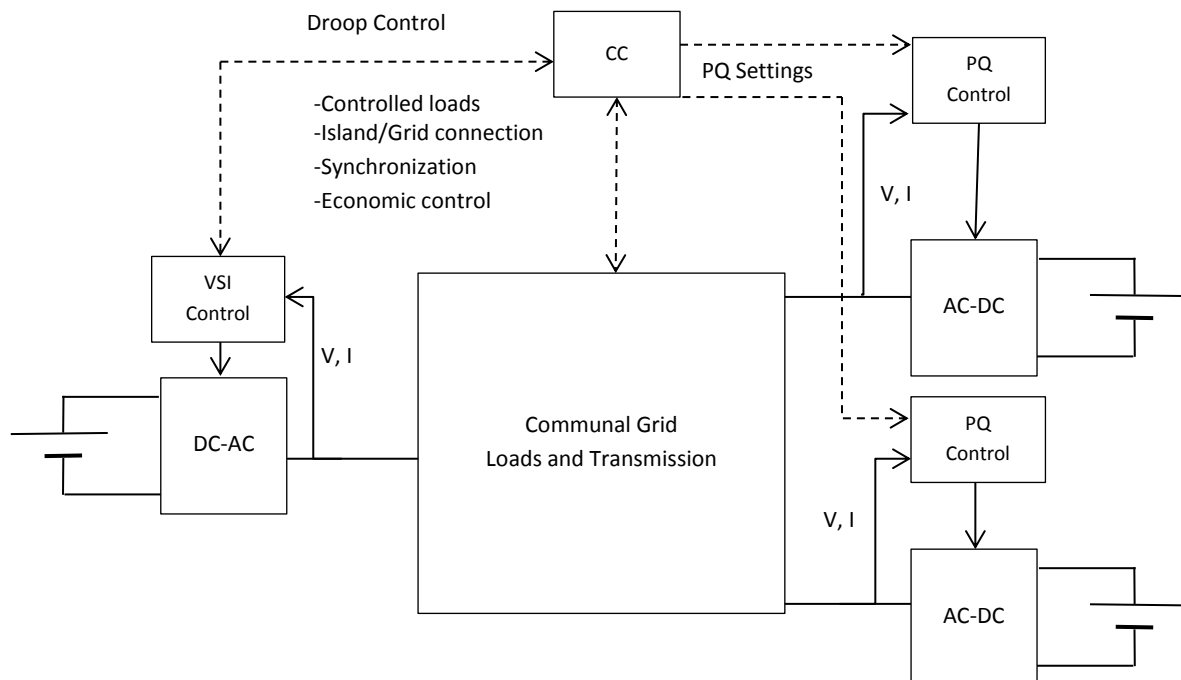


Fig. 6.3: A Centrally Controlled Single Master Communal Grid

In decentralized configuration every decentralized PV system, including the master has a built-in generation profile determined by P-f and Q-V droop curves. Each unit therefore determines its own real and reactive power, eliminating the need for communications in the process. The master VSI sets the voltage and frequency based on its droop and the PQ inverters determine the active power from the system frequency set by the master VSI and the reactive power from the local voltage measurements [182]. The pure droop system gives equal priority to all distributed PV systems within the network and enables easy expansion of the system. In grid-connected mode, the utility grid sets

the frequency (with very little variation) ensuring constant power output while in islanded mode, the master VSI uses droops to control the frequency and voltage of the network [182].

6.1.3.2 Multi-Master Operation:

In this mode, all distributed PV systems within a communal grid can act as masters or can be operated as combinations of master generators (VSIs) and PQ inverters [171]. This mode shares many aspects with single master operation and can also be operated in centralized or decentralized configuration. A centrally controlled multi master system uses several VSIs operating at predefined voltage and frequency, determined by the central controller (CC). The principle is almost identical to the centrally controlled single master system. One advantage is that battery interfaced VSIs can be distributed throughout the network [164]. Figure 6.4 shows a centrally controlled VSI-PQ multi master operation [171,181].

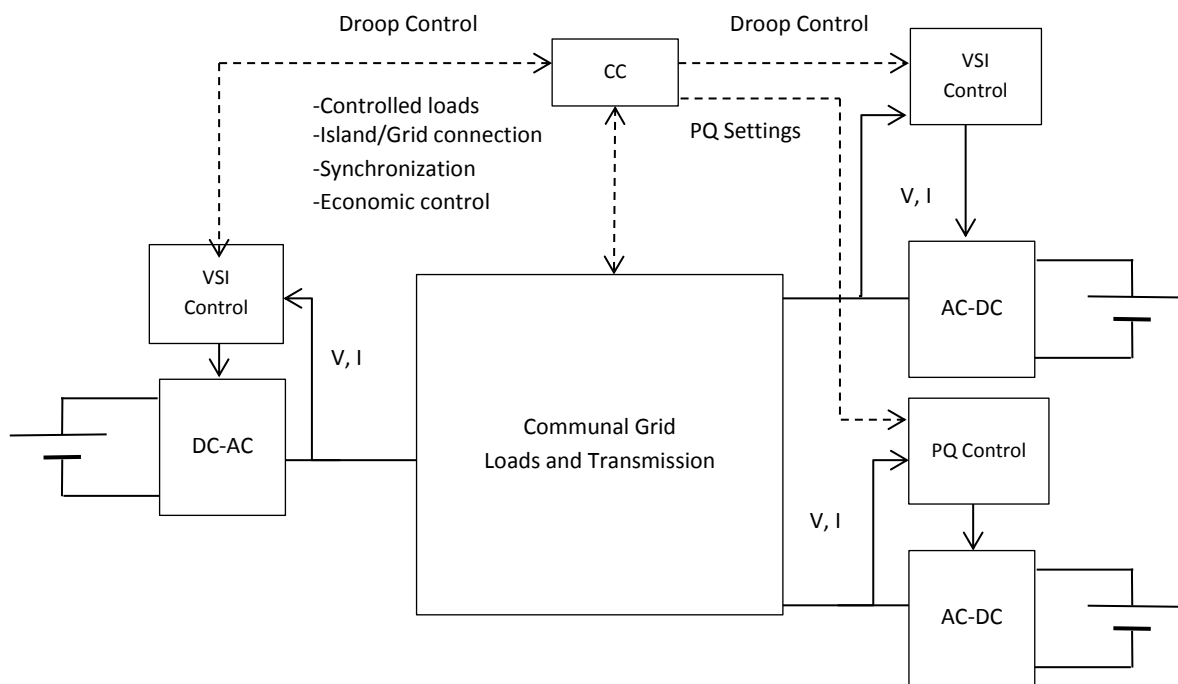


Fig. 6.4: A Centrally Controlled Combined VSI-PQ Multi Master Communal Grid

Compared with single master, the centralised control for multi master requires a higher level of communication between master VSIs. This adds complexity, although it does have the advantage of built-in redundancy as the system will continue to operate if one of the master VSIs goes off-line [178]. Decentralized configuration for multi master is almost identical to the single master mode. All distributed PV systems are able to regulate their power outputs in grid-connected and islanded modes by using individual droop controls. Multi master pure droop systems are well suited to

systems with multiple integrated, renewable energy/storage generators spread throughout a communal grid. When implemented in this way the load will be shared equally across all distributed PV systems [166].

6.2 Methodology:

In this section different communal grid architectures, revolving about energy storage, are modelled and simulated in Matlab/Simulink to determine the most cost-effective option for a given transmission and distribution network. The outputs of the simulations are then fed into the agent-based model (ABM) developed in Netlogo, in chapter 5, which then simulates temporal diffusion of the communal grids based on cost and other preferences. Kendu Bay survey data are used to inform the ABM. The communal grids are classified as islanded and grid connected; in Kendu Bay 92.2% of the residents do not have access to electricity due to various reasons, the main one being cost. For these people, and as explained in chapter 4, small PV systems act as stepping stones to electrification. Such small systems are islanded and thus come with storage devices for power supply stability. This is the norm with many private PV systems installed in rural Kenya irrespective of the sizes, since they are mostly islanded. On the other hand, it is likely that the national utility grid will stabilize and eventually reach every part of the country as the government invest in more power generation, transmission, and distribution. It is therefore important to look at systems which are grid-connected juxtaposed to those that are islanded.

The communal grids could either be DC-coupled or AC-coupled; a grid using a DC bus avoids many of the power conversion steps required when using an AC bus leading to higher energy efficiency and cost-saving. Traditionally, AC enabled efficient voltage transformation and high-voltage power transmission over long distances. Recently however, technology advances have led to highly efficient AC/DC and DC/DC converters, making high-voltage DC long-distance bulk power transmission more efficient [183]. In summary, DC power distributions over DC networks have many benefits including:

- Higher power system efficiency due to fewer AC/DC or DC/AC conversion losses
- DC systems tend to be more modular and scalable than AC systems because DC converters are easier to control and to parallel. This allows for more flexibility in systems designs and expansions, and thus more effective capital investment management
- DC system components tend to be more compact than equivalent AC components because of higher efficiency and due to not being frequency dependent
- Lower capital costs due to fewer electronic components used (no inverters),

- Higher survivability (lower power control system complexity) when subjected to external and internal disturbances due to elimination of synchronization requirements associated with AC systems
- Most distributed energy sources and storage devices have inherently DC outputs, making DC architectures more natural options for their integrations
- Most modern loads require a DC input; even AC classical loads like induction motors rely on inherently DC input variable speed drives (VSDs) to achieve a more efficient and flexible operation.
- Availability: DC is several times more reliable than AC according to NTT data from 30,000 systems due to fewer electronic components (points of failure) used (no inverters) [184]

Due to lower power and energy rating, stability issues are more prevalent in communal grids than in utility grids. Analyses of stability issues in AC-coupled communal grids follow the same concepts as with utility grids, i.e.:

- Voltage and frequency values need to both be regulated through active and reactive power control
- If a decentralized power source is a traditional synchronous generator with an AC output, and is connected directly to the utility grid without power electronic interfaces, stability is controlled through the machine shaft's torque and speed control

In DC systems there are no reactive power interactions which suggests that there are no stability issues; system control seems to be oriented towards voltage regulation only.

6.2.1 Islanded Communal Grids with Decentralized Storage:

Communal grids are operated in islanded mode if they are far from existing grid lines and are thus not connected to the national grid, or if there is a fault with the national grid. Some communities may also intentionally opt for islanded communal grids, even if the national grid is nearby, for various reasons including costs, reliability, independence of ownership, etc. PV-based communal grids operating in islanded modes should have storage systems to ensure stability of power supply. Batteries are the most widely used storage devices with PV systems and shall be the storage devices used in all simulations in this work. Households forming a communal grid could have their own decentralized storage systems or they could decide to have a centralized storage system somewhere within the village. To be allowed to join a communal grid, a house must have electricity needs

beyond lighting and must demonstrate this by having installed PV of a given minimum capacity (power-threshold). They must also be within a given sensing radius of other homes with PV that meet the power-threshold. The idea to join a communal grid returns true if

$$\frac{H_{CGRID-SR}}{H_{Total-SR}} \times 100 > T_{CGRID-SR} \quad (6.12)$$

where $H_{CGRID-SR}$ is the number of households with PV within the sensing radius that meet the power-threshold ($T_{CGRID-P}$), $H_{Total-SR}$ is the total number of households within the same sensing radius, and $T_{CGRID-SR}$ is the communal grid neighbourhood threshold, minimum percentage of neighbours with PV that meet the $T_{CGRID-P}$ required within the sensing radius for a household to think about joining a communal grid.

Households with decentralized storage have their own PV systems, including storage, independently installed before joining a communal grid. The size of the installed PV system is calculated using the formula

$$PV(W_p) = \left(\frac{P \times h}{\eta_{inv(PV)} \times \eta_{batt(PV)} \times \eta_{cc} \times (1 - f_{temp}) \times (1 - f_{dust}) \times (1 - f_{mismatch}) \times EHFS} \right) \quad (6.13)$$

where P is the household's power load, h is the number of hours the load is operated per day, η_{cc} is the charge controller efficiency, f_{temp} , f_{dust} , and $f_{mismatch}$ are the losses in PV module due to cell temperature, dust, and mismatch amongst several cells due to shadow and other factors, and $EHFS$ is the equivalent hours of full sunshine. P is calculated from a list of stochastically allocated appliances based on active occupancy, time of the day, and day of the week (chapter 4). The list of appliances is based on Kendu Bay survey data.

The required battery capacity for the household is given by

$$Batt(Ah) = \left(\frac{P \times h}{\eta_{inv(PV)} \times V \times MDOD \times \eta_{batt(PV)}} \right) \times D \quad (6.14)$$

where V is the operating voltage of the battery, $\eta_{inv(PV)}$ is the efficiency of inverter, $MDOD$ is the maximum depth of battery discharge, $\eta_{batt(PV)}$ is the charging/discharging efficiency of the battery, and D is the days of autonomy

For a communal grid consisting of N households, the total PV capacity needed is given by

$$CGrid_PV(kW_p) = \left(\frac{P \times h}{\eta_{inv(CGrid)} \times \eta_{batt(CGrid)} \times \eta_{cc} \times (1 - f_{temp}) \times (1 - f_{dust}) \times (1 - f_{mismatch}) \times DF \times EHFS} \right) \quad (6.15)$$

where $\eta_{inv(CGrid)}$ is the cumulative efficiency of inverters used in the communal grid, $\eta_{batt(CGrid)}$ is the cumulative charging/discharging efficiency of the batteries used in the communal grid, and DF is the diversity factor, ratio of the sum of all individual peak loads to the maximum load of the entire communal grid.

The total battery capacity required for the communal grid is given by

$$CGrid_Batt(Ah) = N \times \left(\frac{P \times h}{\eta_{inv(CGrid)} \times V \times MDOD \times \eta_{batt(CGrid)} \times DF} \right) \times D \quad (6.16)$$

Generally, $CGrid_PV(kW_p)$ should equal $N \times PV(W_p)$, while $CGrid_Batt(Ah)$ should equal $N \times Batt(Ah)$; the deficit should be evenly distributed between the households forming the communal grid. i.e., they may need to increase the sizes of their installed systems.

6.2.1.1 DC-Coupled Communal Grids:

In these systems generated DC voltage by the PV systems is distributed throughout the communal grid in the DC form. Inverters are therefore not required for common bus connections. However, individual households may purchase small DC-AC inverters for their AC appliances. Each DC-DC converter for each PV system is necessary for maximum power point tracking (MPPT) and for charge controlling of the storage system. There is no need for control system as there is no frequency or voltage amplitude to regulate. However, the DC-DC converter regulates and conditions the DC bus voltage. The overall cost of such a network is therefore low compared to a similarly sized AC-coupled network.

From chapter 5, the average total power generated by a communal grid is 400kW. The PV arrays modelled in this chapter are therefore sized at 100kW, each, for a total output of 400kW. 4 different arrays are used instead of 1 in order to highlight the significance of decentralization. Figure 6.5 shows a schematic diagram of a DC-coupled communal grid with decentralized storage while figure 6.6 shows a Simulink model used to implement the network. Each PV array in the system delivers about 100kW at 1,000 W/m² irradiance; each array consists of 66 parallel strings, each comprising 5 PV 330 SunPower (SPR-305-WHT-D) modules connected in series (66 x 5 x 305.2 = 100.7 kW). Each array is connected to a 5 kHz boost DC-DC converter with maximum power point tracking (MPPT)

and charge-controlling capabilities. Each converter uses the perturb-and-observe method to extract maximum voltage (273V DC) from each array and then boosts it to 500V DC. Each Converter is connected to a decentralized lead acid battery bank rated at 1,040Ah, with a 25% depth of discharge (DOD), and 3 days of autonomy. The battery is then connected to a 500 V DC common bus. The load across each converter is stochastically allocated between 10 kW and 25 kW, based on Kendu Bay data and potential number of households served by each array.

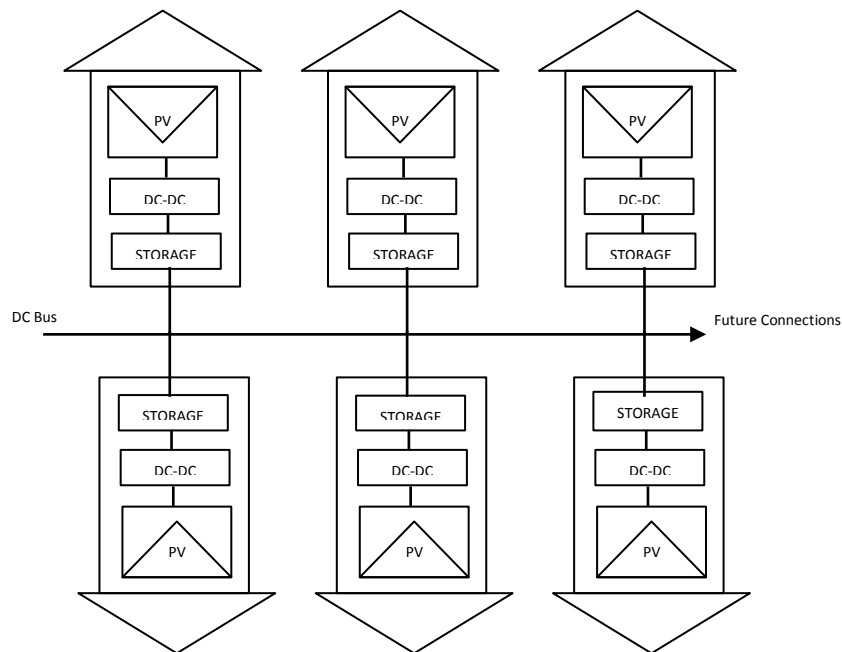


Fig. 6.5: Islanded DC-Coupled Communal Grid with Decentralized Storage

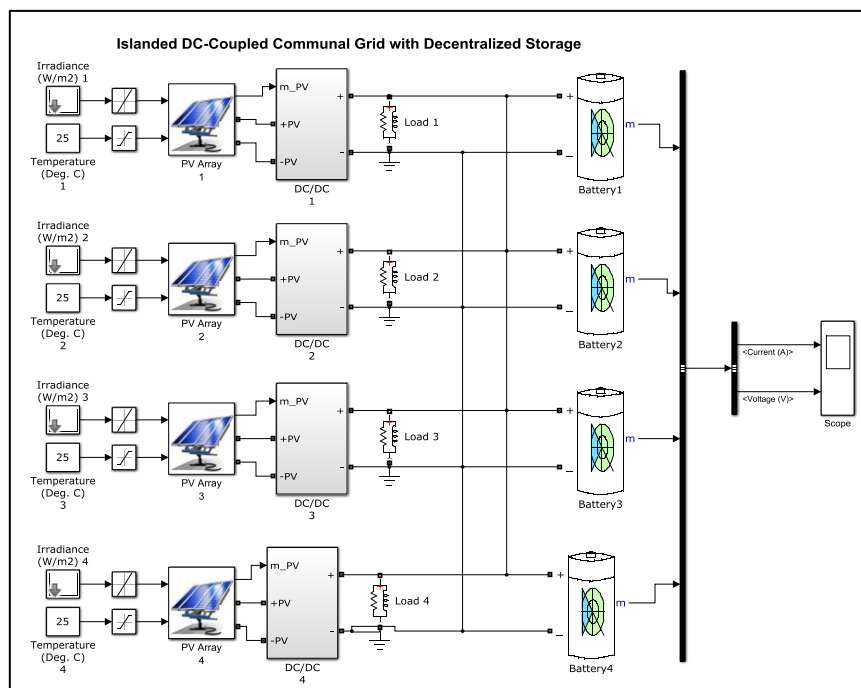


Fig. 6.6: Simulink Model of Islanded DC-Coupled Communal Grid with Decentralized Storage

6.2.1.2 AC-Coupled Communal Grids:

Figure 6.7 shows a schematic diagram of an AC-coupled communal grid with decentralized storage. In these systems generated DC voltage by the PV systems are first inverted into AC form before being distributed throughout the network. Due to decentralized storage, each household has its own DC-AC inverter for connection to the common AC bus. A decentralized control system is used to set the network voltage amplitude and frequency. The system works by using a virtual communication system to independently determine the operating points of each decentralized PV system and load within the communal grid network, effectively eliminating the need for communication links and thus increasing system reliability as well as reducing cost [178]. This enables easy and cost-effective expansion of the communal grid by enabling decentralized PV systems and loads to have plug-and-play capabilities [178]. Every decentralized PV system, including the master has a built-in generation profile determined by P-f and Q-V droop curves. Each unit therefore determines its own real and reactive power, eliminating the need for communication networks in the process. The master VSI sets the voltage and frequency based on its droop and the PQ inverters determine the active power from the system frequency set by the master VSI and the reactive power from the local voltage measurements [182].

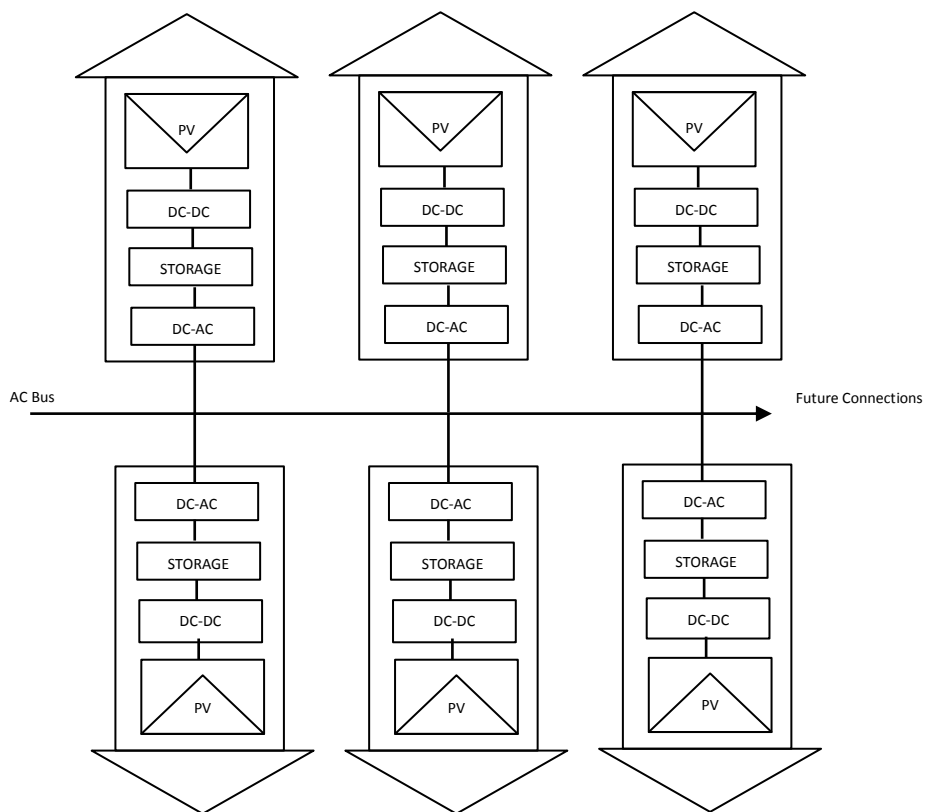


Fig. 6.7: Islanded AC-Coupled Communal Grid with Decentralized Storage

Figure 6.8 shows a Simulink model used to implement the diagram in figure 6.7. Here the DC-DC converter is connected to a 1980-Hz three-phase three-level DC-AC inverter through a DC link capacitor. The inverter inverts the 500V DC to 260V AC, while keeping a unity power factor. It uses two control loops: one which regulates DC link voltage to +/-250 V and an internal control loop which regulate active and reactive current. Active current reference is the output of the DC voltage external controller while reactive current reference is set to zero in order to maintain unity power factor.

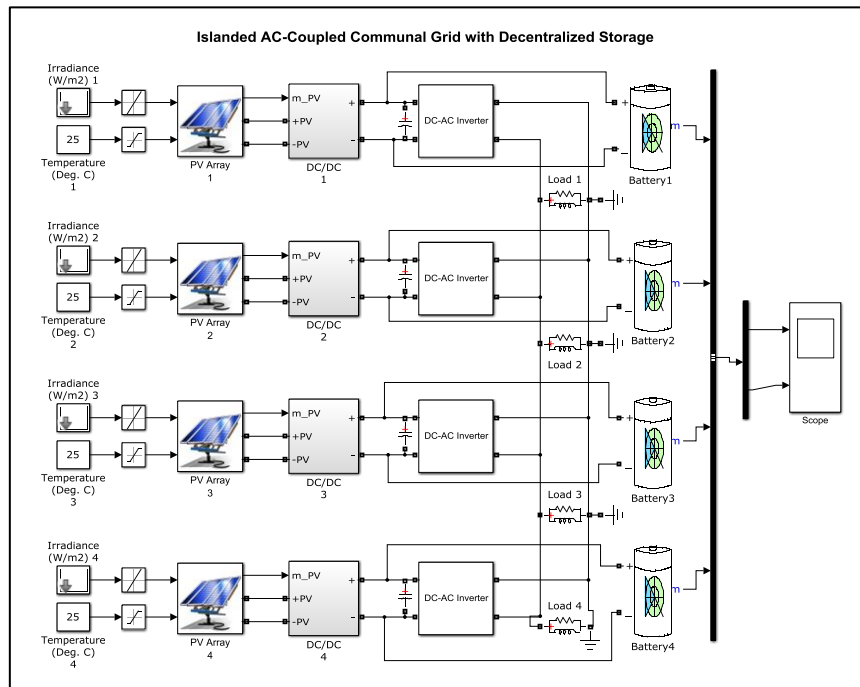


Fig. 6.8: Simulink Model of Islanded AC-Coupled Communal Grid with Decentralized Storage

6.2.2 Islanded Communal Grids with Centralized Storage:

Households with PV systems within a given sensing radius may decide to come together to form a communal grid if they meet the required power and neighbourhood thresholds. However, instead of every household having its own storage system, they may opt for a centralized storage system, by bringing together all their batteries to a central location, or by buying a larger capacity battery bank. Each DC-DC converter for each PV system is still necessary for maximum power point tracking, however, the task of charge controlling is now performed by an appropriately sized central converter/inverter connected to the central storage system. The required battery capacity is given by equation 6.16, where $\eta_{inv(CGrid)}$ now represents the efficiency of the central converter/inverter used with the communal grid while $\eta_{batt(CGrid)}$ represents the charging/discharging efficiency of the central storage system.

6.2.2.1 DC-Coupled Communal Grids:

Figure 6.9 shows a schematic diagram of a DC-coupled communal grid with centralized storage while figure 6.10 shows a Simulink model used to implement it. These systems are similar to DC-coupled systems with decentralized storage, with the exception being that the storage system is now centralized.

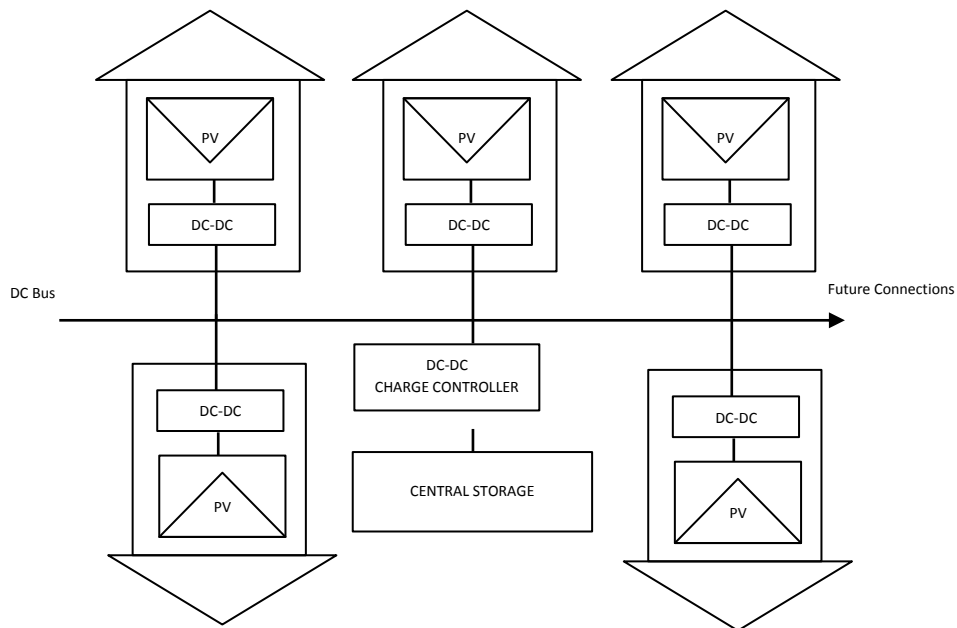


Fig. 6.9: Islanded DC-Coupled Communal Grid with Centralized Storage

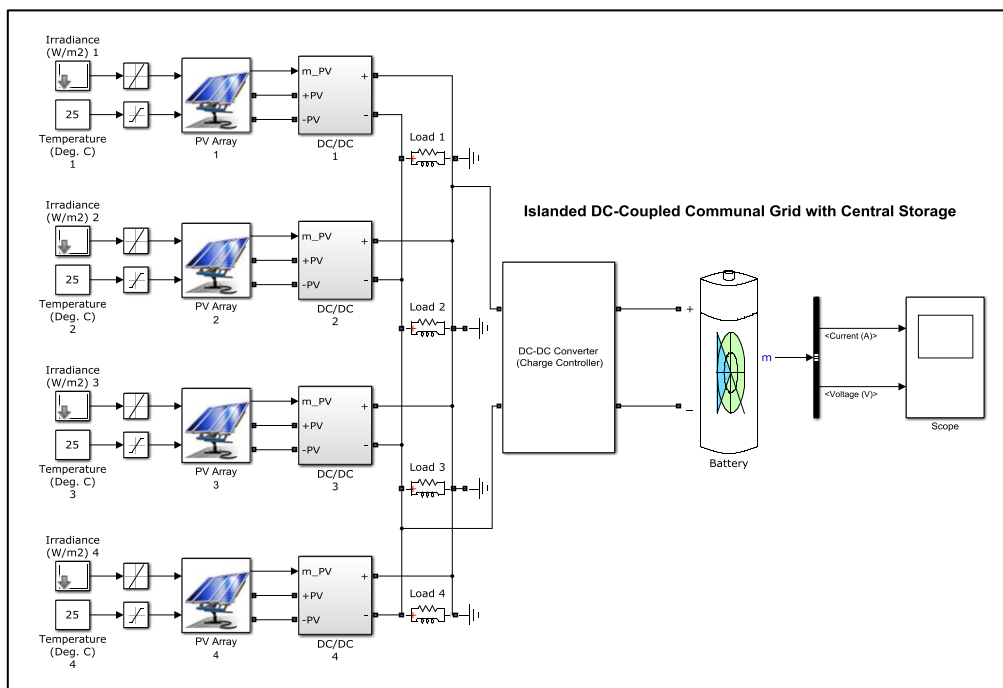


Fig. 6.10: Simulink Model of Islanded DC-Coupled Communal Grid with Centralized Storage

A centralized DC-DC converter with charge controlling capabilities is used to connect the central storage system to the common DC bus. This is an added cost compared to systems with decentralized storage. These systems also don't require control and thus no inverters are required. Future connections to the communal grid are complicated by the fact that each time the storage capacity is increased to meet the increased demand, a new appropriately sized DC-DC charge controller must be purchased for the network. Putting such a cost on the new entrant would dissuade more households from joining the communal grid. DC-DC charge controller connects the DC common bus to the central battery bank. Here, the battery bank capacity is increased to 4,160 Ah while the DOD is kept at 25%. The days of autonomy are also kept at 3 as discussed in section 6.2.1.1.

6.2.2.2 AC-Coupled Communal Grids:

Figure 6.11 shows a schematic diagram of an AC-coupled communal grid with centralized storage. In these systems, each household has its own PV system connected to a DC-DC converter for maximum power point tracking. The converter is then connected to a DC-AC converter for connecting to the common AC bus. A bi-directional AC-DC inverter with charge controlling capabilities is used to connect the central energy storage system to the common AC bus. Since the central inverter is large compared to the individual household inverters, it could act as master VSI for setting up reference line voltage amplitude and frequency while household inverters function as PQ inverters.

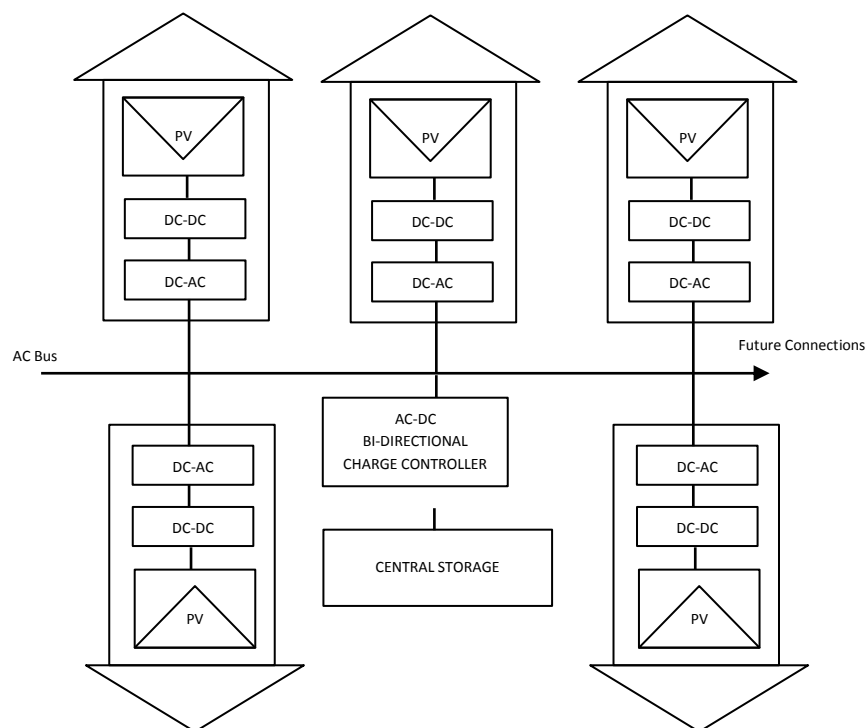


Fig. 6.11: Islanded AC-Coupled Communal Grid with Centralized Storage

Figure 6.12 shows a Simulink model used to implement the network. Here each DC-DC converter extract maximum power from the PV array and then boosts it to 500V DC. Each converter is connected to a DC-AC inverter which then inverts the 500V DC to 260V AC and then feeds it to the common bus. Each DC-DC converter is also connected to a central storage system through a central DC-DC charge controller.

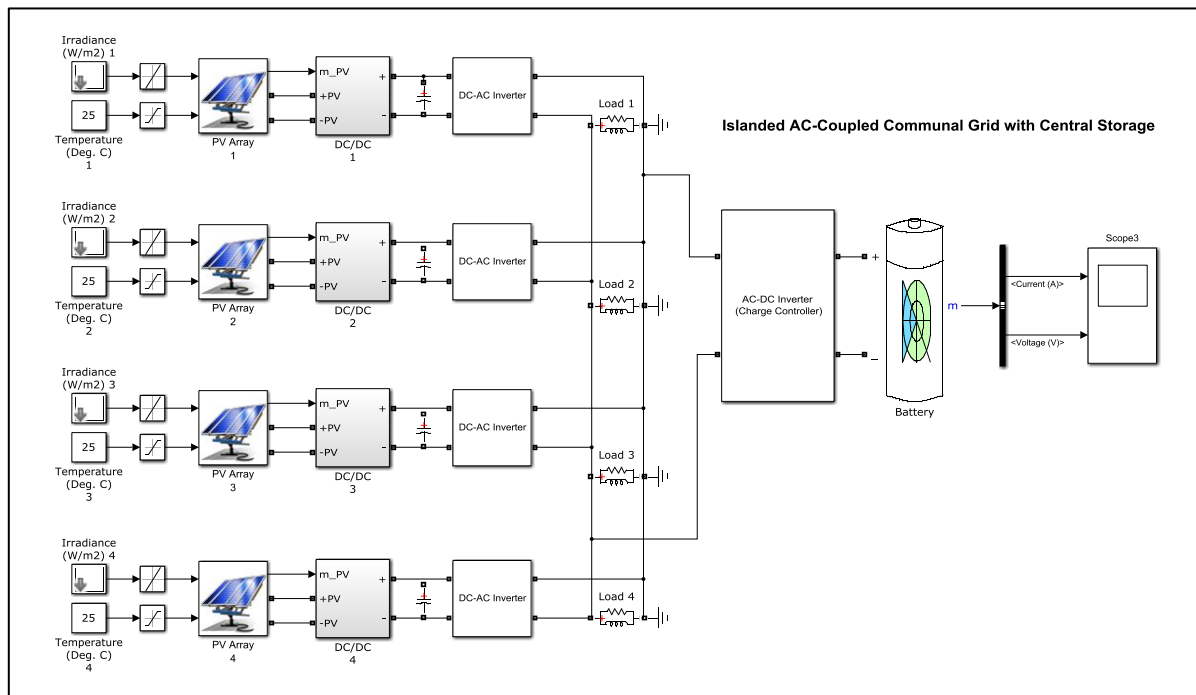


Fig. 6.12: Simulink Model of Isolated AC-Coupled Communal Grid with Centralized Storage

Future connections to the communal grid are complicated by the fact that each time the storage capacity is increased to meet the increased demand, a new appropriately sized AC-DC inverter must be purchased for the network. Putting such a cost on the new entrant would dissuade more people from joining the communal grid.

6.2.3 Grid-Connected Communal Grids:

Even though the national grid is not widespread in most of sub-Saharan Africa, it is inevitable that it will reach most parts of rural areas in the future. It is therefore important to plan for such an eventuality. The national grid brings with it many benefits including unlimited virtual storage, increased reliability and availability of electricity supply, and stability of the system. Even though currently the utility grid in Kenya is quite unreliable due to strain and corruption, in the future it is expected that increased investments in power generation will lead to a more stable national grid. It

is also expected that with increased advancements in technology, corruption will be arrested. This would most likely make the grid more attractive. However, before that happens, it is also likely that many rural communities would have formed many islanded and stable communal grids all over Kenya, contributing to the national power output, and increasing the utility grid capacity once interfaced with it. It is therefore likely that a good percentage of increased national power generation will be from communal grids, spread all over the country. In this section we look at different communal grid control architectures with grid connections. Here again we compare the merits and demerits of DC-coupled and AC-coupled networks with centralized and decentralized storage. i.e., we connect the communal grid architectures discussed in section 6.2.1 above to the national utility grid. The utility grid voltage levels are set at 25kV for all simulations, and the acceptable range of point-of-common-coupling (PCC) voltage variation is $\pm 5\%$. The active powers supported by the inverters are shown as positive quantities since they are leading, while the reactive powers are shown as negative quantities since they are lagging. For simplicity, the simulation results are expressed in per unit (pu), with base voltage of 25kV and base power of 250kVA. The feeder lines parameters are: $0.08 + j0.04$ ohm/km and lengths are 1km for sensing radii of 500m.

Figure 6.13 shows a Thevenin equivalent of a feeder connected to an inverter. The figure represents a power source ($E_{PV} \angle \phi$) where Z_{th} represents the feeder as well as inverter coupling impedance, ϕ is the phase angle difference between PCC and grid voltages, while θ is the impedance angle due to Z_{th} [185]. The following equations are used to control the active and reactive power flows ($S = P + jQ$) from the inverter (the power source) to the feeder (the grid) [185]:

$$P = \frac{V_{th}}{Z_{th}} [(E_{PV} \cos \phi - V_{th}) \cos \theta + E_{PV} \sin \theta \sin \phi] \quad (6.17)$$

$$Q = \frac{V_{th}}{Z_{th}} [(E_{PV} \cos \phi - V_{th}) \sin \theta - E_{PV} \cos \theta \sin \phi] \quad (6.18)$$

Since ϕ is usually very small, i.e., $\cos \phi \approx 1$, and $\sin \phi \approx \phi$, the equations above are reduced to [185]:

$$P = \frac{V_{th}}{Z_{th}} [(E_{PV} - V_{th}) \cos \theta + E_{PV} \phi \sin \theta] \quad (6.19)$$

$$Q = \frac{V_{th}}{Z_{th}} [(E_{PV} - V_{th}) \sin \theta - E_{PV} \phi \cos \theta] \quad (6.20)$$

Equations 6.19 and 6.20 show the dependency of delivered active and reactive power on the impedance angle θ and the phase difference angle ϕ [185].

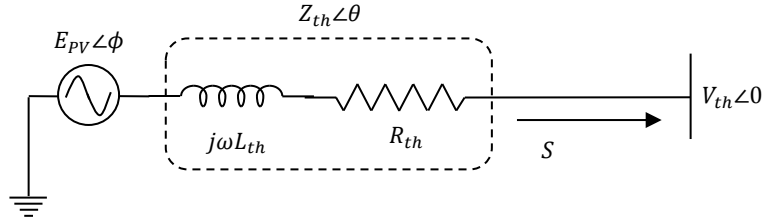


Fig. 6.13: Thévenin Equivalent Circuit of a Feeder (Grid) Connected to an Inverter (PV Source)

For communal grid networks with high resistive (R) values and low reactance (X), i.e. low X/R ratios, the P-f droop control method is used. This makes the impedance angle θ equals to zero hence, from equation 6.19, the active power delivered by the inverter is proportional to the voltage difference ($E_{PV} - V_{th}$) and thus proportional to the inverter E_{PV} . The reactive power of the inverter is proportional to the phase difference angle ϕ , i.e. proportional to the frequency f of the system. It should be noted that ϕ is varying within a small range. P remains constant irrespective of any change in ϕ while Q significantly changes with changing ϕ . On the other hand, P significantly increases with increasing E_{PV} while Q is hardly affected by changes in E_{PV} [185].

For communal grid networks with high X/R ratios, i.e. low line resistance and high reactance and thus the impedance angle θ goes to 90° , the Q-V droop control method is used. The reactive power of the inverter is proportional to the inverter voltage E_{PV} and the active power is proportional to the frequency f . P significantly changes with changing ϕ while Q remains constant regardless of any changes in ϕ . On the other hand, P hardly changes with changing E_{PV} while Q significantly changes with E_{PV} . The Q-V droop control method is one of the widely used methods for voltage regulation; unlike the P-f droop method where additional provision for real power is required, Q-V droop method does not need such a source of real power for generating the necessary Q for compensation [185].

For communal grid networks with complex line impedances, i.e. where neither the line resistance nor the reactance is more significant than the other and therefore neither can be ignored, P-Q-V droop control method is used. In such systems, the X/R ratio is near unity and therefore neither the P-f nor the Q-V droop method is sufficient to regulate the PCC voltage. In such networks, both the active and reactive power are simultaneously affected by changes in voltage magnitude E_{PV} and the phase difference angle ϕ . Since in these systems both active and reactive power affect the voltage magnitude, the system can be represented by the following equation [185]

$$V = V_{pcc} - (n_L * P) - j (m_L * Q) \quad (6.21)$$

where n_L and m_L are the electric load droop coefficients while V_{pcc} is the PCC voltage before compensation and is given by

$$V_{pcc} = V_{ref} + (n_d * P) + j (m_d * Q) \quad (6.22)$$

where n_d and m_d are the active and reactive power coefficients for the proposed P-Q-V droop method while V_{ref} is the desired reference value of PCC voltage, i.e. 1 pu.

6.2.3.1 DC-Coupled Communal Grids with Decentralized Storage:

Figure 6.14 shows a schematic diagram of a DC-coupled communal grid interfaced with the national utility grid while figure 6.15 shows a Simulink model used to implement the network. The storage systems are unnecessary but they assure stability in case the communal grid gets islanded due to a fault with the utility grid. It is also assumed that initially all systems are islanded due to lack of utility grid, and therefore investments into storage systems had been made before the grid arrived.

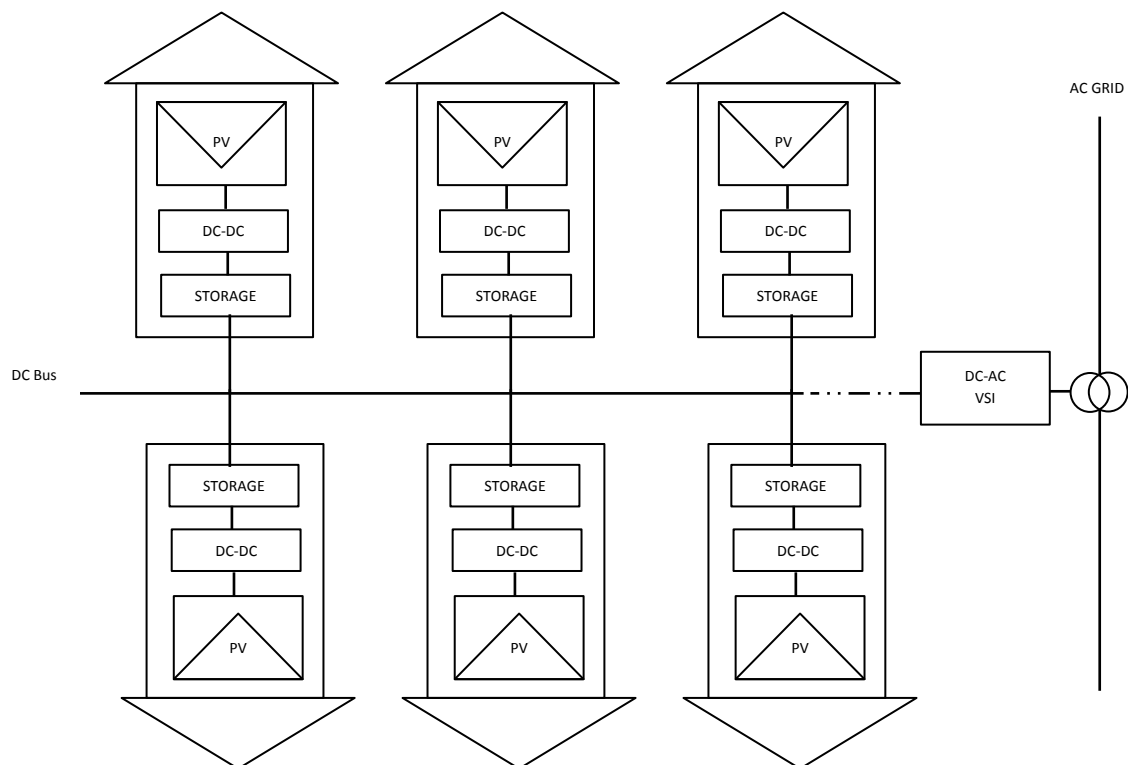


Fig. 6.14: Grid-Connected DC-Coupled Communal Grid with Decentralized Storage

A 1980-Hz three-phase three-level DC-AC inverter, connected to the common bus, inverts the DC bus voltage to 260V AC, while keeping a unity power factor. The inverter uses two control loops: one

which regulates DC link voltage to ± 250 V and an internal control loop which regulates active and reactive current. Active current reference is the output of the DC voltage external controller while reactive current reference is set to zero in order to maintain unity power factor. A 40-kvar capacitor bank is used to filter harmonics produced by the inverter. The inverter is connected to the utility grid through a 400-kVA 260V/25kV step-up transformer. As long as the DC bus voltage is kept stable at a certain level, future connections to the communal grid are easy as no modifications to the interfacing inverter are necessary.

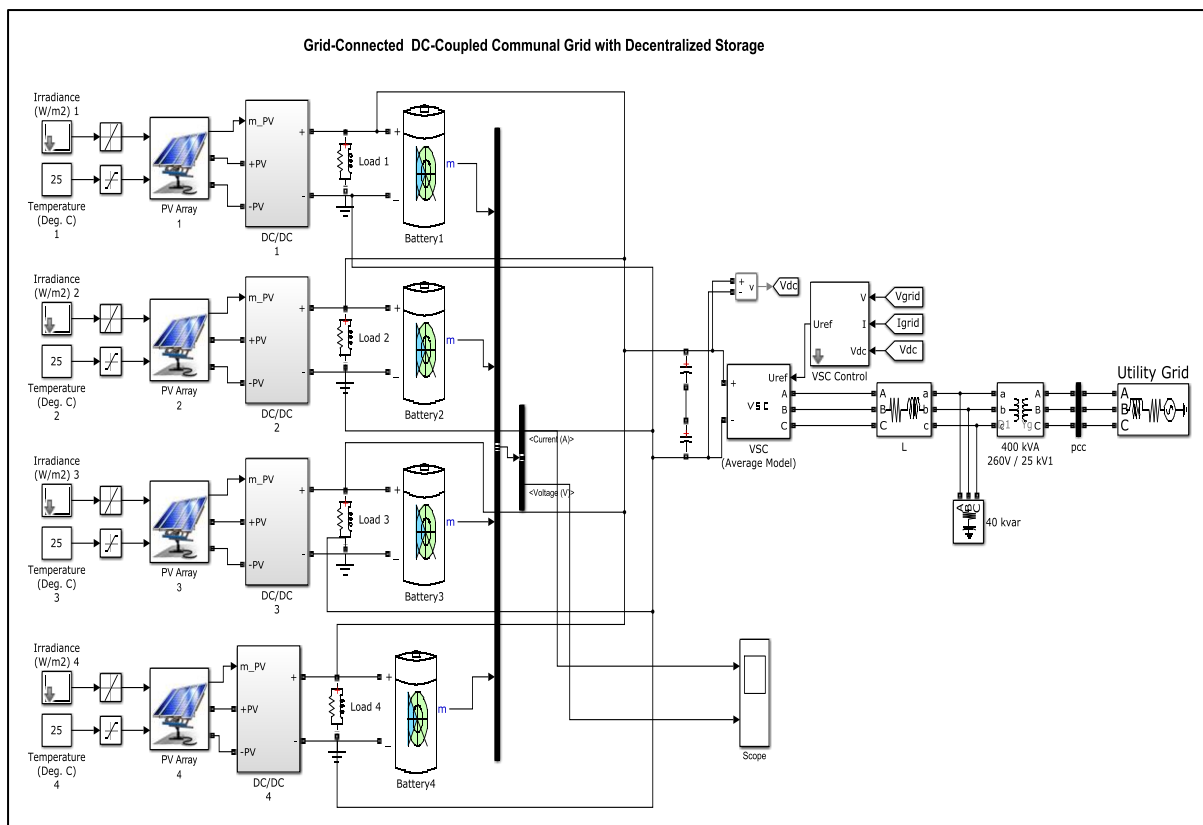


Fig. 6.15: Simulink Model of Grid-Connected DC-Coupled Communal Grid with Decentralized Storage

6.2.3.2 AC-Coupled Communal Grids with Decentralized Storage:

Even though here the common bus voltage is in AC form, it is at a different frequency and voltage from the utility grid; another AC-AC converter is therefore needed to act as a master control for the entire system to set it to the line frequency and voltage amplitude of the utility grid, as shown in figure 6.16. A 40-kvar capacitor bank is used to filter harmonics produced by the inverter. The inverter is connected to the utility grid through a 400-kVA 260V/25kV step-up transformer. Future connections to the communal grid are easy as no modifications to the interfacing inverter are necessary. Figure 6.17 shows the Simulink model used to implement the network.

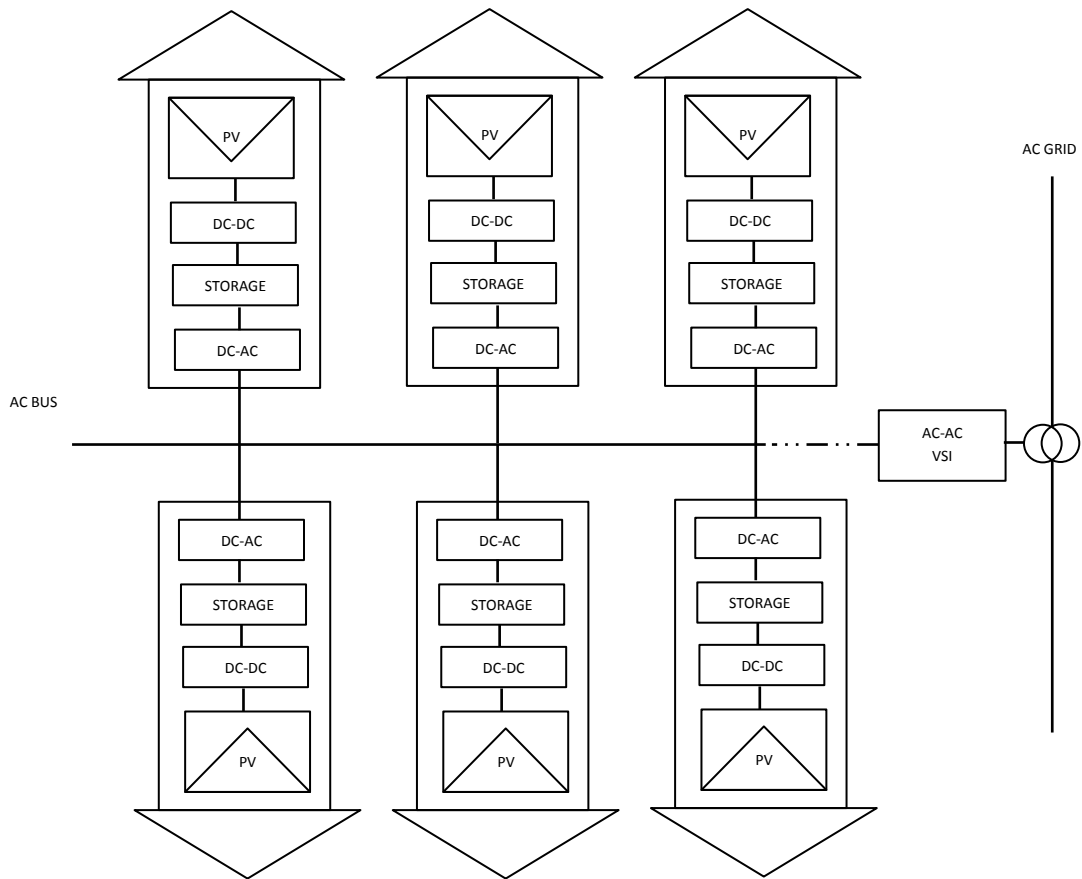


Fig. 6.16: Grid-Connected AC-Coupled Communal Grid with Decentralized Storage

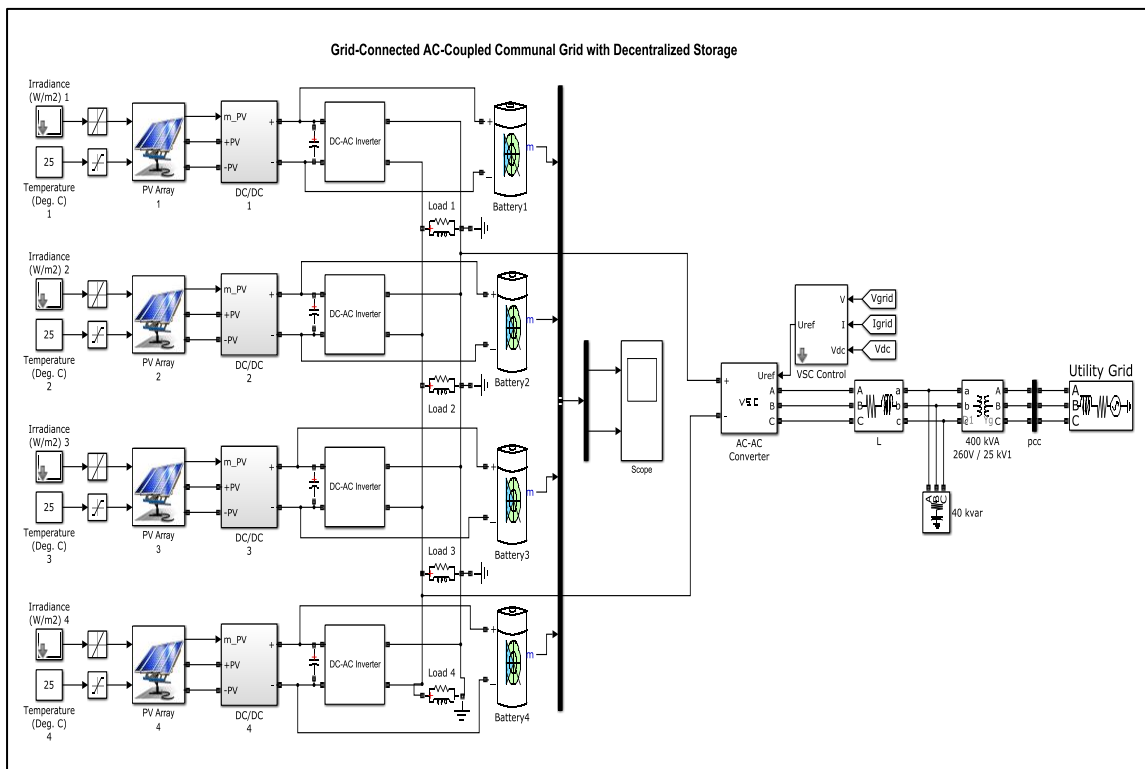


Fig. 6.17: Simulink Model of Grid-Connected AC-Coupled Communal Grid with Decentralized Storage

6.2.3.3 DC-Coupled Communal Grids with Centralized Storage:

Figure 6.18 shows a schematic diagram of a DC-coupled communal grid interfaced with the national utility grid while Figure 6.19 shows a Simulink model used to implement the above network.

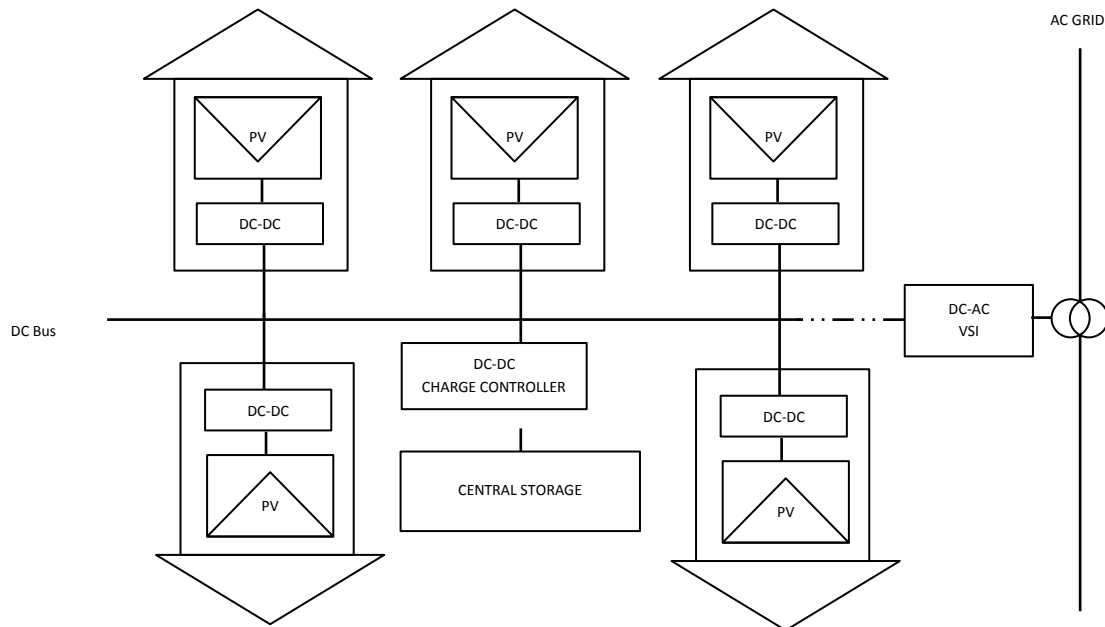


Fig. 6.18: Grid-Connected DC-Coupled Communal Grid with Centralized Storage

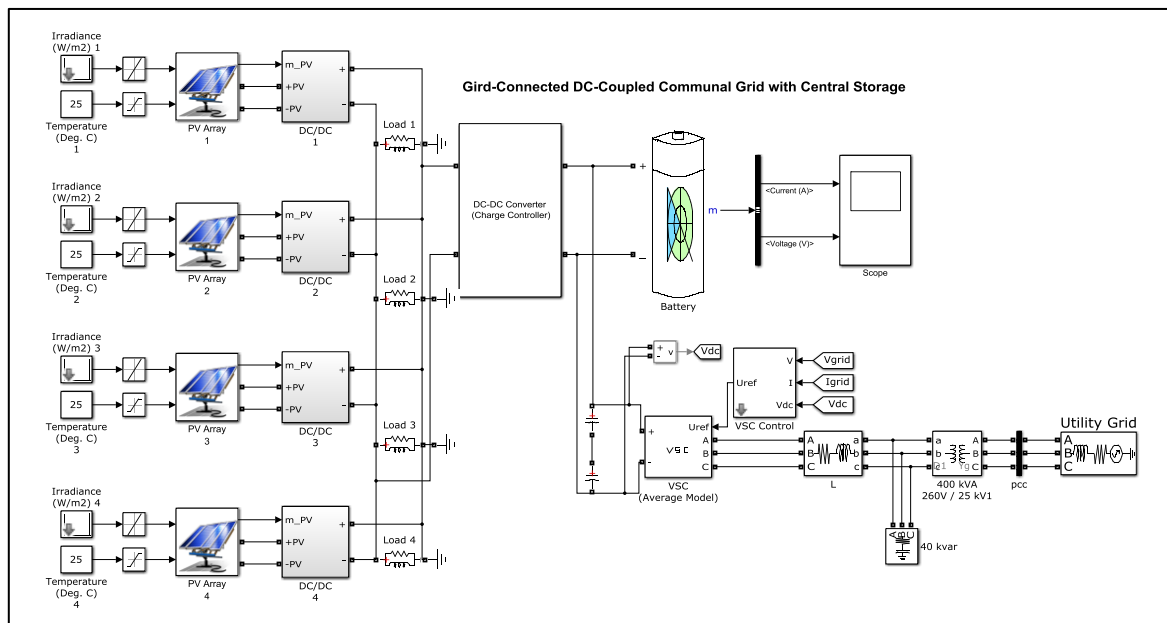


Fig. 6.19: Simulink Model of Grid-Connected DC-Coupled Communal Grid with Centralized Storage

The central storage system is unnecessary but it assures stability in case the communal grid gets islanded due to a fault with the utility grid. Interfacing of the DC common bus with the utility grid is

done using a DC-AC inverter as discussed above. The central location of the charge storage and associated charge controller makes modifications to this system difficult. Once utility grid interfacing has been achieved, future households wishing to join such a communal grid may decide not to invest in the storage system. However, this puts the entire system at risk of power shortage in case it gets islanded due to problems with the utility grid. It is therefore necessary that the storage system and associated power electronics are modified with additional connections. The VSI is connected to a central charge controller through DC link capacitors. All other line parameters are kept the same as with all grid connected networks for comparative analysis.

6.2.3.4 AC-Coupled Communal Grids with Centralized Storage:

Figure 6.20 shows a schematic diagram of an AC-coupled communal grid interfaced with the national utility grid while figure 6.21 shows a Simulink model used to implement it.

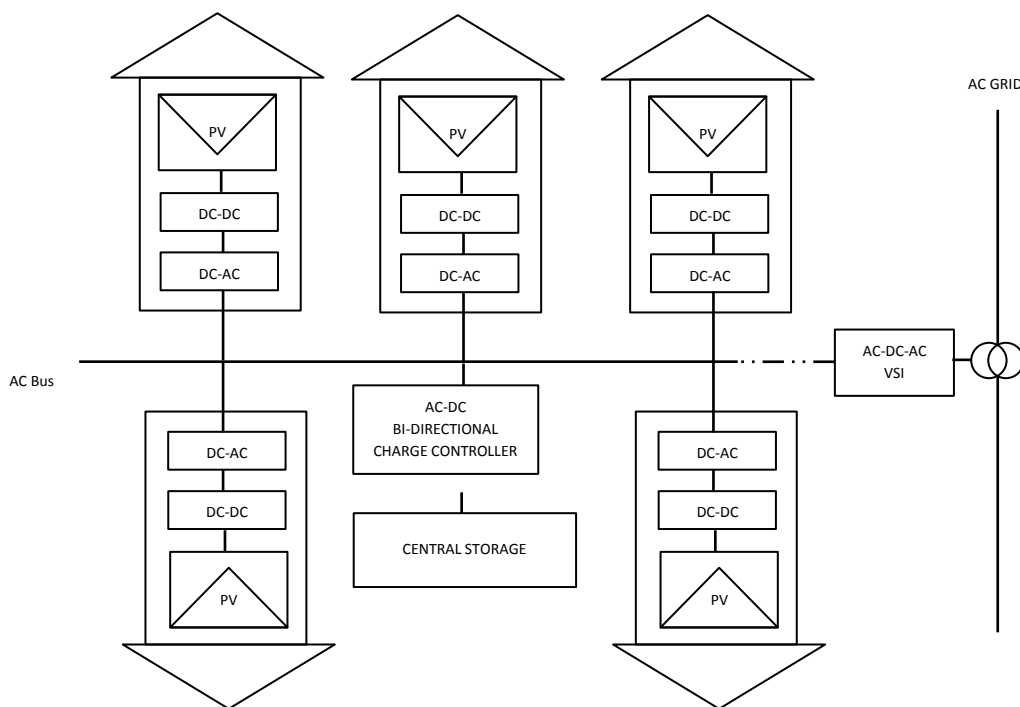


Fig. 6.20: Grid-Connected AC-Coupled Communal Grid with Centralized Storage

Once utility grid interfacing has been achieved, future households wishing to join such a communal grid may decide not to invest in the storage system. However, this puts the entire system at risk of power shortage in case it gets islanded due to problems with the utility grid. It is therefore necessary that the storage system and associated power electronics are modified with additional connections. The system therefore does not facilitate the ease of future connections.

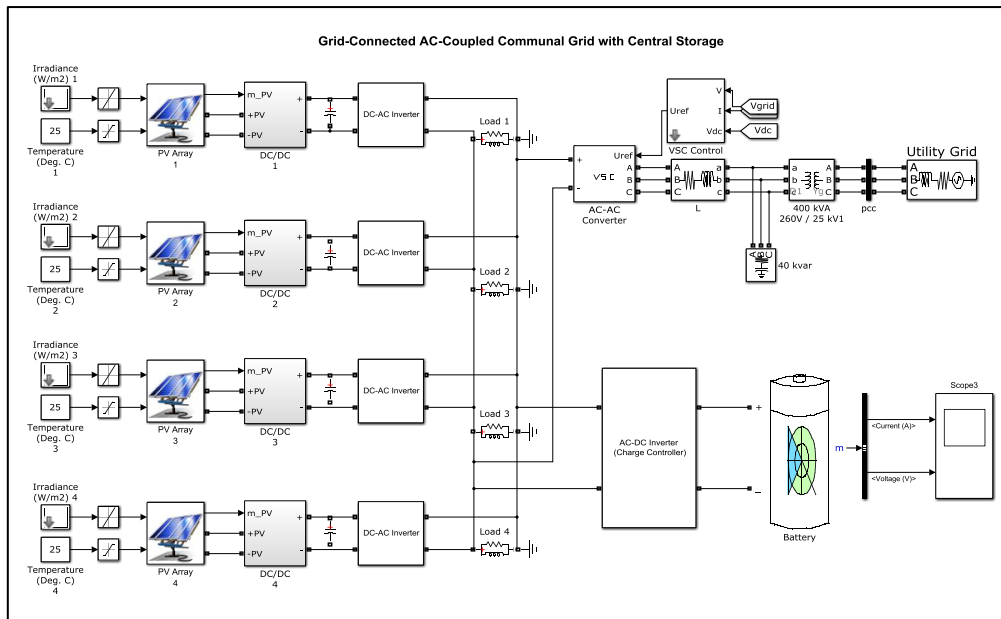


Fig. 6.21: Simulink Model of Grid-Connected AC-Coupled Communal Grid with Centralized Storage

6.2.4 Integrated Communal Grids:

A regional grid consisting of many communal grids of various configurations, depending on cost, socio-economic demographics, and geographical conditions could be used to provide electricity-beyond-lighting to many rural households. For example, consider the regional grid shown in figure 6.22 below. It consists of 10 communal grids, some AC-coupled, while others DC-coupled, connected to an AC utility grid. Grids A to E are DC-coupled and are connected to a central DC bus network. Grids A and D have central storage systems while grids B, C, and E have decentralized storage systems. The System is connected to the utility grid through one DC-AC VSI and a step up transformer. The DC network does not require a communication network and also does not require control. Households could consider joining each individual communal grid independently depending on their preferences and location. On the other hand, grids F to J are AC-coupled. Grids F, I, and J have decentralized storage systems while grids G and H have centralized storage systems. An AC-AC converter is used to interface the common AC but to the utility grid. The converter also acts as a master controller to set the frequency and voltage amplitude of the AC common bus to that of the utility grid it is interfacing with. In case all the communal grids within the network are forced to operate in islanded mode due to a fault with the utility grid, each of the communal grids could have localized decentralized control, with one household's DC-AC inverter acting as a master control, or the entire network connected to a common AC bus could have one centralized master control. Especially at the point of common coupling (PCC) with the utility grid. Here again, depending on location, household preferences, and other conditions, a household may join whichever communal

grid best suits its needs. It is clear that based on architectures, there is no limit to the size and layout of a potential communal (regional) grid.

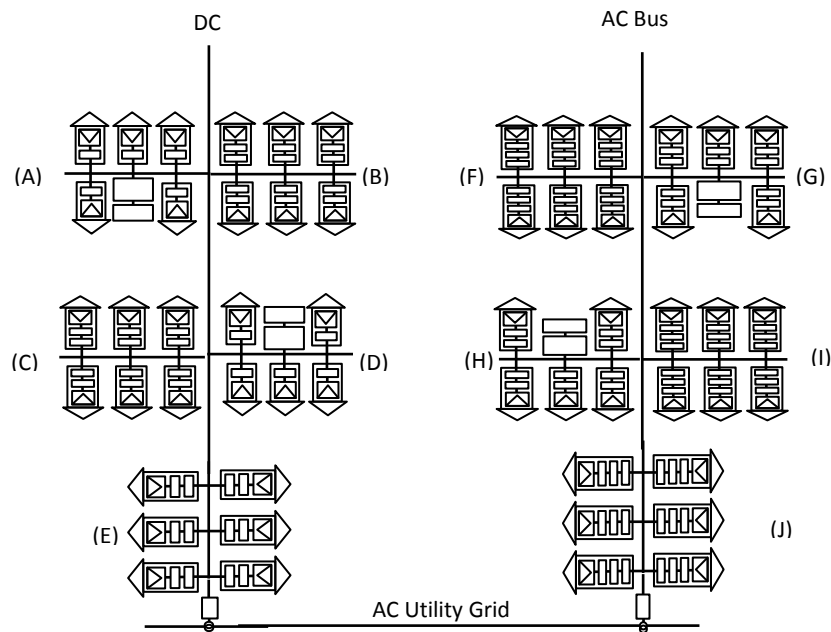


Fig. 6.22: Integrated Regional Grid

6.3 Results and Discussion:

Communal grid control architectures determine initial investment costs, operations and maintenance costs, and future expansion possibilities. Communal grids should be able to efficiently and reliably operate in both utility grid-connected mode and islanded mode. Energy storage systems are needed for stability of power supply in case of islanded operations. To achieve this, power electronics are needed for operational control and grid interfacing. In this section impacts of communal grid architectures on their temporal diffusion in a rural developing community are simulated. We specifically look at islanded and grid-connected communal grid with either centralized or decentralized storage in DC-coupled or AC-coupled networks. From chapter 6, the average power output from a communal grid was is 400 kW. Therefore each of the PV arrays simulated have 4 PV arrays, each rate at 100 kW at 1000 W/m² radiation and 25 °C. Figure 6.23 shows a comparison of irradiances hitting the 4 PV arrays shown in all simulations within 3 seconds (duration of simulation). In PV 1, 1000 W/m² radiation hits the array for 0.5 seconds before falling sharply to 50 W/m² for 2 seconds, before rising again to 1000 W/m² for the remainder of the simulation. In PV 2 1,000 W/m² radiation hits the array for the first 1.5 seconds before falling to 200 W/m² until 2.3 seconds when it rises again to 1,000 W/m². In PV 3 1,000 W/m² radiation hits the array for the first 0.5 seconds before falling to 600 W/m² until 1.5 seconds when it rises again to

1,000 W/m². In PV 4 1,000 W/m² radiation hits the array for the first 1.0 second before falling to 350 W/m² until 2.0 seconds when it rises again to 1,000 W/m². During all simulations the temperature is kept constant at 25 °C.

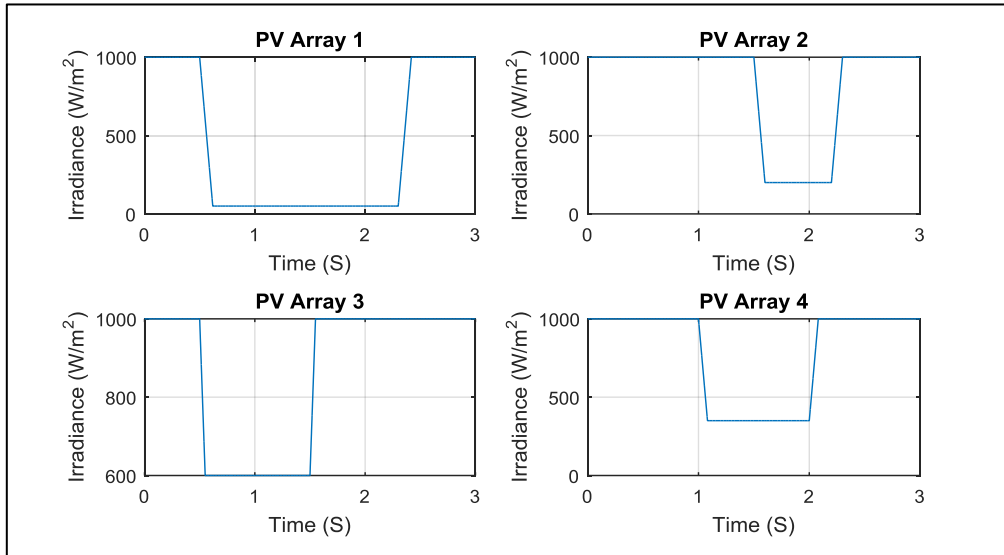


Fig. 6.23: Mean Irradiances Hitting the PV Arrays

Figure 6.24 shows the voltages produced by each of the 4 PV arrays as a result of the irradiances shown above; each array is connected to a DC-DC boost converter with maximum power point tracking (MPPT) capabilities, keeping the average voltage at about 250 V for each array. The blips in the figure correspond to points of changes in irradiances. The maximum voltage produced by each array at any given time is 273 V. This is then boosted to 500 DC by the converters for the common bus.

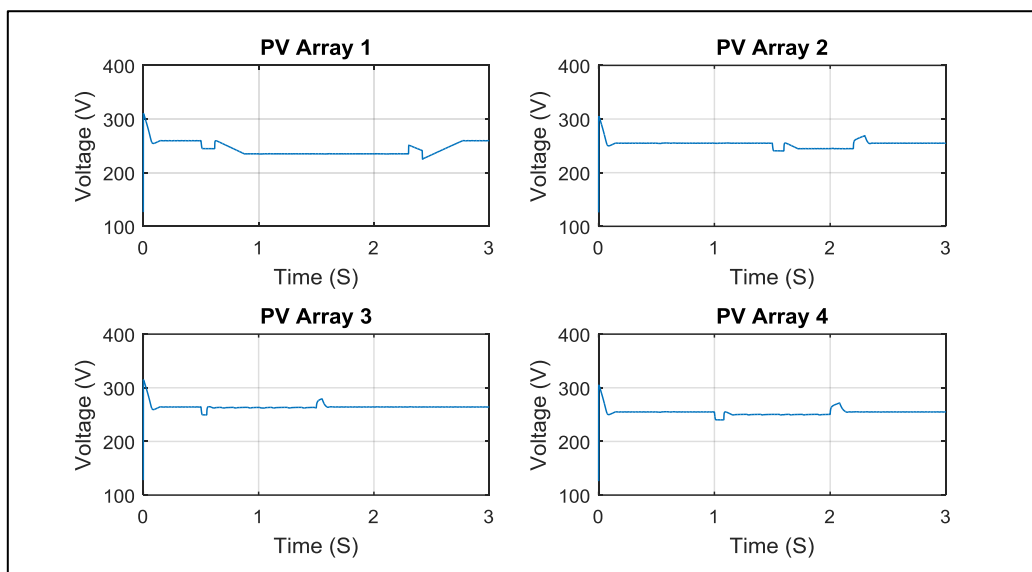


Fig. 6.24: Mean Voltages Produced by the PV Arrays

Figure 6.25 shows the current outputs from the 4 PV arrays. Since the current generated is directly proportional to the irradiance hitting the arrays, the plots mirror those of the irradiances hitting the arrays.

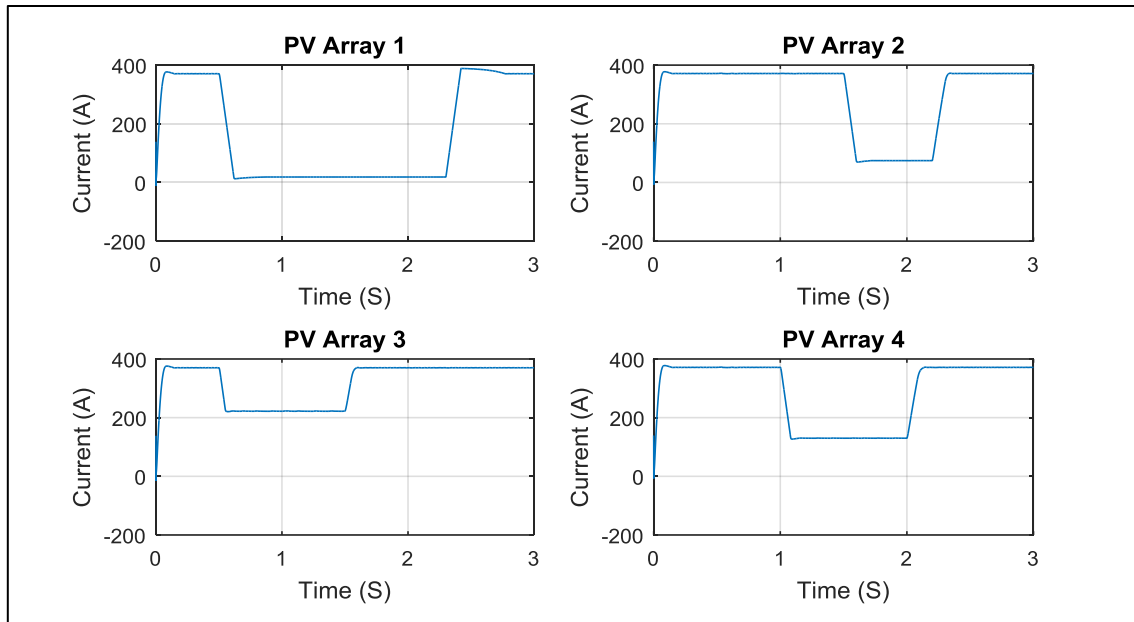


Fig. 6.25: Mean Currents Generated by the PV Arrays

As with current outputs, power outputs from the 4 PV arrays also mirror the irradiances hitting the arrays as shown in figure 6.26. The four power outputs from the PV arrays sum up to the active power injected into the control inverter as shown in figure 6.27.

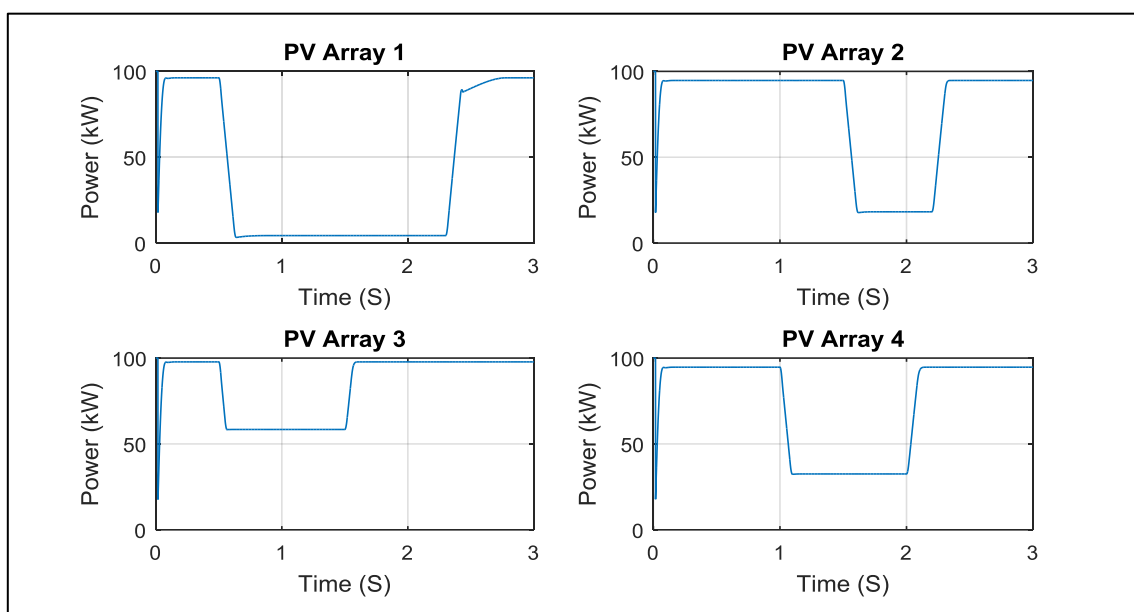


Fig. 6.26: Mean Power Outputs from the PV Arrays

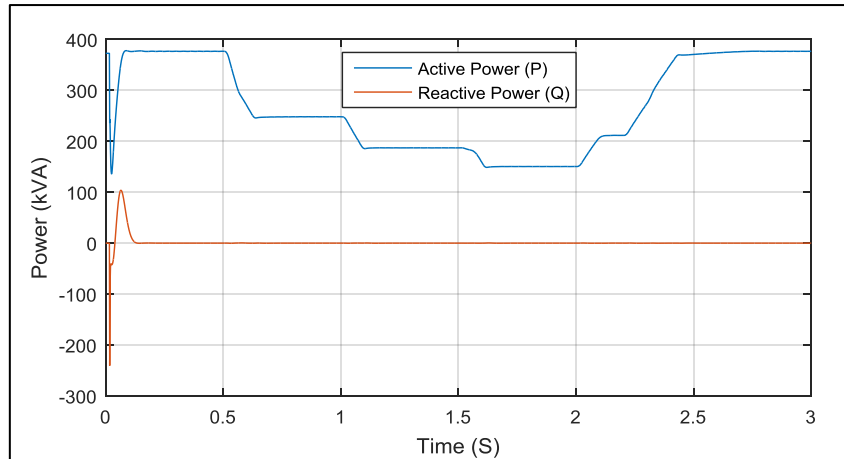


Fig. 6.27: Active and Reactive Power

Table 6.2 shows a comparison of additional power electronics required for different layouts. From the table it is clear that in islanded modes, DC-coupled networks with decentralized storage are the cheapest options for rural developing communities, with no additional costs beyond costs common to all other communal grid architectures. These are followed by DC-coupled networks with centralized storage which required additional investments into centralized charge controllers. AC-coupled networks with decentralized storage which need 4 DC-AC inverters come in third, followed by AC-coupled networks with centralized storage which need a central charge controller in addition to the 4 DC-AC inverters. Grid connection requires additional investments for all of the networks in forms of VSI, 40-kvar capacitor banks to filter harmonics produced by the VSIs, and 400-kVA 260V/25kV step-up transformers. It is assumed that all communal grids are initially islanded, and that investments into utility grid connections are made when it finally arrives at a given location. Depending on costs, some communal grids may opt to remain islanded.

Additional Power Electronics	Islanded				Grid-Connected			
	Centralized		Decentralized		Centralized		Decentralized	
	DC	AC	DC	AC	DC	AC	DC	AC
VSI	0	0	0	0	1	1	1	1
Central Charge Controller	1	1	0	0	1	1	0	0
DC-AC Inverter	0	4	0	4	0	4	0	4
Transformer	0	0	0	0	1	1	1	1
Filter	0	0	0	0	1	1	1	1
Total Additional Cost (\$)	250	950	0	700	250 + GC	950 + GC	GC	700 + GC

Table 6.2: Comparison of Additional Power Electronics Required by Networks. (GC =Connection Grid Cost)

6.3.1 Islanded Communal Grids:

6.3.1.1 DC-Coupled Communal Grids:

Figure 6.28 shows a comparison of households connected to communal grids in centralized and decentralized storage configurations after 25 years while figure 6.29 shows their corresponding percentages.

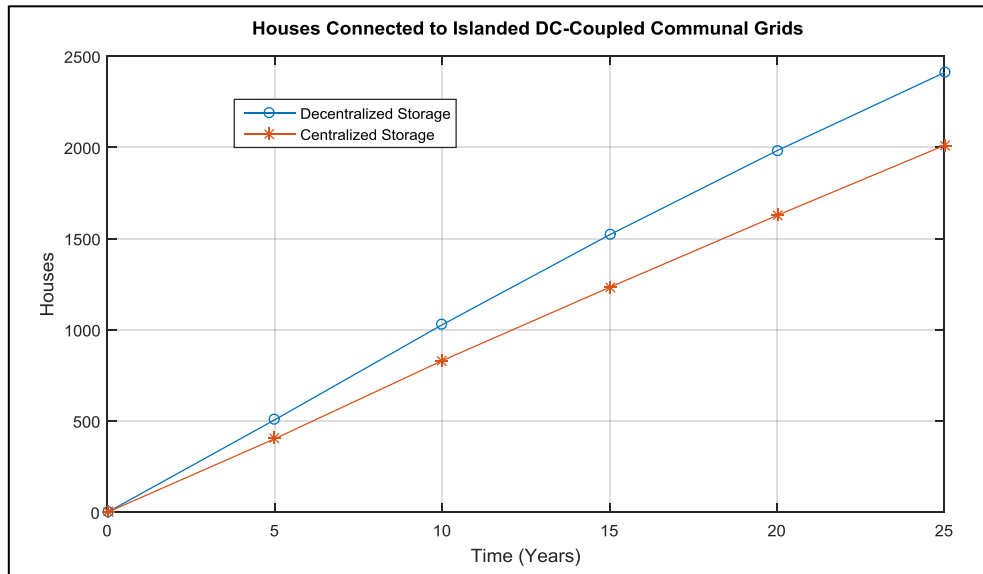


Fig. 6.28: Houses Connected to Islanded DC-Coupled Networks

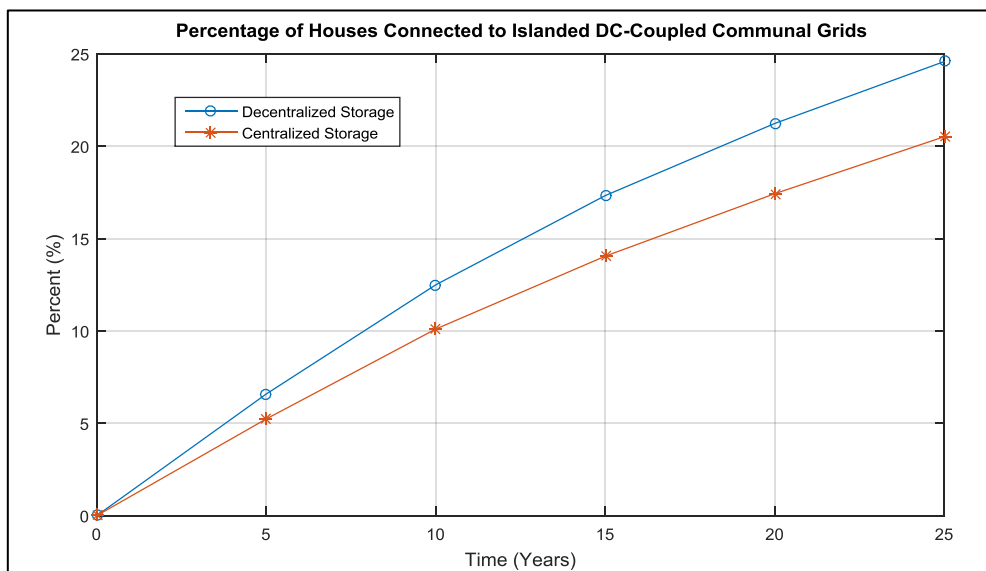


Fig. 6.29: Percentage of Houses Connected to Islanded DC-Coupled Networks

It is assumed that the total storage capacities in both centralized and decentralized systems are the same and that the total investment costs in both are also equal. The determining factor in what

choice of communal grid to join is therefore the additional cost brought about by the central charge controller and the ease of joining or leaving a particular communal grid architecture. In the simulations, the total number of households are increased annually as per national population growth rate, and based on the most recent census. After 25 years, 2,410 households would have joined communal grids with decentralized storage systems, representing 24.6% of all households. This is slightly higher than the 2,011 households that would have joined networks with centralized storage systems, representing 20.5% of all households. It is clear that the additional investment cost required for centralized storage drive more people towards networks with decentralized storage.

6.3.1.2 AC-Coupled Communal Grids:

Figure 6.30 shows a comparison of households connected to communal grids in centralized and decentralized storage configurations after 25 years while figure 6.31 shows their corresponding percentages. In addition to investments costs incurred with similar DC-coupled networks, AC-coupled networks also require DC-AC inverters for each PV array for common bus interfacing. Here also it is assumed that the total storage capacities in both centralized and decentralized systems are the same and that the total investment costs in both are also equal. After 25 years, 2,179 households would have joined communal grids with decentralized storage systems, representing 22.2% of all households. This is higher than the 1,728 households that would have joined networks with centralized storage systems, representing 17.6% of all households.

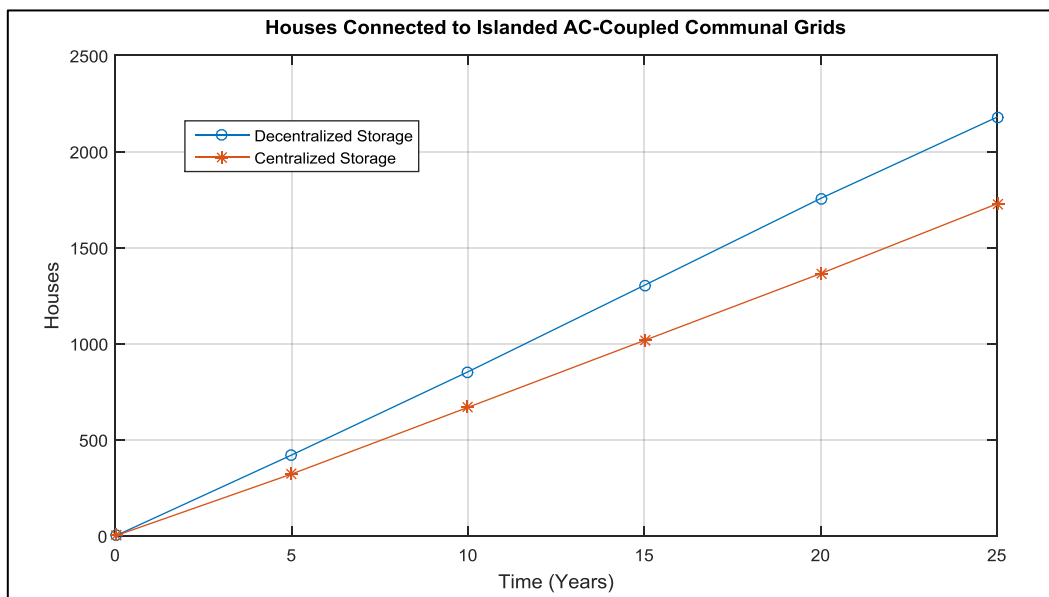


Fig. 6.30: Houses Connected to Islanded AC-Coupled Networks

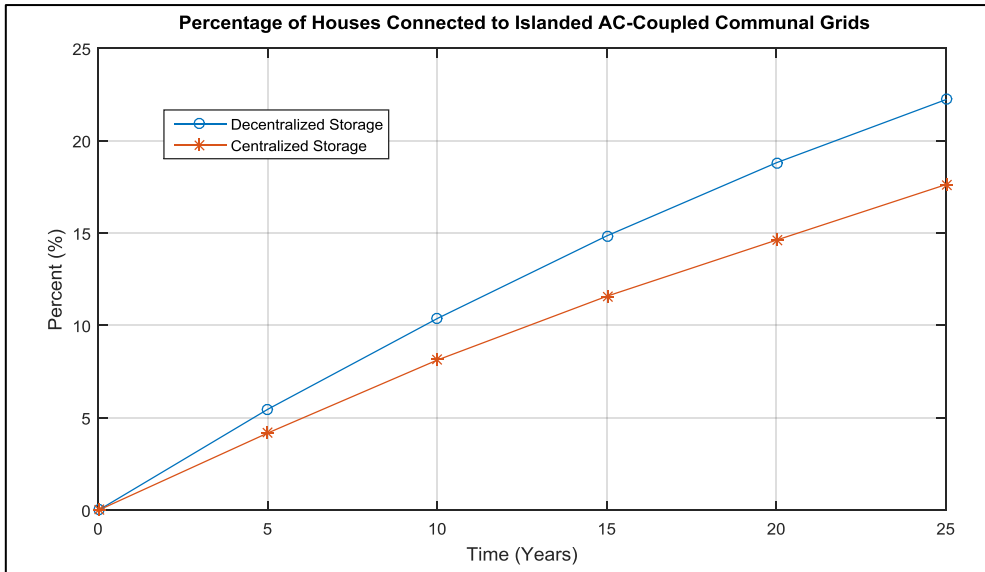


Fig. 6.31: Percentage of Houses Connected to Islanded AC-Coupled Networks

Table 6.3 below shows a comparison of households connected to various islanded communal grids after 25 years. It is clear from the table that more households will have joined networks with decentralized storage systems, whether they be DC- or AC-coupled. In the same category, i.e. decentralized or centralized storage, more households would join DC-coupled networks than AC-coupled networks. This is due to additional costs incurred in DC-AC inverter purchases.

Time (Years)	DC-Coupled		AC-Coupled	
	Decentralized Storage	Centralized Storage	Decentralized Storage	Centralized Storage
0	0	0	0	0
5	507	403	421	322
10	1028	831	854	669
15	1521	1233	1304	1017
20	1982	1627	1756	1365
25	2410	2011	2179	1728

Table 6.3: Comparison of Houses Connected to Communal Grids under Different Islanded Architectures

6.3.2 Grid-Connected Communal Grids:

Communal grid control architectures determine initial investment costs, operations and maintenance costs, and future expansion possibilities. Communal grids should be able to efficiently and reliably operate in both utility grid-connected mode and islanded mode. Energy storage systems are needed for stability of power supply in case of islanded operations. To achieve this, power

electronics are needed for operational control and grid interfacing. In this section impacts of communal grid architectures on their temporal diffusion in a rural developing community are simulated. We specifically look at islanded and grid-connected communal grid with either centralized or decentralized storage in DC-coupled or AC-coupled networks.

Each of the PV arrays simulated have 4 PV arrays, each rate at 100 kW at 1000 W/m² radiation and 25 °C. In all systems, if the PCC voltage rises by more than 5%, a PV array is used to inject active power into the system while if the PCC voltage drops below 5% a heavy load is connected to the feeder. At t_1 (0.0 S), the inverter starts operation to regulate the feeder PCC voltage based on P-f, Q-V, or P-Q-V droop control methods with normal loads. At t_2 (0.5 S) the feeder PCC voltage is increased above 5% due to active power injected from another PV array. At t_3 (1.0 S) the feeder PCC voltage is decreased below 5% limit due to increased load and no additional active power injection.

Figure 6.32 shows the performance of the feeder at t_1 , t_2 , and t_3 if the PCC voltage is regulated using to the P-f droop control method. Figure 6.32 (a) shows the PCC voltage before and after compensation, figure 6.32 (b) shows the PCC voltage before and after active and reactive powers injected by the inverter, figure 6.32 (c) shows the circulated active power, and figure 6.32 (d) shows the apparent power S circulated through the inverter with respect to its rated capacity of 250 KVA.

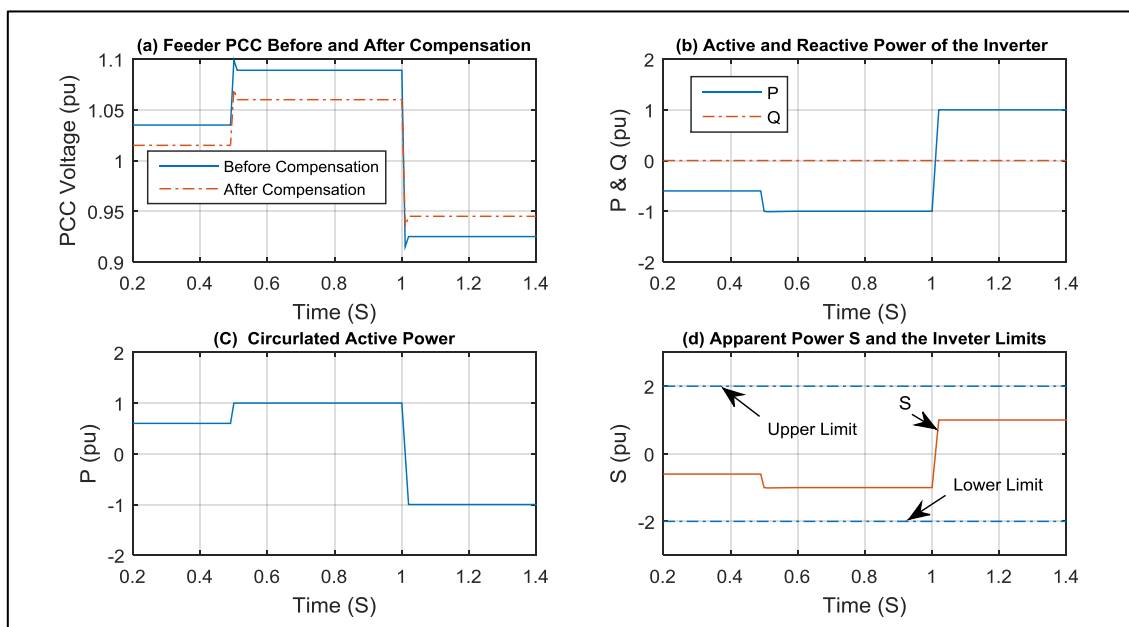


Fig. 6.32: Feeder PCC Voltage Performance with P-f Droop Control Method

From t_1 to t_2 , the PCC voltage is 1.035 pu, and it is reduced to 1.015 pu using P-f droop method; 0.6 pu of active power is absorbed through the inverter. From t_2 to t_3 , the PCC voltage is increased to

1.089 pu and then it is reduced to 1.06 pu. This is done by absorbing 1 pu active power. Even though the inverter could absorb up to 2 pu to regulate the PCC voltage, it has been limited to a maximum of 1 pu for active power injection in order to maintain its voltage within acceptable limits. From t_3 to 1.4 sec, the PCC voltage falls to 0.925 pu due to heavy load on the feeder. The inverter then injects maximum allowable 1 pu active power to improve the PCC voltage from 0.925 to 0.945 pu. The droop coefficient for this method is 0.02 pu/kW for all the operating conditions.

Figure 6.33 shows the performance of the feeder with Q-V droop control method. The conditions for the PCC voltage before compensation are kept identical to that for P-f droop method. From t_1 to t_2 the PCC voltage is reduced from 1.035 pu to 1.02 pu as shown in figure 6.33 (a) by injecting 1.0 pu inductive reactive power through the inverter. From t_2 to t_3 , the PCC voltage is regulated at around 1.055 pu by absorbing 2 pu inductive reactive power capacity of the inverter as shown in figure 6.33 (b). From t_3 to 1.4 seconds, the PCC voltage is raised from 0.925 to 0.948 pu by injecting capacitive reactive power of 2 pu as shown in figure 6.33 (c). The droop coefficient for this method is 0.01 pu/kVAR. Figure 6.33 (d) shows the total apparent power S handled by the feeder. The Q-V droop method utilizes the full inverter rating to compensate for voltage rise and voltage drop; a low X/R ratio system would require higher capacity of inverter to regulate the PCC voltage below the set margin of $\pm 5\%$ [185].

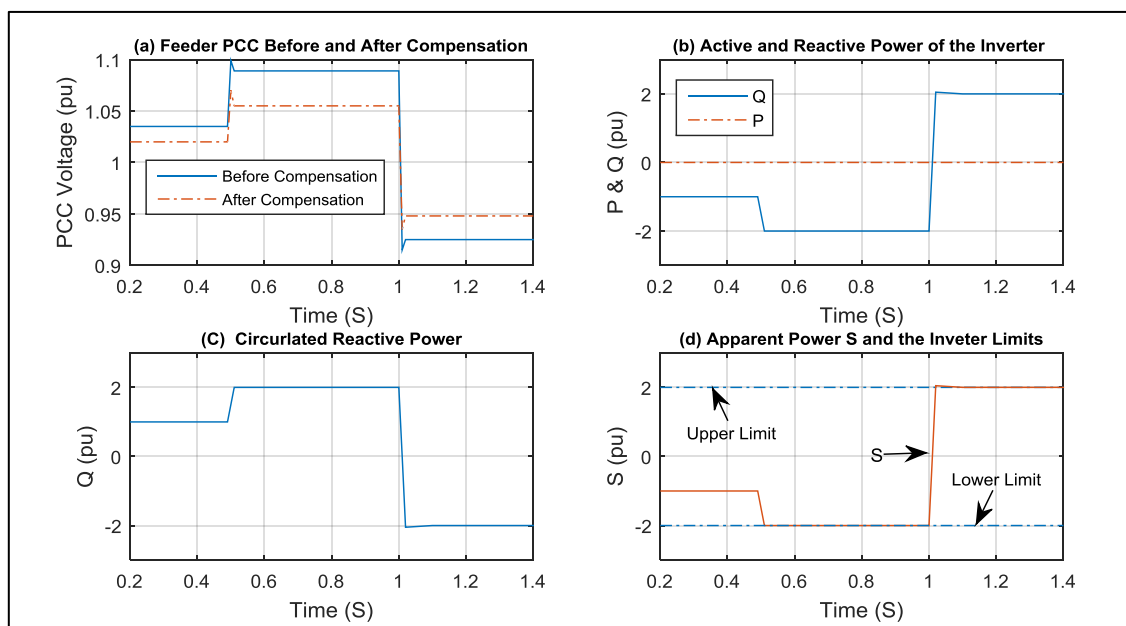


Fig. 6.33: Feeder PCC Voltage Performance with Q-V Droop Control Method.

Figure 6.34 shows the performance of feeder 2 with P-Q-V droop control method. The conditions for the PCC voltage before compensation are kept identical to those for P-f and Q-V droop method.

From t_1 to t_2 the PCC voltage is reduced from 1.035 pu to 1.025 pu as shown in figure 6.34 (a) by absorbing 1.0 pu inductive reactive power through the inverter. The active power coefficient is 0 since the controller mainly uses the reactive power for compensation; the reactive power coefficient is 0.04 pu/kW. From t_2 to t_3 , the PCC voltage is regulated at 1.04 pu by absorbing 1.4 pu inductive reactive power and 0.8 pu active power as shown in figure 6.34 (b). The active droop coefficient is 0.08 pu/kW, while the reactive power coefficient is 0.018 pu/kVAR. The reactive power coefficient is thus reduced as more reactive power is absorbed from the inverter. From t_3 to 1.4 seconds, the PCC voltage is increased from 0.925 pu to 0.96 pu by injecting 1.4 pu capacitive reactive power and 0.7 pu active power simultaneously as shown in figure 6.34 (c). The active droop coefficient is 0.1 pu/kW, while the reactive power coefficient is 0.024 pu/kVAR. Figure 6.34 (d) shows the total apparent power S handled by the feeder. The inverter capacity is more efficiently utilized for voltage regulation with the P-Q-V method than with P-f or Q-V droop methods individually.

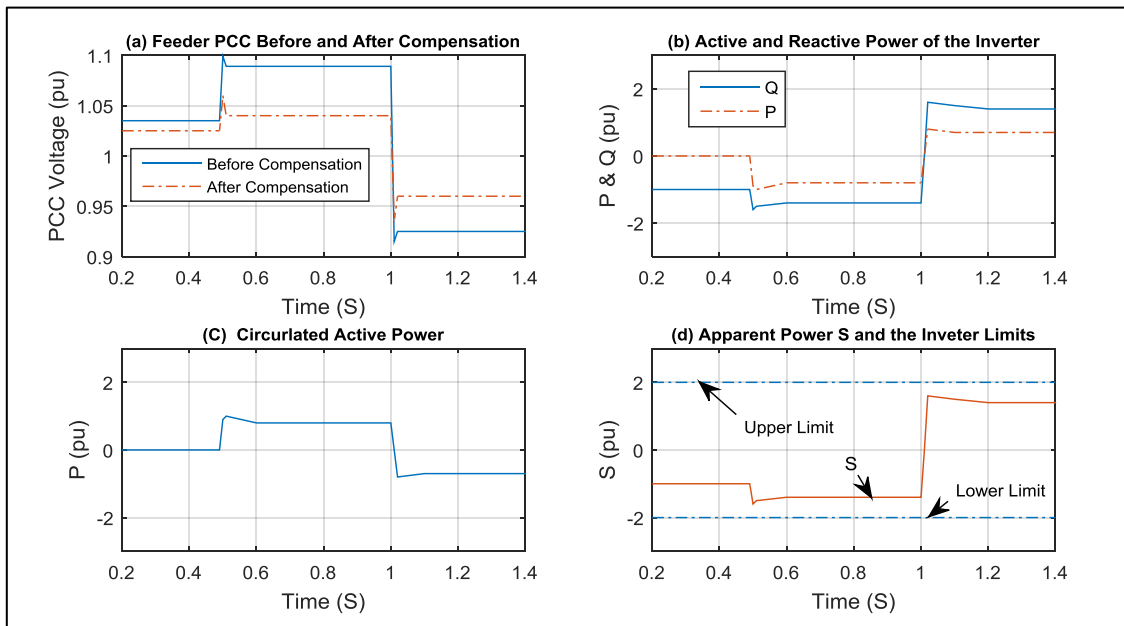


Fig. 6.34: Feeder PCC Voltage Performance with P-Q-V Droop Control Method.

6.3.2.1 DC-Coupled Communal Grids:

Figure 6.35 shows a comparison of households connected to communal grids in centralized and decentralized storage configurations after 25 years while figure 6.36 shows their corresponding percentages. Grid connections add additional costs of VSI, transformer and filter to all networks. After 25 years, 2,103 households would have joined communal grids with decentralized storage systems, representing 21.5% of all households. This is higher than the 1,571 households that would have joined networks with centralized storage systems, representing 16% of all households.

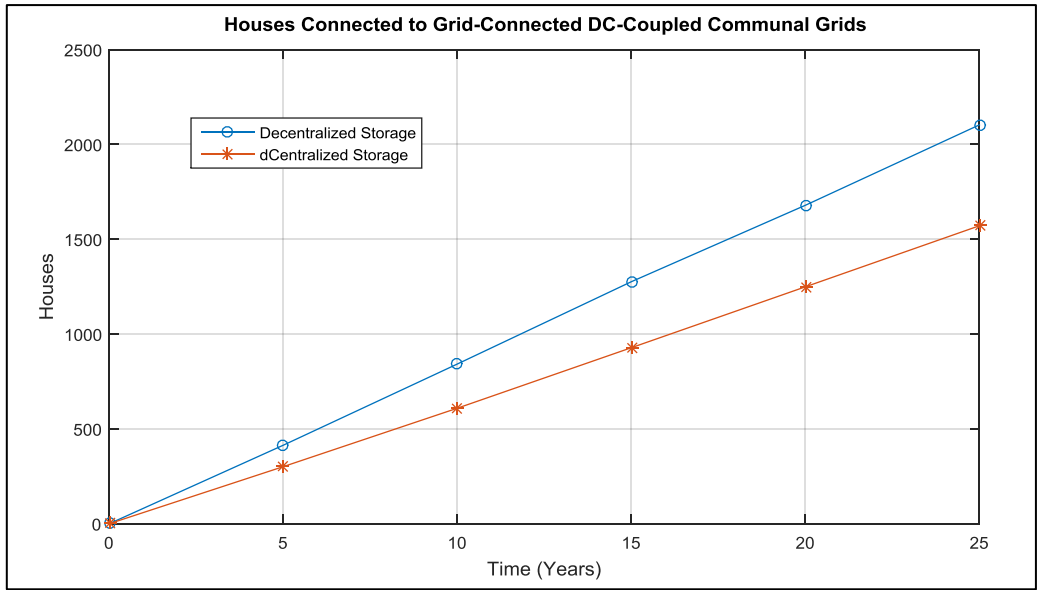


Fig. 6.35: Houses Connected to Grid-Connected DC-Coupled Networks

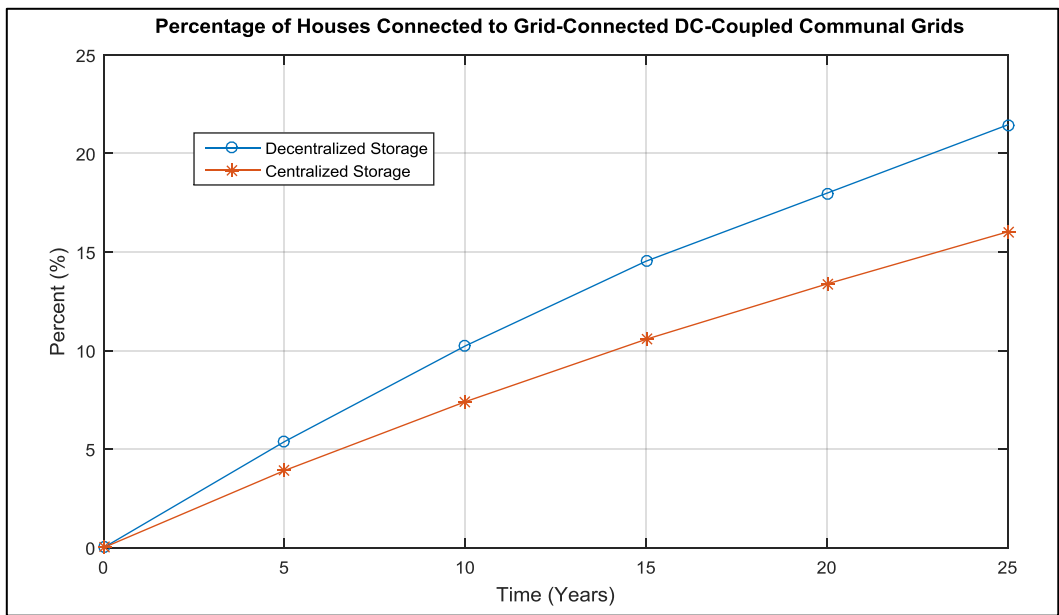


Fig. 6.36: Percentage of Houses Connected to Grid-Connected DC-Coupled Networks

6.3.2.2 AC-Coupled Communal Grids:

Figure 6.37 shows a comparison of households connected to communal grids in centralized and decentralized storage configurations after 25 years while figure 6.38 shows their corresponding percentages. After 25 years, 1,887 households would have joined communal grids with decentralized storage systems, representing 19.2% of all households. This is higher than the 1,286 households that would have joined networks with centralized storage systems, representing 13.1% of all households.

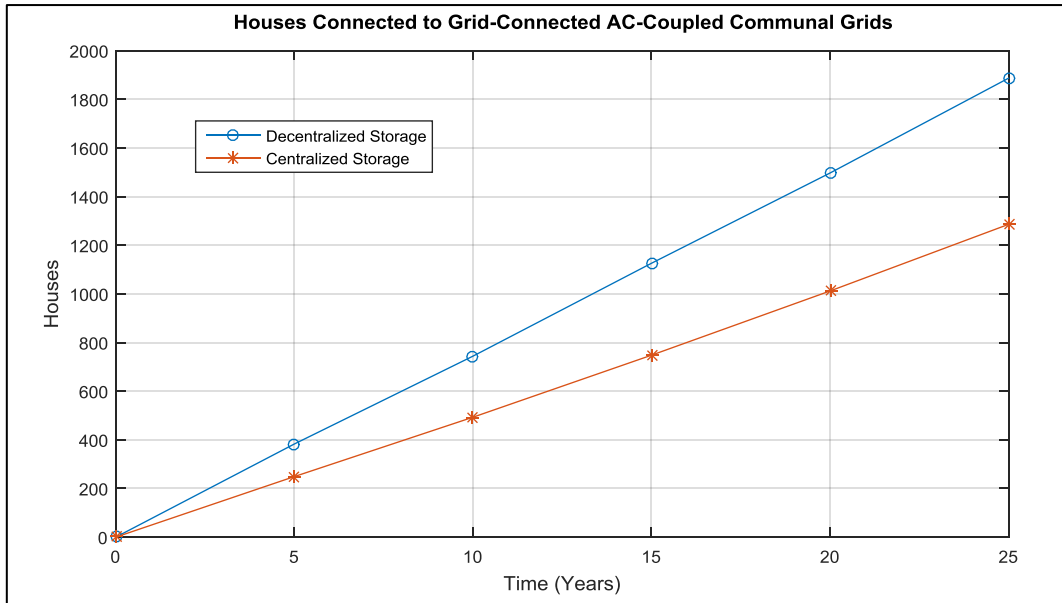


Fig. 6.37: Houses Connected to Grid-Connected AC-Coupled Networks

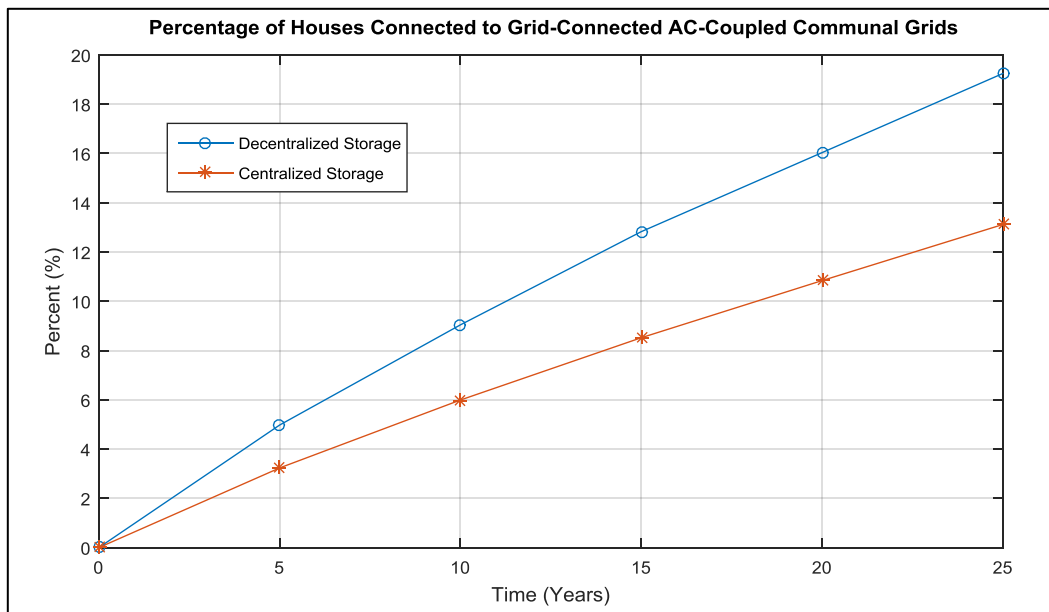


Fig. 6.38: Percentage of Houses Connected to Isolated AC-Coupled Networks

Table 6.4 below shows a comparison of households connected to various grid-connected communal grids after 25 years. Here again it is clear from the table that more households will have joined networks with decentralized storage systems, whether they be DC- or AC-coupled. In the same category, i.e. decentralized or centralized storage, more households would join DC-coupled networks than AC-coupled networks. This is due to additional costs incurred in DC-AC inverter purchases.

Time (Years)	DC-Coupled		AC-Coupled	
	Decentralized Storage	Centralized Storage	Decentralized Storage	Centralized Storage
0	0	0	0	0
5	414	301	383	249
10	842	609	744	493
15	1276	928	1126	748
20	1679	1249	1497	1012
25	2103	1571	1887	1286

Table 6.4: Comparison of Houses Connected to Communal Grids under Different Grid-Connected Architectures

6.4 Concluding Remarks:

In this chapter different control methods and communal grid architecture are modelled. It is shown that P-f droop control method is suitable for networks with low X/R ratios while Q-V droop control method is recommended for systems with high X/R ratios. P-Q-V, is recommended for systems with complex line resistances and reactance, i.e. near unity X/R ratios, as it enables more efficient utilization of inverter capacity for voltage regulation than with P-f or Q-V droop methods individually.

Table 6.5 compares the number of households connected to communal grids based on different control architectures. Communal grids with decentralized storage systems seem to be preferred by more households than systems with centralized storage. This is due to cost considerations and ease of connection/disconnection for each household.

Time (Years)	Decentralized Storage				Centralized Storage			
	Islanded		Grid-Connected		Islanded		Grid-Connected	
	DC	AC	DC	AC	DC	AC	DC	AC
0	0	0	0	0	0	0	0	0
5	507	421	414	383	403	322	301	249
10	1028	854	842	744	831	669	609	493
15	1521	1304	1276	1126	1233	1017	928	748
20	1982	1756	1679	1497	1627	1365	1249	1012
25	2410	2179	2103	1887	2011	1728	1571	1286

Table 6.5: Comparison of Households Connected to Different Communal Grids

These findings may not be intuitive if only viewed from the macro-level perspective rather than the household level perspective because an economy-of-scale framework would typically dictate that larger systems should generally be cheaper and more efficient than smaller systems, and therefore a larger central converter/inverter is assumed to be cheaper and more efficient than many smaller converters/inverters. Similarly, a large battery bank is assumed to perform better than small storage systems. However, such assumptions do not take into consideration the unique path taken by rural residents in developing communities towards joining a communal grid. To recap, initially most rural households install small PV systems, which act as stepping stones to future grid-level electrification. These small systems usually come with energy storage systems, and related power electronics. To be able to join a communal grid, a household must demonstrate the need for electricity-beyond-lighting by having installed a system of minimum 2000 W capacity. This takes time and requires stepwise modifications to the original system. By the time households are ready or permissible to join a communal grid, they would have already made substantial investments in decentralized storage systems and accompanying power electronics. This explains why most households prefer this route, as it allows modest and gradual investments towards a communal grid connection. Centralizing the energy storage system after such a path therefore adds cost to the total investment a household incurs, and thus fewer households prefer this route.

Generally, DC-coupled networks seem to fair better than AC-coupled networks in all categories. This is also due to cost and ease of set-up of such networks. As explained above, DC systems tend to be more modular and scalable than AC systems because DC converters are easier to control and to parallel. This allows for more flexibility in system design and expansion, and thus more effective capital investment management. Also, DC system components tend to be more compact than equivalent AC components because of higher efficiency and by not being frequency dependent. This therefore leads to lower capital costs due to fewer electronic components being used. Also, most distributed energy sources and storage devices have inherently DC outputs, making DC architectures more natural options for their integrations. Due to lower power and energy rating, stability issues are more prevalent in communal grids than in utility grids. However, in DC systems where there are no reactive power interactions, there are no stability issues; system control seems to be oriented towards voltage regulation only.

Regional grids comprising of many communal grids of different architectures could be used to provide electricity-beyond-lighting to rural developing communities such as Kendu Bay, and thus to stimulate rural microeconomic activities. This would eliminate the need to extend the national grid

to these regions. An alternative approach to rural electrification would be feasible if these islanded regional grids eventually spread towards existing national transmissions lines, and eventually fed into the national grid, thus boosting the national power output; the results from this work show that microgeneration systems could be used to cost-effectively provide electricity-beyond-lighting to rural developing communities like Kendu Bay area of Kenya, and to spur rural socio-economic development, with the potential to also increase the national power supply in developing nations in a more sustainable manner, thus allowing sustainable development at both regional and national levels.

Chapter 7: Conclusion and Future Work

7.1 Conclusion:

In this research solar electricity microgeneration systems have been explored as cost-effective alternatives to national grid extensions in providing electricity-beyond-lighting to rural developing communities; a survey-informed agent-based model has been developed as a tool for evaluating temporal diffusion of solar electricity microgeneration systems in a rural developing community. The model uses a location's social, economic, and geographic data to simulate its households' electrification choices with time, given various options. The novelty of the model developed in this work is that it simultaneously simulates how technical, socio-economic, and political factors affect temporal diffusion of PV microgeneration systems in a typical rural developing community. The model further simulates how households with PV, driven by demand for more power, by need for more storage, and by need for improved stability, reliability, and availability of power supply, come together to form communal grids. The model uniquely integrates engineering and policy aspects into one model, by modelling and simulating technical aspects of a PV microgeneration system and a PV-based communal grid, and then looking at how these technical aspects affect the overall costs of such systems, and thus their temporal diffusion within a given developing community. Specifically, the research looked at the technical aspects of PV power generators, power electronics, control systems, communal grid network architectures, and energy storage. These technical sub-systems affected the overall cost of the whole systems, and thus their diffusion within a given community.

Results show that given various options, a household would opt for the most cost-effective electrification path that offers independence over one's own power source and also that is sized to match the household's power demands. This requirement is met by small PV microgeneration systems. Initially, most households in Kendu Bay purchase small PV systems for lighting and to power small electronic devices. These small systems act as the stepping stones to full grid-level electrification; once households have experienced the benefits of electricity, they start to demand more. As their incomes increase with time, households start to modify their systems to match their increasing power demands. Eventually nearby households come together to form communal grids based on their PV systems, or to join already existing communal grids. The increasing PV installations, coupled with the increasing communal grid formations, leads to increased electrification rates through PV systems, as opposed to greater reliance on the national grid. Specifically, results show that the main factor driving PV installations in Kendu Bay is the need for

electricity for basic lighting and to power small electronic appliances such as phone chargers and radios. Results also show that the main inhibiting factor to PV installations in Kendu Bay is cost or inability to afford such systems upfront.

Costs could be influenced by many factors including location, efficiency, demand, and government policies. Increased PV installations could therefore be achieved through introduction of positive incentives such as subsidies; introduction of both capital-based, and power-based subsidies resulted in substantial increases in overall PV installations. The difference between the subsidies was insignificant. Power-based subsidies enables the government to distribute the cost over many years, with the risk of future governments not honouring the debt. On the other hand, capital-based subsidies would require immediate investments from the government, a feat which might not be possible in financially strapped developing countries. A solution lies in striking a balance between debt and upfront investment. Subsidies should only be offered to households that afford, or nearly afford to purchase small PV systems. The amount of subsidies offered should be dictated by the amount a household is willing to invest in a PV system, with households with large PV systems getting more incentives. Families earning a minimum of \$200 per month are able to transition into the PV income threshold bracket after 1 year, and therefore this should be the lowest income threshold for subsidies applications.

Introduction of government-supported low-interest microcredit facilities for those unable to afford small PV system upfront could also result in increased PV installations as shown in simulation results. Currently, some retailers offer PV to civil servant on an interest-free hire-purchase arrangement. This enables the retailers to sell more systems over six months, than they would normally. Such an arrangement could be extended to those without formal employments but with clear and stable monthly incomes, evidenced by bank statements. Such an arrangement could be supported by government guarantees, in case of defaults. This way, more households and small business owners could be able to install PV and pay for it in 6 equal monthly instalments as opposed to paying the full amount upfront. With introduction of a low interest rate, the length of payment could even be extended to 1 or more years. It is therefore recommended to the government to consider stimulating electricity demand in rural Kenya by enabling purchases of small PV systems by provisions of guarantees to small retailers willing to sell PV systems to non-civil servants on hire-purchase or loan arrangements. The government could also consider introducing small microcredit facilities to enable such households to install PV.

Increasing neighbourhood influence could also lead to more PV installations as the socio-economic benefits of such systems become known to more households either through observations, word-of-mouth, or through advertisements. Sensing radius could be increased through local administrative campaigns, billboards and flyers, radio advertisements (most households use dry-cell powered radios), and social activities. Similar methods were used to popularize mobile telephony and related services such as mobile telephone banking and money transfer in Kenya. In fact, most people with low incomes, and most small business owners use mobile telephone banking as opposed to conventional commercial banking. The government should therefore consider increasing sensing radius as a method of sensitizing rural households on the benefits of PV microgeneration systems and on their potential in arresting low rural electrification rates.

In conclusion, for optimum PV installations and subsequent communal grid formations or connections, a combination of many factors must be simultaneously considered, with the most important factors being introduction of subsidies, introduction of favourable microcredit facilities, increased social acceptance through increased neighbourhood influence, and use of cost-effective control methods and architecture. The agent-based model developed in this work could be used by policy-makers and stake-holders in planning, prioritizing, and implementing rural electrification policies for a given community. The only inputs required are a location's socio-economic demographics and its electricity microgeneration potential. The ABM would then simulate temporal diffusion of a given electricity microgeneration system for the area.

7.2 Chapter Summaries:

In chapter one a brief literature review is carried out to highlight the poor electrification states in many rural developing communities, with a focus on sub-Saharan Africa. The importance of electrification to rural socio-economic development is highlighted. The emergence of decentralized electricity generation and distribution as alternatives to national grid extensions is also highlighted. Communal grids are introduced as potential means of providing electricity-beyond-lighting to these developing communities. A review of solar electricity microgeneration is also carried out. It is noted that there is an exponential growth in installations of PV microgeneration systems all around the world as the cost of delivered electricity continues to fall. This is a result of decades of research and development which has resulted in efficient, rapid, and mass production of high quality PV systems, which have in turn also translated into continuously falling prices of PV systems.

In chapter two technical aspects of solar electricity microgeneration systems are modelled and simulated. In the first section PV power generators are reviewed, modelled and simulated. This section simulates I-V and P-V characteristics of solar cells, modules, and arrays in different configurations. Factors affecting PV power output such as partial shading and maximum power point are also modelled and simulated. In the second section, PV power electronics are reviewed, modelled and simulated. PV systems need converters for maximum power point tracking, power conditioning, and voltage buck or boost. PV systems also need inverters for utility grid interfacing and for AC loads; different types of converters/inverters are modelled and simulated. In the third section, energy storage technologies are reviewed. Batteries for PV systems are reviewed, modelled and simulated. Batteries are essential for islanded PV systems and for system stability in grid-connected PV systems. The merits and demerits of different battery technologies are discussed, with lead-acid batteries emerging as the preferred option due to affordability and maturity of technology. It is also shown that lithium-ion batteries have potential for extensive PV use in the future with more research and development and thus fall in costs. Environmental impacts of batteries are also reviewed.

Before the agent-based model that forms the core of this research could be developed, it was necessary to gather survey data that would later be used to inform it. This was done in two stages; the first stage involved identifying a suitable location for the survey and modelling its PV microgeneration potential while the second stage involved developing and carrying out the actual survey. Kendu Bay area of Kenya was identified as the most suitable area for the survey due to its proximity to the equator and thus plenty of sunlight all year round and to its demographics which mirror those of many other rural communities in sub-Saharan Africa. PV microgeneration potential for Kendu Bay area of Kenya are then modelled and simulated in chapter four. First, high resolution irradiance data for Kendu Bay is simulated using a stochastic clear-sky model and based on available empirical data. The irradiance data is then used to model and simulate PV microgeneration potential for a single household, 25 households (microgrid), and 100 households (minigrid). Minutely household power demands are modelled and simulated using a stochastic active occupancy model. The results are used to calculate power imported and exported by the households on a minutely basis, and overall. Results show that there is a great potential for solar microgeneration in Kendu Bay, with strong solar insolation throughout the year; there are little seasonal variations and little cloud cover, boosting PV microgeneration potential. For efficient generation and consumption, results show that connecting many solar microgeneration systems into communal grids reduces power losses due to improper storage or due to demand versus generation mismatches; a single

household imported more power than is exported during a weekday simulation run while 25 or 100 such households connected in a communal grid exported more power than they imported. The stochastic nature of the household power demand model produces different demand profiles for every simulation run; however, it is clear from the data obtained that gridding enables more efficient power consumption than stand-alone systems. In addition, gridding provides effective storage for generated power while also reducing the overall expenses incurred by an individual household vis-à-vis battery costs.

Having obtained satisfactory results from chapter three, a survey of solar electricity microgeneration systems in Kendu Bay was developed and carried out in chapter four. Results show that currently 92.2% of Kendu Bay households are unelectrified due to financial barriers, 4.7% have basic electricity through small PV systems, while 3.1% are connected to the national grid. From the survey, four possible routes to electrification in Kendu Bay are identified as through national grid connections, through stand-alone PV systems, through PV-based communal grids, or through grid-connected PV systems. As there are currently no communal grids in Kendu Bay, only the first three options are operational. However, with more homes installing PV systems, and based on responses to survey questions, potential for communal grids formations remains high. From the survey, it is clear that there is a serious distrust of the national grid, with many respondents describing it as too unreliable due to frequent and long-lasting blackouts, too expensive due to high connection fees, or too corrupt with technicians demanding kickbacks and customers complaining of uneven monthly bills. For these people, any affordable and reliable alternative would be preferred. On the other hand, typical stand-alone PV systems offer limited power capacity and hardly provide electricity-beyond-lighting; a properly sized system to meet all of a household's power demands would be too expensive for most of the Kendu Bay residents, since as it currently stands, 92.2% cannot afford even the most basic of PV systems. Small stand-alone PV systems therefore cannot stimulate rural micro-economic activities. Communal grids based on PV systems could provide the bridge between stand-alone systems and the national grid by providing sustainable, clean, and affordable electricity-beyond-lighting to rural residents.

In chapter five temporal diffusion of solar electricity microgeneration systems in Kendu Bay area are modelled and simulated using an agent-based model developed in Netlogo. Survey data gathered in chapter five are used to inform the model. Results show that after 25 years, more households will be electrified through PV systems than through the national grid. Results also show that the electrification rate in the area will steadily rise from the current 7.8% to about 57.6%. Of these,

44.1% will be electrified through PV systems, with 24.6% being connected to PV-based communal grids. Another 13.5% will be electrified through the national grid. Introduction of subsidies would see further increases in households installing PV systems, leading to substantial increases in electrified households. Similarly, increasing neighbourhood influence, modelled as sensing radius, would lead to increased PV installations and subsequent communal grid connections. On the other hand increasing neighbourhood and power thresholds would lead to fewer PV installations and communal grid connections, respectively. Since electrification rate will generally temporally increase, falling PV installations will mean more electrification through the utility grid.

In chapter six impacts of control methods and architectures on temporal diffusion of PV-based communal grids in Kendu Bay area are modelled and simulated. System performances with different droop control methods are simulated, with results showing that P-f droop control method is suitable for systems with high line resistance (R) and low impedance (X), i.e., low X/R ratio while Q-V droop method is suitable for systems with low line resistance and high impedance and thus high X/R ratio. For systems with near unity X/R ratios, P-Q-V droop control method that efficiently utilizes inverter capacity for voltage control is proposed. Decentralized control in multi-master mode allows all distributed PV systems within the communal grid to regulate their own power outputs in utility-grid-connected and islanded modes by using individual droop controls and thus ensures equal load sharing across all of the distributed PV systems forming the communal grid network. It is the best performing configuration vis-à-vis cost and reliability and is thus the assumed mode in all simulations in future work.

7.3 Future Work:

Future research will expand on the work done so far by looking at methods of integrating energy storage systems into PV-based communal grids. Such power networks face great challenges in transmission and distribution to meet unpredictable daily and seasonal variations in demand. Energy storage systems have been recognized as having great potential in meeting these challenges, whereby energy is stored in a certain state, according to the technology used, and is converted to electricity when needed. Specifically, energy storage systems can be used to time-shift renewable energy from off-peak generation to on-peak times. This leads to reduction in transmission bottleneck by storing the energy close to the end user or by using underutilized transmission paths at night. This raises the overall capacity factor on the lines involved, and has the potential to increase overall revenues for transmission providers who might not be able to carry the same

renewable energy at peak load hours, causing the energy to be dumped or sold at lower value market.

Significant research over the last decade has been geared towards improving cost and reliability of energy storage systems. However, little work has been done on engineering tools for integrating energy storage into existing or future electric grids. Many existing modelling tools consider energy storage in more limited environments. Despite the range and quality of these resources, no models or tools have been found that specifically deal with sizing and locating energy storage under any optimality criterion that would be useful for infrastructure development. This is mainly due to complexity of the problem, requirements for multidisciplinary resources, lack of familiarity on the part of utility transmission and distribution engineers with energy storage technologies, utilities engineer's preferences for wires and substations, and most importantly, the opinion of many engineers involved in energy storage is that such a model cannot be built.

The future implementation of a reliable and low-carbon electricity infrastructure may depend, in part, on the availability of infrastructure-specific models; making models and analytical tools available to the planning communities could significantly enhance the planning process to improve grid future operation to enable higher utilization of the infrastructure with a lower carbon footprint. Future research will focus on development of a model that reflects the market environment for energy storage including an open ancillary service market and the ability to allow the aggregation of multiple value streams including both generation and transmission services characteristics. The model should be tailored for use in a communal grid environment, with the following desirable characteristics:

- Fast modelling capability, meaning a limited number of nodes for analysis with the ability to aggregate models up from distribution to transmission and include balancing area market factors
- Capability to economically optimize energy storage siting against competing technologies by node-in transmission or distribution applications against predetermined load profiles to include the aggregation of ancillary services
- Options to optimize the storage solution around particular uses such as ancillary services, renewable integration (at generation side or end use), energy or capacity use, stationary or modular siting
- Means for inputting updatable equipment costs, maintenance costs and power conversion system options that show ramp rates

References:

1. U.S. Energy Information Administration (EIA), *International Energy Outlook*, 2013
2. International Energy Agency (IEA), *World Energy Outlook*, 2012
3. Ministry of Foreign Affairs of Netherlands, *Renewable Energy: Access and Impact; a Systematic Literature Review of the Impact on Livelihoods of Interventions Providing Access to Renewable Energy in Developing Countries*, IOB Study, 2013
4. WHO, *Global Burden of Disease*, 2010
5. Zerriffi, H., *Distributed Rural Electrification in Brazil*, in *Rural Electrification* 59-87, 2011, Springer, Netherlands
6. Yadoo, A., Cruickshank, H., *The Value of Cooperatives in Rural Electrification*, *Energy Policy* **38**:2941-2947, 2010
7. Reiche, K., Covarrubia, J., Martinot, E., *Expanding Electricity Access to Remote Areas: Off-Grid Rural Electrification in Developing Countries*, *World Power* 52-60, 2000
8. Short, W., Packey, D., Holt, T., *A Manual for the Economic Evaluation of Energy Efficiency and Renewable Energy Technologies*, National Renewable Energy Laboratory (NREL), 1995
9. National Renewable Energy Laboratory (NREL), *Energy Analysis: Technology Cost and Performance*, NREL, 2012
10. World Bank, *Technical and Economic Assessment of Off-Grid, Mini-Grid and Grid Electrification Technologies*, ESMAP Paper, 2007
11. Kerr, R., *Sun's Role in Warming is Discounted*, *Science* **268**: 28-29, 1995
12. Klein, R., Schipper, E., Dessai, S., *Integrating Mitigation and Adaptation into Climate and Development Policy: Three Research Questions*, *Environmental Science and Policy* **8**: 579–588, 2005
13. Earth Policy Institute, http://www.earth-policy.org/data_center/C23, 2015
14. Cadwell, J., *Photovoltaic Technology and Markets*, *Contemporary Economic Policy* **12**: 97–111, 1994
15. Zerriffi, H., Wilson, E., *Leapfrogging Over Development? Promoting Rural Renewables for Climate Change Mitigation*, *Energy Policy* **38**: 1689–1700, 2010
16. Lysen, E., *Photovoltaics for Villages*, *IEEE Spectrum* **31**:34-39, 1994
17. Adner, R., *When Are Technologies Disruptive? A Demand-Based View of the Emergence of Competition*, *Strat. Mgmt. J.* **23**:667-688, 2002

18. Fleetwood, T., *An Investigation into the Disruptive Capacity of Distributed Power Technologies*, M.Sc. Dissertation, Manchester School of Management, Manchester, 2001
19. Patterson, W., *Transforming Electricity*, Earthscan, London, 1999
20. Magnussen, T., Watson, F., *Sticking to your Knitting or Changing Business Model? Discontinuities and Capabilities in Electrical Power Generation Equipment Manufacturing*, Paper Submitted to Industrial and Corporate Change, 2003
21. Maycock, P., *The World PV Market: Production Increases 36%*, Renewable Energy World, 2002
22. Watson, J., *Co-Provision in Sustainable Energy Systems: the Case of Micro-Generation*, Energy Policy **32**:1981-1990, 2004
23. Chappells, H., Klintman, M., Linden, A., et al., *Domestic Consumption Utility Services and the Environment: Final Project Report*, University of Lancaster, Wageningen and Lund, 2,000
24. Udwaيدا, F., Kumar, K., *Impact of Consumer Co-Construction in Product/Service Markets*, Technol. Forecast Soc. **40**:261-272, 1991
25. Fliess, S., Klienaltenkamp, M., *Blueprinting the Service Company: Managing Service Processes Efficiently*, J. Bus. Res. **5701**:1-13, 2002
26. Van Vliet, B., Chappells, H., *The Co-Provision of Utility Services: Resources, New Technologies and Consumers, Paper for Consumption, Everyday Life and Sustainability Summer School*, University of Lancaster, 1999
27. Weinmann, O., *Experience in Operating Hydrogen Systems*, Presentation to UK Energy Network Meeting, Rutherford Appleton Laboratory, 10th July, 2002
28. Institution of Electrical Engineers, *The Enternet – The Power to Transform the Electricity Industry*, Seminar Held at IEE, Savoy Place, London, 20th February, 2002
29. Sauter, R., Watson, J., *Strategies for the Deployment of Micro-Generation Implications for Social Acceptance*, Energy Policy **35**:2770-2779, 2007
30. Semadeni, M., Hansmann, R., Flueeler, T., *Public Attitudes in Relation to Risk and Novelty of Future Energy Options*, Energy & Environment **15**:755-777, 2004
31. Kaldellis, J., *Social Attitude Towards Wind Energy Applications in Greece*, Energy Policy **33**:595-602, 2005
32. Faiers, A., Neame, C., *Consumer Attitudes Towards Domestic Solar Power Systems*, Energy Policy **34**:1797-1806, 2006
33. Penson, S., *Car and Household Emissions Threaten UK's CO₂ Goals*, Reuters/Planetark, www.planetark.com/dailynewsstory.cfm/newsid/32537/story.htm, October 6th, 2005

34. Fischer, C., *Users as Pioneers: Transformation in the Electricity System, Micro CHP and the Role of the Users*, in: Jacob, K., Binder, M., Wieczorek, A., (Eds), *Governance for Industrial Transformation*, Proceedings of the 2003 Berlin Conference on Human Dimensions of Global Environmental Change, Environmental Policy Research Centre, Berlin, 319-337, 2004
35. Fischer, C., *From Consumers to Operators: the Role of Micro CHP Users*, in: Pehnt, M., Cames, M., Fischer, C., et al., (Eds), *Microgeneration: Towards a Decentralized Energy Supply*, Springer, Heidelberg, 2006, 2006
36. London Renewables, *Attitudes to Renewable Energy in London: Public and Stakeholder Opinion and the Scope for Progress*, A Report Commission by London Renewables and Carried Out by Brook Lyndhurst Ltd in Association with MORI and Upstream, Greater London Authority, 2003
37. Ellison, G., *Renewable Energy Survey*, Draft Summary Report of Findings, www.london.gov.uk/assembly/reports/environment/power_survey_orc.pdf, August 10th, 2005
38. Dobbyn, J., Thomas, G., *Seeing the Light: the Impact of Micro Generation on Our Use of Energy*, Sustainable Consumption Roundtable, London, 2005
39. Jones, H., *Achieving Energy Efficiency through Domestic CHP: An Analysis of Market Barriers in the UK*, A Report Submitted in Partial Fulfilment of the Requirements for the MSc and the DIC, Imperial College of Science, Technology and Medicine, 2003
40. Naesje, P., Andersen, T., Saele, H., *Consumer Response on Price Incentives*, in: ECEEE 2005 Summer Study 'Energy Savings: What Works and Who Delivers?', Mandelieu La Napoule **3**:1259-1269, 2005
41. World Bank, *World bank Mission to India Nov 4-15*, IREDA Review, World Bank, Washington DC, 1996
42. Cabraal, A., Davies, M., C., Schaeffer, L., *Best Practices for Photovoltaic Household Electrification Programs*, World Bank, Washington DC, 1996
43. Erickson, J., Chapman, D., *Photovoltaic Technology: Markets, Economics, and Rural Development*, World Development **23**: 1129-1141, 1995
44. Foley, G., *Photovoltaic Applications in Rural Areas of the Developing World*, World Bank, Washington DC, 1995
45. Acker, R., Kammen, D., *The Quiet Energy Revolution: Analysing the Dissemination of Photovoltaic Power Systems in Kenya*, Energy Policy **24**: 81-111, 1996
46. Saha, H., *Design of a Photovoltaic Electric Power System for an Indian Village*, Solar Energy **27** (2): 103 – 107, 1981

47. Aulich, H.A., Raptis, F., Schmid, J., *Rural Electrification with Photovoltaic Hybrid Plants – State of the Art and Future Trends*, Progress in Photovoltaics: Research and Applications **6**: 325–339, 1998
48. Dakkak, M., Hirata, A., Muhida, R., Kawasaki, Z., *Operation Strategy of Residential Centralised Photovoltaic System in Remote Areas*, Renewable Energy **28**: 997–1012, 2003
49. Schmidt-Kuntzer, Schafer, G., *Village Power Plants Versus SHS*, SunWorld **17**: 17–20, 1993
50. Vallve, X., Serrasolses, J., *Design and Operation of a 50 kWp PV Rural Electrification Project for Remote Sites in Spain*, Solar Energy **59**: 111–119, 1997
51. European Photovoltaic Industry Association (EPIA), *Global Market Outlook for Photovoltaics 2013-2017*, 2013
52. International Energy Agency (IEA), *Key World Energy Statistics*, 2011
53. Greacen, C., Engel, R., Quetchenbach, T., *A Guidebook on Grid Interconnection and Islanded Operation of Mini-Grid Power Systems Up to 200 kW*, Lawrence Berkeley National Laboratory, Schatz Energy Research Centre, 2013
54. Tyagi, M., *Introduction to Semiconductor Materials and Devices*, John Wiley & Sons, Hoboken, NJ, 1991
55. Masters, G., *Renewable and Efficient Electric Power Systems*, John Wiley & Sons, New Jersey, 2004
56. Rekioua, D., Matagne, E., *Optimization of Photovoltaic Power Systems – Modelization, Simulation and Control*, Springer-Verlag, London, 2012
57. Gow, J. A., Manning, C. D., *Development of a Photovoltaic Array Model for Use in Power-Electronics Simulations Studies*, IEE Proceedings-Electric Power Applications **146**: 193-200, 1999
58. Protopogopoulos, C., Brinkworth, B. J., Marshall, R. H., et al., *Evaluation of Two Theoretical Models in Simulating the Performance of Amorphous-Silicon Solar Cells*, 10th E.C Photovoltaic Solar Energy Conference Proceedings, 412-415, 1991
59. Markvart, T., *Solar Electricity*, 2nd Edition, Wiley, ISBN: 0471988537, 1999
60. Lorenzo, E., *Solar Electricity: Engineering of Photovoltaic Systems*, PROGENSA, ISBN 8486505550, 1994
61. Veissid, N., Bonnet, D., Richter, H., *Experimental Investigation of the Double Exponential Model of a Solar Cell Under Illuminated Conditions: Considering the Instrumental Uncertainties in the Current, Voltage and Temperature Values*, Solid-State Electronics **38**: 1937-1943, 1995
62. BP Solar, www.bpsolar.us, 2008

63. Rahmann, C., *Mitigation Control Against Partial Shading Effective in Large-Scale PV Power Plants*, IEEE Trans. Sustain. Energy **7**: 173-180
64. Hohm, D.P., Ropp, M. E., *Comparative Study of Maximum Power Point Tracking Algorithms*, Progress in Photovoltaics: Research and Application **11**: 47- 62, 2003
65. Hussein, K. H., Muta, I., Hoshino, T., et al., *Maximum Photovoltaic Power Tracking: An Algorithm for Rapidly Changing Atmospheric Conditions*, IEE Proceedings, Generation, Transmission and Distribution **142**: 59-64, 1995
66. Khaehintung, N., Wiangtong, T., Sirisuk, P., *FPGA Implementation of MPPT Using Variable Step-Size P and O Algorithm for PV Applications*, 2006 International Symposium on Communications and Information Technologies, 212-215, 2006
67. *IEEE Standard for Interconnecting Distributed Resources with Electric Power Systems*, IEEE Std **1547-2003**: 1 –16, 2003.
68. Turitsyn, K., Sulc, P., Backhaus, S., et al., *Local Control of Reactive Power by Distributed Photovoltaic Generators*, First IEEE International Smart Grid Communications (Smart-GridComm) Conference 79 –84, 2010
69. Paal, E., Tatai, E., *Grid Connected Inverters Influence on Power Quality of Smart Grid*, 14th International Power Electronics and Motion Control Conference (EPE/PEMC), T6–35 –T6–39, 2010
70. Etehad, M., Ghasemi, H., Vaez-Zadeh, S., *Reactive Power Ranking for dg Units in Distribution Networks*, 10th Environment and Electrical Engineering (EEEIC) Conference 1 –4, 2011
71. Jewell, W., Hu, Z., *The Role of Energy Storage in Transmission and Distribution Efficiency*, Transmission and Distribution Conference and Exposition (T&D), IEEE PES, 1–4, 2012
72. Manz, D., Piwko, R., Miller, N., *Look Before You Leap: The Role of Energy Storage in the Grid*, Power Energy Mag. IEEE **10**: 75– 84, 2012
73. Jiang, Q., Wang, H., *Two-Time-Scale Coordination Control for a Battery Energy Storage System to Mitigate Wind Power Fluctuations*, Energy Conversion, IEEE Trans. **28**: 52–61, 2013
74. Roberts, B., Sandberg, C., *The Role of Energy Storage in Development of Smart Grids*, Proc. IEEE **99**: 1139–1144, 2011
75. Hadjipaschalis, I., Poullikkas, A., Efthimiou, V., *Overview of Current and Future Energy Storage Technologies for Electric Power Applications*, Renew. Sustain. Energy Rev. **13**: 1513–1522, 2009
76. Roberts, B., McDowall, J., *Commercial Successes in Power Storage*, Power Energy Mag. IEEE **3**: 24–30, 2005

77. Ter-Gazarian, A., *Energy Storage for Power System*, First Edition, the Institute of Engineering and Technology, London, United Kingdom, 1994
78. Lindley, D., *Smart Grids: The Energy Storage Problem*, *Nature* **463**: 18–20, 2010
79. Electricity Storage Association, *Electricity Storage*, <http://www.electricitystorage.org/>
80. Wahl, K., *A Short History of Electrochemistry*, *Galvanotechnik* **96**: 1820–1828, 2005
81. Gnanaraj, J. S., Thompson, R. W., Iaconatti, S. N., et al., *Formation and Growth of Surface Films on Graphitic Anode Materials for Li-Ion Batteries*, *Electrochemical and Solid-State Letters* **8**: A128–A132, 2005
82. Teofilo, V., Merritt, L., Hollandsworth, R., *Advanced Lithium Ion Battery Charger*, *IEEE Aerospace and Electronic Systems Magazine* **12**: 30-36, 1997
83. Tremblay, O., Dessaint, L. A., Dekkiche, A. I., *A Generic Battery Model for the Dynamic Simulation of Hybrid Electric Vehicles*, *Vehicle Power and Propulsion Conference (VPPC 2007)*, 284-289, 2007
84. Chiasson, J., Vairamohan, B., *Estimating the State of Charge of a Battery*, *Control Systems Technology*, *IEEE Transactions on* , **13**: 465- 470, 2005
85. Tyagi, M., *Introduction to Semiconductor Materials and Devices*, John Wiley & Sons, Hoboken, NJ, 1991
86. Xiao, B., *A Universal State-of-Charge Algorithm for Batteries*, *DAC* 687–692, 2010.
87. Tremblay, O., Dessaint, L.-A. *Experimental Validation of a Battery Dynamic Model for EV Applications*, *World Electric Vehicle Journal*, 2009
88. Solar Energy International. *Photovoltaics Design and Installation Manual*. 4th ed. British Columbia, New Society Publishers, 2004.
89. Baert, D., Vervaet, A., *Lead-acid Battery Model for the Derivation of Peukert's Law*, *Electrochimica Acta* **44** (20), 1999
90. www.pveducation.org/pvcdrom/properties-of-sunlight/
91. Green, M. A., *Solar Cells: Operating Principles, Technology and System Applications*, University of New South Wales, 1992
92. http://upload.wikimedia.org/wikipedia/commons/thumb/0/0b/Band_gap_comparison.svg/2000px-Band_gap_comparison.svg.png
93. Renewable Resource Data Centre, National Renewable Energy Laboratory, *Solar Spectra*, 2008
94. Badescu, V., *Verification of Some Very Simple Clear and Cloudy Sky Models to Evaluate Global Solar Irradiance*, *Solar Energy* **61**: 251-264, 1997

95. Stoffel, T., Renne, D., Myers, D., et al., *Concentrating Solar Power: Best Practices Handbook for the Collection and Use of Solar Resource Data (CSP)*, NREL/TP-550-47465, 2010
96. Lanetz, A., Kudish, A., *A Method for Determining the Solar Global and Defining the Diffuse and Beam Irradiation on a Clear Day*, in, *Modelling Solar Radiation at the Earth's Surface*, Badescu, V., Ed., Heidelberg, Germany, 2008
97. Daneshyar, M., *Solar Radiation Statistics for Iran*, *Solar Energy* **21**: 345-349, 1978
98. Paltridge, G., Proctor, D., *Monthly Mean Solar Radiation Statistics for Australia*, *Solar Energy* **18**: 235-243, 1976
99. Kasten, F., Czeplak, D., *Solar and Terrestrial Radiation Dependent on the Amount and Type of Cloud*, *Solar Energy* **25**: 177-189, 1980
100. Haurwitz, B., *Insolation in Relation to Cloudiness and Cloud Density*, *Journal of Meteorology* **2**: 154-166, 1945
101. Haurwitz, B., *Insolation in Relation to Cloud Type*, *Journal of Meteorology* **3**: 123-124, 1946.
102. Robledo, L., Soler, A., *Luminous Efficacy of Global Solar Radiation for Clear Skies*, *Energy Conversion and Management* **41**: 1769-1779, 2000
103. Meinel, A., Meinel, M., *Applied Solar Energy*. Reading, MA: Addison-Wesley Publishing Co., 1976
104. Laue, E., *The Measurement of Solar Spectral Irradiance at Different Terrestrial Elevations*, *Solar Energy* **13**: 51-57, 1970
105. Kasten, F., *A Simple Parameterization of the Pyrheliometric Formula for Determining the Linke Turbidity Factor*, *Meteorologische Rundschau* **33**: 124-127, 1980
106. Linke, F., *Transmissions-Koeffizient und Trubungsfactor*, *Beitr. Phys. fr. Atmos* **10**: 91-103, 1922
107. Davies, J., McKay, D., *Evaluation of Selected Models for Estimating Solar Radiation on Horizontal Surfaces*, *Solar Energy* **43**: 153-168, 1989
108. Davies, J., McKay, D., *Estimating Solar Irradiance and Components*, *Solar Energy* **29**: 55-64, 1982
109. Badescu, V., *Use of Sunshine Number for Solar Irradiance Time Series Generation*, in, *Modelling Solar Radiation at the Earth's Surface*, V. Badescu, Ed., Heidelberg, Germany, 2008
110. Bird, R., *A Simple Solar Spectral Model for Direct-Normal and Diffuse Horizontal Irradiance*, *Solar Energy* **32**: 461-471, 1984
111. Bird, R., Riordan, C., *Simple Solar Spectral Model for Direct and Diffuse Irradiance on Horizontal and Tilted Planes at the Earth's Surface for Cloudless Atmospheres*, *J Clim Appl Meteorol* **25**: 87-97, 1986

112. Bird, R., Hulstrom, R., *Simplified Clear Sky Model for Direct and Diffuse Insolation on Horizontal Surfaces*, SERI/TR-642-761, 1981
113. Gueymard, C., *REST2: High-Performance Solar Radiation Model for Cloudless-Sky Irradiance, Illuminance, and Photosynthetically Active Radiation – Validation with a Benchmark Dataset*, *Solar Energy* **82**: 272-285, 2008
114. Gueymard, C., *Critical Analysis and Performance Assessment of Clear Sky Solar Irradiance Models Using Theoretical and Measured Data*, *Solar Energy* **51**: 121-138, 1993
115. Kenya Meteorological Department, *Integrated PV and Irradiance Simulator*, Ministry of Science and Technology, Kenya, 2013
116. Jackson, J. D., *Elettrodinamica Classica*, Zanichelli, 2001
117. Dusabe, D. , Munda, J., Jimoh, A., *Modelling of Cloudless Solar Radiation for PV Module Performance Analysis*, *Journal of Electrical Engineering* **60**: 192-197, 2009
118. Masters, G., *Renewable and Efficient Electric Power Systems*, John Wiley & Sons, New Jersey, 2004
119. Skartveit, A., Olseth, A., *The Probability Density and Autocorrelation of Short-Term Global and Beam Irradiance*, *Solar Energy* **49**: 477-487, 1992
120. Richardson, I., Thomson, M., Infield, D., et al., *Domestic Electricity Use: A High-Resolution Energy Demand Model*, *Energy and Buildings* **40**: 1878-1887, 2010
121. Central Bureau of Statistics, Office of the Vice President, and Ministry of Planning and National Development, *Economic Survey*, Nairobi, 2011
122. Capasso, A., Grattieri, W., Lamedica, R., et al., *A Bottom-up Approach* Fernandez, M., Ruddell, A. J., Vast, N., et al., *Development of a VRLA Battery with Improved Separators, and a Charge Controller, For Low Cost Photovoltaic and Wind Powered Installations*, *J. Power Sources* **95**: 135–140, 2001
123. Wright, A., Firth, S., *The Nature of Domestic Electricity-Loads and Effects of Time Averaging on Statistics and on-site Generation Calculations*, *Applied Energy* **84**: 389-403, 2007
124. Ministry of Energy and Petroleum, Republic of Kenya, *The Energy Act*, 2013
125. Foster, V., Steinbuks, J., *Paying the Price for Unreliable Power Supplies In-House Generation of Electricity by Firms in Africa*, WPS, 2009
126. Acker, R., Kammen, D.M., *The Quiet (Energy) Revolution: Analysing the Dissemination of Photovoltaic Power Systems in Kenya*, *Energy Policy* **24**: 81-111, 1996
127. Hankins, M., *Market Potentials for German Solar Energy Companies in East Africa*, GTZ, Hannover, 2009

128. Greacen, C., Engel, R., Quetchenbach, T., *A Guidebook on Grid Interconnection and Islanded Operation of Mini-Grid Power Systems Up to 200 kW*, Lawrence Berkeley National Laboratory, Schatz Energy Research Centre, 2013
129. Zerriffi, H., *Rural Electrification: Strategies for Distributed Generation*, Vancouver, British Columbia, Canada, 2011
130. Yadoo, A., Cruickshank, H., *The Role for Low Carbon Electrification Technologies in Poverty Reduction and Climate Change Strategies: A Focus on Renewable Energy Minigrids with Case Studies in Nepal, Peru and Kenya*, *Energy Policy* **42**: 591-602, 2012
131. Parshall, L., Pillai, D., Mohan, S., et al., *National Electricity Planning in Settings with Low Pre-existing Grid Coverage: Development of a Spatial Model and Case Study of Kenya*, *Energy Policy* **37**: 2395-2410, 2009
132. Sanoh, A., Parshall, L. Sarr, O., et al., *Local and National Electricity Planning in Senegal: Scenarios and Policies*, *Energy for Sustainable Development* **16**: 13-25, 2012
133. Levin, T., Thomas, V., *Least-Cost Network Evaluation of Centralized and Decentralized Contributions to Global Electrification*, *Energy Policy* **41**: 286-302, 2012
134. Foster, V., Steinbuks, J., *Paying the Price for Unreliable Power Supplies In-House Generation of Electricity by Firms in Africa*, WPS, 2009
135. Bhattacharyya, S., Timilsina, G., *Modelling Energy Demand of Developing Countries: Are the Specific Features Adequately Captured?*, *Energy Policy* **38**: 1979-1990, 2010
136. Urban, F., Benders, R., Moll, H., *Modelling Energy Systems for Developing Countries*, *Energy Policy* **35**: 3473-3482, 2007
137. Zhao, J., Mazhari, E., Celik, N, Son, Y., *Hybrid Agent-Based Simulation for Policy Evaluation of Solar Power Generation Systems*, *Simulat Pract Theory* **19**: 2189-2205, 2011
138. Beise, M., *The International Adoption of Photovoltaic Energy Conversion: Is Japan a Lead Market?* Discussion Paper Series 153, Research Institute for Economics & Business Administration, Kobe University, 2004
139. Guidolin, M., Mortarino, C., *Cross-country Diffusion of Photovoltaic Systems: Modelling Choices and Forecasts for National Adoption Patterns*, *Technological Forecasting and Social Change* **77**: 279-296, 2010
140. Wustenhagen, R., Bilharz, M., *Green Energy Market Development in Germany: Effective Public Policy and Emerging Customer Demand*, *Energy Policy* **34**: 1681 – 1696, 2006
141. Zhang, Y., Song, J., Hamori, S., *Impact of Subsidy Policies on Diffusion of Photovoltaic Power Generation*, *Energy Policy* **39**: 1958 – 1964, 2011
142. Rogers, E., *Diffusion of Innovations*, Free Press, New York, NY, 2003.

143. Sauter, R., Watson, J., *Strategies for the Deployment of Micro-Generation Implications for Social Acceptance*, *Energy Policy* **35**: 2770-2779, 2007
144. Semadeni, M., Hansmann, R., Flueeler, T., *Public Attitudes in Relation to Risk and Novelty of Future Energy Options*, *Energy & Environment* **15**:7 55-777, 2004
145. Kaldellis, J., *Social Attitude Towards Wind Energy Applications in Greece*, *Energy Policy* **33**: 595-602, 2005
146. Fischer, C., *Users as Pioneers: Transformation in the Electricity System, Micro CHP and the Role of the Users*, in: Jacob, K., Binder, M., Wieczorek, A., (Eds), *Governance for Industrial Transformation*, Proceedings of the 2003 Berlin Conference on Human Dimensions of Global Environmental Change, Environmental Policy Research Centre, Berlin, 319-337, 2004
147. Fischer, C., *From Consumers to Operators: the Role of Micro CHP Users*, in: Pehnt, M., Cames, M., Fischer, C., et al., (Eds), *Microgeneration: Towards a Decentralized Energy Supply*, Springer, Heidelberg, 2006, 2006
148. London Renewables, *Attitudes to Renewable Energy in London: Public and Stakeholder Opinion and the Scope for Progress*, A Report Commission by London Renewables and Carried Out by Brook Lyndhurst Ltd in Association with MORI and Upstream, Greater London Authority, 2003
149. Ellison, G., *Renewable Energy Survey*, Draft Summary Report of Findings, www.london.gov.uk/assembly/reports/environment/power_survey_orc.pdf, August 10th, 2005
150. Young, H., *Innovation Diffusion in Heterogeneous Populations: Contagion, Social Influence, and Social Learning*, *The American Economic Review* **99**: 1899-1924, 2009
151. Bollinger, B., Gillingham, K., *Peer Effects in the Diffusion of Solar Photovoltaic Panels*, *Marketing Science* **31**: 800-812, 2012
152. Narayanan, S., Nair, H., *Estimating Causal Installed-Base Effects: A Bias-Correction Approach*, November 2, 2012
153. Rai, V., Robinson, S., *Effective Information Channels for Reducing Costs of Environmentally Friendly Technologies: Evidence from Residential PV Markets*, *Environmental Research Letters* **8**: 014044, 2013
154. Jaffe, A., Newell, R., Stavins, R., *A Tale of Two Market Failures: Technology and Environmental Policy*, *Ecological Economics* **54**: 164-174, 2005
155. Brown, J., Reingen, P., *Social Ties and Word-of-Mouth Referral Behaviour*, *Journal of Consumer Research* **14**: 350-362, 1987

156. Krishnamurthy, S., *A Comprehensive Analysis of Permission Marketing*, Journal of Computer Mediated Communication **6**, 2001
157. Rode, J., Weber, A., *Knowledge Does Not Fall Far from the Tree - A Case Study on the Diffusion of Solar Cells in Germany*, ERSA Conference Papers ersa11p497, European Regional Science Association, 2011
158. Bass, F., *A New Product Growth Model for Consumer Durables*, Management Science **15**: 215–227, 1969
159. Kim, Sang-Hoon, Srinivasan, V., *A Conjoint-Hazard Model of the Timing of Buyers' Upgrading to Improved Versions of High-Technology Products*, Journal of Product Innovation Management **26**: 278-290, 2009
160. Islam, T., Meade, N., *The Impact of Competition, and Economic Globalization on the Multinational Diffusion of 3G Mobile Phones*, Technological Forecasting and Social Change **79**: 843-850, 2012
161. Ministry of Energy and Petroleum, Republic of Kenya, *Solar Energy*, 2012
162. Huang, W., Lu, M., Zhang, L., *Survey on Microgrid Control Strategies*, Energy Procedia **12**: 206-212, 2011
163. Hatziargyriou, N., *Microgrids: Architecture and Control*, F. Edition, John Wiley & Sons, New York, 2014
164. Huang, J., Jiang, C., Xu, R., *A Review on Distributed Energy Resources and Microgrids*, Renewable and Sustainable Energy Review **12**: 2472-2483, 2008
165. Basak, P., Saha, A., Chowdhury, S., *Microgrid: Control Techniques and Modelling*, Proceedings of the 44th International Universities Power Engineering Conference (UPEC), Glasgow , 2009
166. Pedrasa, M., Spooner, T., *A Survey of Techniques Used to Control Microgrid Generation and Storage during Island Operation*, 16th Australasian Universities Power Engineering Conference (AUPEC2006), Melbourne, Australia, 2006,
167. De Brabandere, K., Bolsens, B., *A Voltage and Frequency Droop Control Method for Parallel Inverters*, IEEE Trans. on Power Electronics **22**: 1107-1115, 2007
168. Renewable Academy (renac), ReGrid: Frequency and Voltage Regulation in Electrical Grids, 2003 (<http://docplayer.net/6038884-Regrid-frequency-and-voltage-regulation-in-electrical-grids.html>)
169. Bevrani, H., Shokoochi, S., *An Intelligent Droop Control for Simultaneous Voltage and Frequency Regulation in Islanded Microgrids*, IEE Transactions on Smart Grid **4**: 1505-1514, 2013

170. Pecas-Lopes, J., Moreira, C., Mandureira, A., *Defining Control Strategies for Microgrids Islanded Operation*, IEEE Transactions on Power Systems **21**: 916-924, 2006
171. Pecas-Lopes, J., Moreira, C., Mandureira, A., et al., *Control Strategies for Microgrids Emergency Operation*, International Conference on Future Power Systems, Amsterdam, 2005
172. Ashbani, S., Abdel-Rady, M., *General Interface for Power Management of Micro-Grids Using Nonlinear Cooperative Droop Control*, IEEE Transactions on Power Systems **20**: 2929-2941, 2013
173. Bergen, A., Vittal, V., *Power Systems Analysis*, Prentice Hall, NJ, USA, 1999
174. Engler, A., Soultanis, N., *Droop Control in LV-grids*, International Conference on Future Power Systems, Amsterdam, 2005
175. Yao, W., Chen, M., *Design and Analysis of the Droop Control Method for Parallel Inverters Considering the Impact of the Complex Impedance on the Power Sharing*, IEEE Trans. on Industrial Electronics **58**: 576-588, 2011
176. Alatrash, H., Mensah, A., Mark, E., et al., *Generator Emulation Controls for Photovoltaic Inverters*, 8th International Conference on Power Electronics - ECCE Asia, Jeju, 2011
177. Abusara, M., Shark, S., Guerrero, J., *Improved Droop Control Strategy for Grid-Connected Inverters*, Sustainable Energy, Grids and Networks **1**: 10-19, 2015
178. Bidram, A., Davoudi, A., *Hierarchical Structure of Microgrids Control System*, IEEE Transactions on Smart Grid **3**: 1963-1976, 2012
179. De Brabandere, K., Vanthournout, K., Driesen, J., et al., *Control of Microgrids*, Power Engineering Society General Meeting, IEEE, Tampa, 2007.
180. Chowdhury, S., Chowdhury, P., Crossley, P., *Microgrids and Active Distribution Networks*, The Institution of Engineering and Technology, London, 2009
181. Banerji, A., Sen, D., Paul, D., et al., *Microgrid: A Review*, Global Humanitarian Technology Conference: South Asia Satellite (GHTC-SAS), Trivandrum , 2013
182. Baert, D., Vervaet, A., *Lead-acid Battery Model for the Derivation of Peukert's Law*, Electrochimica Acta **44** (20), 1999
183. Vallve, X., Serrasolses, J., *Design and Operation of a 50 kWp PV Rural Electrification Project for Remote Sites in Spain*, Solar Energy **59**: 111–119, 1997
184. Chaurey, A., Kandpal, T., *A Techno-Economic Comparison of Rural Electrification Based on Solar Home Systems and PV Microgrids*, Energy Policy **38**: 3118-3129, 2010

185. Khadkikar, V., Kirtley, J., *Interline Photovoltaic (I-PV) Power System—A Novel Concept of Power Flow Control and Management*, Proc. Power and Energy Society General Meeting, Detroit, MI, USA, 2011

Appendix A:

UNIVERSITY OF LEEDS RESEARCH ETHICS COMMITTEE APPLICATION FORM ¹																
UNIVERSITY OF LEEDS																
<p>Please read each question carefully, taking note of instructions and completing all parts. If a question is not applicable please indicate so. The superscripted numbers (eg³) refer to sections of the guidance notes, available at http://ris.leeds.ac.uk/oleir/leasapplication. Where a question asks for information which you have previously provided in answer to another question, please just refer to your earlier answer rather than repeating information.</p>																
<p>Research ethics training courses: http://www.sddu.leeds.ac.uk/sdcu-research-ethics-courses.htm</p>																
<p>To help us process your application enter the following reference numbers, if known and if applicable:</p>																
Ethics reference number:																
Student number and/ or grant reference:	200797083															
PART A: Summary																
<p>A.1 Which Faculty Research Ethics Committee would you like to consider this application?²</p> <p> <input type="radio"/> Arts and PVAC (PVAR) <input type="radio"/> Biological Sciences (BIOSCI) <input type="radio"/> ESSU/ Environment/ LUBS (AREA) <input checked="" type="radio"/> MaPS and Engineering (MEEC) <input type="radio"/> Medicine and Health (Please specify a subcommittee): <ul style="list-style-type: none"> <input type="radio"/> School of Dentistry (DREC) <input type="radio"/> School of Healthcare (SHREC) <input type="radio"/> School of Medicine (SoMREC) <input type="radio"/> Institute of Psychological Sciences (IPSREC) </p>																
<p>A.2 Title of the research³</p> <p>Modelling Solar Microgeneration and Grid Electrification Pathways for Rural Kenya Taking into Account Local Socio-Economic and Political Factors.</p>																
<p>A.3 Principal Investigator's contact details³</p> <table border="1" style="width: 100%; border-collapse: collapse;"> <tr> <td style="width: 40%;">Name (Title, first name, surname)</td> <td>Mr Nicholas Opiyo</td> </tr> <tr> <td>Position</td> <td>PhD Student</td> </tr> <tr> <td>Department/ School/ Institute</td> <td>Energy Research Institute</td> </tr> <tr> <td>Faculty</td> <td>Engineering</td> </tr> <tr> <td>Work address (including postcode)</td> <td>ERI, Faculty of Engineering, University of Leeds, Leeds, LS2 9JT</td> </tr> <tr> <td>Telephone number</td> <td>07561 360 033</td> </tr> <tr> <td>University of Leeds email address</td> <td>elno@leeds.ac.uk</td> </tr> </table>			Name (Title, first name, surname)	Mr Nicholas Opiyo	Position	PhD Student	Department/ School/ Institute	Energy Research Institute	Faculty	Engineering	Work address (including postcode)	ERI, Faculty of Engineering, University of Leeds, Leeds, LS2 9JT	Telephone number	07561 360 033	University of Leeds email address	elno@leeds.ac.uk
Name (Title, first name, surname)	Mr Nicholas Opiyo															
Position	PhD Student															
Department/ School/ Institute	Energy Research Institute															
Faculty	Engineering															
Work address (including postcode)	ERI, Faculty of Engineering, University of Leeds, Leeds, LS2 9JT															
Telephone number	07561 360 033															
University of Leeds email address	elno@leeds.ac.uk															

Performance, Governance and Operations
Research & Innovation Service
Charles Tickrath Building
101 Clarendon Road
Leeds LS2 9JT. Tel: 0113 343 4873
Email: ResearchEthics@leeds.ac.uk



Nicholas Opiyo
Energy Research Institute
University of Leeds
Leeds, LS2 9JT

**MaPS and Engineering Joint Faculty Research Ethics Committee (MEEC FREC)
University of Leeds**

11 September 2014

Dear Nicholas

Title of study **Modelling Solar Microgeneration and Grid Electrification
Pathways for Rural Kenya Taking Into Account Local
Socio-Economic and Political Factors.**

Ethics reference **MEEC 14-003**

I am pleased to inform you that the application listed above has been reviewed by the MaPS and Engineering joint Faculty Research Ethics Committee (MEEC FREC) and following receipt of your response to the Committee's initial comments, I can confirm a favourable ethical opinion as of the date of this letter. The following documentation was considered:

DOCUMENT	Version	Date
MEEC 14-003 Faculty Research Ethics Committee.docx	1	11/09/14
ME-C 14-003 Ethical_Review_Form_V3_opt_10.pdf	1	04/09/14
MEEC 14-003 KENYA DAY SOLAR HOME SYSTEMS SURVEY INFORMATION SHEET.pdf	1	05/09/14
MEEC 14-003 Consent Form.pdf	1	04/09/14
ME-C 14-003 Kenya Day Solar Home Systems Survey.pdf	1	04/09/14
MEEC 14-003 Risk Assessment.pdf	1	04/09/14

Please notify the committee if you intend to make any amendments to the original research as submitted at date of this approval, including changes to recruitment methodology. All changes must receive ethical approval prior to implementation. The amendment form is available at <http://ris.leeds.ac.uk/EthicsAmendment>.

Please note: You are expected to keep a record of all your approved documentation, as well as documents such as sample consent forms, and other documents relating to the study. This should be kept in your study file, which should be readily available for audit purposes. You will be given a two week notice period if your project is to be audited. There is a checklist listing examples of documents to be kept which is available at <http://ris.leeds.ac.uk/EthicsAudits>.

We welcome feedback on your experience of the ethical review process and suggestions for improvement. Please email any comments to ResearchEthics@leeds.ac.uk.



Fieldwork Assessment Form (Low Risk Activities)

Fieldwork Project Details	
Faculty School/Service	Engineering
Location of Fieldwork	Kenya Bay, Kenya
Brief description of Fieldwork activity and purpose <i>(include address, area, grid reference and map where applicable)</i>	Survey on solar homes systems in Kenya Bay, Kenya. Targeted area is about 65 square kms.
Fieldwork itinerary <i>e.g. flight details, hotel address, down time and personal time.</i>	I will fly to Kenya on 30 th of November 2014. I will be staying at my rural home in Kenya Bay during the survey. I will spend an average of 10 hours per day for 20 days during the survey.
University Travel Insurance Policy Number	None
Organiser Details	Contact details <i>Name, email, telephone</i>
Fieldwork Activity Organiser / Course Leader	Nicholas Opiyo, eluo@leeds.ac.uk, 07561 369 0433
Departmental Co-ordinator	Dr Rolf Crook, r.crook@leeds.ac.uk, 0113 3437737
Nature of visit <i>Size of Group, time working, staff, undergraduate, undergraduate.</i>	Postgraduate (none working)
Participant Details <i>Attach information as separate list if required.</i>	Contact details <i>Name, Address, email, telephone, gender and next of kin contact details</i>
	Nicholas Opiyo, eluo@leeds.ac.uk, 07561 369 0433



UNIVERSITY OF LEEDS

KENDU BAY ELECTRIFICATION SURVEY CONSENT FORM:

I have read the introduction letter handed to me by the surveyor, Nicholas Opiyo, and I have asked all the questions that I can think of at this moment. I have been informed of my right to withdraw from this survey at any moment without having to give a reason why. I have also been assured that my personal data will be handled professionally and with utmost respect and anonymity.

I CONSENT to participate in the survey:

NAME:

SIGNATURE:

DATE:



UNIVERSITY OF LEEDS

KENDU BAY ELECTRIFICATION SURVEY INTRODUCTION:

Dear Resident,

I am NICHOLAS OPIYO from the University of Leeds in the UK

I am carrying out a survey on electrification options in Kendu Bay area, and in particular on PV systems installed in the area. I specifically seek to gather the following information:

1. Your source of electricity if any, and appliances served
2. Reasons behind your electrification status
3. Your choices of other household energy needs
4. Your education and income levels
5. Your household size
6. Your opinions on the national utility grid

The information you give me will be immediately anonymized and your name or address will not appear on the final report. Only I will be able to identify your response, and the data will be destroyed once the research is complete.

Thank you for your time

Kind Regards

A handwritten signature in black ink, appearing to read 'Nicholas Opiyo'.

Nicholas Opiyo



KENDU BAY PV SYSTEMS SURVEY REPORT

The main sources of electricity for Kendu Bay residents are grid and solar home systems. Grid electricity passes along the main roads, Kendu-Oyugis and Kendu-Homa Bay, and is mainly available to people to live along the roads. Solar home systems (SHS) are retailed by Africa Retail Traders (ART) which has a big shop in Kendu Bay town. The SHS come in two standard packages: a 45 W system with a 12 V 100 AH lead acid battery and a non-grid-tie dc/ac inverter installed at \$250, and a 100 W system with a 24 V 100 AH lead acid battery pack and a non-grid-tie dc/ac inverter installed at \$400. Both of these systems are cheaper than grid electricity connection fee of \$750. ART sells the SHS to civil servants on an interest-free higher purchase (credit) arrangement payable over 6 months, with deductions taken directly from purchasers' salaries. Other buyers have to pay the full amounts before installations.

The main sources of cooking fuels are firewood, charcoal, kerosene, and liquid petroleum gas (LPG). Most of the locals, i.e. those with farms and thus own their residences, use firewood and charcoal for cooking. Firewood is freely collected from local bushes while charcoal is easy to burn or cheap to purchase. Kerosene is used by few who aren't locals and thus live in rented properties or cannot access bushes for firewood collections. LPG is used by well-off (by local standards) families, all of whom have electricity.

SURVEY SUMMARY

The survey area was divided into three sections namely Gendia, Kanam, and Pala, to ensure equal distribution of samples and to make it easier to manage the travel logistics. The surveyed samples were divided into two sections: commercial and institutional establishments which covered 3 schools and 15 shops, and individual households which covered 513 household, representing about 1.77% of the population of Kendu Bay. Below is a summary:

COMMERCIAL AND INSTITUTIONAL ESTABLISHMENTS:

- 3 schools surveyed:
 - These are public primary schools run and managed by the government
 - Pupils in classes 6-8 are required to attend morning (5.00am-7.30am) and evening (6.00pm – 9.00pm) tutorial classes, periods during which lighting is required
 - 1 school had grid electricity connection and thus enough power for any need

- 1 had solar systems installed on the roof of every classroom, each with the following specifications:
 - 100W solar panel
 - 24V 100AH lead acid battery pack
 - DV/AC non-grid-tie inverted
 - Each system was used to power 2 fluorescent tubes and 2 socket outlets for TV or radio lessons
 - All systems are locally manufactured or branded (EVEREADY)
 - The installation was funded by the government through a rural institutions electrification program
- 1 had neither grid nor solar systems but was on course for solar systems installations this year. Students in classes 6-8 used kerosene pressure lamps for tutorial classes
- 15 shops surveyed:
 - 3 shops had grid electricity and thus enough power for their needs
 - 4 shops had SHS installed with the following specifications:
 - 1 had the standard 45 W system
 - 2 had the 100 W system
 - 1 originally had the 45 W system but upgraded to the 100 W system
 - 8 shops had neither grid electricity nor SHS

INDIVIDUAL HOUSEHOLDS:

- Traditional houses are defined as houses with grass-thatched roofs and with walls and floors constructed with clay soil mixed with cow dung.
- Transitional houses are traditional houses with corrugated iron sheets for roofs
- Modern houses are described as houses constructed with either bricks (red bricks are locally baked) or stones (also locally mined). The roofs are usually made of corrugated iron sheets.
- Unless otherwise stated, no home has internal washrooms, shower-rooms and pit latrines are constructed as separate buildings near the main houses
- Some homes (those along the main road and government owned) have piped water; 99% of homes in Kendu Bay do not have piped water. Water is fetched from a local river (Awach) and for those near the lake, the lake. Some NGOs constructed few sparsely placed boreholes with hand pumps but these usually produce hard water which is not good for drinking or washing.
- 513 household surveyed and divided into 3 groups:

- Grid electricity connected:
 - 16 households surveyed (3.1%)
 - All live along the main roads (less than 50 m from grid lines)
 - 8 live in rented furnished apartments or houses
 - 8 own their homes
 - All houses are modern
 - Standard grid connection fees is \$750, way too high for many rural residents
 - 4 had SHS installed before grid electricity:
 - 2 had 45 W systems, upgraded them to 100W systems due to increasing load capacities, and then connected to the grid when it finally arrived. 1 sold the SHS after grid installation while 1 kept his system independent of the grid for emergency power during blackouts
 - 2 had only 45 W systems; 1 kept his system for stand-by power, independent of the grid, while the other sold his to a neighbour
 - Appliances common in grid connected homes are: fridge with freezer, colour TVs with home theatre systems, iron, microwave, blender, electric kettle, toaster, water dispensers, fans, phone chargers, electric bulbs, laptop computers, and in one case, a printer.
 - Income levels are above \$450 per month
 - Education levels are college degree and above
 - Cooking fuels are LPG and charcoal
 - Reasons for grid connection:
 - Grid is available
 - More power required than supplied by SHS
 - Appropriately sized SHS more expensive than grid connection
 - Rented property already grid connected

- SHS installed (No grid):
 - 24 households surveyed (4.7%)
 - All houses are modern
 - 20 lived in owned homes
 - 4 live in rented homes
 - Income levels are between \$250 - \$400

- Education levels are mainly college education and above
 - Cooking fuels are firewood and charcoal
 - 12 had 45 W systems
 - 9 had 100 W systems
 - 2 initially had 45 W systems but upgraded to 100 W systems
 - 1 initially had 100W system but upgraded it to a 400W system (4x100W systems)
 - Main appliance powered by the 45 W systems are light bulbs, phone chargers, and in some cases, simple radios
 - Main appliances powered by the 100 W system as the same as the 45 W system with the only addition being small colour TVs
 - The 400W system is also used to power a small fridge and a laptop
 - Main reasons for choosing SHS are:
 - Grid electricity is too expensive
 - Grid is unreliable
 - Lives far from grid
 - SHS is affordable and reliable
 - Basic need for electricity with low load profile
 - Credit facility available (only to civil servants)
- No Grid or SHS:
- 473 households interviewed and divided into three groups according to education levels and correlating income levels:
 - Group 1
 - 160 households interviewed (31.2%)
 - Primary school education or lower
 - Income below \$75 per month
 - Live in owned traditional houses on ancestral lands and are subsistence farmers and casual labourers
 - Cooking fuels are firewood collected from local bushes
 - Kerosene lanterns or firewood are used for lighting
 - No electricity because:
 - Too poor to afford grid electricity or SHS
 - Live far from grid

- Group 2
 - 224 households interviewed (43.7%)
 - Have some level of high school education
 - Income levels are \$75 - \$200
 - Live in owned traditional houses on ancestral lands and are subsistence farmers
 - Most are skilled casual labourers
 - Cooking fuels are firewood collected from local bushes
 - Kerosene lanterns are used for lighting
 - No electricity because:
 - Too poor to afford grid connection or SHS
 - Live far from grid
- Group 3
 - 89 households interviewed (17.3%)
 - Educated up to tertiary college level
 - Income levels are \$200 – 250
 - Live in owned transitional houses on ancestral lands and are subsistence farmers
 - They are mainly low level civil servants or small business owners
 - Cooking fuels are firewood and charcoal
 - Kerosene lanterns are used for lighting
 - No electricity because:
 - Grid is too expensive
 - Cannot afford SHS upfront (some are saving to buy SHS)
 - Live far from grid

SUMMARY

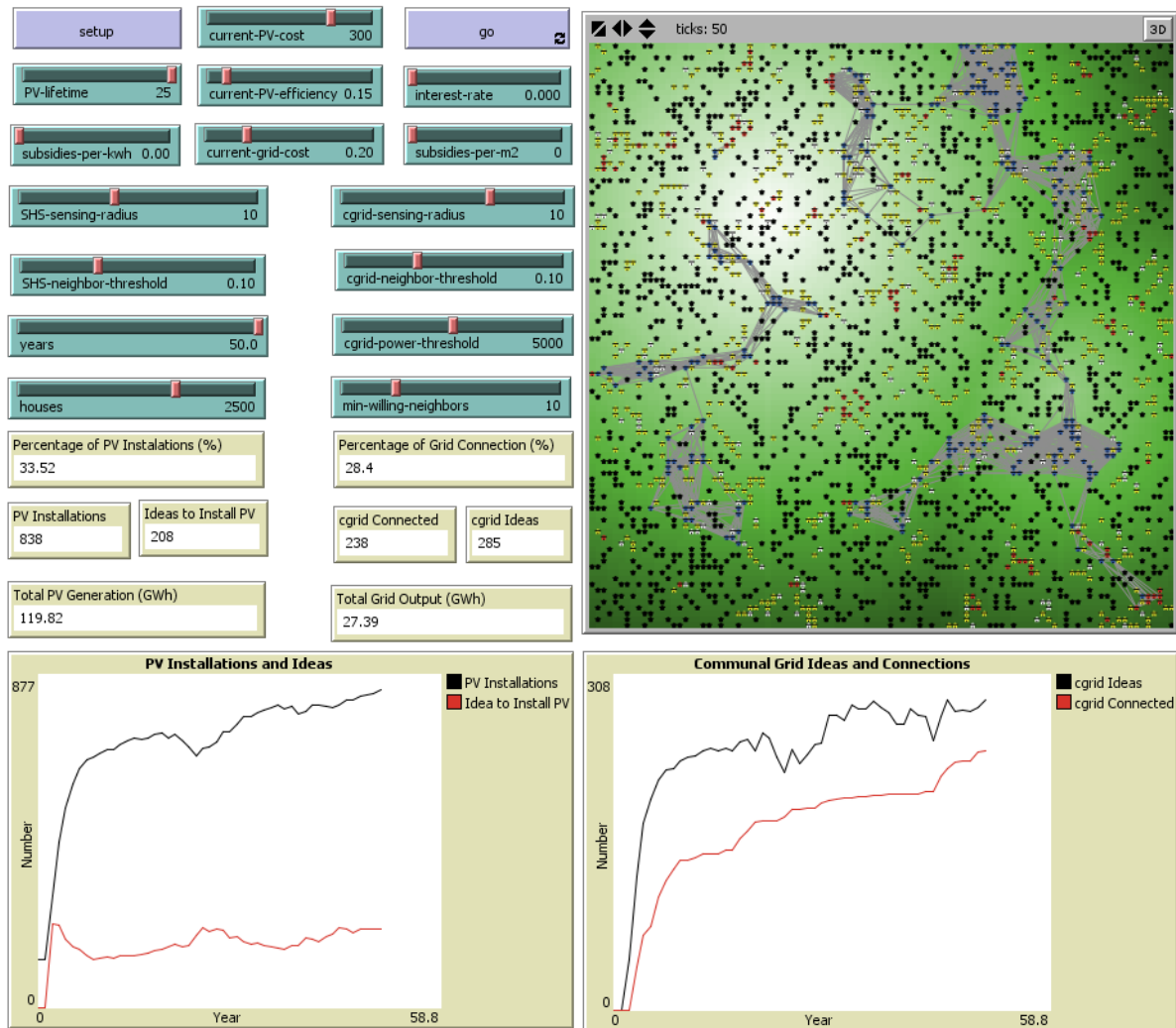
- Of the 513 households surveyed, only about 3.1% have access to grid electricity, this is in line with the national data which puts rural Homa Bay County electrification rate at below 3%
- About 4.7% of surveyed household have installed solar home systems for provision of electricity for basic needs, also in line with national statistics which puts such installations at about 4%

- Majority of residents (92.2% of those surveyed) do have access to electricity of any source and depend on kerosene lanterns and firewood for lighting
- For those with grid electricity:
 - The main advantage is access to unlimited power
 - The main complaints are frequent blackouts, uneven monthly bills, and high connection fee
 - Household appliances mirror modern households with nearly all appliances necessary for a comfortable available in the house
 - All live in modern homes
 - Education level are college degree and above
 - Income levels are above \$400/month
 - Cooking fuels are mainly LPG and charcoal, as with those in urban centres like Nairobi
- For those with SHS but no grid:
 - The main advantages are reliability, affordability, and environmental safety
 - The main disadvantage is capacity
 - All are willing to be part of communal grids
 - All live in modern homes
 - Education levels are college degree and above
 - Income level are between \$250 and \$400 per month
 - Cooking fuels are firewood, charcoal, kerosene, and in some cases, LPG
- For those with neither grid nor SHS
 - The main obstacle is poverty
 - Poverty and education levels are correlated, meaning, most individual in this group do not have modern education; most have no college education
 - Live mainly in traditional home with few living in transitional homes
 - Income levels are below \$250 per month, with many earning below \$75 per month.
 - Cooking fuels are firewood and charcoal
 - Kerosene lanterns and firewood are used for lighting



Photos of PV Systems in Kendu Bay

Appendix B:



A View of Netlogo Interface

; Kendu Bay PV-Diffusion Model (Combines SHS and Communal Grids Diffusion Models into one)

; Author: Nicholas N. Opiyo

; The model predicts future electrification topologies in Kendu Bay area of Kenya given current electrification structures

; Socio-economic Data from Kendu Bay SHS Survey are used in the model

```
globals [PV-cost-per-m2 PV-efficiency grid-electricity-costs total-
PV-generation total-cgrid-generation household-income]
patches-own [elevation insolation patch-quality roof-size PV cgrid-
connected ngrid-connected PV-age PV-output cgrid-output]
```

```

turtles-own [PV-building-decision cgrid-connection-decision ngrid-
connection-decision]

; Clear everything including plots
; Set artificial topography of landscape and assume one turtle
(house) per patch
; Calculate insolation;
; Set all relevant decisions to 'false'
; cgrid stand for communal grid while ngrid stand for the national
grid

to setup

  clear-all

  ask patches [
    set-artificial-landscape
    set patch-quality 0.3 + random-float 0.7
    set PV false
    set cgrid-connected false
    set ngrid-connected false
    calculate-insolation ]

; Create a given number of houses (7393 for Kendu Bay)
; Randomly set roof sizes available for PV installations to between
10m2 and 50m2
; Divide the houses according to electrification and income status
using Kendu Bay survey data

  create-turtles houses [
    set shape "house"
    move-to one-of patches with [ not any? turtles-here ]
    set roof-size 10 + random 50
    set cgrid-connected false
    set cgrid-output 0
    set PV-building-decision false
    set cgrid-connection-decision false
    set ngrid-connection-decision false
    set PV-cost-per-m2 current-PV-cost
    set PV-efficiency current-PV-efficiency
    set grid-electricity-costs current-grid-cost
    set total-cgrid-generation 0 ]

; Group 1 consists of houses that are connected to the national grid
; This group comprised 3.1% of the survey sample
; All of these households reported incomes of $400 and above per
month
; It is assumed that they all initially don't have PV but could
choose to install some in the future
; Houses that are connected to the national grid are coloured blue

  let group1 3.1 * 0.01 * houses
  let grid-connected n-of group1 turtles
  ask grid-connected [

```

```

    set color blue
    set household-income random income > 400
    set PV false
    set PV-output 0
    set total-PV-generation 0
    set ngrid-connected true]

; Group 2 consists of houses with PV but with no grid connection
; These group comprised 4.7% of the survey sample
; All households in this category reported incomes of between $250
and $400 per month
; None of the houses in this category are grid connected but could
choose to do so in the future
; Houses in this category are coloured yellow

    let group2 4.7 * 0.01 * houses
    let houses-with-PV n-of group2 turtles
    ask houses-with-PV [
        set color yellow
        set PV true
        set PV-age random PV-lifetime
        set total-PV-generation sum [PV-output] of turtles with [PV]
        set household-income random income >= 250 and income <= 400
        set ngrid-connected false]

; Group 3 comprised of houses with no source of electricity
whatsoever
; This group comprises 92.2% of Kendu Bay households.
; Income levels are below $250 per month
; In the future, with incrtcreasing incomes, houseolds in this group
could become electrified
; Houses in this category are coloured black
; This group is further divided into 3 group according to incomes as
follows:

; Group 3a cromprises of houses with incomes below $75/month.
; They comprise 31.2% of Kendu Bay households

    let group3a 31.2 * 0.01 * houses
    let unelectrified-houses1 n-of group3a turtles
    ask unelectrified-houses1 [
        set color black
        set household-income random income <= 74
        set PV false
        set PV-output 0
        set total-PV-generation 0
        set ngrid-connected false]

; Group 3b cromprises of houses with incomes between $75 and $200
per month.
; They comprise 43.7% of Kendu Bay households

    let group3b 43.7 * 0.01 * houses
    let unelectrified-houses2 n-of group3b turtles
    ask unelectrified-houses2 [
        set color black

```

```

    set household-income random income >= 75 and income <= 199
    set PV false
    set PV-output 0
    set total-PV-generation 0
    set ngrid-connected false]

; Group 3c comprises of houses with incomes between $200 and $250
per month.
; They comprise 17.3% of Kendu Bay households

    let group3c 17.3 * 0.01 * houses
    let unelectrified-houses3 n-of group3c turtles
    ask unelectrified-houses3 [
        set color black
        set household-income random income >= 200 and income <= 249
        set PV false
        set PV-output 0
        set total-PV-generation 0
        set ngrid-connected false]

    let unelectrified-houses n-of (group3a + group3b + group3c)
turtles

    reset-ticks

end

; Create artificial landscape to mirror Kendu Bay area with both
Pala and Wire hills
; Calculate insolation using available empirical data

to set-artificial-landscape
    let elev1 100 - distancexy 30 70
    let elev2 70 - distancexy 80 40
    ifelse elev1 > elev2
    [set elevation elev1]
    [set elevation elev2]
    set pcolor scale-color green elevation 0 100
end

to calculate-insolation
    let particle-reduction 0.95 ; Dust in air affect radiation
    if elevation > 50 [set particle-reduction 1]
    let orientation 180
    let lowest-neighbor min-one-of other patches in-radius 4
[elevation]
    set orientation atan ([pxcor] of lowest-neighbor - pxcor) ([pycor]
of lowest-neighbor - pycor)
    set insolation 600 + (1000 * particle-reduction * (1 - cos
orientation) / 2)
end

; Stop simulations after given number of years (ticks)

```

```

; Houses without PV must first develop the idea to do so if they
earn over $250/month
; Every year, household income is increased by a growth rate to
carter for discount rates in Kenya
; Every 10 years, prevailing PV cost is halved based on Swanson's
law
; Old PV systems are randomly killed off if their age falls within 5
years of PV lifetime limit

to go

    tick
    if ticks >= years [stop]
    if ticks = 10 [set current-PV-cost current-PV-cost * 0.5]
    ask turtles with [PV] [
        set PV-age PV-age + 1
        if PV-age > random-normal PV-lifetime 5 [
            set PV false
            set PV-age 0
            set PV-output 0
        ]
    ]

    ask turtles with [PV-building-decision] [set PV-building-decision
false]
    ask turtles with [PV = false] [determine-idea-to-install-PV]
    ask turtles with [PV-building-decision] [calculate-balance-and-
decide]

    ask turtles with [cgrid-connection-decision] [set cgrid-
connection-decision false]
    ask turtles with [PV = true] [determine-idea-to-connect-to-cgrid]
    ask turtles with [cgrid-connection-decision] [calculate-cgrid-
decision]

    ask turtles with [ngrid-connection-decision] [set ngrid-
connection-decision false]
    ask turtles with [ngrid-connection-decision] [determine-idea-to-
connect-to-ngrid]
    ask turtles with [ngrid-connection-decision] [check-income-and-
decide]

    set household-income income * growth-rate
    set PV-cost-per-m2 current-PV-cost
    set total-PV-generation total-PV-generation + sum [PV-output] of
turtles with [PV]
    set total-cgrid-generation total-cgrid-generation + sum [PV-
output] of turtles with [cgrid-connected]
end

; Households without PV but with incomes above $250/month can
develop ideas to install PV
; Households which meet neighbourhood threshold can also develop
ideas to install PV
; Houses that are thinking of installing PV are coloured white

```

```

to determine-idea-to-install-PV
  if (income >= 250) and (PV = false) [
    set PV-building-decision true
    set color white]
  if any? neighbors with [PV] in-radius SHS-sensing-radius [
    if (count neighbors with [PV and any? turtles-here] in-radius
SHS-sensing-radius /
    count neighbors with [any? turtles-here] in-radius SHS-
sensing-radius) > SHS-neighbor-threshold
    [set PV-building-decision true
    set color white]
  ]
end

```

```

; If a household is thinking of installing PV, it must meet the
income requirement - earn over $250/month
; A household can then compare the cost of PV power/kWh and grid
power/kWh before making a decision
; If PV is cheaper, decision to install is made
; Houses with PV are coloured yellow
; If there are no subsidies, subsidies/kWh and subsidies/m2 are set
to zero
; If the system is purchased cash, interest rate is set to zero.

```

```

to calculate-balance-and-decide
  if (income >= 250) and (PV-building-decision = true) [
    let AF (1 + interest-rate) ^ PV-lifetime
    let total-cost (PV-cost-per-m2 - subsidies-per-m2) * roof-size *
AF
    set PV-output insolation * patch-quality * PV-efficiency * roof-
size
    let generation-cost-per-kwh total-cost / (PV-output * PV-
lifetime)
    let avoided-cost-per-kwh grid-electricity-costs
    if generation-cost-per-kwh < avoided-cost-per-kwh + subsidies-
per-kwh [
      set PV true
      set color yellow
      set PV-age 0]
    ]
end

```

```

; Houses with PV that meet a certain minimum power threshold can
develop idea to join a communal grid
; Such an idea is only developed if there are enough neighbours
within a given sensing radius who meet...
; ... minimum power requirement
; Such houses are coloured red
; All communal grids are ac-coupled with each individual system
contributing its panels and batteries ...
; ...to the grid.

```

```

to determine-idea-to-connect-to-cgrid
  if any? neighbors with [PV-output >= cgrid-power-threshold] in-
radius cgrid-sensing-radius [

```

```

    if (count neighbors with [PV-output >= cgrid-power-threshold and
any? turtles-here] in-radius cgrid-sensing-radius /
    count neighbors with [any? turtles-here] in-radius cgrid-
sensing-radius) > cgrid-neighbor-threshold [
    set cgrid-connection-decision true
    set color red]
]
end

; If a given minimum number of households within a given sensing
radius meet the requirements to join/form a communal grid...
; ... they can do so.
; Total Power output of such a communal grid is the sum of each PV
output in the system

to calculate-cgrid-decision
  if count turtles with [cgrid-connection-decision and any? turtles-
here] in-radius cgrid-sensing-radius >= min-willing-neighbors [
    set cgrid-connected true
    set color yellow
    create-links-with other turtles with [cgrid-connected] in-radius
cgrid-sensing-radius]
    set cgrid-output sum [PV-output] of turtles with [cgrid-connected]
end

; Houses that are not connected to the national grid can decide to
so if their monthly incomes rise above $400

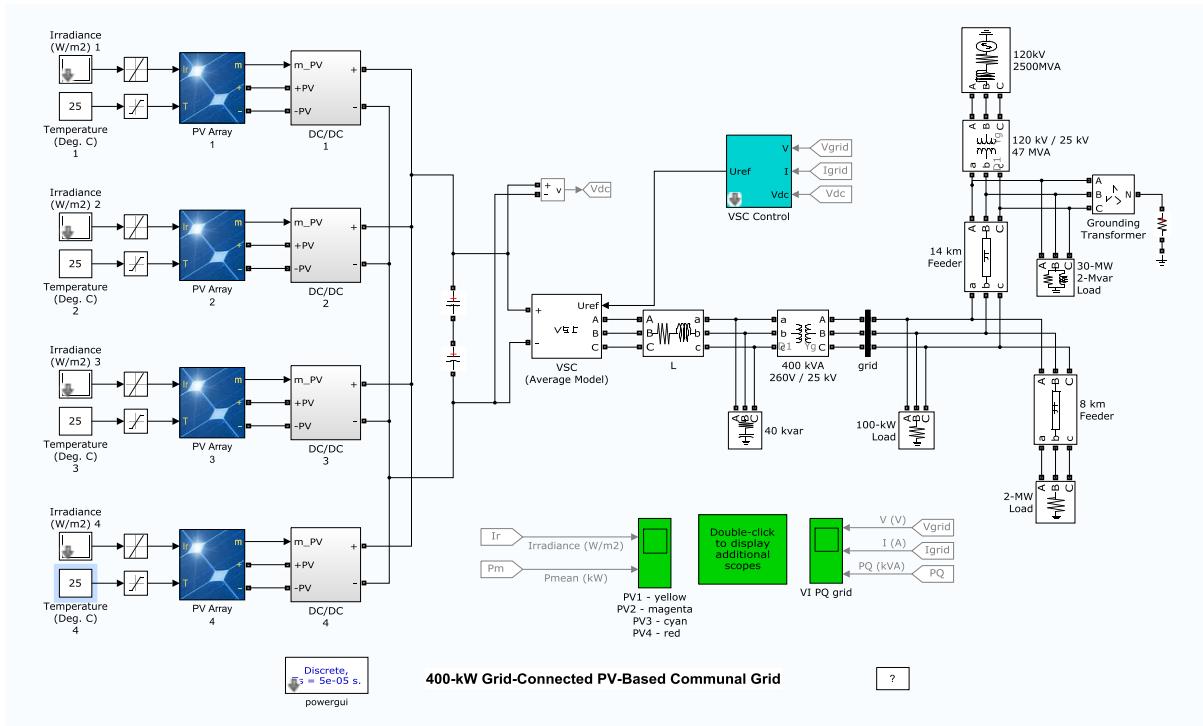
to determine-idea-to-connect-to-ngrid
  if income >= 400 [
    set ngrid-connection-decision true]
end

; Once the income requirement has been met, cost comparison is done
to ensure that it is cheaper to connect to the grid...
; ... than to install PV
; Houses that are connected to the national grid are coloured blue

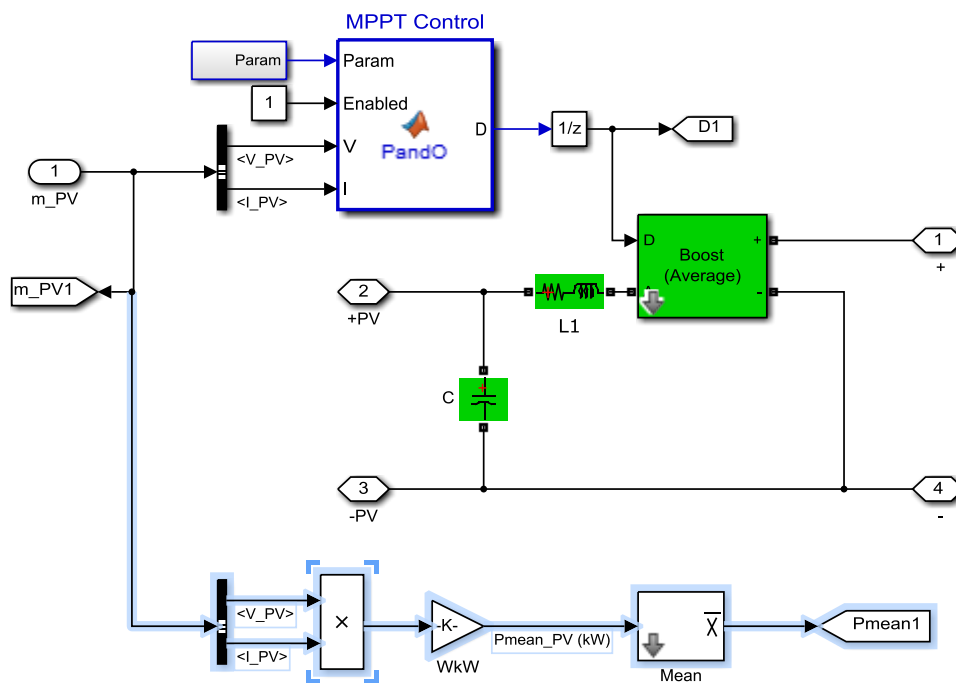
to check-income-and-decide
  if (income >= 400) and (ngrid-connection-decision = true)[
    let AF (1 + interest-rate) ^ PV-lifetime
    let total-cost (PV-cost-per-m2 - subsidies-per-m2) * roof-size *
AF
    set PV-output insolation * patch-quality * PV-efficiency * roof-
size
    let generation-cost-per-kwh total-cost / (PV-output * PV-
lifetime)
    let avoided-cost-per-kwh grid-electricity-costs
    if grid-electricity-costs < generation-cost-per-kwh [
    set ngrid-connected true
    set color blue]
  ]
end

```

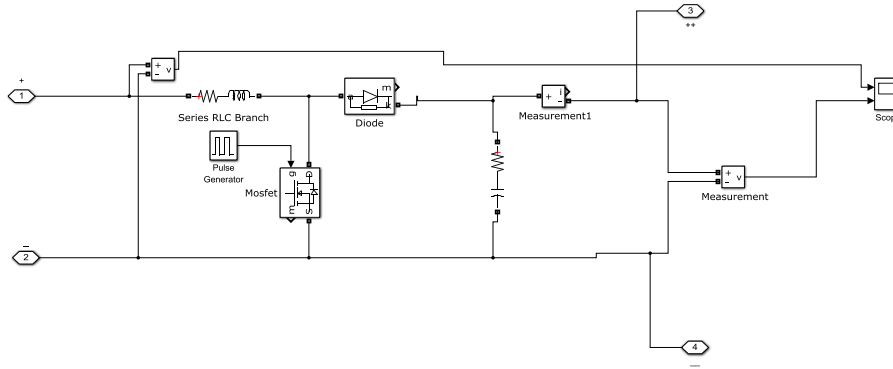
Appendix C:



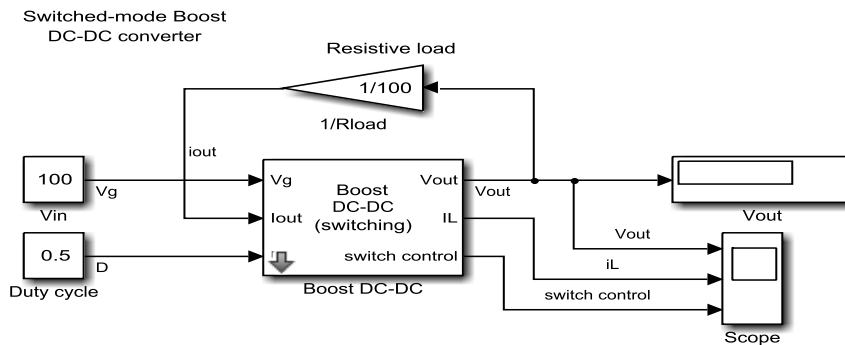
Under DC-AC Inverter Subsystem



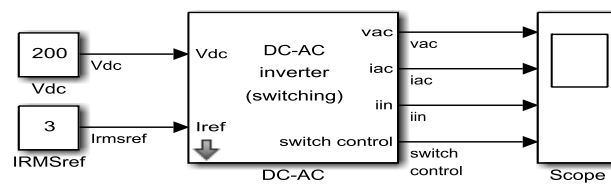
Under DC-DC Converter Subsystem



Under DC-A C Inverter Subsystem



Switched-Mode DC-AC Inverter



Matlab Codes for Perturb and Observe

```
function D = PandO(Param, Enabled, V, I)

% MPPT controller based on the Perturb & Observe algorithm.

% D output = Duty cycle of the boost converter (value between 0 and 1)
%
% Enabled input = 1 to enable the MPPT controller
% V input = PV array terminal voltage (V)
% I input = PV array current (A)
%
% Param input:
Dinit = Param(1); %Initial value for D output
Dmax = Param(2); %Maximum value for D
Dmin = Param(3); %Minimum value for D
deltaD = Param(4); %Increment value used to increase/decrease the duty
cycle D
% ( increasing D = decreasing Vref )
%
persistent Vold Pold Dold;
```

```

dataType = 'double';

if isempty(Vold)
    Vold=0;
    Pold=0;
    Dold=Dinit;
end
P= V*I;
dV= V - Vold;
dP= P - Pold;

if dP ~= 0 & Enabled ~=0
    if dP < 0
        if dV < 0
            D = Dold - deltaD;
        else
            D = Dold + deltaD;
        end
    else
        if dV < 0
            D = Dold + deltaD;
        else
            D = Dold - deltaD;
        end
    end
    D=Dold;
end

if D >= Dmax | D<= Dmin
    D=Dold;
end

Dold=D;
Vold=V;
Pold=P;

Initialize MPPtrackIref
%
global Iref;
global Increment;
global Pold;
Pold = 0; % initial value for the sensed power
Iref = 4; % initial value for the current reference
Increment = -1; % initial direction: decrease reference current

% Simple MPP "perturb and observe" tracking algorithm
% using Boost DC-DC input current Iref as the control variable
% Pold, Iref and Increment are initialized in InitializeMPPtrackIref.m
%
% Input: power P to be maximized
% Output: reference current

function y = MPPtrackIref(P)

global Pold;
global Iref;
global Increment;

```

```

IrefH = 5; % upper limit for the reference current
IrefL = 0; % lower limit for the reference current
DeltaI = 0.02; % reference current increment

if (P < Pold)
    Increment = -Increment; % change direction if P decreased
end

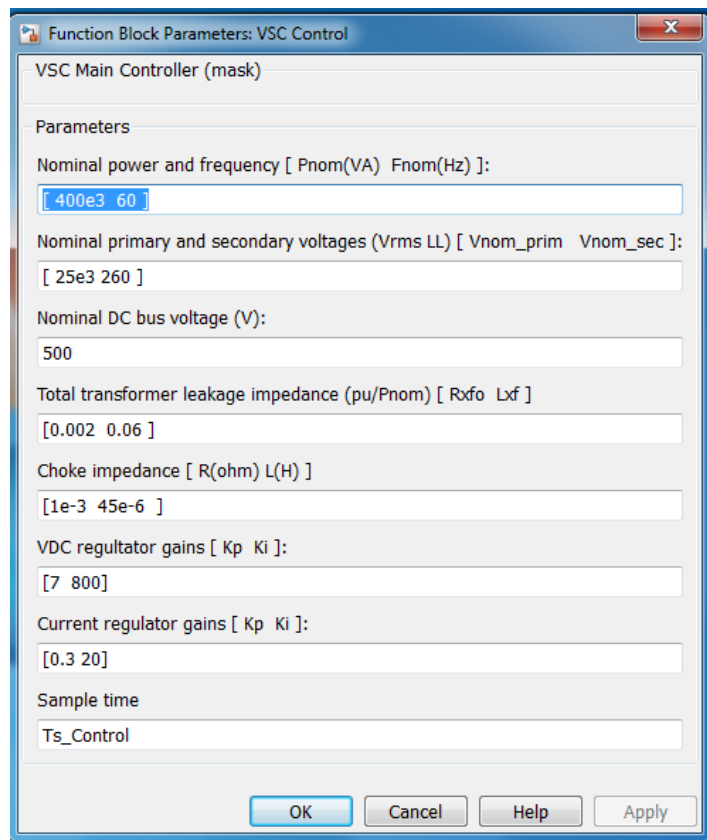
% increment current reference
Iref=Iref+Increment*DeltaI;

% check for upper limit
if (Iref > IrefH)
    Iref = IrefH;
end

% check for lower limit
if (Iref < IrefL)
    Iref = IrefL;
end

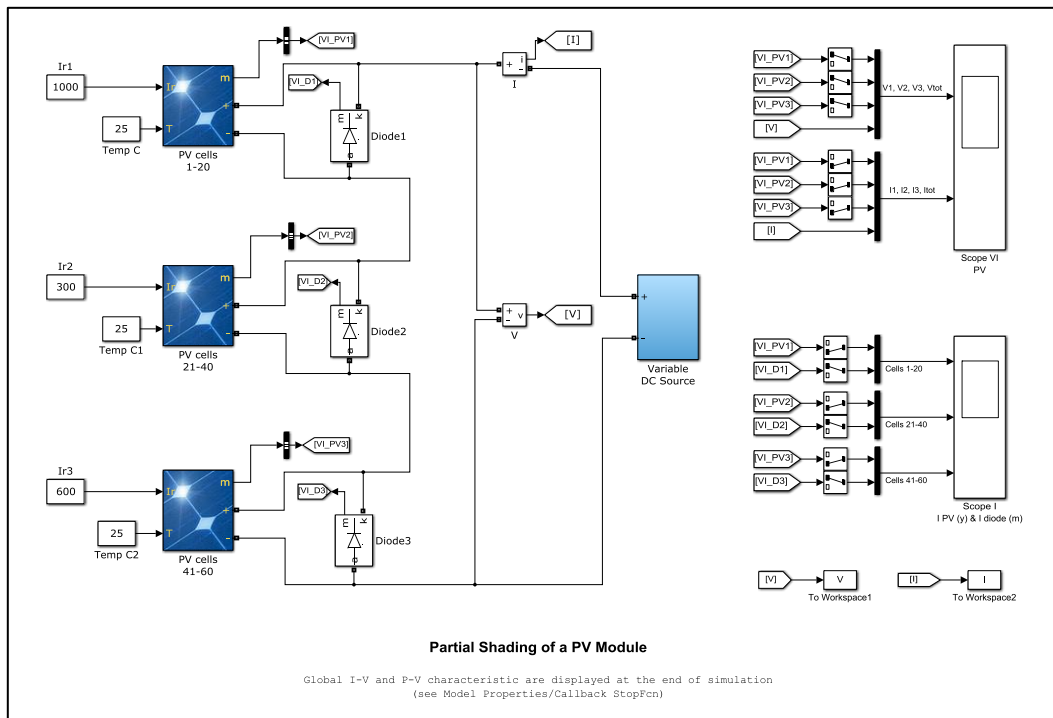
% save power value
Pold = P;
% output current reference
y = Iref;

```

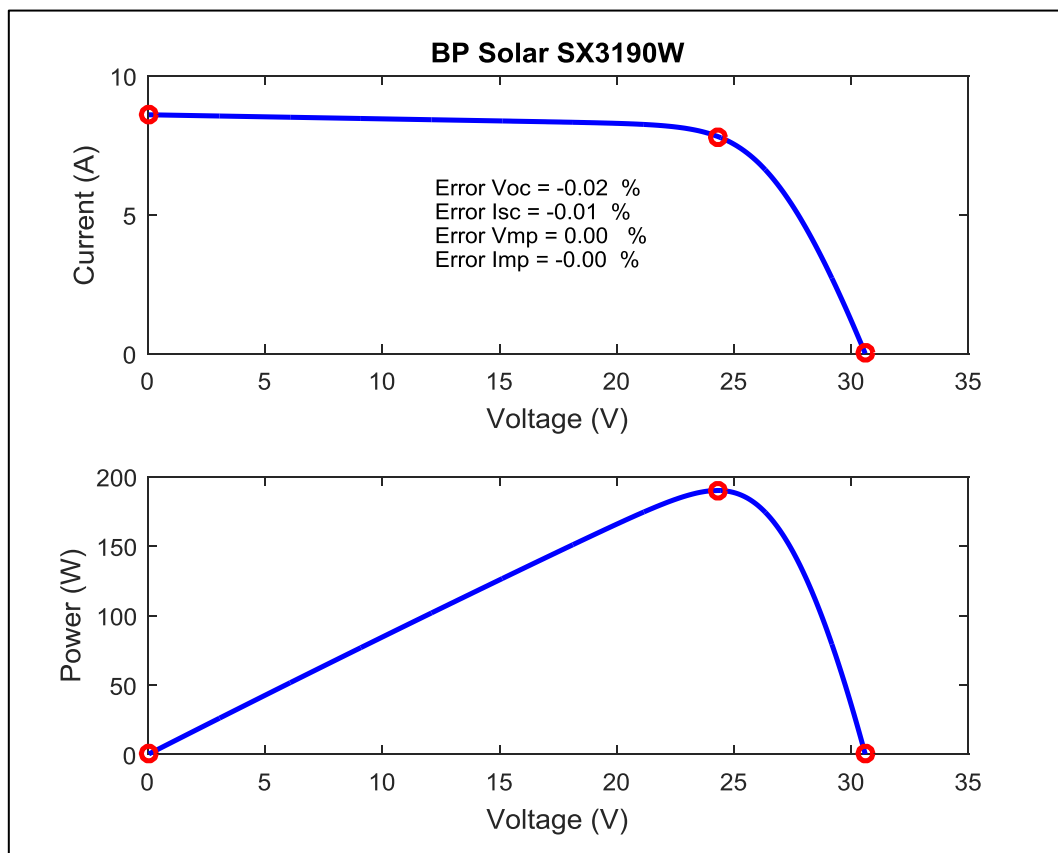


VSI Block Parameters

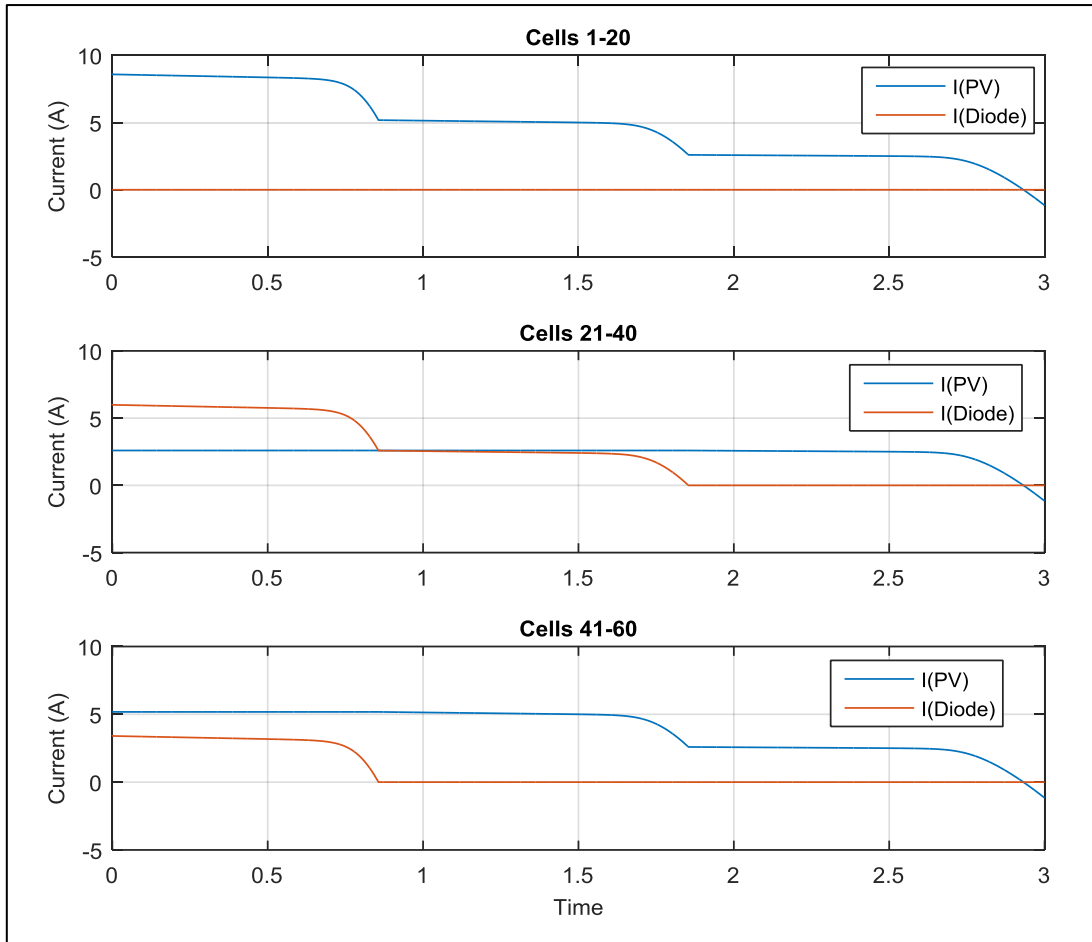
Matlab Model for PV Characteristics:



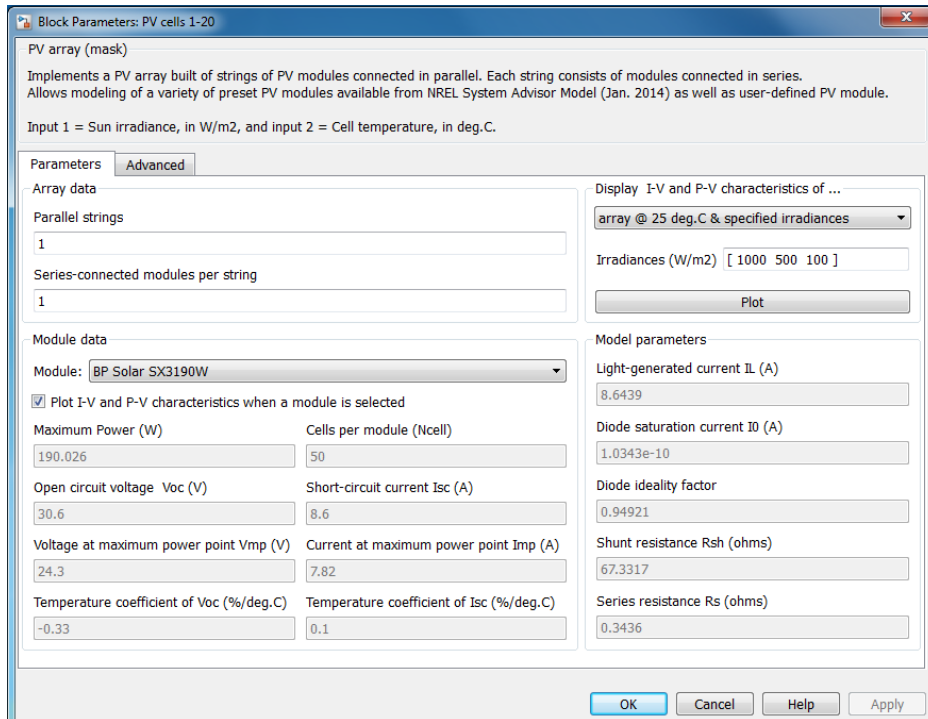
Complete Figure 3.8 Simulink Model

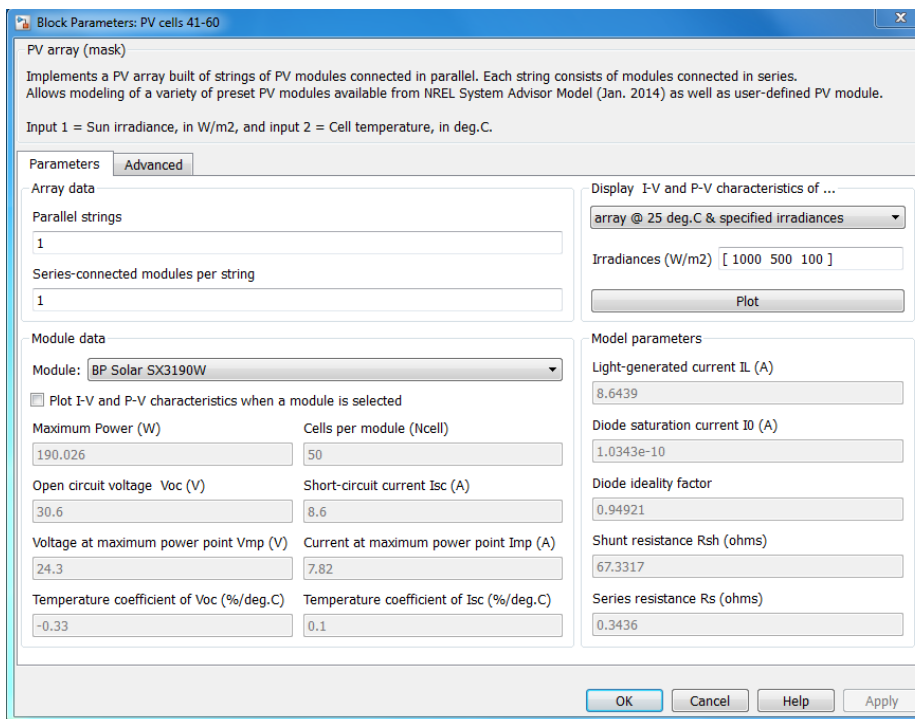
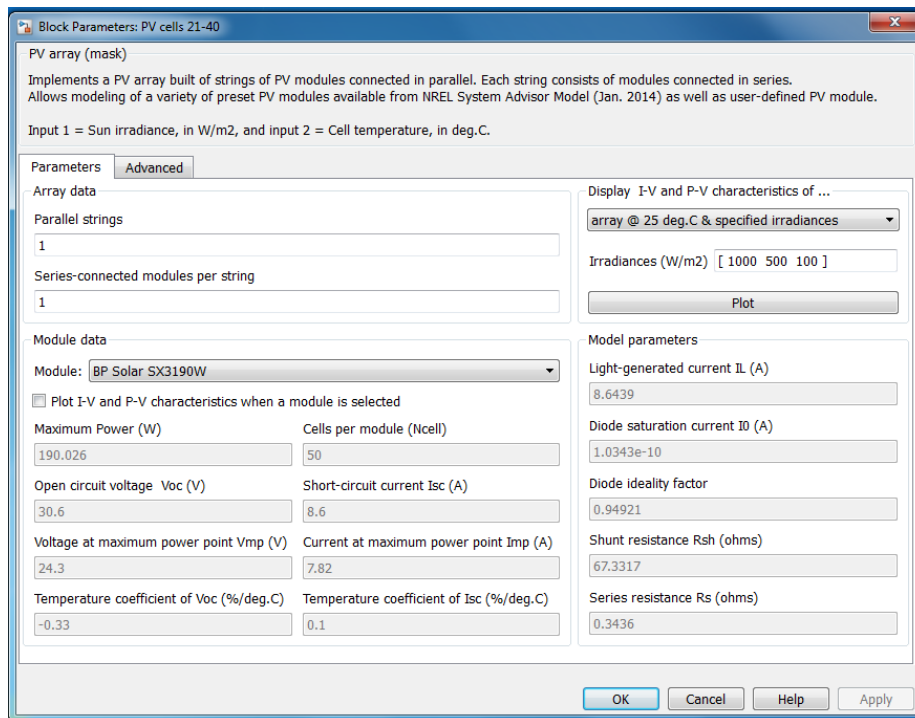


Module I-V and P-V Characteristics



Comparison on Diode and PV Currents





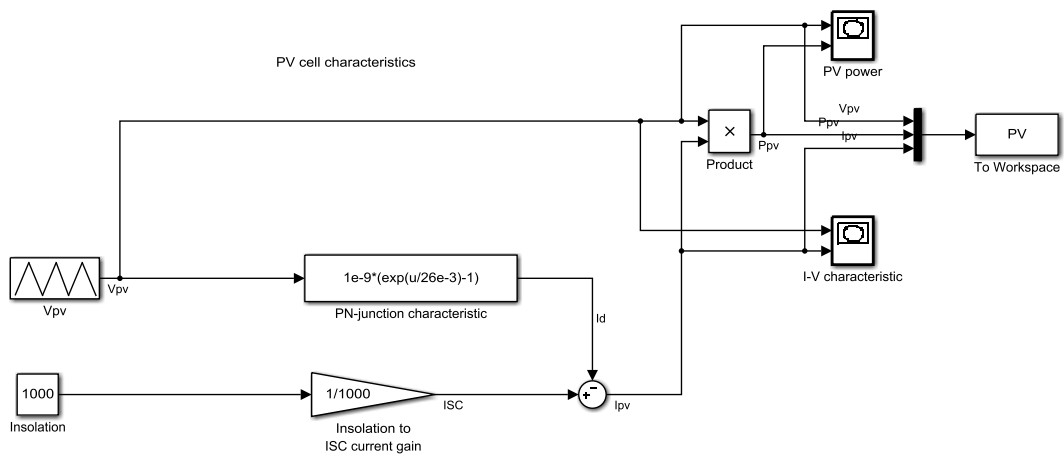
Block Parameters for the PV Cells

```
%PVcharacteristics.m
%This code plots the P-V and I-V curves of the photovoltaic array
clc
clear
Tcell = 25; %Ambient cell temperature (degrees celcius)
G = 1000;%Solar Irradiation (W/m2)
Voc = 43.2; %Open circuit voltage
%Uses photovoltaic model to calculate values
```

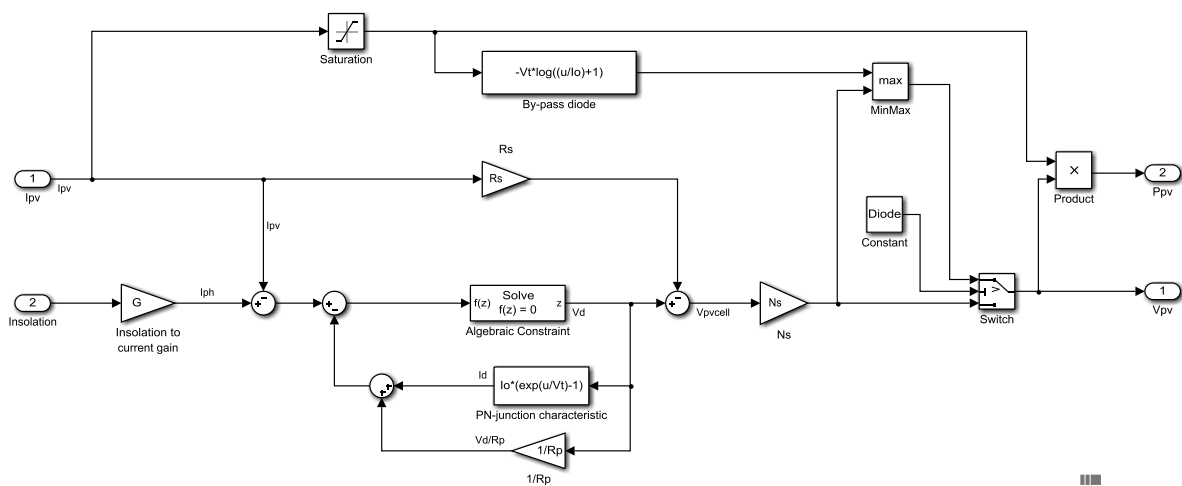
```

Va = 0:0.01:Voc;
Ipv = PVcharacteristics_func(Va,G,Tcell);
Ppv = Va.*Ipv; %Calculating PV output power
Pmax = max (Ppv); %Finding the maximum power of the array
%Plots P-V characteristic
% plot(Va,Ppv,'r','Linewidth', 3)
% title('P-V Characteristic (Irradiance 1kW/m^2)');
% xlabel('Voltage (V)');
% ylabel('Power (W) ');
% grid on
%Plots I-V characteristic
plot(Va,Ipv,'b','Linewidth', 1)
title('I-V Characteristic (Irradiance 1kW/m^2)');
xlabel('Voltage (V)');
ylabel('Current (A)');
grid on

```



PV Cell Model



PV Module Model

```

% find maximum power point in the PV cell data generated by pv1.mdl

```

```

pmax = max(PV.signals.values(:,2));
vrange = max(PV.signals.values(:,1));
irange = max(PV.signals.values(:,3));
[tf,index]=ismember(pmax,PV.signals.values(:,2));
disp(' MPP power: ')
disp(PV.signals.values(index,2));
disp(' MPP voltage: ')
disp(PV.signals.values(index,1));
disp(' MPP current: ');
disp(PV.signals.values(index,3));
figure(1)
plot(PV.signals.values(:,1),PV.signals.values(:,2)); % plot P(Vpv)
axis([0 vrange 0 pmax]);
figure(2)
plot(PV.signals.values(:,1),PV.signals.values(:,3)); % plot Ipv(Vpv)
axis([0 vrange 0 irange]);

function Ia = msx60 (Va, Suns, TaC)
% constants used
k = 1.38e-23; % Boltzman's const
q = 1.60e-19; %charge on an electron
%Enter the following constants here, and the model will
%be calculated based on these for 1000W/m^2
A = 1.2;
Vg = 1.12;
Ns = 36;
T1 = 273 + 25;
Voc_T1 = 21.06/Ns;
Isc_T1 = 3.80;
T2 = 273 + 75;
Voc_T2 = 17.05/Ns;
Isc_T2 = 3.92;
TaK = 273 + TaC; % array working temp
TrK = 273 + 25; % reference temp
dVdI_Voc = -1.15/Ns/2; % dVdI at Voc per cell;
% when Va = 0, light generated current Iph_T1 = array short cct current
% constant 'a' can be determined from Isc vs T
Iph_T1 = Isc_T1*Suns;
a = (Isc_T2-Isc_T1)/Isc_T1*1/(T2-T1);
Iph = Iph_T1*(1+a*(TaK-T1));
Vt_T1 = k*T1/q ;
Ir_T1 = Isc_T1/(exp(Voc_T1/(A*Vt_T1))-1);
Ir_T2 = Isc_T2/(exp(Voc_T2/(A*Vt_T1))-1); % not used
b = Vg*q/(A*k);
Ir = Ir_T1*(TaK/T1)^(3/A)*exp(-b*(1/TaK-1/T1));
X2v = Ir_T1/(A*Vt_T1)*exp(Voc_T1/(A*Vt_T1));
Rs = -dVdI_Voc - 1/X2v; % series resistance per cell
% Ia = 0:0.01: Iph
Vt_Ta = A*k*TaK/q;
% Ia1 = Iph -Ir*(exp((Vc+Ia*Rs)/(Vt_Ta) - 1) ;
% solve for Ia: f (Ia) =Iph-Ia-Ir*(exp((Vc+Ia*Rs)/Vt_Ta)-1) =0;
% Newton's method: Ia2 = Ia1 - f (Ia1)/f'(Ia1)
Vc = Va/Ns;
Ia = zeros (size (Vc));
% Iav = Ia;
for j = 1:5;
Ia = Ia - (Iph-Ia-Ir*(exp((Vc+Ia*Rs)/Vt_Ta)-1))/ (-1-
(Ir*(exp((Vc+Ia*Rs)/Vt_Ta)-1))*Rs/Vt_Ta);
end

```

```

% Script to show I-V characteristics of msx60 solar panel
% at 600, 800 and 1000 W/m^2 and 25 degC
Va = 0:0.5:24;
N = 0;
for V = 0:0.5:24;
N= N+1;
Ia (1, N) = msx60 (V, 0.6, 25);
end
plot (Va, Ia, Vb, Ia);
axis([0 24 0 4]);
xlabel('Voltage(V)');
ylabel ('Current (A)');
Title ('MSX-60 I-V Characteristics');
hold on;
N= 0;
for V = 0:0.5:24;
N=N+1;
Ia (1, N) = msx60 (V, 0.8, 25);
end
plot (Va, Ia, 'g');
N=0;
for V=0:0.5:24;
N=N+1;
Ia (1, N) = msx60 (V, 1, 25);
end
plot (Va, Ia, 'r');

% Script to show I-V characteristics of msx60 solar panel
% at 0, 25, 50 and 75 deg C
Va = 0:0.5:24;
N = 0;
for V = 0:0.5:24;
N= N+1;
Ia (1, N) = msx60 (V, 1, 0);
end
plot (Va, Ia, 'b');
axis([0 24 0 4]);
ylabel ('Current (A)');
Title ('MSX-60 I-V Characteristics');
hold on;
N= 0;
for V = 0:0.5:24;
N=N+1;
Ia (1, N) = msx60 (V, 1, 25);
end
plot (Va, Ia, 'g');
N=0;
for V=0:0.5:24;
N=N+1;
Ia (1, N) = msx60 (V, 1, 50);
end
plot (Va, Ia, 'r');
N=0;
for V=0:0.5:24;
N=N+1;
Ia (1, N) = msx60 (V, 1, 75);
end
plot (Va, Ia, 'm');

% Script to show P-V characteristics of msx60 solar panel
% at 25 deg C

```

```

Va = 0:0.5:24;
N = 0;
for V = 0:0.5:24;
N= N+1;
Ia (1, N) = msx60 (V, 1, 25);
P (1, N) = Ia (1, N)*Va (1, N);
end
plot (Va, P, 'b');
axis([0 24 0 80]);
xlabel('Voltage(V)');
ylabel('Power (W)');
Title ('MSX-60 P-V Characteristics at G=1000W/m^2 and T=25 degC');

function Ia = msx120 (Va, Suns, TaC)
% constants used
k = 1.38e-23; % Boltzman's const
q = 1.60e-19; %charge on an electron
%Enter the following constants here, and the model will
%be calculated based on these for 1000W/m^2
A = 1.4;
Vg = 1.12;
Ns = 72;
T1 = 273 + 25;
Voc_T1 = 42.2/Ns;
Isc_T1 = 3.81;
T2 = 273 + 75;
Voc_T2 = 34.09/Ns;
Isc_T2 = 3.96;
TaK = 273 + TaC; % array working temp
TrK = 273 + 25; % reference temp
dVdI_Voc = -2.15/Ns/2; % dVdI at Voc per cell;
% when Va = 0, light generated current Iph_T1 = array short cct current
% constant 'a' can be determined from Isc vs T
Iph_T1 = Isc_T1*Suns;
a = (Isc_T2-Isc_T1)/Isc_T1*1/(T2-T1);
Iph = Iph_T1*(1+a*(TaK-T1));
Vt_T1 = k*T1/q ;
Ir_T1 = Isc_T1/(exp(Voc_T1/(A*Vt_T1))-1);
Ir_T2 = Isc_T2/ (exp (Voc_T2/ (A*Vt_T1))-1); % not used
b = Vg*q/ (A*k);
Ir = Ir_T1*(TaK/T1)^(3/A)*exp(-b*(1/TaK-1/T1));
X2v = Ir_T1/(A*Vt_T1)*exp(Voc_T1/(A*Vt_T1));
Rs = -dVdI_Voc - 1/X2v; % series resistance per cell
% Ia = 0:0.01: Iph
Vt_Ta = A*k*TaK/q;
% Ia1 = Iph -Ir*(exp ((Vc+Ia*Rs)/ (Vt_Ta) - 1) );
% solve for Ia: f (Ia) =Iph-Ia-Ir*(exp ((Vc+Ia*Rs)/Vt_Ta)-1) =0;
% Newton's method: Ia2 = Ia1 - f (Ia1)/f' (Ia1)
Vc = Va/Ns;
Ia = zeros (size (Vc));
% Iav = Ia;
for j = 1:5;
Ia = Ia - (Iph-Ia-Ir*(exp ((Vc+Ia*Rs)/Vt_Ta)-1))/ (-1-
(Ir*(exp((Vc+Ia*Rs)/Vt_Ta)-1))*Rs/Vt_Ta);
end

% model of the Maximum Power Point Tracker (MPPT)
function [ Vmpp,Imppp,Pmax ] = MPPT(Vmin , dV , Vmax,G,T)
%initialize Vmpp, Imppp and Pmax
Imppp = 0;

```

```

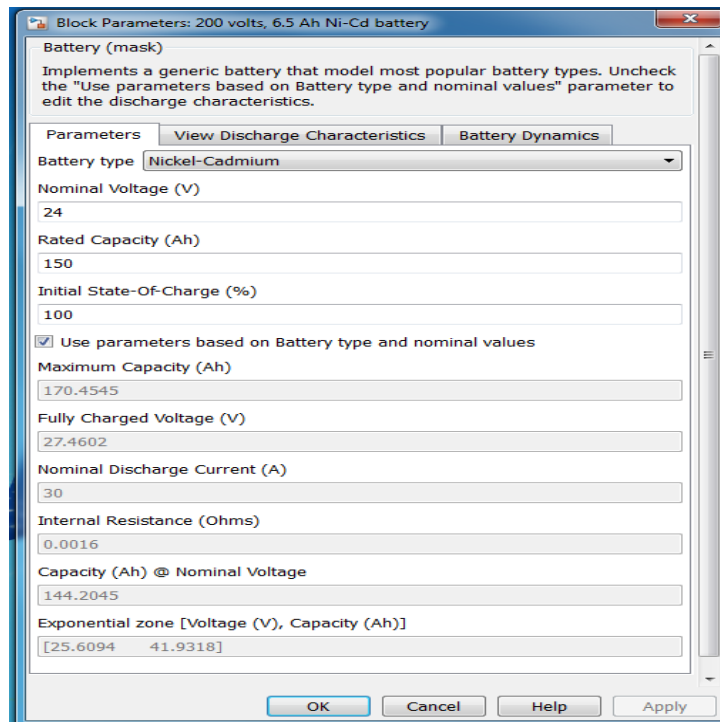
Vmpp = 0;
Pmax = 0;
for V = Vmin: dV: Vmax;
Ia = msx60(V,G,T);
P = Ia*V ;
if P > Pmax;
Pmax = P;
Vmpp = V;
Impp = Ia;
else
end
end

function [Psw_on,Pon,Psw_off,Ploss] = Mosfet(Va,Ia,p,T)
% constants gm, rdson, Vt, Cgs, tr, tf
gm = 42*((T+273)/300) ^ (-2.3); % Forward Transconductance in Siemens
rdson = 0.008*((T+273)/300)^2.3 ; % static Drain-to-Source On-
Resistance
Vt = 3.0 -(6*10^(-3))*T; % Gate Threshold Voltage
Cgs = 4000*10^(-12) ; % Input Capacitance in F
Cgd = 480*10^(-12); % Reverse Transfer Capacitance in F
tr = 100*10^(-9) ;% Rise Time in Sec
tf = 70*10^(-9) ;% Fall Time in Sec
Rg = 2.5; % gate resistance
%-----
Vf = Ia*rdson;
fs = 2*p*50;
t2_t1 = Rg*(Cgs+Cgd)*log ((gm*Va)/ (gm*(Va-Vt)-Ia));
Vgp = Vt + (Ia/gm);
Ig = (Va-Vgp)/Rg;
t3_t2 = (Va-Vf)*Cgd/Ig;
%-----
% losses for four transistors in a Full bridge configuration
Psw_on = 2*fs*(Va*Ia*(t2_t1)/2 + Ia*((Va-Vf)*tr/2 + Vf*tr));
Pon = 2*Vf*Ia;
Psw_off = 2*fs*(Ia*((Va-Vf)*tf/2 + Vf*tf) + Va*Ia*t3_t2/2);
%-----
Ploss = Psw_on + Pon +Psw_off;

home
disp ('')
disp ('Simulation Program for Grid connected PWM inverter with PV as aDC
source')

disp ('')
Vmin = input ('Enter minimum Voltage for MPPT Algorithm :');
dV = input ('Enter the increment value for MPPT Algorithm :');
Vmax = input ('Enter the Maximum Voltage for MPPT algorithm :');
Go = input ('Enter the solar Irradiation :');
G = Go/1000;
T = input ('Enter the Ambient temperature in degC :');
[Impp, Vmpp, Pmax] = MPPTtracking (Vmin, dV, Vmax, G, T);
[Vout, Iout, theta] = PWM (Impp, Vmpp);

```



Block Parameters for Battery Model